THE IMPACT OF MONOMER SEQUENCE AND STEREOCHEMISTRY ON THE BULK PROPERTIES OF REPEATING SEQUENCE POLY(LACTIC-*CO*-GLYCOLIC ACID) MATRICES

by

Michael Andrew Washington

Bachelors of Science, Seton Hill University, 2010

Submitted to the Graduate Faculty of the

Kenneth P. Dietrich School of Arts and Sciences in partial fulfillment

of the requirements for the degree of

Doctor of Philosophy in Chemistry

University of Pittsburgh

2017

UNIVERSITY OF PITTSBURGH

DIETRICH SCHOOL OF ARTS AND SCIENCES

This dissertation was presented

by

Michael Andrew Washington

It was defended on

April 7th, 2017

and was approved by

Geoffrey R. Hutchison, Assistant Professor, Department of Chemistry

W. Seth Horne, Associate Professor, Department of Chemistry

Steven R. Little, William Kepler Whiteford Endowed Professor and Chair, Department of

Chemical Engineering, Bioengineering, Pharmaceutical Sciences, Ophthalmology,

Immunology, and the McGowan Institute for Regenerative Medicine

Dissertation Advisor: Tara Y. Meyer, Associate Professor, Department of Chemistry and the

McGowan Institute for Regenerative Medicine

THE IMPACT OF MONOMER SEQUENCE AND STEREOCHEMISTRY ON THE BULK PROPERTIES OF REPEATING SEQUENCE POLY(LACTIC-*CO*-GLYCOLIC ACID) MATRICES

Michael Andrew Washington, PhD

University of Pittsburgh, 2017

Poly(lactic-*co*-glycolic acid) (PLGA)-based biodegradable materials have attracted considerable interest in the field of bioengineering due to their biocompatibility, FDA approval and tunable physico-chemical properties. Current methods for tuning the properties of PLGAs for a specific therapeutic application are, however, limited to changing the monomeric ratio and stereochemistry of cyclic diesters prior to ring-opening polymerization (ROP), a reaction that produces an unsequenced random copolymer. To understand how sequence, both structural and stereochemical, can be exploited to tune PLGA properties for specific applications, copolymers bearing periodic repeating sequences of lactic and glycolic acid were prepared using segmer assembly polymerization (SAP), an approach for controlling the sequence and stereochemistry within PLGA. A series of sequenced PLGAs were prepared, fabricated into various therapeutic devices, and characterized both in their initial states and after exposure to physiological conditions to promote hydrolytic degradation. Changes in sequence, stereochemistry, and monomeric ratios were shown to have a profound effect on such properties as *in vitro* erosion, swelling, compressive modulus, ultimate compressive stress, internal morphology, and crystallinity in implantable pellets. Data acquired from thermal analysis, gel permeation chromatography, and proton nuclear magnetic resonance established that the onset of molecular weight loss and oligomer formation via hydrolytic cleavage may be delayed based on backbone sequence. Two-photon microscopy studies of PLGA microparticles dramatically illustrate the

profound influence of backbone sequence on the hydrolysis profile and development of the internal acidic microclimate. Sequenced PLGA microparticles were found to maintain their initial internal pH over a 28 d time period compared to their random analogues. These results were confirmed by evaluating the *in vivo* foreign body response to subcutaneous microparticle injections. After 28 d *in vivo*, the alternating stereopure PLGA, poly LG, had minimal giant cell infiltrate compared to the commonly used random analogue, PDLGA-50. These discoveries establish a greater understanding of the role of sequence in controlling properties for bioengineering applications in addition to providing valuable insight into the preferential hydrolysis mechanism of sequenced PLGAs.

TABLE OF CONTENTS

LIST OF TABLES

LIST OF FIGURES

xviii

LIST OF SCHEMES

LIST OF EQUATIONS

LIST OF ABBREVIATIONS

AcOH   acetic acid

atm   atmosphere

Bn   benzyl protecting group

°C   degrees Celsius

Đ   dispersity (polymer chain dispersity)

Da   dalton

DCC   N,N'-dicyclohexylcarbodiimide

DIC   N,N'-diisopropylcarbodiimide

DMAP   4-dimethylaminopyridine

DPTS   4-(Dimethylamino)pyridinium 4-toluenesulfonate

DSC   Differential scanning calorimetry

EtOAc   ethyl acetate

G   glycolic acid monomeric unit

GPa   gigapascal

GPC   gel permeation chromatography

Hz   hertz

kDa   kilodalton

L   (*S*)-lactic acid monomeric unit

L$_{rac}$	racemic lactic acid monomeric unit
M	molar (moles per liter)
MALDI-ToF-MS	matrix-assisted laser desorption/ionization time-of-flight mass spectrometry
mg	milligram
MHz	megahertz
min	minute
mL	milliliter
M$_n$	number average molecular weight
M$_{n(0)}$	number average molecular weight at time = 0
M$_{n(t)}$	number average molecular weight at time = t
mol	mole
MPa	megapascals
M$_w$	weight average molecular weight
nm	nanometer
NMR	nuclear magnetic resonance spectroscopy
O/O	oil/oil single-emulsion
PDLGA-50	50:50 poly(D,L-lactide-*co*-glycolide)
PDLGA-65	65:35 poly(D,L-lactide-*co*-glycolide)
PGA	poly(glycolic acid)
PLA	poly(lactic acid)
PLGA	poly(lactic-*co*-glycolic acid)
PLGA (50/50)	50:50 poly(D,L-lactide-*co*-glycolide)

PLGA (70/30)	70:30 poly(D,L-lactide-*co*-glycolide)
PLGA (75/25)	75:25 poly(D,L-lactide-*co*-glycolide)
PLGA (80/20)	80:20 poly(D,L-lactide-*co*-glycolide)
PLGA (90/10)	90:10 poly(D,L-lactide-*co*-glycolide)
PLLGA-50	50:50 poly(L-lactide-*co*-glycolide)
ppm	parts per million
ROP	ring-opening polymerization
rt	room temperature
Si	*tert*-butyldiphenyl silyl protecting group
TBDPS	*tert*-butyldiphenyl silyl protecting group
SAP	segmer assembly polymerization
TBAF	tetra-n-butylammonium fluoride
T_g	glass transition temperature
THF	tetrahydrofuran
T_m	melting transition temperature
TPM	two-photon microscopy
UCS	ultimate compressive stress
W/O	water/oil single-emulsion
W/O/W	water/oil/water double-emulsion
XRD	x-ray powder diffraction
χ	Flory-Huggins parameter
δ	chemical shift
λ	wavelength

μL	microliter
τ	hydrolytic induction time period

PREFACE

The work presented herein was conducted at the University of Pittsburgh. I was the lead researcher whom was responsible for areas of concept formation, data collection and analysis, as well as manuscript composition. Dr. Tara Y. Meyer was the supervisory author and primary investigator on this project and was involved throughout the project in concept formation and manuscript composition. The work presented within this thesis was funded by the National Science Foundation (CHE-1410119).

DEDICATION

To my parents and brother,

Carol S., Dale R., and Gregory A. Washington

grandparents,

Helen E. and Alphonse S. Gilius & Alma C. and Robert Washington

and fiancé,

Kasey E. Riddle

Without whom none of my success would be possible. Words cannot express how much your

love and support has meant to me throughout this journey.

"Your future hasn't been written yet. No one's has. Your future is whatever you make it, so

make it a good one." – Emmett Brown

ACKNOWLEDGEMENTS

First, I would like to express my deepest gratitude to my advisor, Prof. Tara Y. Meyer for her mentorship throughout my Ph.D. I was sincerely blessed to have had the opportunity to work with such a patient, passionate, motivated, and dedicated advisor. Thank you to the members of my thesis committee: Prof. Steven R. Little, Prof. Geoffrey R. Hutchison, and Prof. W. Seth Horne for providing me with insightful comments, guidance, and positive encouragement.

I would like to extend my sincere thanks to Seton Hill University's chemistry faculty: Prof. John A. Cramer, Sr. Susan Yochum, Prof. Demetra Chengelis-Czegan, Prof. Diana Hoover, and Prof. Tony Parker for believing in me and providing me with opportunities to grow as a scientist throughout my collegiate career. To the late Dr. JoAnne W. Boyle, whose devotion to learning and deep care and concern for my career was truly inspirational, thank you for making your vision of Seton Hill a reality –"Hazard Yet Forward." To all the past and present members of the Meyer Group: Ryan M. Stayshich, Jian Li, Ryan M. Weiss, Amy L. Short, Jeffrey T. Auletta, Shaopeng Zhang, Colin D. Ladd, Jamie A. Nowalk, Jordan H. Swisher, and Emily F. Barker, thank you for the wonderful memories and continual support; we are forever a chemistry family. Thank you to my undergraduates, Kerri R. Bell and Devin J. Swiner, who assisted with portions of data acquisition reported in Chapter 2.

To my family, specifically Kristin N. Washington, Gary A. Riddle, Kimberly S. Riddle, Ron P. Gilius, and Susan L. Gilius, thank you for your continual love and words of

encouragement. To my nephews, Bryce O. Washington and his new baby brother, Baby W., don't be afraid to dream and always remember to do what you can't.

1.0   INTRODUCTION

1.1   SIGNIFICANCE

Poly(lactic-*co*-glycolic acid) (PLGA) has emerged as the most investigated biodegradable polymer over the past three decades due to its tunable release profiles, biocompatibility, and non-toxicity.[1] Additionally, unlike other biodegradable polymers, the U.S. Food and Drug Administration (FDA) and European Medicine Association (EMA) have approved PLGA for human use making it a strong candidate for biodegradable medical devices.[2] Currently, 15 PLGA-based parenteral drug delivery systems are commercially available for treating various ailments, such as prostate cancer, acromegaly, periodontitis, and malignant gliomas.[3] Despite its success in the aforementioned applications, PLGA-based technologies have made minimal progress in clinical applications outside of controlled drug delivery. We hypothesize that the lack of control over important characteristics, such as the rate of hydrolysis and retention of mechanical properties, have limited PLGAs transition into other clinical applications. Furthermore, we propose that sequence, an aspect of PLGA structure little explored prior to our work, can be used to tune and improve the bulk properties of PLGAs.

Using a sequence-controlled polymerization method, segmer assembly polymerization (SAP), a series of sequenced PLGAs were synthesized and compared to commonly used random analogues with similar lactic (L) and glycolic (G) ratios to evaluate differences in swelling,

erosion, hydrophilicity, internal acidic distribution, *in vivo* inflammatory response, internal and external morphology, mechanical properties, thermal properties, molecular weight distribution, and end group formation rate as a function of degradation. This is the *first* comprehensive report that compares the bulk properties of a set of novel sequence-defined PLGA copolymers to random analogues.

1.2 SYNTHETIC METHODS AND MICROSTRUCTURAL CONTROL

Random poly(lactic-*co*-glycolic acid) (PLGA) is generally synthesized using one of two synthetic pathways: 1) metal-catalyzed bulk ring-opening polymerization (ROP) of cyclic diesters or 2) condensation of the α-hydroxy acids (Fig. 1).[4-5] For ROP, the reaction is generally catalyzed using tin(II) bis(2-ethylhexanoate) (Sn(Oct)$_2$), which despite the known toxicity of tin, has been accepted by the FDA as "generally recognized as safe (GRAS)." This approach routinely produces high-molecular-weight polymers (10^5 – 10^6 Da) that are suitable for biomedical applications. In contrast, polycondensation of the α-hydroxy acids generally yields low-molecular-weight copolymers (10^2 – 10^3 Da) unless coupled to an azeotropic dehydration strategy.[6]
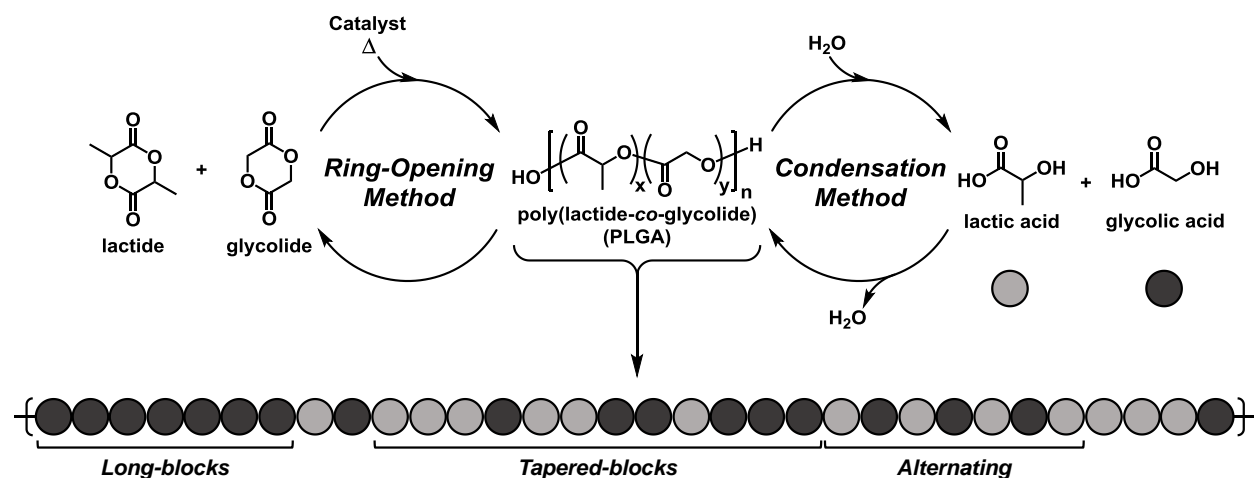
Figure 1. Ring-opening and condensation polymerizations produce random poly(lactic-*co*-glycolic acid)s with various microstructures.

Although ROP has been successfully utilized to make high-molecular weight PLGAs, transesterification processes can occur in parallel. Under concentrated and bulk conditions in conjunction with high temperature and long reaction times, polyesters readily undergo intra- and inter-molecular transesterification side-reactions. Using ^{1}H and ^{13}C NMR, Hu and coworkers monitored microstructural changes in PLGA copolymers comprising L-lactic (L_S) and glycolic acid (G) units and observed a decrease in L_S and G block lengths and concomitant racemization of L_S units with increasing reaction time.[7] Similar results were observed by Kasperczyk and coworkers in monitoring the appearance of transesterification induced LGL signals via ^{1}H and ^{13}C NMR.[8-9] These detrimental sequence scrambling side-reactions and differing monomeric reactivity ratios make batch-to-batch reproducibility of PLGA nearly impossible and result in limited control over properties.

Interestingly, the homopolymer, poly(lactic acid) (PLA), can be synthesized with a high degree of stereoselectivity and reproducibility.[4, 10-12] Similar to PLGA, high-molecular-weight PLAs are traditionally synthesized using ROP of lactide. Various diastereomers of lactide can be prepared (i.e., L-lactide, D-lactide, *meso*-lactide, or *rac*-lactide) using a polycondensation-

3

depolymerization strategy of the chiral lactic acid. Stereochemically tailored PLAs of varying tacticity can be prepared (e.g., atactic, heterotactic, isotactic, isotactic stereoblock, and syndiotactic) depending on the identity of the input lactide monomer(s) and metal catalyst (Fig. 2A).[13-15] Coates, Spassky and coworkers have made significant progress in developing a library of stereoselective catalysts for tailoring the tacticity of lactide using ROP.[14, 16-19] These catalysts consist of transition, rare-earth, or main group metal coordination complexes that offer superior control over tacticity and limit transesterification and epimerization side-reactions. Importantly, stereochemical control is lost when ROP is performed on mixtures of lactide and glycolide monomers and no control of the sequences of G and L units is achieved. [20] The higher reactivity and achirality of glycolide significantly limits the microstructural diversity of PLGA to random copolymers with long G-block and short atactic or isotactic L-blocks (Fig. 2B). The only sequenced PLGA copolymer that can be prepared by ROP is the simple alternating (LG)$_n$ sequence. Dong *et al.,* recently synthesized atactic alternating PLGA from a single monomer, D,L-3-methyl glycolide.[21] Overall, it is not possible to use ROP to create complex L- and G-sequences.
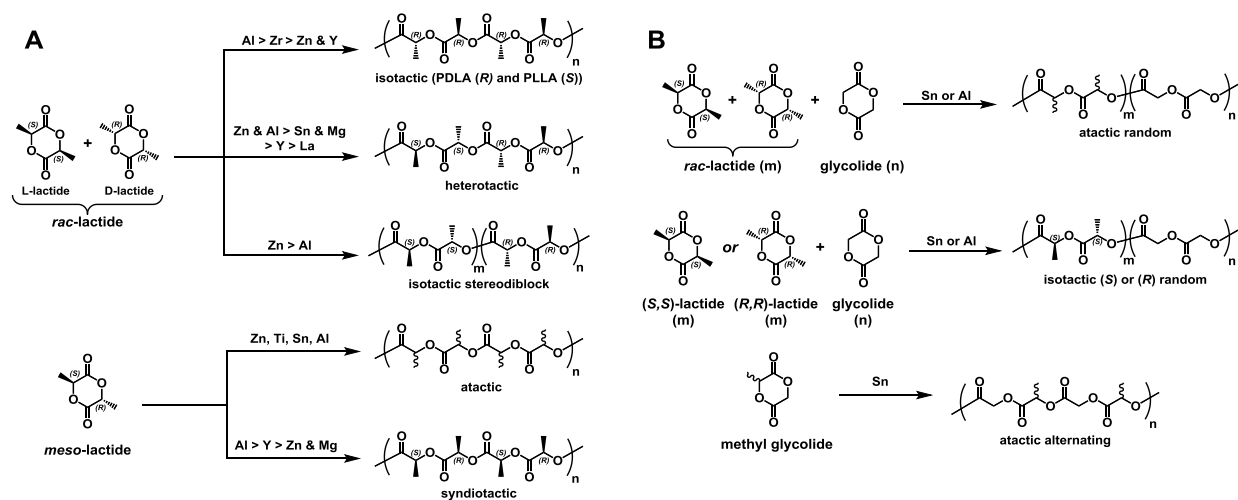
Figure 2. Microstructural variants of (A) poly(lactide) and (B) poly(lactide-*co*-glycolide) using metal-mediated ring-opening polymerizations.

1.3   MICROSTRUCTURE – PROPERTY RELATIONSHIPS

Although sequence exploration in PLA and PLGA has been limited as described in the previous section, there is evidence in the literature that suggests that controlling the microstructure of PLA and PLGA copolymers offers specific advantages for tailoring various thermophysical and physicochemical properties. For example, thermal properties, such as glass transition temperature (T_g), melting temperature (T_m), and crystallinity, largely depend on the monomer- and stereo-sequence of the copolymer. The thermal properties for PLAs vary based only on tacticity; isotactic and syndiotactic are semi-crystalline with T_ms of 175 and 155 °C, respectively, whereas heterotactic and atactic are amorphous.[22] The T_gs for PLAs tend to decrease as stereoregularity decreases. Contrary to PLA, the thermal properties of PLGA are largely affected by the lactic acid (L) to glycolic acid (G) ratio. Gilding and Reed evaluated a set of poly(L-lactide-*co*-glycolide)s and determined that PLGAs with an L-content > 80% were semi-crystalline with T_ms of 185 °C (100%), 165 °C (90 %), and 120 °C (80%) and T_gs ~55 – 60 °C; all other PLGAs were amorphous with T_gs ~50 – 55 °C.[23]

The mechanical properties of PLA and PLGA have also been shown to depend on stereo- and structural sequence, again limited to the example sequences that can be prepared by ROP. PLA (specifically isotactic PLA) is preferred over PLGA for load bearing applications due to its osteo-similar and superior mechanical properties and cell adhesion compatability.[24-27] Isotactic PLA has a higher mechanical strength than amorphous atactic PLA, 2.7 and 1.9 GPa, respectively, due to its semi-crystalline thermal properties. Mechanical strengths similar to atactic PLA have been reported for semi-crystalline PLGAs with L-contents > 82%; however, mechanical properties are retained over significantly shorter time periods compared to PLAs. Decreasing the L-content below 80% results in lower mechanical strengths and shorter property

retention time periods. PLGAs are only utilized in short-term low-load bearing devices, such as craniomaxillofacial plates, pins and staples and bioresorbable sutures and suture anchors, for these reasons.[28]

It has been reported that the degradation behaviors of PLA and PLGA are drastically different despite having similar thermophysical properties (Fig. 3).[28] PLA stereovariants typically degrade of the course of 20 − 24 months with isotactic PLA having the slowest degradation rate.[26] However, decreasing the L-content in isotactic random PLGA to 85% results in a 4-fold decrease in degradation time, (i.e., 5 − 6 months). Shorter degradation time periods of 4 − 5 months and 1 − 2 months are typical for PLGA (75/25) and PLGA (50/50), respectively.

For PLGAs, not surprisingly, degradation is found to depend strongly on the L:G composition of the copolymer. Controlling the input monomer ratio is the most common method for adjusting the hydrolytic rates of PLGAs. For example, in a microparticle degradation study conducted by Park, PLGA (50/50) and PLGA (70/30) microspheres degraded faster than microspheres composed of PLGA (80/20) and PLGA (90/10). There were no significant differences in molecular weight in this case, leading to the conclusion that the differences in hydrolysis rates for specific linkage types (i.e., G-G > L-G & G-L > L-L) led to the variations in degradation behavior.[29] Although sequence control is limited in these systems, studies that compare random copolymers with differing L- and G-block lengths suggest that the exploration of sequence could prove fruitful.[30-31]
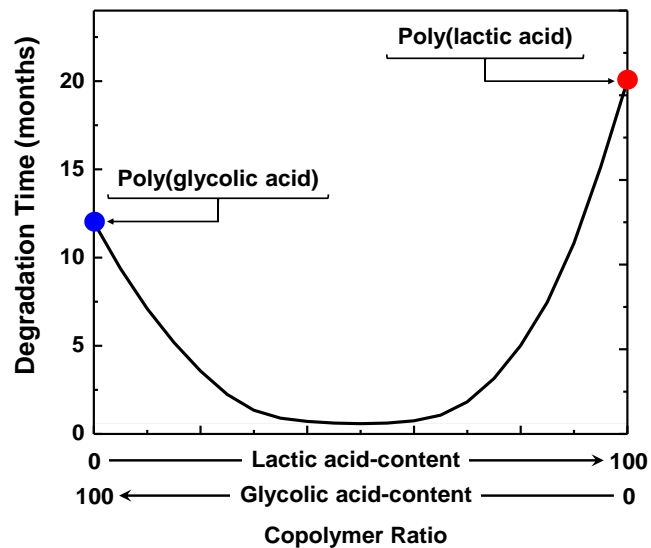
Figure 3. Degradation times for various copolymers of lactic and glycolic acid including the homopolymers. Image adapted from "Synthetic biodegradable polymers as orthopedic devices," by J.C. Middleton, 2000, *Biomaterials*, *21*, 2338. Copyright 2000 Elsevier Science Ltd. Adapted with permission.

1.4   STRATEGIES FOR SEQUENCE – CONTROLLED POLYMERS: BIOLOGICAL AND SYNTHETIC

The importance of sequence can be seen in Nature where monomer sequence regulation strategies are readily employed to control the structure, properties, and dynamic functions of biomacromolecules. The diverse needs of all living organisms are fundamentally satisfied by the molecular framework of deoxyribonucleic acid (DNA). The nucleotide sequence within the backbone of DNA encodes information that is translated into instructions for assembling complex biopolymers, such as polypeptides and proteins.[32] These biopolymers adopt unique three-dimensional structures to accomplish various biological tasks based on the amino acid

sequences. Mimicking the dynamic abilities of these biopolymers with a sequenced copolymer is particularly attractive from a synthetic point-of-view; however, our current synthetic approaches for producing sequence-regulated copolymers are underdeveloped.

Sequence-regulated polymerization processes, chain-growth and step-growth, are currently used to produce a variety of sequenced microstructures.[33-36] Chain-growth living radical and ring-opening polymerization methods, such as atom transfer radical polymerization (ATRP),[37] reversible addition/fragmentation chain transfer polymerization (RAFT),[38] nitroxide-mediated polymerization (NMP),[39] and ring-opening metathesis polymerization (ROMP),[40] have been used to synthesize short sequenced-defined repeats within block, alternating, and gradient copolymers (Fig. 4). These polymerization methods are synthetically practical, accommodate an array of monomers, and offer control over molecular weight distribution ($Đ \approx 1.05$). The precision of the repeat-unit sequence is mechanistically limited due to instantaneous and continuous propagation of monomer, making iterative single monomer propagations difficult.[41] Controlled radical chain-growth polymerization methods excel in controlling polymer topology (e.g., cyclic, linear, star, graft or brush, dendrimer, hyperbranched, networks) despite having chain composition limitations. Using ATRP, Matyjaszewski and coworkers have led the charge in synthesizing and characterizing the properties of these complex architectures.[42-43]
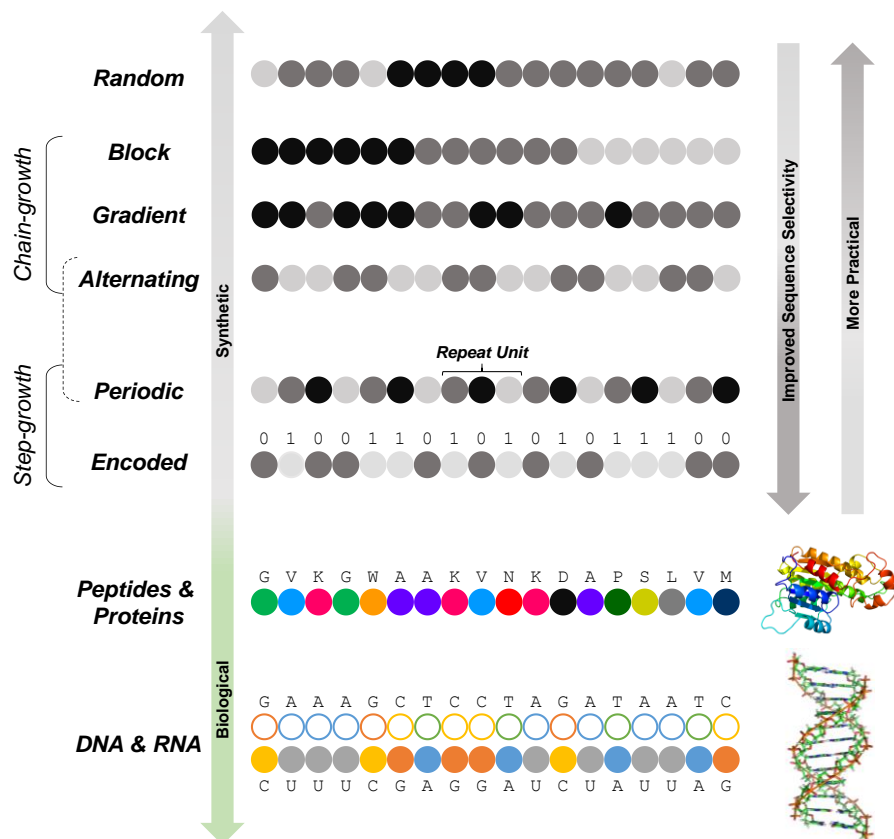
Figure 4. Progress in synthetic polymerization methods towards achieving architectures similar to those produced by biological systems.

Levels of microstructural control similar to biological systems may only be achieved using step-growth polymerizations.[44-46] Unlike the previously mentioned chain-growth processes, which rely on radical or transition metal mediated propagation mechanisms, step-growth polymerization methods utilize reactive AB or AA + BB type monomers. These monomers are sequentially coupled using a one-pot synthetic approach or solid support synthetic approach in which orthogonal chemistries, such as copper-catalyzed azide-alkyne cycloaddition (CuAAC),[47] thiol-ene,[48] Passerini,[49] and esterification[50] reactions, are utilized to produce periodic and encoded microstructures. Monodisperse precision polymers (Đ = 1.01 − 1.08) can be obtained using the linear iterative solid support synthetic method; however, the production of high molecular weight polymers requires numerous couplings-purification iterations and high reaction

yields.[35, 51] The most complex sequenced macromolecules have been synthesized by Lutz and coworkers[52-53] and Börner and coworkers[54] using solid-phase methods. Alternating and periodic architectures are accessible using solid support methods; however, the more practical one-pot approach has been utilized on gram scales by Meyer and coworkers[55] and Joy and coworkers[56-57] yielding polymers of high molecular weight.

1.4.1   Segmer Assembly Polymerization: Tailor-Made Sequences

Although recent progress has been made with controlling sequence in polymers, few studies have produced a significant family of sequenced polymers based on a specific group of monomers. The Meyer group, in contrast, has developed a step-growth polymerization method, segmer assembly polymerization (SAP), which has been utilized to produce more than 30 periodic copolymers.[55] This method offers superior control over monomeric sequence compared to traditional condensation methods (Fig. 5). Using the SAP methodology, sequenced $(A_mB_n)_x$ copolymers are prepared using discrete monodisperse repeat units, termed "segmers." Each segmer is assembled using orthogonally protected building blocks that are coupled using traditional esterification chemistry. A and B sequences of modest length ($m + n = 2 - 7$) may be produced using an iterative divergent-convergent strategy consisting of sequential coupling-deprotection reactions. The segmers are then polymerized using optimized condensation conditions to yield periodic repeat sequences within the polymer backbone.
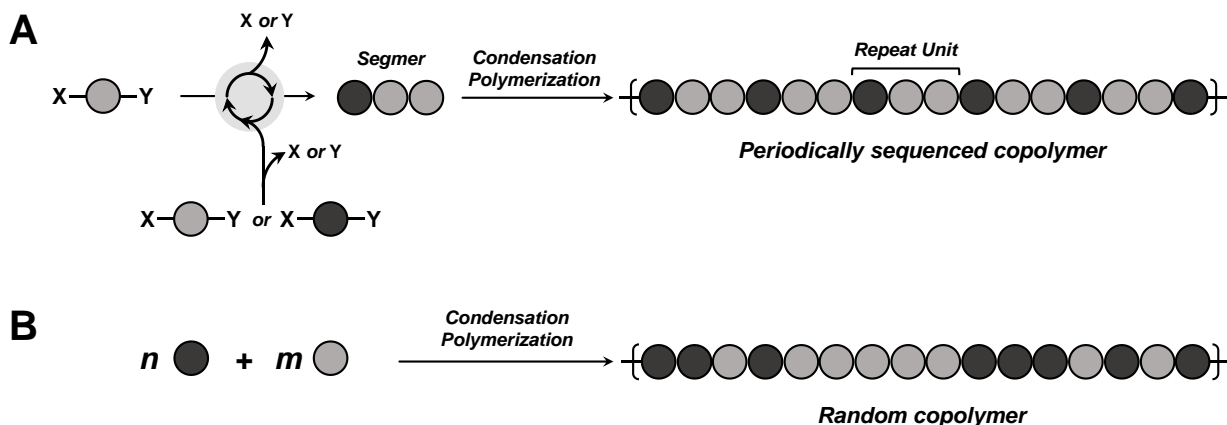
Figure 5. Comparison of segmer assembly polymerization methodology (A) and traditional condensation polymerizations (B) for preparing binary copolymers. Here, X and Y represent orthogonal protecting groups.

Various pilot experiments were conducted by the Meyer group using SAP in which sequenced copolymer variants of commonly used biodegradable copolymers were synthesized. Stayshich *et al.*,[55] synthesized a library of periodic copolymers comprising L-, D-, and *rac*- lactic acid and glycolic acid units with molecular weights of 14 − 40 kDa. Meyer and coworkers expanded the aforementioned polyester family by including caprolactic acid units and (*S*)-3-benzyloxy-2-hydroxypropionic acids in periodic copolymers where molecular weights ranged from 18 − 49 kDa and 17 − 48 kDa, respectively.[58-59] These model systems illustrated the synthetic versatility and precision of SAP, but most importantly demonstrated that a family of sequenced copolymers with similar molecular weights can be routinely produced.

1.5   EXPLOITING SEQUENCE TO CONTROL PROPERTIES

Portions of the background discussed in this section were previously published in "J.H. Swisher, J.A. Nowalk, M.A. Washington, T.Y. Meyer "1. Properties and Applications of Sequence-Controlled Polymers" and "J. Li, M.A. Washington, K.L. Bell, R.M. Weiss, S.M. Rothstein, S.R.

11

Little, H.M. Edenborn, T.Y. Meyer "Chapter 18. Engineering Hydrolytic Degradation Behavior of Poly(lactic-*co*-glycolic acid) through Precise Control of Monomer Sequence" Sequence-Controlled Polymers: Synthesis, Self-Assembly, and Properties. American Chemical Society: 2014; Vol. 1170, p 271-286.

The Meyer group has previously reported sequence-based property correlations for PLGAs and PLGCAs (C = caprolactic unit; 6-hydroxyhexanoic acid). For binary copolymers in which the composition was allowed to vary, as is the case with the series of polymers with repeating units of LLLLC, LLLC, LLC, LLCLC, LLCCLC, and CLC, the T_gs were found to closely adhere to the predictions of the Fox equation.[58] However, when ternary copolymers with identical compositions but different sequences were compared, **poly GLC** vs. **poly LGC**, a difference of nearly 8 ºC was observed. The tendency towards crystallization and the T_m was found to be very sensitive to sequence. In the pair described above, **poly GLC** was semi-crystalline with a T_m = 37.7 ºC while **poly LGC** remained amorphous. Stereosequence also affected the crystallinity in a significant fashion. The isotactic **poly L$_S$L$_S$G**, for example, is slow to crystallize (T_m = 114 ºC) whereas both **poly L$_S$L$_R$G** and **poly L$_R$L$_S$G** crystallize easily and exhibit a higher T_m (~ 155 ºC for both).[55]

The most dramatic sequence based behavior for PLGAs occurs, however, during hydrolytic degradation. Behaviors that were by monitored by Meyer and coworkers during degradation included molecular weight, lactic acid release, and rhodamine B release.[60-61] All were found to have a dramatic dependence on sequence. Molecular weight, for example, drops exponentially for random PLGA controls, while the molecular weight of sequenced materials with similar compositions decrease gradually. In addition, the molecular weight profile of 50:50 poly(D,L-lactide-*co*-glycolide) (PDLGA-50) broadened and became distinctly polymodal over

the course of degradation while the profiles of sequenced PLGAs exhibited only slight broadening over the same time period. Lactic acid release was also sequence dependent, with the random copolymers exhibiting rapid release of lactic acid while all other sequenced samples were significantly slower. The lactic acid release of sequenced PLGAs followed in accordance with the aforementioned hydrolysis rate hierarchy; **poly GLG** > **poly L$_{rac}$G** > **poly LG** > **poly L$_{rac}$LG** > **poly LLG**. Meyer and coworkers have also discovered that both guest molecule loading efficiencies and *in vitro* release rates depend on sequence. When rhodamine B dye was loaded into microparticles prepared from both **PDLGA-50** and **poly LG**, the random copolymer consistently exhibited higher maximum loading efficiencies. When exposed to physiological conditions, however, the dye was more gradually released from the sequenced copolymer, **poly LG**, compared to the random **PDLGA-50** copolymer.

1.6   THESIS OVERVIEW

Meyer and coworkers have demonstrated that monomer- and stereo-sequence strongly influence the degradation properties of PLGA; sequence-defined PLGAs hydrolyze slower and more uniformly compared to random analogues (Fig. 6). The overall objective of the current work is to expand upon these findings and improve our understanding of how monomer-by-momoner sequence affects the bulk properties of PLGA using matrices, which are commonly used in biomedical applications (e.g, solid implants and microparticles). We hypothesize that matrices fabricated with sequence-defined PLGAs will be able to retain a bulk property of interest over longer time periods compared to random PLGA analogues due to their more homogenous degradation profiles.
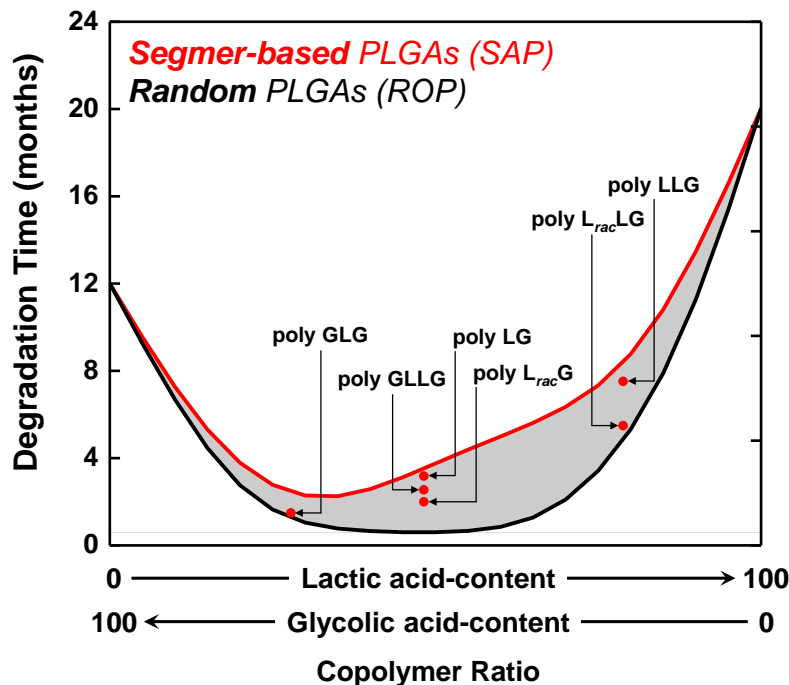
Figure 6. Deviations from typical random PLGA degradation times for various sequence-defined PLGAs. Here, the gray space between the two curves represents the accessible degradation times for sequenced PLGAs.

In Chapter 2 of this dissertation, a comprehensive examination of the swelling and erosion behaviors of sequence-defined and random PLGA solid cylindrical matrices (3 mm x 3 mm and 3 mm x 1.5 mm) as a function of degradation time are reported. The goal of this study was to monitor the *in vitro* degradation behavior of sequence-defined PLGAs over 8-week (swelling) and 20-week (erosion) time periods to determine if the erosion mechanism of sequence-defined PLGAs align more closely with a bulk or surface erosion mechanism; random PLGAs erode via a bulk mechanism.

In Chapter 3 we focus on expanding our understanding of the degradation behaviors of sequence-defined PLGAs by monitoring the evolution and release of acidic by-products from PLGA microparticles, ~200 μm and ~30 μm, which has been considered a most serious drawback for PLGA-based drug delivery systems. An innovative two-photon microscopy

14

method was utilized to map the *in vitro* internal acidic microclimate pH of sequence-defined and random PLGA analogues over an 8-week time period. In addition, the release of acidic by-product was qualitatively analyzed using subcutaneous microparticle injections in mice, where the foreign body response was evaluated 2- and 4-weeks post-injection. This is the first report in which a sequence-defined PLGA copolymer was utilized *in vivo*.

In Chapter 4 we focus on determining how monomer sequence affects the retention of mechanical properties for solid cylindrical matrices, 3 mm x 3 mm. In this study, the microstructural and macroscopic bulk properties of a series of sequence-defined and random PLGAs were monitored *in vitro* over a 9-week time period. The results of this study provide valuable insights into the preferential hydrolysis mechanism for sequence-defined PLGAs.

2.0 THE IMPACT OF MONOMER SEQUENCE AND STEREOCHEMISTRY ON THE SWELLING AND EROSION OF BIODEGRADABLE POLY(LACTIC-*CO*-GLYCOLIC ACID) MATRICES

2.1 OVERVIEW

This work presented in this chapter describes the mechanism of swelling and erosion for sequenced and random poly(lactic-*co*-glycolic acid)s. This chapter has been previously published and is summarized in Fig. 7.[62]
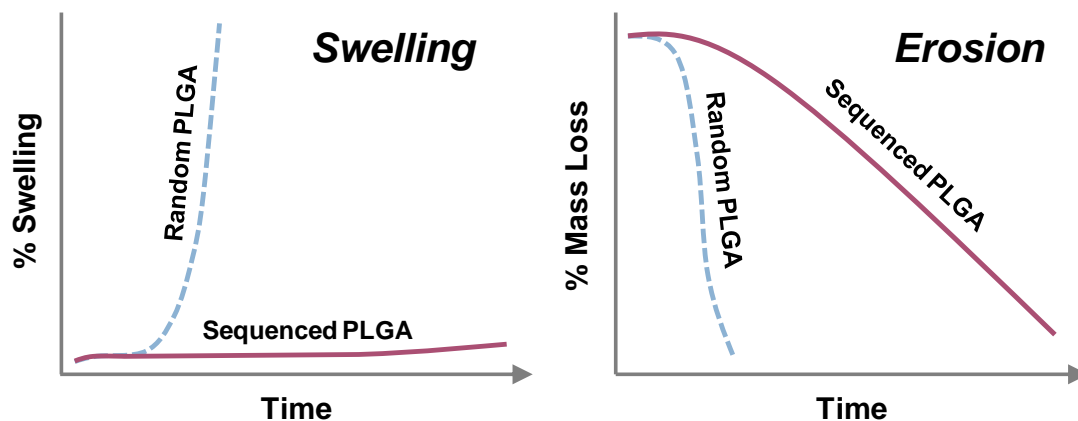
Figure 7. Graphical abstract for Chapter 2 – The impact of monomer sequence and stereochemistry on the swelling and erosion of biodegradable poly(lactic-co-glycolic acid) matrices.

Monomer sequence is demonstrated to be a primary factor in determining the hydrolytic degradation profile of poly(lactic-*co*-glycolic acid)s (PLGAs). Although many approaches have been used to tune the degradation of PLGAs, little effort has been expended in exploring the sequence-control strategy exploited by nature in biopolymers. Cylindrical matrices and films prepared from a series of sequenced and random PLGAs were subjected to hydrolysis in a pH 7.4 buffer at 37 °C. Swelling ranged from 107% for the random racemic PLGA with a 50:50 ratio of lactic (L) to glycolic (G) units to 6% for the sequenced alternating copolymer poly LG. Erosion followed an inverse trend with the random 50:50 PLGA showing an erosion half-life of 3-4 weeks while poly LG required ca. >10 weeks. Stereosequence was found to play a large role in determining swelling and erosion; stereopure analogues swelled less and were slower to lose mass. Molecular weight loss followed similar trends and increases in dispersity correlated with the onset of significant swelling. The relative proportion of rapidly cleavable G-G linkages relative to G-L/L-G (moderate) and L-L (slow) correlates strongly with the degree of swelling observed and the rate of erosion. The dramatic sequence-dependent variation in swelling, in the absence of a parallel hydrophilicity trend, suggest that osmotic pressure, driven by the differential accumulation of degradation products, plays an important role.

2.2   INTRODUCTION

We have discovered that sequence can be used to control the degradation behavior of poly(lactic-*co*-glycolic acid)s (PLGAs). Random PLGAs have been utilized extensively in controlled drug delivery systems and clinical applications due to their biocompatibility, biodegradability, and regulatory acceptance. Target applications include controlled release devices for anticancer

17

agents,[63-65] surgical sutures and screws,[1, 66] and porous scaffolds for tissue regeneration.[67] Despite the number of literature reports on the utility of PLGAs for bioengineering, however, there are currently only 15 FDA-approved PLA/PLGA-based drug products on the US market.[68] We hypothesize that one contributing factor to the poor translation into application is the relatively narrow range of performance of the random copolymer PLGAs during degradation, a deficiency that has been addressed by others with a variety of strategies including adjusting molecular weight, controlling ratio of lactic (L) and glycolic (G) units; tuning average L and G block lengths, adding comonomers and chemical additives, and through the design and configuration of devices.[69-70]

Our approach to expanding the accessible range of degradation profiles is to move beyond random copolymers through the control the sequence of the monomers, an approach which in biological polymers has been shown to provide diverse structure and function from a limited monomer set. The potential for impact of this approach is further supported by the recent promising reports of sequence control in other synthetic copolymers [34-35, 45-46, 58-59, 71-73] and by intriguing studies by Sarasua *et al.*, that link properties with statistical variations in chain microstructure for selected biopolyesters.[74-79]

To probe the relationship between monomer order and properties, we have developed a synthetic route that yields PLGAs with repeating sequences.[55] For example, we have prepared **poly LG**, which consists of an exact repeat of the LG dimer for the length of the polymer (i.e., $(LG)_n$). Similarly, we have been able to prepare a variety of polymers bearing periodic repeats of varying lengths (e.g., $(LLG)_n$, $(GLLG)_n$, etc…). Using NMR spectroscopy, which is uniquely powerful for the characterization of this particular class of polymer due to solution phase conformational preferences, the periodic structure of these polymers has been confirmed.

18

Moreover, sequence errors are easily detected and can be quantified.[55] The ability to both synthesize exact sequences and verify them enables, for the first time, a thorough exploration of structure and function in PLGAs.

In initial properties studies of this new class of periodic PLGAs [60-61] we have found a surprisingly strong correlation between sequence and properties. In microparticles prepared from these copolymers, we observed a correlation of sequence with molecular weight loss, lactic acid release, and thermal properties. In general, the sequenced PLGAs exhibited a slower and more gradual loss of molecular weight and a longer preservation of morphology, including T_g, than the random analogues. Differences were also observed between sequences, both structural- and stereoisomers. The release of an encapsulated guest molecule, rhodamine B, was also studied and found to depend directly on monomer order; the simple alternating copolymer **poly LG** released the guest more slowly and gradually than did the random PLGA control.

Based on these results, we hypothesize that sequenced PLGAs may have positive implications for bioengineering applications where prolonged delivery times and/or structural integrity are particularly important. For example, a longer release time would be beneficial for long-lasting intraocular implants. These implants, which are designed to replace eye drop regimens, which have low patient compliance, allow for continuous drug release.[80] We also expect that the slower degradation of the sequenced PLGAs will minimize the accumulation of pH-lowering acidic by-products compared to random PLGAs. This behavior could provide a protective effect for tissues such the retina, which is known to be particularly sensitive to non-physiological pH.[81] The improved maintenance of morphology for the sequenced PLGAs could also offer advantages for certain applications (e.g., the repair of craniofacial bony defects) which

require longer term mechanical strength during the delivery of critical osteogenic growth factors.[82]

Swelling and erosion are deeply relevant to these application goals and their study should also lend insight into any sequence-based differences in the underlying mechanism of erosion. It has been previously reported and substantiated by numerous studies that matrices of random PLGAs below certain dimensions degrade by bulk erosion.[83-84] Observable behaviors associated with this mechanism include, in most cases, significant swelling and a rapid loss of mass after an initial latent period. At the other end of the continuum lie materials that decompose by surface erosion. These materials (e.g., polyanhydrides) degrade without significant water uptake and mass loss is gradual as the inner layers only begin to degrade as the outer layers are sequentially hydrolyzed.[85-89] This distinction is particularly important for the use of PLGA in drug delivery, as it is expected and has been observed that the release profile of encapsulated drugs depends on swelling and erosion.[90] Herein, we examine the swelling and erosion of sequenced PLGAs to determine, in part, whether their degradation behavior aligns more closely with a bulk or surface mechanism.

2.3   MATERIALS AND METHODS

2.3.1   Materials

Periodic PLGA copolymers were prepared as previously described.[55, 91] Poly(D,L-lactide-*co*-glycolide) with a 50:50 ratio of lactic to glycolic acid-derived units and carboxylate end groups

(**PDLGA-50**) and poly(D,L-lactide-*co*-glycolide) with a 65:35 ratio of lactic to glycolic acid-derived units and carboxylate end groups (**PDLGA-65**) were obtained from Durect Corporation (Birmingham, AL) as a pelletized solid. Prior to use, the polymers were dissolved in methylene chloride (CH$_2$Cl$_2$) and precipitated in methanol to yield off white amorphous solids. Poly(L-lactide-*co*-glycolide) with a 50:50 ratio of lactic to glycolic acid-derived units and carboxylate end groups (**PLLGA-50**), was obtained from Changchun SinoBiomaterials Co. Ltd. (Changchun, China) as a fibrous white solid and was used as provided. Phosphate buffered saline (PBS, pH = 7.4, 10 mM) was purchased from Life Technologies (Carlsbad, CA).

2.3.2   Characterization

Molecular weights and dispersities were acquired on a Waters GPC system (THF, 0.5 mL/min) with Jordi 500 Å, 1000 Å, and 10000 Å divinylbenzene (DVB) columns and refractive index detector (Waters), which was calibrated relative to polystyrene standards. Thermal properties of all polymers were obtained using TA Instruments Q200 DSC. Standard data were collected with a heating and cooling rate of 10 °C/min. Melting transitions (T$_m$) were collected from the first heating cycle and glass transition temperatures (T$_g$) were collected during the second heating cycle. Inflection points of glass transition temperatures are reported. All samples were prepared by drop-casting (CH$_2$Cl$_2$) into DSC pans followed by vacuum drying for 24 h and annealing at 85 °C for 3 h. The ^{1}H and ^{13}C NMR spectra were obtained in CDCl$_3$ using a 500 MHz Bruker spectrometer at 293 K and calibrated to the residual solvent peak at δ 7.26 ppm (^{1}H) and δ 77.00 ppm (^{13}C). Matrix assisted laser desorption/ionization time-of-flight (MALDI-ToF-MS) spectra were obtained on a Voyager-DE PRO instrument with a 337 nm N$_2$ laser and 25 kV accelerating voltage. The mass spectra of the polymers were obtained in reflector mode. The matrix consisted

of *trans*-2-[3-(4-*t*-butyl-phenyl)-2-methyl-2-propenylidene]malononitrile (DCTB) and sodium trifluoroacetate as the cationization agent.

2.3.3   Preparation of cylindrical-shaped pellets

Cylindrical-shaped pellets of all PLGAs were prepared by heated compression molding in a custom press. The colorless polymer (20-30 mg) was loaded into the press that was warmed to 85-95 °C and compressed with a 1,200-1,400 lb load for 10 min using a Carver press (Hydraulic unit model #3912; Wabash, IN). The press and sample were then re-heated for 10 min in an oven at 85 °C, and compressed again for 5 min under the same temperature and load. The resulting pellets were opaque or translucent depending on the polymer used and had dimensions of 3 x 3 mm (swelling) or 3 x 1.5 mm (erosion), corresponding to a weight of ~26 mg and ~15 mg, respectively.

2.3.4   *In vitro* swelling of sequenced and random PLGAs

Two samples of each polymer (26 mg each) were placed in separate Eppendorf tubes containing 2 mL of PBS. All tubes were incubated at 37 °C on a rotating mixer (8 rpm). Samples were removed every 2 d for the first 10 d, then weekly depending on the degree of swelling. Both **PDLGA-50** and **PLLGA-50** were removed every 2 d until sample degradation progressed to the point that the remaining material could not be handled or weighed. Each sample was blotted dry for 30 s and weighed on an analytical balance ($\pm$ 1.0 x 10^{-4} g) until a stable reading was displayed for 15 s. The phosphate buffer was replaced each week for the entirety of the study.

2.3.5 *In vitro* erosion of sequenced and random PLGAs

Ten samples of each polymer (15 mg each) were placed in separate Eppendorf tubes containing 2 mL of PBS. Samples of each polymer were then divided into 5 groups of 2 samples, each to determine the mass loss at 5 different time intervals. All tubes were incubated at 37 °C on a rotating mixer (8 rpm). The tubes were refilled with fresh PBS (2 mL) every week. At each time point, duplicate samples of each polymer were collected, blotted dry for 15 s, flash-frozen in liquid N_2, then lyophilized for 2 d. After freeze-drying, the pellets were weighed on an analytical balance ($\pm 1.0 \times 10^{-4}$ g). Masses were recorded once a stable reading was displayed for 15 s.

2.3.6 Water contact angle experiments

Water contact angle measurements were recorded using a VCA optima XE video contact angle system at 24 °C and 42-48% relative humidity. A droplet with a volume of 1 μL was formed at the end of the needle and then lowered carefully until contact was made with the sample. The needle was withdrawn immediately so that the droplet was left on the sample surface. An image of the droplet was acquired with a charge-coupled device (CCD) camera 5 s after contact with the surface of the film. The static contact angle was calculated automatically by the VCA software. Approximately 45 s was required to complete the whole measurement process. Each measurement was repeated 5x per sample at different locations.

Films of all PLGAs were prepared using a drawdown coating method. Each of the copolymer samples was dissolved in dichloromethane at a concentration of 250 mg/mL. A 20-30 μm film was deposited on a glass microscope slide using a 180-200 μL aliquot of the polymer solution. The resulting film was dried in an oven at 70 °C for 1 h and stored in a vacuum

desiccator until used. Samples were exposed to PBS at 23 °C and the hydrated contact angle was monitored over an 8 d time period. After the hydrated water contact angle was recorded, the films were flash-frozen in liquid N_2, lyophilized for 3 d, and the lyophilized film contact angle was determined using the same method.

2.4   RESULTS

2.4.1   Naming conventions and characterization of PLGA copolymers

The L-lactic unit, racemic lactic unit, and glycolic unit are abbreviated as **L**, **L**$_{rac}$, and **G**, respectively. The periodic copolymers utilized in this study were prepared using segmer assembly polymerization (SAP). In this method, we prepare well-defined oligomers and polymerize them using condensation conditions that have been optimized to preclude sequence scrambling by transesterification (Fig. A1). The resulting copolymers are termed periodic copolymers because they consist of a nearly perfect repetition of the input segmer. As such, a segmer consisting of a lactic and glycolic acid-derived unit, would be termed **LG** and the polymer would be named **poly LG** (Scheme 1). The SAP method was also used to prepare a random copolymer, **R-SAP**, by condensation of a 1:1:1:1 ratio of the segmers **LG**, **GL**, **LL** and **GG**. The random copolymers, **PLLGA-50**, **PDLGA-50** and **PDLGA-65**, prepared by ring-opening polymerization (ROP) of lactide and glycolide, were purchased. In this case, the **PLLGA-50** and **PDLGA-50** are the stereopure and racemic versions of the copolymers with a 50:50 L:G-ratio and **PDLGA-65** is the racemic derivative of a copolymer with a 65:35 L:G-ratio. Sequenced copolymers prepared by SAP range in molecular weight from 18 to 30 kDa and are

24

comparable to purchased random PLGA controls (Table 1, Fig. A2). All polymers exhibited T_gs in the range of 44 to 49 °C (Table 1, Fig. A3).
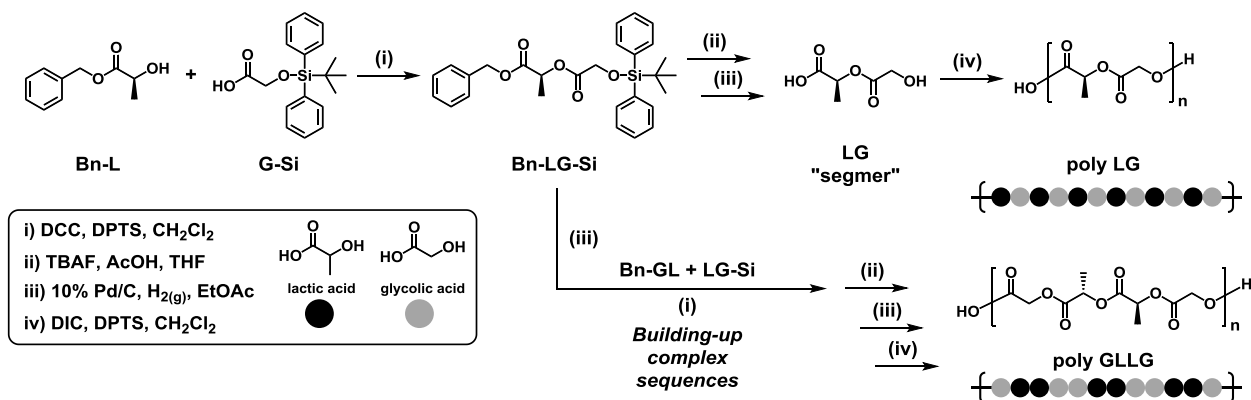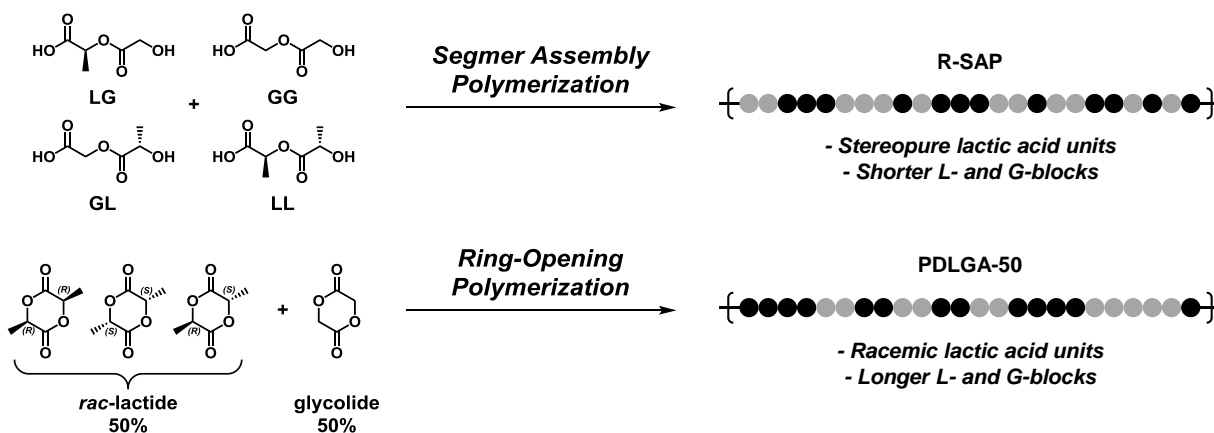
Scheme 1. Synthesis of periodic PLGA copolymers using segmer assembly polymerization (SAP) method along with random analogues synthesized by SAP and ring-opening polymerization (ROP).

Table 1. Characterization data for sequence-defined and random PLGAs utilized in swelling and erosion studies.

Polymer	M_n^a (kDa)	M_w^a (kDa)	$Đ^a$	T_g (°C)[b]	ratio L:G[c]
Poly LG	23.5	30.0	1.3	44	50:50
Poly L$_{rac}$G	30.8	44.4	1.4	49	50:50
Poly GLG	21.6	28.3	1.3	45	34:66

Poly GLLG	18.7	25.1	1.3	45	50:50
R-SAP	24.1	33.3	1.4	46	44:56
PDLGA-50	30.7	38.4	1.3	48	51:49
PLLGA-50	23.9	38.8	1.6	47	54:46
PDLGA-65	28.3	39.2	1.4	47	65:35

[a] Determined by size exclusion chromatography in THF relative to polystyrene standards.

[b] Obtained in the second heating cycle at 10 °C/min.

[c] Results based on ^{1}H NMR spectroscopy and presented as the ratio of the lactic (L) and glycolic (G) units.

2.4.2 Characterization

The copolymers were characterized by ^{1}H NMR, ^{13}C NMR, and MALDI-ToF mass spectrometry (Figs. 8, 9, A4 – A22). As we have previously described in detail the assignment of ^{1}H and ^{13}C NMR spectra of these polymers,[55] we will comment on only few key features. Most importantly, we note that these sequenced copolymer exhibit unusually sharp and well-resolved ^{1}H NMR peaks, even for high molecular weight samples. These copolymers have strong sequence-based conformational preferences, which result in unique and assignable resonances for each variant. The diastereotopic glycolyl protons are particularly useful in the ^{1}H NMR spectrum. The combination of clear sequence based differences in chemical shift, along with high resolution means sequence mistakes are readily identifiable and quantifiable.
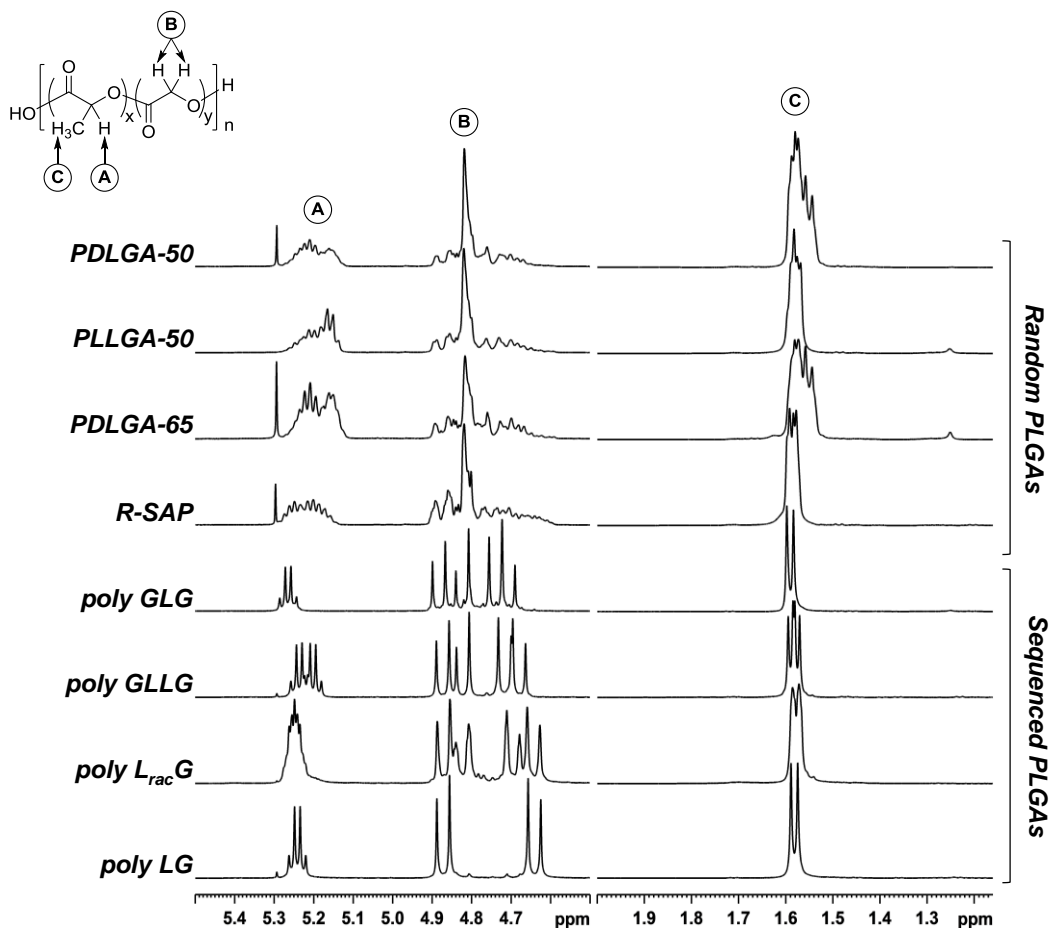
Figure 8. ^{1}H NMR (500 MHz) spectra of sequenced and random PLGAs (δ 5.5 – 4.5 and 2.0 – 1.2 ppm). Labels corresponding to the locations of methine (A), methylene (B), and methyl (C) proton chemical shifts for poly(lactic-*co*-glycolic acid) are included for reference.

MALDI-ToF mass spectra (Fig. A22) of these copolymers also confirms the periodic structure of these copolymers as the chain lengths observed are all multiples of the target sequence. With the exception of **Poly GLG** the sequenced copolymers, while not perfect, exhibit very small amounts of error and epimerization. The **Poly GLG** sample, as can be seen in both the ^{1}H and MALDI-ToF spectra does contain a slightly higher rate of sequence errors, primarily consisting of the loss/addition of G or LG units. The rate is fairly low, with no more than one error per chain seen for chains in $(GLG)_{10}$ region of the MALDI-ToF spectrum. We believe the error arises, in this case, from the relatively low stability of the GLG segmer from which it is

prepared. Again, it should be noted that the assignment of these NMR spectra has been extensively investigated and is described in detail elsewhere.[55] The ^{1}H NMR spectra of the random copolymers, **PDLGA-50, PLLGA-50** and **R-SAP** were also acquired and the actual L:G unit ratio (Table 1) was calculated by integration of the glycolic methylene and lactic methine resonances.

The ^{13}C NMR spectra of the carbonyl region of the sequenced and random copolymers are particularly interesting to the current discussion as they highlight the dramatic difference in numbers and types of sequence environments (Fig. 9). The random copolymers show a large variety of carbonyl environments, while the sequenced copolymers exhibit only a few. The introduction of stereosequences also increases the complexity of this region, even for the periodic copolymer **poly L$_{rac}$G**.
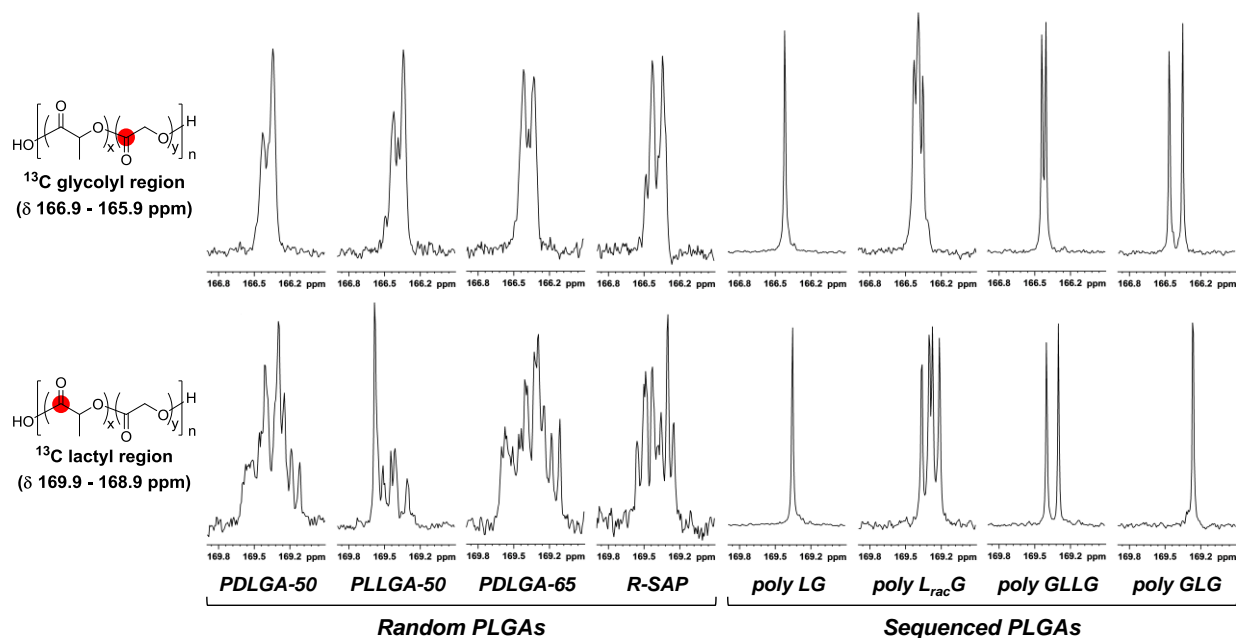
Figure 9. ^{13}C NMR (500 MHz) spectra of glycolyl (top) and lactyl (bottom) carbonyl regions of sequenced and random PLGAs.

As **R-SAP** had been prepared from the dimers LL, GG, LG, and GL, we expect that the average L and G block lengths are most probably shorter than those in commercial **PDLGA-50**

and **PLLGA-50** produced from the ROP of lactide and glycolide. We were not, surprisingly, able to confirm this hypothesis spectroscopically because we found that the ^{13}C NMR resonances of the periodic copolymers produced for this study and others overlapped in a way that precludes a simple interpretation of this region for random mixtures (Fig. A23 for an example). We note that the prior assignments of resonances that have been proposed based on ROP copolymer syntheses [7, 9, 92-93] cannot be applied in the case of **R-SAP** because those analyses were based on the predicted absence of resonances for certain sequences that are not forbidden in the R-SAP case. That being said, it is clear from the observed differences in the glycolyl carbonyl region of **PLLGA-50** and **R-SAP**, that there are significant microstructural differences. These differences should, based on our sequence hypothesis, be reflected in the properties.

2.4.3 *In vitro* swelling of sequenced and random PLGAs

PLGA performance has been examined in a variety of constructs including microparticles,[29, 90] films,[94-95] and solid matrices in a variety of geometries.[84, 96] For the current studies, which focus on bulk properties rather than drug release, we have chosen to fabricate the polymers into macroscale cylindrical matrices to increase their relevance to larger implantable devices (e.g., screws and plates). To determine dependence of the uptake of water on sequence, swelling studies were performed on cylindrical pellets (3 x 3 mm), two per polymer, prepared using heated compression molding. For random PLGA, these matrices would be expected to degrade by a bulk hydrolysis mechanism since they are thinner in all dimensions than the critical thickness of 7.4 cm that has been identified as the transition point between bulk and surface erosion for poly(α-hydroxy ester)s.[84] Data for cylindrical constructs similar to those used in this

study, prepared using random PLGAs, were reported by von Bukersroda *et al.,* in their efforts to develop improved osteosynthetic devices.[97-99]

The samples were exposed to buffer at physiological temperature and pH and their hydrated mass was recorded over an eight-week time period. The size and shape of the hydrated pellets at each time point were documented photographically (Fig. 10). The swelling % of the duplicate samples was calculated according to Eq. 1 where m_0 is the initial sample mass and m_t is the mass of the hydrated pellet at time t (Fig. 11).

Equation 1.

$$swelling \% = \frac{m_t - m_0}{m_0} \times 100\% \tag{1}$$
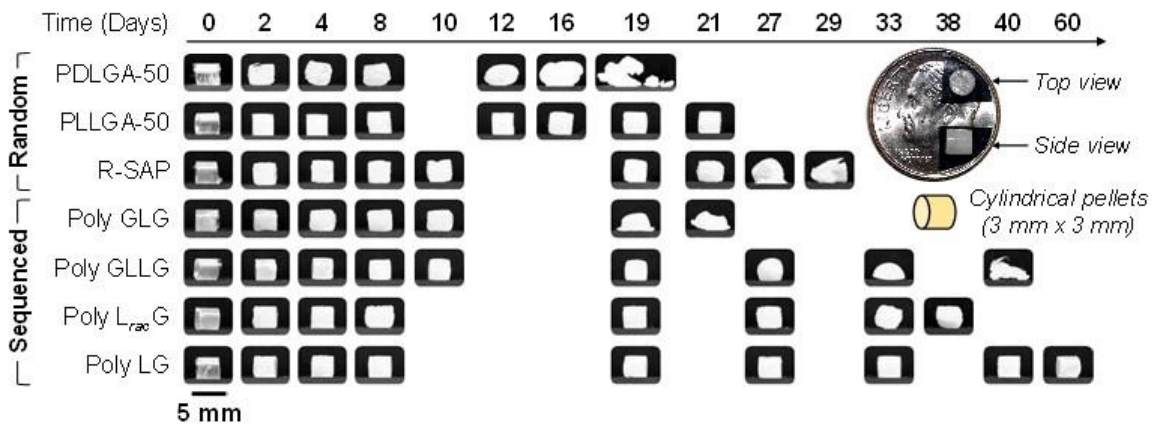
Figure 10. Side-view appearance of water-swollen cylindrical pellets as a function of hydrolysis time.
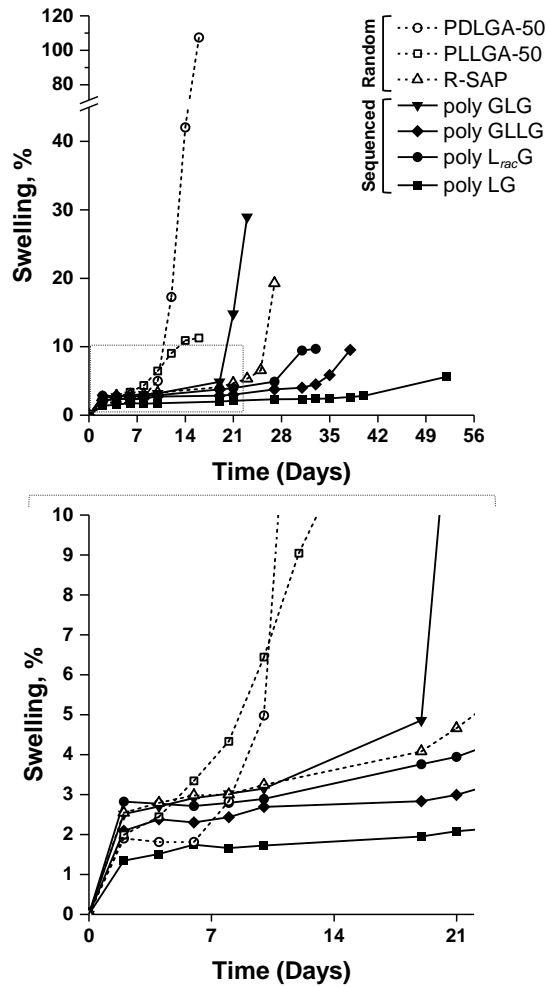
Figure 11. Swelling profiles of sequenced and random PLGAs over 8 weeks (top); enlargement of the first 3-week time period (bottom). Open symbols represent random copolymer controls and closed symbols represent sequenced copolymers.

In examining the swelling data, it can be seen that upon immersion there was an initial increase in swelling of ~2% for all polymers during the first two days. The pellet size and morphology remained constant during this time period but gradually changed over the first week depending on the sequence of the PLGA. The onset of swelling for both random PLGAs, **PDLGA-50** and **PLLGA-50**, occurred during the first week. Interestingly, the morphology of **PDLGA-50** changed during this time period and **PLLGA-50** remained unchanged.

31

During the second week, swelling increased from 5% to 42% for **PDLGA-50**; significant swelling and altered shape morphology was also observed. The stereopure random analogue **PLLGA-50** slowly increased in water content from 6% to 11% while retaining its structural integrity. The swelling of sequenced PLGAs remained unchanged during this time period with only **R-SAP**, the random PLGA analogue prepared by SAP, exhibiting slight changes in morphology. After three weeks of immersion, the influence of sequence and stereochemistry was more pronounced. The water content of **PDLGA-50** reached its maximum of 107% and significant sample fracturing was observed. The loss of integrity precluded any further measurements. **PLLGA-50** exhibited nominal visual swelling and had a maximum of 11% prior to sample failure. No significant changes in swelling were observed for **poly LG**, **poly L$_{rac}$G** and **poly GLLG**, 2%, 4% and 3%, respectively. Noticeable changes in morphology were observed in **poly GLG** (15%) and **R-SAP** (5%), which were followed by a continual increase in swelling resulting in rupture after 23 days for **poly GLG** (30%) and 27 days for **R-SAP** (20%). In the time period of week four to five, the morphology of **poly GLLG** and **poly L$_{rac}$G** begins to change and is accompanied by an increase in swelling, 5-10% and 4-6%, respectively, with each sample failing at a maximum swelling of 10%. Throughout this time period, **poly LG** exhibited minimal changes in swelling and morphology; at 52 days swelling was only 6%.

2.4.4 *In vitro* erosion of sequenced and random PLGAs

To understand the erosion behavior of sequenced and random PLGAs, mass loss experiments were conducted in parallel to the swelling studies. Cylindrical pellets with a height of 1.5 mm and width of 3 mm, prepared by heated compression molding were used. These studies were performed under physiological pH and temperature and mass loss data were obtained on the

32

lyophilized pellets at selected time points over 19 weeks. The size and shape of the lyophilized

pellets were recorded photographically and are reported in (Fig. 12) and erosion profiles of

sequenced and random PLGAs are shown in (Fig. 13). The erosion is reported as % mass loss,

which was calculated using Eq. 2, where m_0 is the initial sample mass and m_t is the mass of the

lyophilized pellet at time t.

Equation 2.

$$\% \text{ mass loss} = \frac{m_0 - m_t}{m_0} \text{ x } 100\% \tag{2}$$
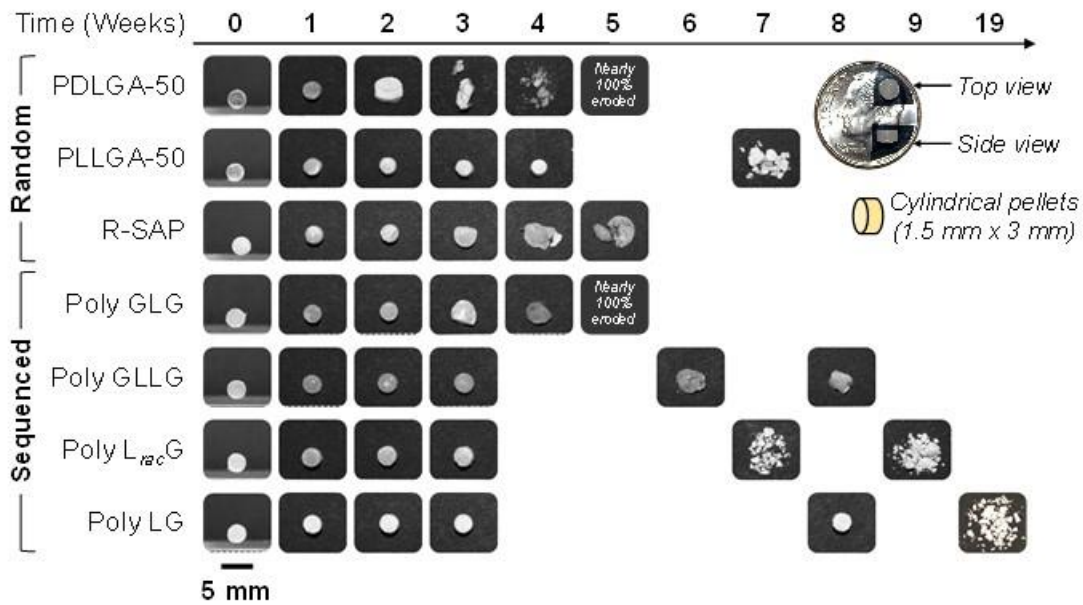
Figure 12. Top-view appearance of eroded cylindrical pellets, after lyophilization, as a function of hydrolysis time.
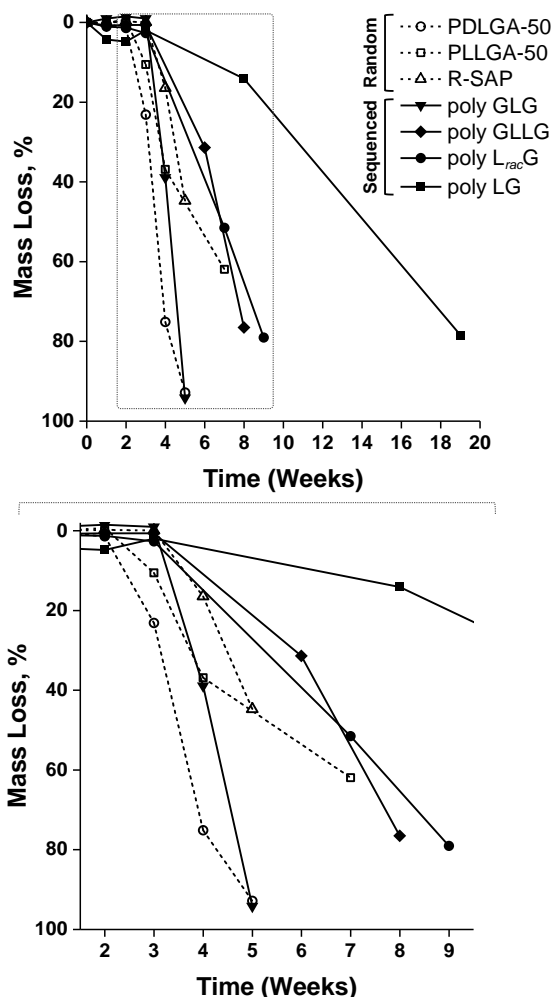
Figure 13. Erosion profiles of sequenced and random PLGAs over 19 weeks (top); enlargement of weeks 2-9 (bottom). Open symbols represent random copolymer controls and closed symbols represent sequenced copolymers.

The mass loss profiles for periodic PLGAs were found to be dramatically different than random PLGAs for a variety of sequences. All samples began with an initial period of stability. After this initial period, the degradation proceeded at a rate that depended on L:G ratio, structural sequence and stereochemistry. For the random PLGAs, **PDLGA-50** and **PLLGA-50**, the onset of erosion occurred at two weeks. The 1:1 LG ratio polymer, **PDLGA-50**, then lost mass rapidly over the next three weeks before losing structural integrity. The random stereopure analogue, **PLLGA-50**, retained its structural integrity after the onset of erosion for an additional two weeks

34

but lost its structural integrity at week seven, at a 62% mass loss. Interestingly, for **PLLGA-50**, the erosion rate plateaued between weeks four and seven.

The sequenced PLGAs, with the exception of **poly LG**, and the random analogue prepared by SAP exhibited an onset of erosion during week three. Interestingly, both **poly GLG** and **R-SAP** lost their structural integrity at week three and had rapid stages of mass loss throughout weeks four and five. During these time periods, **poly GLG** lost 39% of its mass at week four and an additional 55% by week five. **R-SAP** at the same time points lost 16% and an additional 28%. Mass loss for **poly GLLG** and **poly L$_{rac}$G** was more gradual. Despite having the same onset of erosion, **poly GLLG** and **poly L$_{rac}$G** retained their structural integrity over weeks four and five but failed at weeks six and seven, respectively. During the time period of weeks three to six for **poly GLLG**, only 31% eroded and an additional 45% eroded after eight weeks. For **poly L$_{rac}$G**, 49% of the sample was lost between weeks three and seven and an additional 27% after nine weeks. The erosion profile of **poly LG** was more linear and structural integrity was maintained over a longer time period; no pronounced onset of erosion was evident over the time period studied. The structural integrity of **poly LG** was retained for eight weeks with only a 14% mass loss. At the end of the study, **poly LG** had lost 78% of the sample's initial mass.

2.4.5 Correlated trends in swelling and erosion
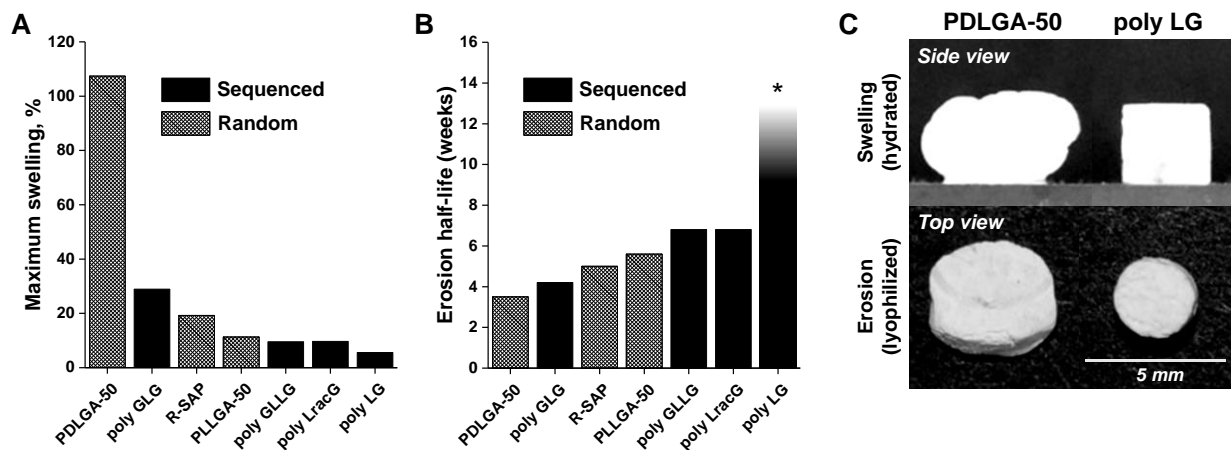
Figure 14. Maximum swelling % (A) and erosion half-life (B) of sequenced and random PLGAs. *Erosion half-life is approximately 10-14 weeks. Enlarged views (C) of cylindrical constructs of PDLGA-50 and poly LG in week 2 of degradation highlighting the dramatic sequence-based differences in swelling and erosion behavior.

When the swelling and erosion behaviors of copolymers are compared, there is a clear inverse relationship. Those polymers that exhibited a higher degree of swelling were also observed to erode more quickly (Fig. 14). Another important observation that can be made by examining these trends is that both the random **PDLGA-50** and **poly LG** are outliers amongst their analogues. **PDLGA-50** swelled by a factor of 3x more than any other sample. On the other end of the spectrum is the alternating copolymer **poly LG**, which erodes 2x more slowly than any other PLGA examined, including other sequences. The dependence of both processes on stereochemistry can also be seen, with the racemic versions exhibiting more swelling and shorter erosion half-lives than their stereopure analogues. Finally, it is interesting to note that **poly GLG**, which would be expected based only on the ratio of L:G units to degrade the quickest, has a half-life that is slightly longer than the random **PDLGA-50**.

36

Although the large and repeatable differences in behavior between sequences suggest that the sequence is retained during the degradation process, esters are known to undergo transesterification in the solid state under some conditions. Indeed the synthesis of random PLGA has been reported by the thermolysis of PLA with PGA.[7] To probe the possibility of transesterification during hydrolysis in these studies, we collected ^{1}H NMR spectra of the simple alternating stereopure **poly LG** as a function of degradation (Fig. A24). As the NMR spectra for these polymers is exquisitely sensitive to changes in sequence and stereochemistry, any changes would be evident.[55] Over 35 days, however, despite evidence of some degradation to form oligomers, there was no observed transesterification nor epimerization of the **poly LG** structure (Fig. A25).

2.4.6   Changes in molecular weight and distribution
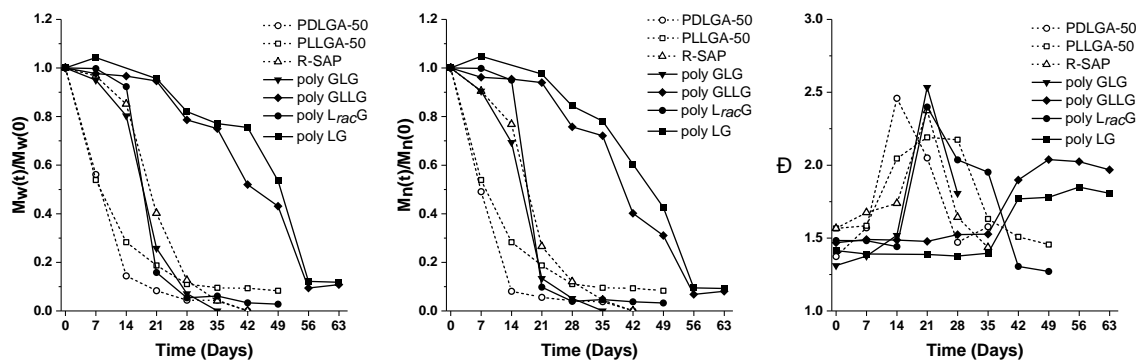
Figure 15. Weight average molecular weight (left); number average molecular weight (center); dispersity (right) of sequenced and random PLGAs as a function of time. Open symbols represent random copolymer controls and closed symbols represent sequenced copolymers.

The molecular weight profiles for all polymers in this study, normalized relative to the original M_w and M_n, along with the dispersity data are plotted in Fig. 15. The molecular weight loss profiles for random PLGAs, **PDLGA-50** and **PLLGA-50**, decreased rapidly with time, which is

typical of 50:50 ratio random PLGAs.[100] In contrast, **R-SAP**, **poly GLG** and **poly L$_{rac}$G** did not exhibit significant molecular weight loss until after 7 d. **Poly LG** and **poly GLLG** retain their initial molecular weights for 3 weeks.

Polymer chain dispersity (*Đ*) was also found to depend on monomer order and stereochemistry. **PDLGA-50**, **R-SAP**, **poly L$_{rac}$G** and **poly GLG** exhibit a sharp increase in dispersity by week 3. During this time period **PLLGA-50** also increases but at a slower rate. The dispersities of **poly LG** and **poly GLLG** remain constant over 35 d, and increase gradually over the following 4 weeks.

2.4.7   Surface water contact angle

To determine if there were significant differences in the inherent hydrophilicity of the sequenced and random PLGAs, the surface contact angles of selected samples, **PDLGA-50**, **PDLGA-65** and **poly LG**, were measured after exposure to hydrolyzing conditions. Thick films (20-30 µm) were submerged in PBS buffer at 23 °C and the hydrated contact angle was monitored over an 8 day time period. The samples were subsequently dried by lyophilization and the dry film contact angles were recorded (Fig. 16).
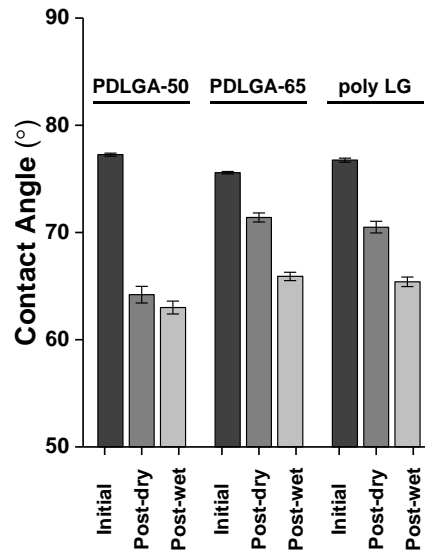
Figure 16. Average water contact angles from unexposed films (initial) and films exposed to physiological conditions over 8 days measured in their hydrated (post-wet) and lyophilized (post-dry) states. Error bars represent the standard error of the mean.

The initial water contact angle for all samples was relatively similar, $76.5 \pm 0.5°$ and agrees with previously reported measurements.[101-102] There were no significant changes in the hydrated film contact angles over an 8 day time period, with the average contact angles for **PDLGA-50**, **PDLGA-65**, and **poly LG** being 63°, 66° and 65°, respectively (Fig. A26). The lyophilized film water contact angles, however, do show initial differences after 1 day of exposure to physiological pH and temperature (Fig. A27). The initial contact angle of **PDLGA-50** decreases from 77° to 63°, which then remains unchanged at around 62-63° for the remaining 8 days of exposure. In contrast, the lyophilized contact angles for **PDLGA-65** and **poly LG** do not change significantly after 1 day of exposure. The change in the lyophilized contact angle for **PDLGA-50** and **poly LG** over 8 days was minimal with the overall averages being 72° and 71°, respectively. The differences observed between sequences in the lyophilized angles appears to correlate with the amount of film degradation—the slower degrading samples maintain their surface hydrophobicity longer.

39

2.5   DISCUSSION

The ultimate goal of this work and that of many researchers in bioengineering is to be able to control the degradation of implantable/injectable polymers. While the architecture (i.e., size, shape, porosity) of particular matrices contributes significantly to their behavior,[103-104] the chemical composition of the material from which they are made is ultimately responsible for determining the degradation mechanism, profile, release rate of encapsulated drugs, and mechanical properties. The most widely adopted strategy for changing polymer composition, and thereby tuning properties, is to add new or modify the current monomers. While this approach works well for materials that will not be employed in biomedical applications, the use of new monomers in a biomaterial presents significant challenges as all of the degradation products must be non-toxic and clearable.

Our approach to composition control, which avoids the introduction of new chemical entities, is to adopt nature's own solution to this problem: use the same monomers but change the order. Despite the obvious nature of this idea, the synthetic challenges in making sequenced copolymers have long inhibited the exploration of this strategy. There are only isolated, nearly anecdotal, studies relating bulk properties to sequence outside of amino and nucleic acid polymers.[34-35, 45-46] We have focused our research on PLGA due to the ubiquity of its use and because the poor match of PLGA properties with those required for particular applications has been cited as the justification for the synthesis of a multitude of polymers based on alternate monomers.[104-106] It was our hypothesis, one now supported by the results herein, that sequence control may offer an alternate approach to adjusting PLGA properties to those required for particular applications.

Swelling and erosion are both intrinsically involved in degradation.[84] While our data conclusively demonstrate that both behaviors depend on sequence, the reason for the correlation is not immediately apparent. One possible explanation, especially given the dramatic differences in swelling, is that the properties correspond to sequence-based variations in hydrophilicity. Although not a true measure of intrinsic hydrophilicity, the fact that the surface contact angle of **PDLGA-50**, which necessarily possesses runs of L and G, is nearly the same the simple alternating **poly LG**, suggests that sequence-based differences in the interaction with water are minimal. More convincingly, we find that the water uptake in the first 3 days of the swelling experiment was nearly the same for all samples. These results suggest that the differences seen are not a function of the initial interaction with water but rather come about as a result of chain degradation processes.

The molecular weight loss profile matches the trends that we reported previously [60-61] and tracks well with the swelling and erosion behaviors. The ROP-random copolymers degrade more quickly than either the **R-SAP** or sequenced copolymers. The dispersity trends are also interesting as the dispersity increase correlates in time with the onset of significant swelling in all of the polymers.

Stereosequence also plays a key role in degradation. Both stereopure **PLLGA-50** and **poly LG** retain their structural integrity over a slightly longer time period than their racemic analogues, **PDLGA-50** and **poly L$_{rac}$G**, respectively. While it is known that crystallinity plays a role in the differences between the random copolymers,[107-108] the sequenced copolymers do not appear to crystallize to a significant extent, even during degradation.[60] A fuller understanding of this phenomenon will require further study outside the scope of the current investigation.

Overall, we hypothesize that the differences in hydrolysis profile, both in swelling and erosion, are due primarily to the variation in kinetic rates of cleavage of the L-L, L-G, G-L and G-G linkages (Fig. 17). This rate difference has long been established in the random copolymer literature and has been used to explain, for example, the increase in L to G ratio during the hydrolysis period.[29, 107, 109-110] The observed molecular weight behavior is consistent as **PDLGA-50**, which has the full spectrum of linkages, exhibited a faster drop in molecular weight as a function of hydrolysis time than did the isomeric **poly LG**, which comprises only L-G and G-L linkages. The dispersity behavior of these copolymers also correlates as rapid cleavage of G-G linkages would be expected to result in earlier increases in polymer chain dispersity.
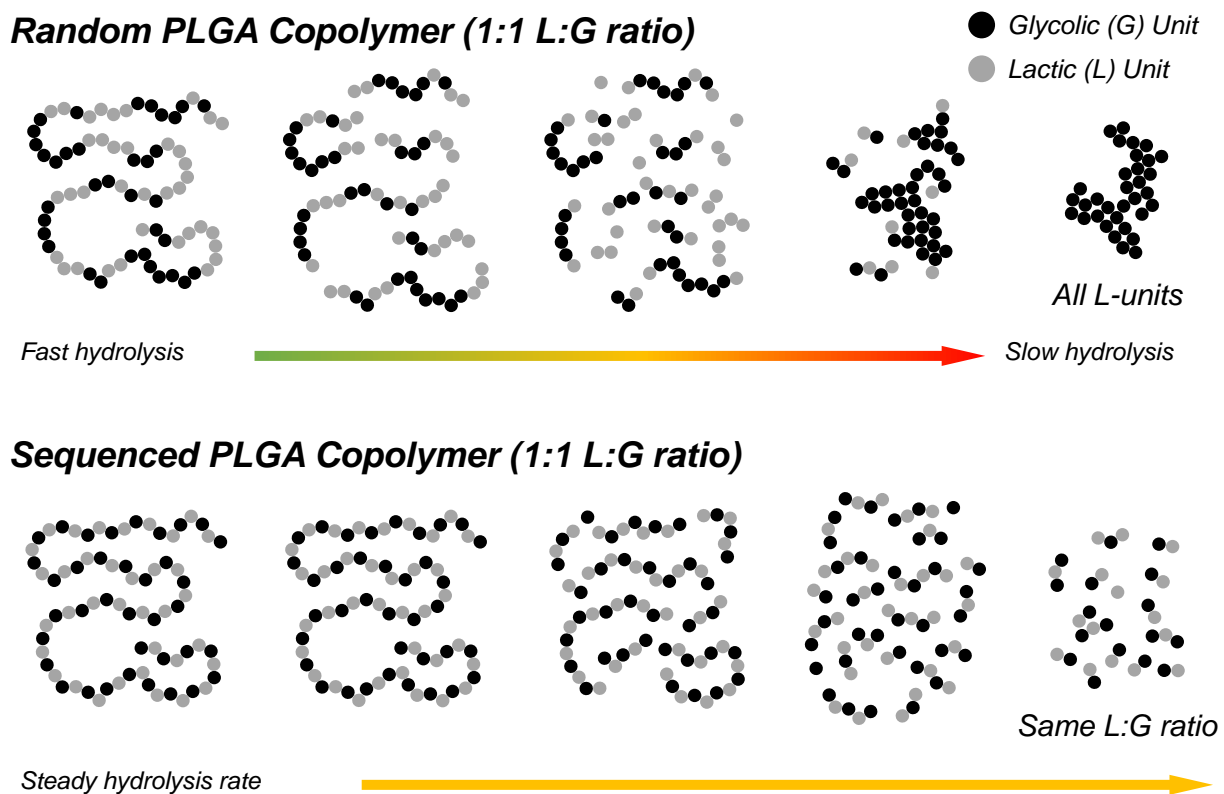
Figure 17. Differences in the rates of hydrolysis for random and sequenced PLGA copolymers with the same L:G ratio.

In the current study, the variation in cleavage rates would be expected to produce significant differences in species population within the pellets, which we propose leads to the observed differences in degradation profile. The rate of chain cleavage and concomitant generation of acidic oligomers and monomers would be expected to correlate with the frequency of G-G linkages within the chain—a larger percentage of G-G linkages should lead to higher local concentrations of hydrolytic products within the construct. Although the higher local concentrations of acidic species would be expected to autocatalytically enhance interior degradation and polymer erosion, [111-113] this effect alone does not explain the swelling behavior. In addition, we propose that osmotic pressure may play an important role in this case because the degradation products are likely produced more rapidly than they are released.[114-116] Under these circumstances a concentration gradient could drive the osmotic uptake of water to give swelling that correlates with the number of entrapped products.[84] While swelling should eventually facilitate clearance, thereby relieving osmotic pressure, the constructs appear to lose both structural integrity and morphological stability before such an equilibrium is reached. This hypothesis is consistent with the observation that pellets with identical compositions but higher numbers of G-G linkages degrade much faster and exhibit dramatic morphological changes.

2.6   CONCLUSIONS

We have demonstrated that swelling and erosion, which are both key properties related to potential applications of PLGAs, depend dramatically on the sequence of the L and G monomers. Specifically, as the number of G-G linkages is decreased, the degree of swelling is diminished and the erosion is slowed. This dependence on sequence allows for the tuning of the hydrolytic profile without additives or other comonomers. Future work will focus on both improving our understanding of the dependence of hydrolysis on sequence and on studies that test the *in vivo* performance of these materials.

3.0 MONOMER SEQUENCE IN PLGA MICROPARTICLES: EFFECTS ON ACIDIC MICROCLIMATES AND *IN VIVO* INFLAMMATORY RESPONSE

3.1 OVERVIEW

This work presented in this chapter describes the *in vitro* acidic microclimate pH distribution, external morphological changes and *in vivo* foreign body response for sequenced and random poly(lactic-*co*-glycolic acid) microparticles. This chapter has been submitted for publication in a peer-reviewed journal and is summarized in Fig. 18: M.A. Washington, S.C. Balmert, M.V. Fedorchak, S.R. Little, S.C. Watkins, T.Y. Meyer. "Monomer sequence in PLGA microparticles: Effects on acidic microclimates and *in vivo* inflammatory response." **2017**.
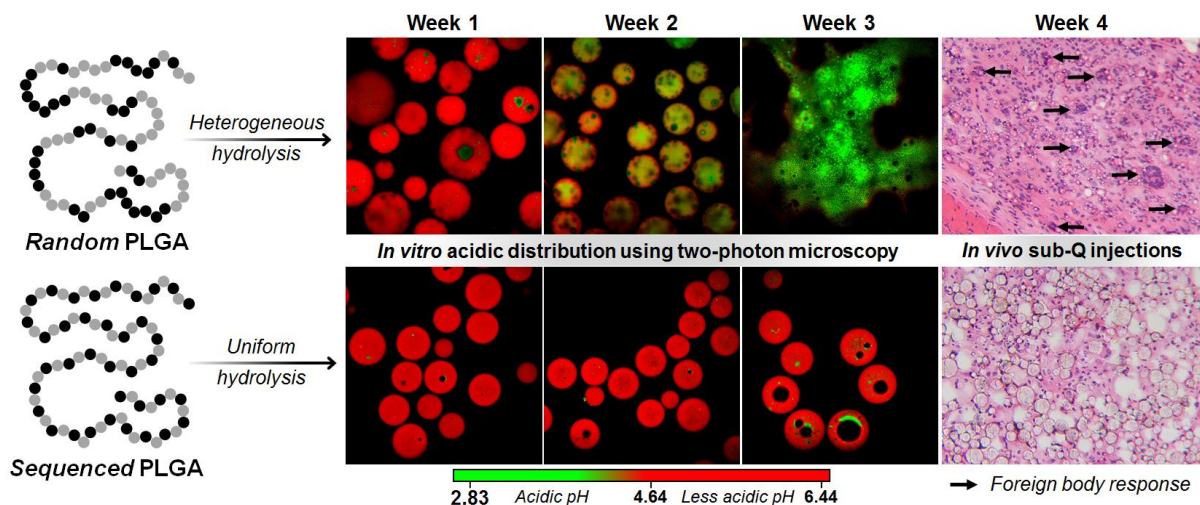
Figure 18. Graphical abstract for Chapter 3 – Monomer sequence in PLGA microparticles: Effects on acidic microclimates and *in vivo* inflammatory response.

Controlling the backbone architecture of poly(lactic-*co*-glycolic acid)s (PLGAs) is demonstrated to have a strong influence on the production and release of acidic degradation by-products in microparticle matrices. Previous efforts for controlling the internal and external accumulation of acidity for PLGA microparticles have focused on the addition of excipients including neutralization and anti-inflammatory agents. In this report, we utilize a sequence-control strategy to tailor the microstructure of PLGA. The internal acidic microclimate distributions within sequence-defined and random PLGA microparticles were monitored *in vitro* using a non-invasive ratiometric two-photon microscopy (TPM) methodology. Sequence-defined PLGAs were found to have minimal changes in pH distribution and lower amounts of percolating acidic by-products. A parallel scanning electron microscopy study further linked external morphological events to internal degradation-induced structural changes. The properties of the sequenced and random copolymers characterized *in vitro* translated to differences in *in vivo* behavior. The sequence alternating copolymer, poly LG, had lower granulomatous foreign-body reactions compared to random racemic PLGA with a 50:50 ratio of lactic to glycolic acid.

3.2 INTRODUCTION

The favorable hydrolytic degradation profiles and biocompatibility of poly(lactic-co-glycolic acid)s (PLGAs) have resulted in extensive research into their application as components in drug delivery systems (DDSs).[69, 117] The performance of DDSs made from PLGAs have been linked in these studies to several characteristics including ester hydrolysis rates, diffusion, swelling, erosion, and local pH drop.[70, 114-115, 118] Although these processes can be tuned to a certain degree by varying the L:G-ratio and molecular weight of the random copolymer, the lack of fine control

46

over the properties may contribute to the surprisingly low commercial use of PLGAs.[95] Despite thousands of literature reports on PLGA DDSs, fewer than 20 PLGA-based products have garnered FDA and EMA approval over the past three decades.[68] This lack of translation suggests that there is a clear unmet need for alternative methods that optimize the performance of PLGA matrices.

We have recently reported that precise control over monomer sequence can be utilized to tune *in vitro* PLGA degradation behavior for various PLGA matrices. In Li *et al.*, for example, we describe sequence-dependent degradation behavior of microparticles, demonstrating that thermal properties, molecular weight loss, lactic acid release, and rhodamine B release rates were dramatically different for random PLGAs vs. sequenced PLGAs prepared with the same L:G-ratio and molecular weights.[60-61] Specifically, we found that *in vitro* degradation and release rates were slower and more gradual for microparticles prepared with periodic sequences (e.g., $(LG)_n$, $(LLG)_n$) relative to random analogues. More recently, in Washington *et al.,* we demonstrated that compression-molded implants fabricated with sequenced PLGAs exhibited minimal *in vitro* changes in swelling, delayed onsets of erosion, and more gradual changes in molecular weight and dispersity compared to random PLGAs with the same overall compositions.[62] Finally, in both of these studies, we were able to show that by varying the structural and/or stereosequence that the degradation-related properties could be tuned. We note that there are a number of recent reports concerning both the development of new general synthetic strategies for creating sequenced copolymers as well as studies correlating sequence with properties.[33-36, 45, 54, 119-121]

Significant precedent for our strategy of controlling sequence can also be found in studies on random poly(α-hydroxy acid)s in which properties are mapped to changes in the statistical distributions of monomers. For instance, Abe and Tabata have demonstrated that the thermal

47

properties and crystalline structures for a class of periodic aliphatic polyesters may be varied over a wide range of temperatures based on stereosequence manipulations.[122-123] Sarasua and coworkers have further linked statistical variations in chain microstructure to various hydrolytic degradation rates in poly(lactide-*co*-ε-caprolactone) matrices.[74, 76-77, 79, 124-125] Finally, Albertsson and coworkers, determined that the distribution of hydrolytically-accessible 1,5-dioxepan-2-one linkages had a profound effect on the release rates of acidic degradation products in triblock, multiblock, and random crosslinked caprolactone/1,5-dioxepan-2-one copolymers.[126]

This study adds to our previous work on sequenced PLGAs, specifically on the characterization of how sequence affects the accumulation, distribution, and release of acidic by-products during PLGA degradation. These by-products represent a significant challenge to using poly(α-hydroxy acid)s in applications because acid can degrade macromolecular payloads that have been encapsulated in PLGA matrices and can lead to local inflammation when implanted *in vivo*.[113] Previous attempts to address this issue have typically involved the addition of neutralizing agents and other excipients to control the internal acidic microclimate pH (μpH)[127] and/or the incorporation of anti-inflammatory agents such as dextramethasone and tripolyphosphate to minimize the impact of acidity on tissues near the injection site.[128-129] Although these methods have proven effective in specific studies, the addition of external agents necessarily introduces new factors that can affect the drug release kinetics, immune response, and degradation profile of the PLGA matrix. Based on our reported observation that lactic acid release rates were greatly suppressed in sequenced copolymers relative to random PLGAs,[60] we hypothesize that sequence can be used as a tool to control the acidic microclimate within a polymer microparticle and acid-induced inflammation of DDSs. This approach is particularly

attractive since the potential complications that could arise from the incorporation of additives can be avoided.

To understand how sequence affects acidity within a PLGA microparticle, we characterized the *in vitro* spatial distribution of low pH regions in PLGA as a function of sequence and stereosequence using a non-invasive ratiometric two-photon microscopy (TPM) method. Non-invasive efforts to visualize the pH within random PLGA microparticles have been previously reported and include electron paramagnetic resonance spectroscopy (EPR)[111, 116, 130-131] and confocal laser scanning microscopy (CLSM).[113, 132-137] Although EPR methods demonstrated that the internal pH of PLGA particles can be as low as pH = 2, CLSM studies, conducted on particles loaded with pH-sensitive dyes, make it possible to spatially map the pH within small particles. Using CLSM methods, Langer and Schwendeman independently reported an internal pH range within microparticles composed of random PLGAs of 1.5 − 3.5 after 15 d and 3.2 − 3.4 after 28 d of *in vitro* hydrolytic degradation, respectively. Moreover, Schwendeman and coworkers extensively studied how L:G-ratio, molecular weight, microparticle size, and emulsion method (W/O/W and O/O) influenced μpH kinetics and determined that L:G-ratio and molecular weight contributed to differences in μpH distribution and kinetics. Random PLGA with an L:G-ratio of 50:50 and low molecular weight were also found to exhibit earlier onsets of acid accumulation, lower acidic distribution after 28 d, and notable changes in morphology. Degradation-induced morphological changes were also observed by Langer and coworkers using scanning electron microscopy (SEM); increasing surface pores and slight plasticization for 50:50 L:G-ratio PLGA microparticles were observed.[113] We note that we have also previously utilized CLSM to map the drug distribution a dextran-labeled Texas Red dye.[138] Other strategies for measuring the acidity of PLGA, aside from the aforementioned non-invasive methods, have been

reported and include indirect pH measurements of the incubation media potentiometric measurements recorded using inserted pH probes.[116, 139-141]

In the current study, we focused upon the difference in pH distribution within microparticles as a function of monomer sequence using two-photon microscopy (TPM). We and others have demonstrated the TPM offers distinct advantages over confocal microscopy for monitoring ratiometric probes within cells and other structures including minimization of data-destroying photobleaching and the ability to image at greater depths.[142-145] Finally, as we are also interested in understanding whether sequence-based differences in pH distribution within microparticles translate into differences in *in vivo* performance we also report herein a comparison of the inflammatory response to implanted sequenced and random copolymer microparticles.

3.3   MATERIALS AND METHODS

3.3.1   Materials

Poly(D,L-lactide-*co*-glycolide) with a copolymer ratio of 50:50 and 65:35 were purchased from Durect Corporation (Birmingham, AL). Poly(L-lactide-*co*-glycolide) with a 50:50 L:G-ratio was purchased from Changchun SinoBiomaterials Co. Ltd. (Changchun, China). The pH sensitive fluorescent probe, LysoSensor[TM] Yellow/Blue DND-160 (PDMPO) (MW 366.42), was purchased from Life Technologies (Eugene, OR, USA) as a 1 mM solution in dimethylsulfoxide (DMSO). Polyvinyl alcohol (PVA, MW 25 kDa, 98% hydrolyzed) was from Polysciences

(Warrington, PA). Sequence PLGA copolymers were prepared using previously reported methods.[55]

3.3.2 Characterization

Molecular weights and dispersities were acquired on a Waters GPC system (tetrahydrofuran (THF), 0.5 mL/min) with Jordi 500 Å, 1000 Å, and 10000 Å divinylbenzene (DVB) columns and refractive index detector (Waters), which was calibrated relative to polystyrene standards. Thermal properties of all polymers prior to and after single-emulsion (O/W) microparticle preparation were obtained using TA Instruments Q200 DSC. Data were collected with a heating and cooling rate of 10 °C/min. The glass transition temperatures (T_g) for polymers as synthesized were collected during the second heating cycle while the O/W microparticles were collected in the first heating cycle. The glass transition temperatures are reported as the half-step Cp extrapolated. The ^{1}H and ^{13}C NMR spectra were obtained in CDCl$_3$ using a 500 MHz Bruker Avance III spectrometer at 293 K and calibrated to the residual solvent peak at δ 7.26 ppm (^{1}H) and δ 77.00 ppm (^{13}C).

3.3.3 Preparation of PLGA microparticles

PLGA microparticles containing the pH sensitive dye, LysoSensor™ Yellow/Blue DND-160 (PDMPO) were synthesized using a single-emulsion process.[69, 146] Briefly, under low light conditions, PLGA (300 mg) was dissolved in dichloromethane (4 mL) followed by the addition of 200 μL of 1.0 mM LysoSensor™ in DMSO and the mixture was vortexed 1 min. The solution was added dropwise through a 250 μm sieve (U.S. Standard sieve series; ASTM E-11

specifications; Dual MFG Co.; Chicago, IL) into a 1% w/v (aq) PVA solution stirred at 600 RPM

for 3 h at 23 °C. The resulting microspheres were centrifuged at 4 °C, 1,000 RPM, 8 min and

washed with deionized (DI) water (4x).The microspheres were briefly re-suspended in deionized

water (5 mL), flash frozen with liquid nitrogen and lyophilized for 3 d (VirTis Benchtop K

freeze dryer, Gardiner, NY; operating at 100 mTorr). For the control, unloaded microparticles,

the procedure described above was used while omitting the addition of the pH sensitive dye.

3.3.4   Fluorescent intensity ratio vs. pH standard curve

Buffers of pH 2.8 to 6.4 were prepared using 0.1 M citric acid and 0.2 M Na_2HPO_4 solutions. An

aliquot of LysoSensor[TM] Yellow/Blue DND-160 was added to the buffer solutions yielding a

concentration of 2.0 µM. A Varian Cary Eclipse Fluorescence Spectrophotometer coupled to a

personal computer with software (cary eclipse software) provided by Varian was utilized to

monitor the emission spectra of the pH probe as a function of pH. The standard dye solutions

were excited at the isosbestic point $\lambda = 360$ nm and the fluorescence spectra were recorded from

$375 - 700$ nm. The standard curve was established by plotting the ratio of the fluorescent

intensities at two emission wavelengths, 450 nm and 530 nm, versus the pH of that solution.

3.3.5   Microclimate pH mapping inside microparticles

PLGA microparticles ($40 - 41$ mg) were incubated in 2.00 mL of phosphate buffer saline (10.0

mM, pH = 7.4) at 37 °C under continuous rotation at 8 rpm (Labquake Tube Rotator, Thermo

Scientific). At specific time points, a 100 µL aliquot was deposited on a glass microscope slide

and imaged using a two-photon microscope system. Fresh buffer was added to maintain the initial sample volume of 2.00 mL.

3.3.6 Two-photon microscopy image acquisition

Two-photon images of sequenced and random PLGAs were captured using an Olympus FV1000MPE multiphoton laser scanning microscope (Olympus Corporation; Tokyo, Japan). The TPM system was configured with a mode-locked Ti:Sapphire laser (Chameleon Vision; Coherent; Santa Clara, CA) capable of emitting excitation wavelengths from 680-1080 nm (excitation wavelength set to 740 nm, 5.4 % intensity) and a Olympus upright optical microscope with a 25x, XL Plan N 1.05 N.A. water immersion objective lens (Olympus). The multiphoton emission of the LysoSensor^{TM} DND-160 pH probe at near neutral and acidic pH was captured using 420 – 460 nm (detector 1; red channel; near neutral pH) and 500 – 550 nm (detector 2; green channel; acidic pH) emission filters. FLUOVIEW Ver. 2.1c software (Olympus) was utilized to acquire multiple XY scans (508 x 508 µm; 0.503 µm/pixel resolution; 12.5 µsec/pixel) in 1.5 µm increments in the Z-direction. Each sample was imaged in 4 additional regions. The whole assembly of the TPM microscope was placed on a vibration isolation table (Kinetics Systems Inc., Boston, MA).

3.3.7 Image processing for pH distribution

TPM images were processed using Nikon-Elements AR 4.50 software package. A threshold was applied to each channel with a 3x smoothing algorithm. The pH vs. I_{450nm}/I_{530nm} titration curve was applied to the images and the corresponding pixel intensity ratio frequency vs. pH

histograms were constructed. The histograms were processed using OriginPro 2016 where a lowess smoothing algorithm was applied to remove the high-frequency components.

3.3.8   Scanning electron microscopy characterization of microparticle morphology

Five samples of microparticles for each PLGA (10 mg) were incubated in 1.00 mL of phosphate buffer saline (10.0 mM, pH = 7.4; Gibco by Life Technologies) at 37 °C under continuous rotation at 8 rpm (Labquake Tube Rotator, Thermo Scientific). This study was run in parallel with the two-photon study. At specific time points, week(s) 1, 2, 3, 4 and 5, the microparticles were flash frozen with liquid nitrogen and lyophilized for 3 d prior to imaging. The structural integrity and surface morphology of sequenced and random PLGAs during degradation were characterized using the JSM-6510LV SEM system. The lyophilized microparticles were sputtered with palladium under an argon atmosphere for 2 cycles of 2.5 min, 30 mA, with a Cressington Sputter Coater 108auto (Ladd Research, Williston, VT). The images were captured under high vacuum at an acceleration voltage of 2.5 – 5 kV with the stage titled 5°. Three images from separate regions of the sample were captured under various magnifications of x150, x350, and x800.

3.3.9   *In vivo* studies and histology

Female C57BL/6J wild-type mice were purchased from The Jackson Laboratory (Bar Harbor, ME) and used at 8 – 12 weeks of age. All mice were maintained under specific pathogen-free conditions at the University of Pittsburgh, and experiments were conducted with the approval of the Institutional Animal Care and Use Committee and in accordance with NIH guidelines. Mice

were subcutaneously injected in the scruff with PLGA microspheres (15 mg) suspended in sterile phosphate buffered saline. Mice were euthanized at 2 weeks and 4 weeks (n = 2 mice per group per time point). Tissues at the injection sites were excised, flash frozen fresh, and cryosectioned. Sections were stained with hematoxylin and eosin (H&E), and imaged using a Nikon Eclipse E400 microscope.

3.4   RESULTS

3.4.1   PLGA copolymer and microparticle synthesis and characterization

The sequenced periodic copolymers **poly LG** and **poly L$_{rac}$G** were prepared as described previously using segmer assembly polymerization (SAP) (Fig. 19A).[55] It is important to note that the synthetic method has been optimized to produce copolymers with a very high degree of sequence fidelity.[147] The naming convention for these polymers includes the description of the exact sequence of monomers in a segmer unit wherein the L-lactic acid unit, *rac*-lactic acid unit, and glycolic acid units are abbreviated as L, L$_{rac}$, and G, respectively. The purchased random copolymers were prepared by ring-opening polymerization (ROP, Fig. 19C). **PDLGA-50** is racemic variant of the random copolymer with and L:G-ratio of 1:1 while **PLLGA-50** is the stereopure analogue. **PDLGA-65** is racemic but has a 2:1 L:G-composition. The molecular weights of sequenced PLGAs prepared by SAP and purchased random PLGA controls were comparable, 21 − 30 kDa (Table 2, Fig. B1).

Microparticles, both with and without the inclusion of the pH-sensitive dye LysoSensor^{TM} Yellow/Blue DND-160, were prepared by a single-emulsion method. The T$_g$s for

55

all polymers were between 47 – 50 °C as synthesized but decreased by 2 – 6 °C after formulation into microparticles (Table 2, Fig. B2). The surface morphology of the non-dye loaded microparticle controls was characterized using scanning electron microscopy (Fig. B3). The microparticles exhibited some dispersity with sizes ranging from 50-150 μm.
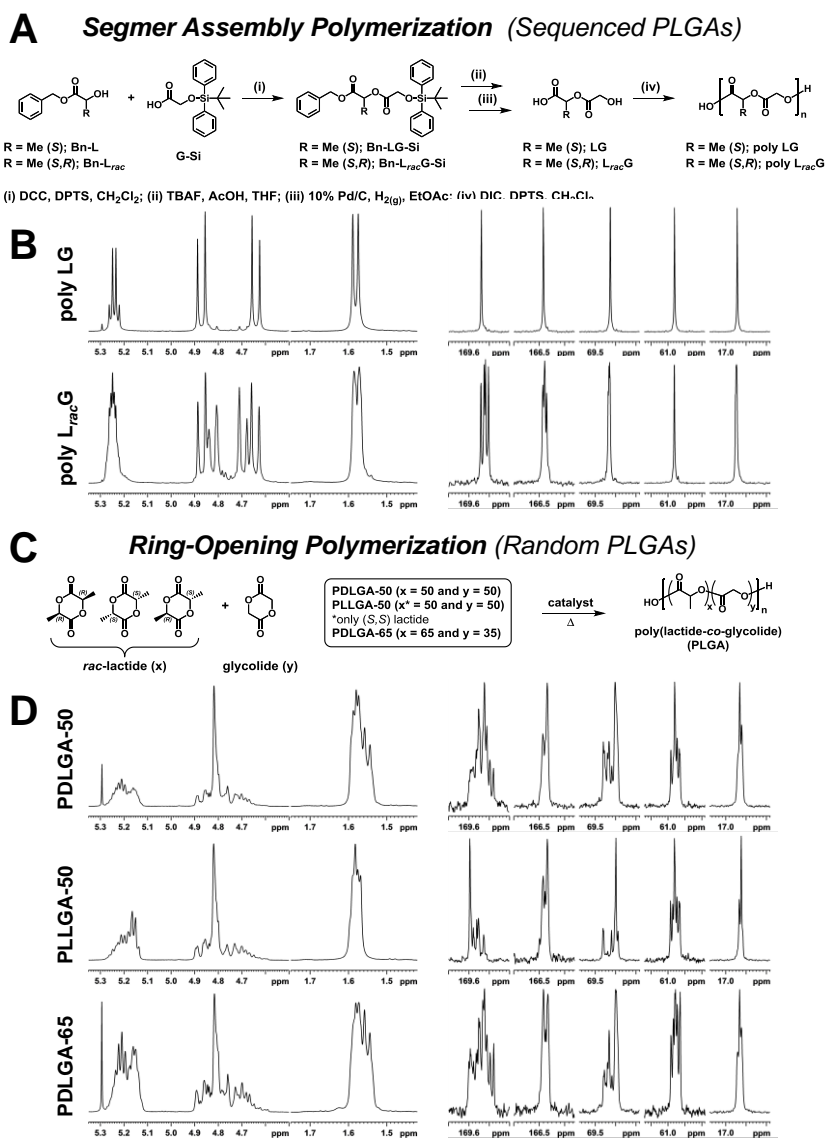
Figure 19. Synthetic preparation of sequenced and random PLGAs and NMR characterization (A) Synthesis of sequenced PLGA copolymers via segmer assembly polymerization (SAP) methodology. (B) ^{1}H NMR spectra (left) and ^{13}C NMR spectra (right) for the sequenced periodic PLGA copolymers. (C) Ring-opening polymerization synthesis of the purchased random PLGAs. (D) ^{1}H NMR spectra (left) and ^{13}C NMR spectra (right) for the random

PLGA copolymers. For all polymers, the 1H NMR spectra display the methine, methylene, and methyl resonances from left to right. ^{13}C NMR spectra display the resonances for glycolyl, lactidyl, methine, methylene, and methyl carbons from left to right.

Table 2. Characterization data for sequenced and random PLGAs utilized in acidic microclimate study.

Polymer	$M_n{}^a$ (kDa)	$M_w{}^a$ (kDa)	$Đ^a$	$T_g{}^b$ (°C)	$T_g{}^c$ (°C)	ratio L:G[d]	Control Yield (%)	Dye-loaded Yield (%)
Poly LG	21.4	32.1	1.5	50	48	50:50	47.1	57.7
Poly L$_{rac}$G	29.7	43.9	1.5	49	45	50:50	61.3	62.0
PDLGA-50	28.9	38.2	1.3	48	42	51:49	60.8	61.7
PLLGA-50	22.4	31.4	1.4	47	44	54:46	65.4	60.2
PDLGA-65	28.5	38.3	1.3	48	45	65:35	64.2	57.3

[a] Molecular weights determined using THF size exclusion chromatography relative to polystyrene standards.
[b] Standard glass transition temperatures were measured in the second heating cycle (10 °C/min, half C_p extrapolated).
[c] Glass transition temperatures of microparticles after single emulsion preparation were measured in the first heating cycle (10 °C/min, half C_p extrapolated).
[d] Ratio of lactic (L) and glycolic (G) units was determined using ^{1}H NMR spectroscopy.

The sequence and stereopurity of the periodic PLGA copolymers were confirmed using ^{1}H and ^{13}C NMR (Figs. 19B and 19D). We have shown previously through extensive studies that the NMR spectra of sequenced PLGAs is extraordinarily sensitive to sequence with the result that we can *unambiguously* assign the sequence of any polymer by comparison to authentic samples and can determine if a particular sample is contaminated with other sequence errors.[55, 147] Particularly sensitive are the chemical shifts of the diastereotopic glycolic methylene peaks that exhibit significant differences that correlate with the relative stereochemistry of nearby lactic units. It can be seen, for example, in Fig. 19B that there is one major pair of doublets associated for the glycolic units of the stereopure **poly LG** while multiple peaks appear in that same regions for **poly L$_{rac}$G**, corresponding to stereoisomers that have been previously shown to correlate to a tetrad-level of resolution (e.g. *iss* vs. *iis*).[9, 55] On that basis, the weak peaks visible in the glycolic

region of the **poly LG** can be attributed to a small amount (<5%) of epimerization. Similar analyses can be made for the ^{13}C NMR spectra, with the carbonyl resonances being the easiest to interpret.

As we will be exploring the degradation behavior of these sequenced copolymers it is important to note that we have previously exploited the sensitivity of these NMR spectra to sequence to verify that sequence scrambling does not occur to a significant extent during hydrolytic degradation.[55, 62]

3.4.2 LysoSensor Yellow/Blue DND-160 pH-dependent fluorescent response

LysoSensor™ Yellow/Blue DND-160 (PDMPO) was used to measure the internal pH of PLGA microspheres. Within a working pH range of 6.4 to 2.8, the emission intensity of this molecular probe shifts from $\lambda_{max} \sim 450$ nm to $\lambda_{max} \sim 530$ nm with acidifying pH (Fig. 20A). A series of citric acid : sodium phosphate dibasic pH buffer solutions were utilized to construct a pH vs. I_{450nm}/I_{530nm} standard curve used for interpretation of the TPM data (Figs. B4 and B5). Briefly, pH buffer solutions of pH 2.83 – 6.44 with 2 μM dye concentrations were excited at the isosbestic point λ_{ex} 360 nm and their ratiometric response intensity was determined. Using a third-order polynomial function ($r^2 = 0.994$), the optimal pH detection range was determined to be between pH 3.4 – 5.8 with the regions of pH 2.8 – 3.4 and pH 5.8 – 6.4 being slightly outside the detection range. Previous reports have verified that the ratiometric emission properties are independent of concentrations above 1 μM.[133, 137] Microparticles were loaded by exposure to a 50 μM solution of the LysoSensor™ dye during single-emulsion fabrication. Quantitative loading efficiencies were not determined in this study. Instead, the loading efficiency was qualitatively determined by the presence of emission bands associated with the dye. We had previously

reported that **poly LG** and **poly L$_{rac}$G** exhibited a lower loading efficiency that the random analogue [60] and the same qualitative behavior was observed for the LysoSensor™ dye in this investigation.
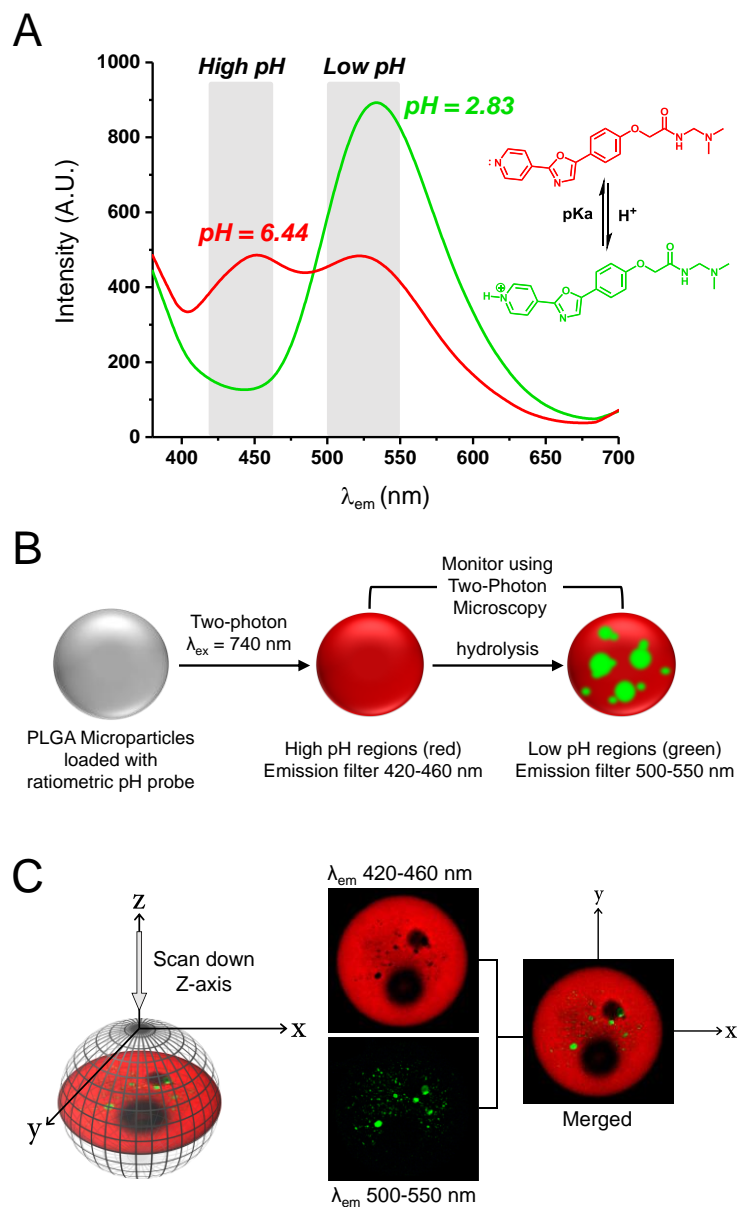
Figure 20. Ratiometric properties of pH-sensitive dye, two-photon microscopy experimental overview, and image acquisition parameters. (A) Chemical structure, emission profiles (λ_{ex} = 360 nm), and emission window regions for the deprotonated and protonated LysoSensor™ pH probe. (B) The low energy two-photon excitation, λ_{ex} = 740 nm ≈ 2x one-photon λ_{ex}, penetrates deep into the interior of the microparticles providing a detailed pH map (C) Z-stack

image acquisition of microparticles in solution were monitored using two separate λ_{em} windows. Merged images are displayed throughout the manuscript.

3.4.3 Internal acidity and morphology changes within sequenced and random PLGA microparticles

The effect of monomer sequence on the evolution and distribution of acidity within PLGA microparticles was investigated using two-photon microscopy (Fig. 20B). The pH probe, LysoSensor^{TM}, was loaded into 50 – 150 μm microparticles using a single-emulsion method. At various time points over 8 weeks, internal slices of aqueous microparticle suspensions were imaged at various depths. The ratiometric pH response was captured using a V/G multiphoton emission filter set, translating to red (near neutral pH) and green (acidic pH) signals (Fig. 20C). The pH distribution studies for sequenced PLGAs, was limited to 3 weeks due to low dye loading and long-term dye leaching. The random 50:50 analogues were monitored over 2 weeks while minimal dye leaching for **PDLGA-65** allowed the pH to be monitored over 8 weeks. Representative images of microparticles over a 2-week time period are shown in Fig. 21. Additional data for **poly L$_{rac}$G**, **poly LG**, and **PDLGA-65** at later time points can be found in Fig. 22. High resolution TPM images of single microparticles displaying characteristic acidic microclimate features are included for reference in Fig. B6.
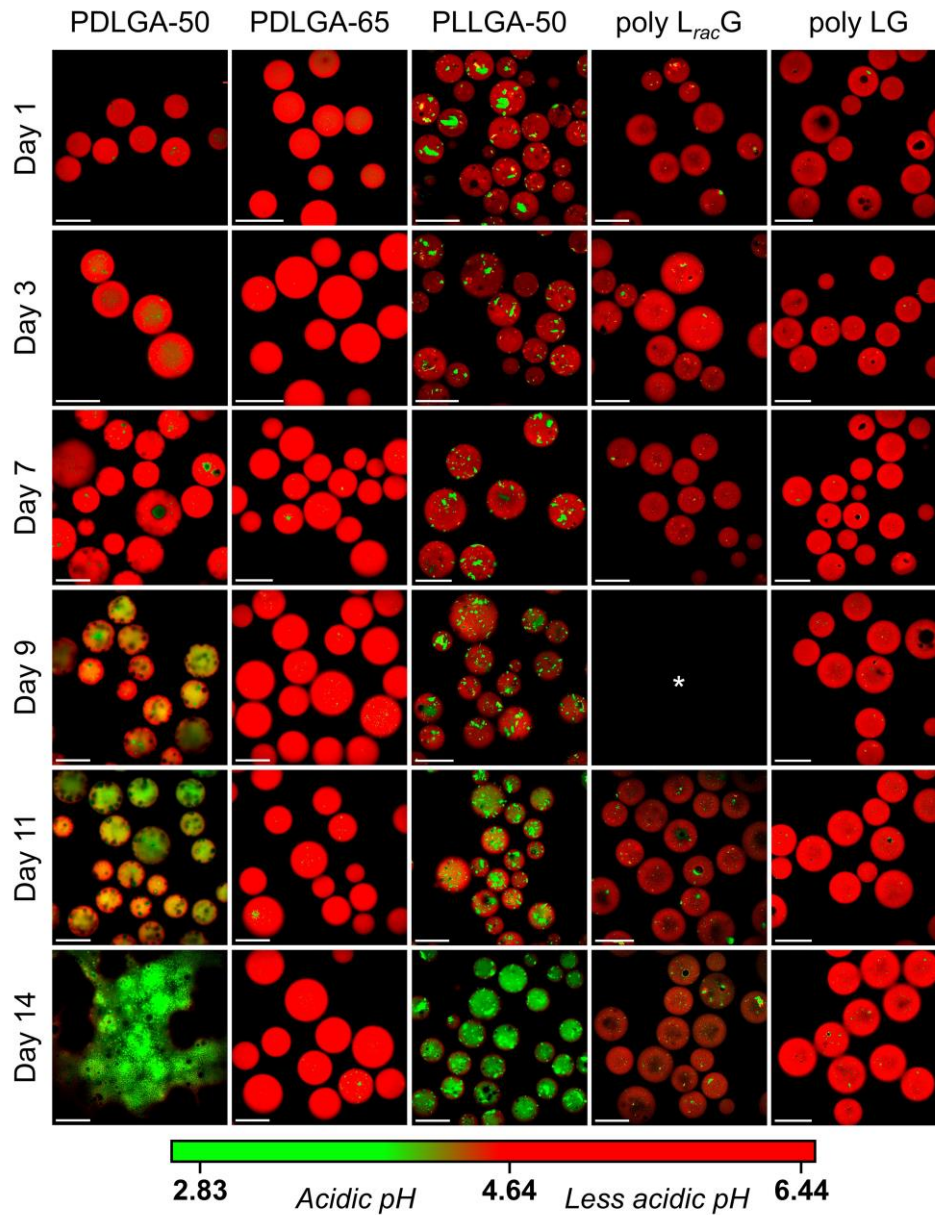
Figure 21. Internal acidic microclimate distributions of sequenced and random PLGA copolymers after 1, 3, 7, 9, 11 and 14 d in vitro (brightness normalized). *Image not obtained due to laser mode-locking complications. Scale bar = 100 μm.

The internal pH of microspheres during the first two weeks of incubation was within the detectable range of the pH probe, $2.83 < pH < 6.44$. Internal pores, which appear as black holes on the micrograph, were present in all particles but were more prevalent in the sequenced PLGAs and **PLLGA-50**. Initially, all samples exhibited minimal acidity with an internal pH > 4.64. It

should be noted that even in the initial image of **PLLGA-50** regions of apparent low pH appear but these artifact are likely due to refracting crystals.[148-150] Consistent with this assignment is the fact that microparticle controls without the pH-sensitive dye exhibited the same features (Fig. B7). In addition, differential scanning calorimetry thermograms contained melting transitions spanning 75 – 125 °C (Fig. B2). After 3 d, the internal pH of **PDLGA-50** slightly decreased while the pH of all other samples remained unchanged. With increasing incubation time, localized regions of acidity appeared in **PDLGA-50** and **PLLGA-50** while the pH within **PDLGA-65**, **poly L$_{rac}$G**, and **poly LG** microparticles remained less acidic. The size of the acidic regions within **PDLGA-50** microparticles were larger compared to **PLLGA-50**. Interestingly, the **PDLGA-50** particles exhibited shape irregularities concomitantly with the onset of increasing acidity at 7 d while all other samples retained their original morphology at this point in time. After 9 d, the once localized regions of acidity within **PDLGA-50** percolated throughout the microparticles resulting in a widespread decrease in pH, pH ≈ 4.5. Similar behavior was present in **PLLGA-50** microparticles at 11 d. At this time the internal structure of **PDLGA-50** had significantly changed, large apparently acid-filled pores had formed and the internal pH became more acidic, pH < 4.5. By contrast, the frequency of acidic μ-pockets within **PDLGA-65**, **poly L$_{rac}$G**, and **poly LG** microparticles was significantly lower. After an additional week of incubation, **PDLGA-50** lost structural integrity and had become an acid-saturated mass with a pH << 4.5. Interesting, **PLLGA-50** microparticles exhibited a similar distribution of acidity to **PDLGA-50** while maintaining structural integrity.
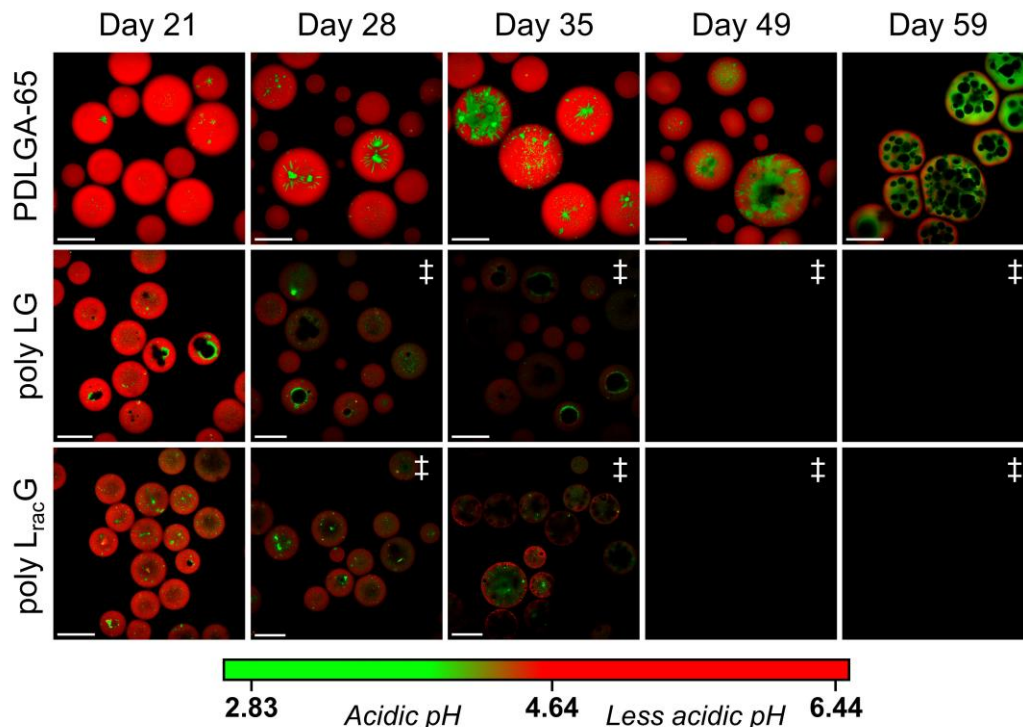
Figure 22. Two-photon microscopy images of the internal acidic microclimate distribution images within PDLGA-65, poly L$_{rac}$G, and poly LG at later time points; 21, 28, 35, 49, and 59 d. ‡ Ratiometric pH probe response was no longer discernable from background autofluorescence resulting from dye-leaching. Scale bar = 100 μm.

Between 14 and 21 d, the acidity distribution within **PDLGA-65**, **poly L$_{rac}$G**, and **poly LG** microparticles remained relatively constant. At 21 d, the frequency of acidic μ-pockets within **poly L$_{rac}$G** microparticles had increased, whereas **poly LG** accumulated acid only around the periphery of the internal aqueous pores (Fig. 22). The presence of acidic μ-pockets within **PDLGA-65** also increased and acidic μ-channels branching form larger acid filled pores were also observed. By 28 d, dye levels in **poly LG** and **poly L$_{rac}$G** microparticles had decreased to the point that dye signal could not be distinguished from the background auto-fluorescence. Despite the absence of dye, however, gross internal structural changes can be observed at 35 d. At this time the prevalence of open pores within **poly L$_{rac}$G** increased resulting in microparticle plasticization after 46 d. In contrast, **poly LG** microparticles retained their original internal

63

structural features until approximately 11 weeks after which the particles exhibit brittle failure to give a powder; no prior plasticization is noted (Fig. B8). For **PDLGA-65**, the frequency and size of acidic μ-pockets increased during the next 2 weeks and significant plasticization was observed by 59 d.

3.4.4   Trends in pH distribution for sequenced and random PLGA microparticles

To visualize more clearly how the overall pH distribution evolves within samples containing a population of particles (n = 10), pH distribution curves for PLGA microparticles were constructed using pixel intensity ratios. The frequency of a specific pH was plotted against the internal pH to monitor any changes in the internal pH distribution (Fig. 23). After 3 d of incubation, the internal pH of all samples remained above pH = 4.5, with the distribution varying based on sequence and stereochemistry. **PDLGA-50** had a significantly narrower distribution, pH = 4.5 – 5.0 compared to all other samples, pH = 4.5 – 6.0+. After 7 d, the pH shifts towards a less acidic pH for **PDLGA-50** and **PLLGA-50** while all other samples remained constant. This initial shift in pH for **PDLGA-50** and **PLLGA-50** was immediately followed by a decreased in pH at 9 d, which continually shifted to a more acidic pH in the following days, 11 and 14. This behavior was also observed in **PDLGA-65** particles but the process was more gradual. The internal pH for **PDLGA-65** particles slowly shifted to a less acidic pH over the second week and then shifted back towards a more acidic pH in the following 5 weeks. Interestingly, the original pH distribution was maintained throughout the course of the experiment for **poly LG** whereas a slight deviation was observed for **poly L$_{rac}$G**, favoring a more acidic pH.
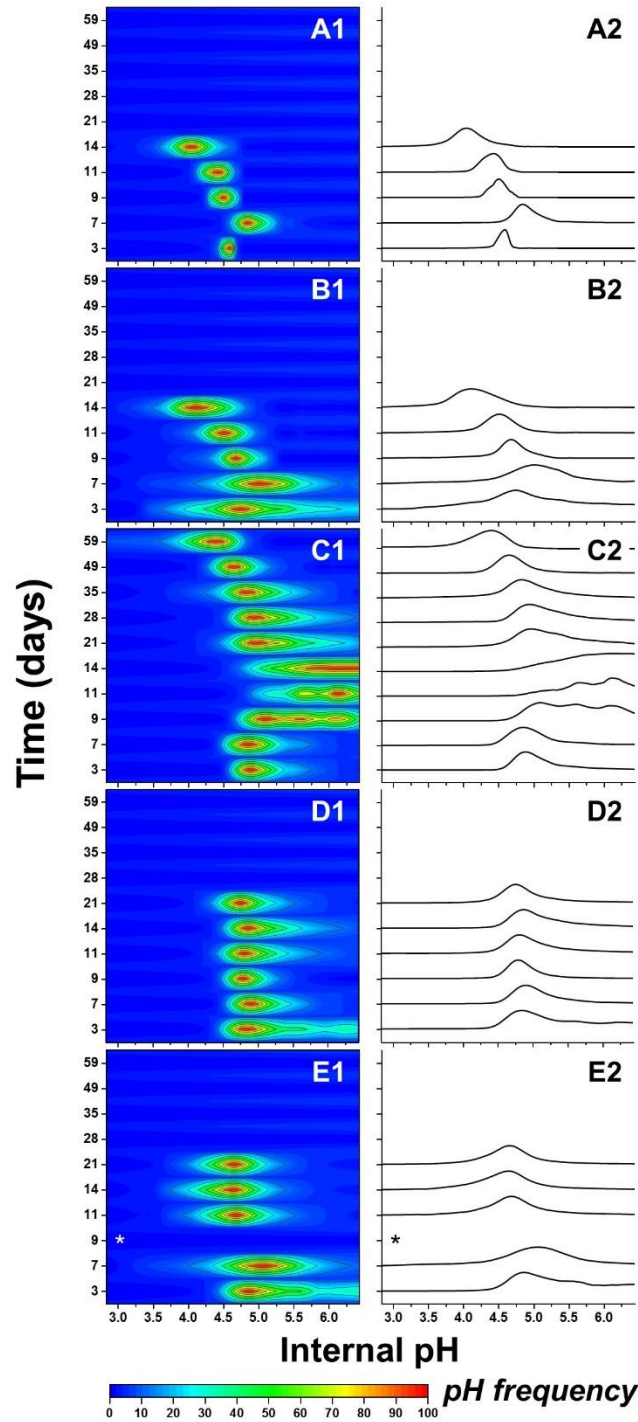
Figure 23. Contour maps of the internal pH of PLGA microparticles at time points 3, 7, 9, 11, 14, 21, 28, 35, 49 and 59 days: (A1) PDLGA-50, (B1) PLLGA-50, (C1) PDLGA-65, (D1) poly LG, (E1) poly L$_{rac}$G and corresponding internal pH distribution histograms (A2-E2). *Profile not obtained due to laser mode-locking complications. Data obtained from images containing multiple microparticles.

3.4.5 External morphology changes in sequenced and random PLGAs

Single-emulsion PLGA microparticle controls, without encapsulated dye, were exposed to physiological conditions over 5 weeks and imaged using SEM to investigate the effects of monomer sequence and stereopurity on microparticle morphology. Representative images of microparticles after 7, 14, 21, 28, and 35 d of incubation are displayed in Fig. 24. After single-emulsion preparation, all microparticles were spherical with non-porous surfaces (Fig. B3). During the first week of incubation, subtle changes in morphology were observed for **PDLGA-50** microparticles. The surface of **PDLGA-50** was slightly textured and small pores had formed on all **PDLGA-50** microparticles. The initial morphology was maintained during this time period for all other samples. Within 14 d of incubation, the external morphology of **PDLGA-50** was severely compromised with evidence of erosion. Large and small pore networks including small channels were observed (Fig. 25A). No changes were observed for the remaining samples until 21 d. At this time, **PDLGA-50** microparticles have lost all structural integrity and have formed plasticized masses. The stereopure random analogue, **PLLGA-50**, no longer retained its spherical shape and changes in surface texture were also observed. In the following week, regions of swelling were observed on the surfaces of **PLLGA-50** microparticles (Fig. 25C), and small pores began to form on the surface of **poly L$_{rac}$G** microparticles. The morphology of **PDLGA-65** and **poly LG** remained unchanged. After 35 d of incubation, **poly L$_{rac}$G** microparticles no longer retained their spherical shape and the frequency of small pores had increased with some forming a circular network of pores (Fig. 25D). The regions of swelling remained on the surface of **PLLGA-50** microparticle at this time **PDLGA-65** and **poly LG** remained unchanged (Figs. 25B and 25E).
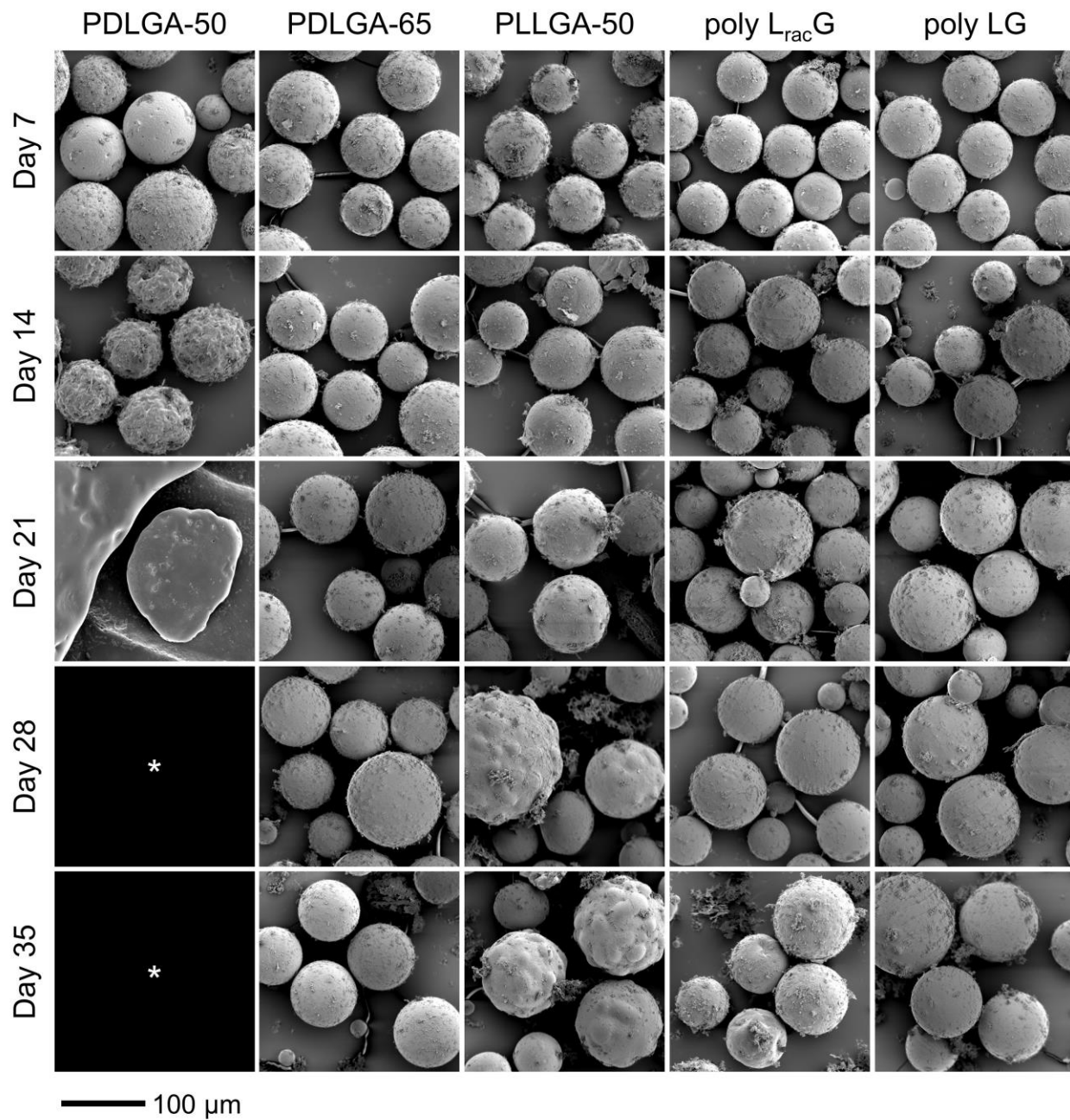
Figure 24. Scanning electron micrographs of sequenced and random PLGAs after 7, 14, 21, 28, and 35 d in vitro under x350 magnification. *Sample no longer retained structural integrity.
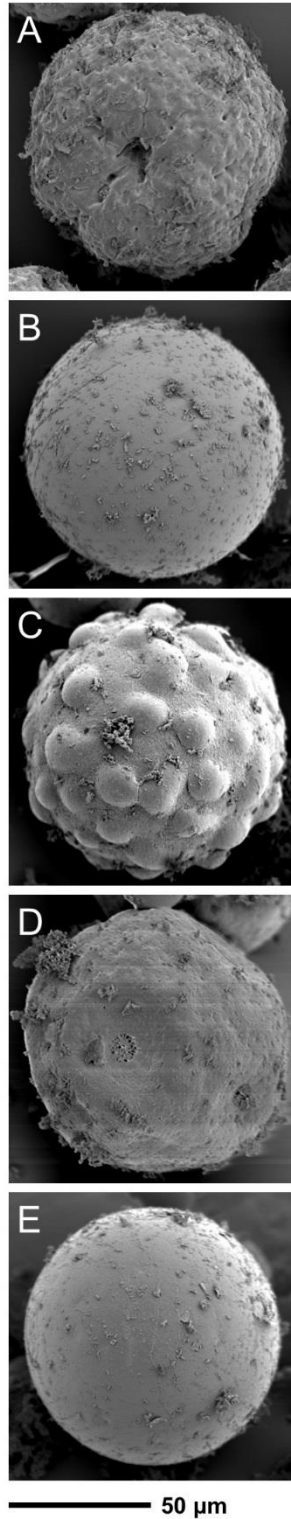
Figure 25. Scanning electron micrographs of single particles of PDLGA-50 (t = 14 d) (A), PDLGA-65 (t = 35 d) (B), PLLGA-50 (t = 35 d) (C), poly $L_{rac}G$ (t = 35 d) (D), and poly LG (t = 35 d) (E) under x800 magnification. All images were taken at 35 d with the exception of PDLGA-50, which only retained a spherical morphology up to 14 d.

3.4.6   Foreign body response to microparticle injections

Microparticles of the sequenced copolymer **poly LG** and the random **PDLGA-50** were subcutaneously injected in mice to monitor the *in vivo* foreign body response at 2 and 4 weeks post-injection (Figs. 26 and B9). These polymers were chosen for comparison because they exhibited a significant difference in acid distribution behavior and degradation profile. The size and morphology of the single-emulsion blank microparticles were similar as confirmed by SEM (Fig. B10). Histological analysis of subcutaneous depots of both microparticle formulations revealed granulomatous foreign-body reactions. Macrophages and neutrophils were present at 2 weeks post-injection, with somewhat greater neutrophil infiltration in **poly LG** microparticle depots. By 4 weeks, neutrophils were absent from both particle depots, and foreign-body reactions were characterized by the presence of macrophage foam cells and multinucleated Langhans and Touton giant cells. At this time **poly LG** microparticle depots had noticeably fewer and less developed multinucleated giant cells compared to **PDLGA-50**. It is important to note that in contrast **PDLGA-50**, which exhibited a significant decrease in the number and size of particles present by week 4, **poly LG** microparticle depots had remained stable in the subcutaneous tissue.
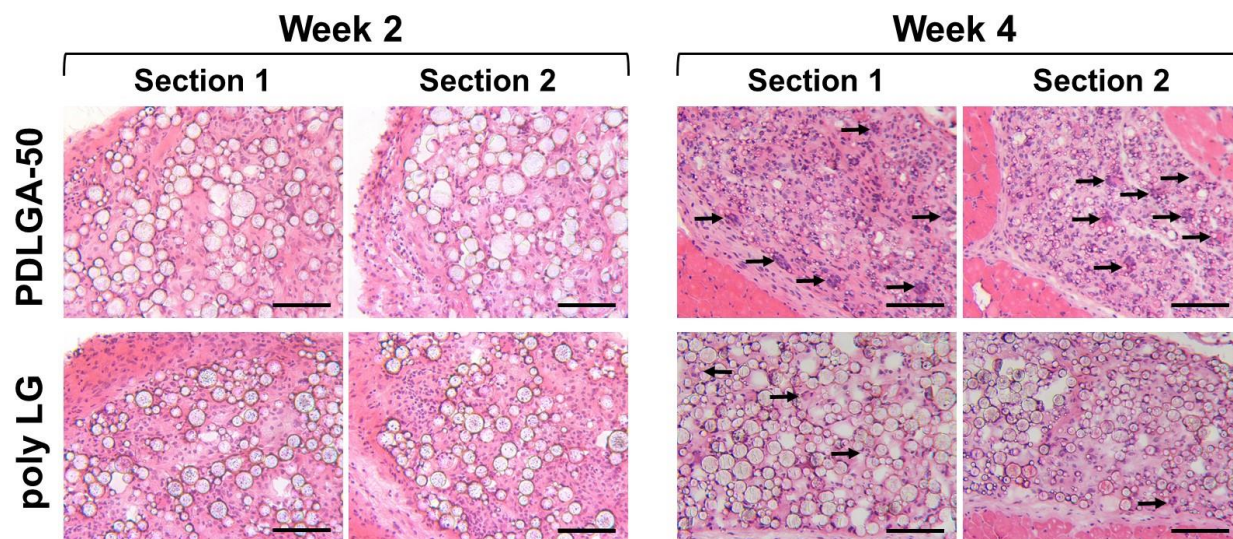
Figure 26. H&E staining of subcutaneous tissue microparticle depot injections in C57BL/6J wild-type mice, 2 and 4 weeks after injections (x25). Section 1 and 2 are representative sections of tissue from two different mice. Arrows indicate presence of foreign body giant-cells. Scale bar = 100 μm.

3.5   DISCUSSION

The current study correlates well with our previous studies on how sequence affects degradation in PLGAs while providing significant new insights into the reasons and consequences of those differences. Perhaps the most fundamental finding and one that echoes our prior *in vitro* sequence-based hydrolysis studies in both trends and observed degradation times, is that sequence has a profound influence on the rate of degradation. **PDLGA-50, PLLGA-50**, **poly L$_{rac}$G**, and **poly LG,** which all have the same 1:1 L:G-composition exhibit dramatically different hydrolysis profiles. Indeed, random **PDLGA-50** fails 8 weeks earlier than the alternating stereopure **poly LG**. The alternating sequenced copolymer exhibits a time to failure that more closely resembles that of the random **PDLGA-65**, which has a nearly 2:1 L:G-ratio. This

70

behavior is interesting because many prior studies have correlated degradation times with L:G-ratio and shown that higher L-content translates into slower degradation.[9, 29, 95-96, 107-108, 151-153] It is also clear that stereochemical sequence is important; stereopure versions of both the random and sequenced copolymer degrade more slowly than the racemic copolymers.

As we have discussed in the context of our previous studies, [60-62] the difference in hydrolysis rates between G-G, L-G/G-L, and L-L units is one of the most significant contributors to the range of degradation rates observed (Fig. 27). In random PLGAs, it is well-established that G-rich blocks degrade much more quickly than L-rich blocks. As a result, random PLGAs are rapidly cleaved into shorter chains and the acidic by-products from the cleavage can further accelerate degradation. In contrast, **poly LG** has only two type of linkages, L-G and G-L, both with intermediate and similar cleavage rates. Initial cleavage of the chains is, thus, expected to proceed more slowly and less localization of the cleavage sites and acidic by-products is expected.
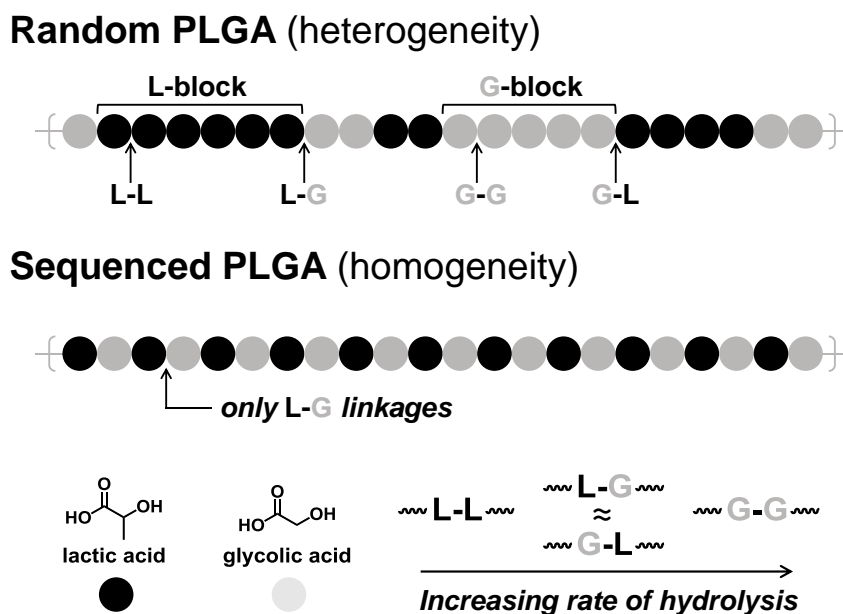
Figure 27. Linkage type(s) and distribution for PDLGA-50 (top) and poly LG (bottom) with relative linkage hydrolysis rates.

71

The microscopy images acquired in this study increase our understanding of how the molecular level phenomena, including cleavage rates, affect the morphology, acid microclimate distribution, and internal structure. The most prominent change observed in the microparticles as a function of degradation is the shape-distorting plasticization of all the polymers, except **poly LG**. The sequence-based differences in this behavior correlate well with molecular weight loss and the degree of buffer infiltration. With regard to molecular weight, our prior study relating sequence to properties has shown that the rate of molecular weight loss and the degree of swelling and erosion for microparticles and implants prepared from these copolymers exhibits the following trend: **PDLGA-50** > **PLLGA-50** > **poly $L_{rac}G$** > **poly LG** (**PDLGA-65** was not reported in this study but has been characterized relative to **PDLGA-50** previously).[62, 94-95] Also, we have seen the plasticization reflected in the broadening and shift of the glass transition temperatures for **PDLGA-50** and **poly $L_{rac}G$**.[60]

Buffer infiltration is likely an important contributor to the observed differences in acid distribution within the particles. The particles that ultimately exhibit low pH throughout the entire particle, **PDLGA-50** and **PLLGA-50**, are also the ones that exhibited a greater degree of swelling during the first week of incubation in a prior study. In this study these samples were found to exhibit an initial increase in their overall internal pH prior after 7 d prior to the onset of degradation. This early increase in pH, which has been observed previously by Schwendeman and coworkers,[133] can be attributed to a combination of buffer solution penetration with concomitant neutralization and/or flushing of acidic by-products. We hypothesize that, in the current study, acid production as a result of hydrolysis then exceeds the intraparticle buffer capacity leading to the observed delocalized acidity. Consistent with this analysis is the local acid distribution pattern observed for **PDLGA-65**, which should both swell less than the random

50:50 PLGAs and produce acid more gradually. **Poly LG** represents the far end of this continuum, with a small degree of swelling and a lack of fast cleaving G-G sequences.

The initial internal particle structure and dye-loading also differs based on sequence, which we hypothesize may correlate with structural homogeneity of the PLGA copolymers. Immediately after preparation, we observe that sequenced-defined **poly L$_{rac}$G** and **poly LG** microparticles exhibit a higher number of internal voids than the microparticles produced from random PLGAs. Although we did not quantify this parameter, the observation was consistent in all micrographs and for multiple particle preparations. The second observation that the sequenced copolymers would not load as much dye as the random copolymers was obvious in the brightness of the initial images and in the fact that dye levels fell to below observable concentrations for both **poly L$_{rac}$G** and **poly LG** before the particles had failed. In a previous study, we had also noted that we were able to achieve a higher loading of rhodamine-B into **PDLGA-50** vs. **poly LG** microparticles. We suggest that these two observations may be related to the homogeneity of the sequenced copolymers relative to the random analogues. Although we do not observe multiple T$_g$s for **PDLGA-50**, which would indicate microphase separation, the presence of L- and G-rich blocks must necessarily result in some degree of heterogeneity in the bulk that will in turn generate areas that have more and less affinity for any solute. The sequenced chains, which due to their uniformity must be characterized by a single Flory-Huggins interaction parameter, χ, will likely favor self-interaction and exclude other possible solutes. In the case of particle formation, such self-interaction can lead to the exclusion of the organic solvent used in the preparation of the microparticles. The excluded solvent will coalesce to form droplets, which will lead to the formation of internal voids. Similarly, the homogeneous sequenced copolymers would be expected to exhibit a lower tendency to interact with most

solutes, including dyes and drugs, relative to the more heterogeneous random PLGAs. We hypothesize that this phenomenon is responsible for the difficulties that we have experienced in loading such solutes into **poly LG**. Although the complete verification of this hypothesis will require experiments outside the scope of the current study, it is clear that encapsulation methodologies for sequenced PLGAs should be further optimized.

Our confidence in the sequence-based differences we see using TPM is supported by the similarity of the behavior we observed for the random copolymers to that reported by both Schwendeman and Langer. Specifically, in both reports a shift towards higher pH values was observed after exposure to physiological conditions. This behavior was most prominent for random PLGA microparticles with a 50:50 L:G-ratio and less for PLGAs with higher L-content (i.e., 85:15 and 100:0).[113, 133, 154] Also, consistent between our studies and others were the reported pH distribution ranges despite the use of different dyes and microscopic techniques. Finally, the morphological changes in the current work were consistent with those reported by Langer and coworkers for **PDLGA-50** microparticles.[113]

Finally, we have observed similarities between *in vitro* and *in vivo* microparticle degradation behaviors for sequenced and random PLGAs, which is of particular importance for translation because not all characteristics observed *in vitro* carry over once the material is implanted. First, we see that the differences in degradation time between **PDLGA-50** and **poly LG** are preserved *in vivo*. The **PDLGA-50** microparticles have mostly degraded by the end of 4 weeks of implantation whereas the **poly LG** particles exhibit minimal changes in the same time period. Secondly, the foreign-body response appears to be diminished for the sequenced **poly LG** microparticles. In previous similar studies on random PLGAs, differences in host tissue response have been associated with changes in microparticle surface chemistry and/or local pH

due to polymer degradation.[155-160] The TPM studies demonstrated that acid production within the **poly LG** particles is minimal in this time period, thus it seems likely that difference in FBGC response in the current pilot study is primarily due to the variance in degradation rates. Although further investigation will be required to ascertain the *in vivo* response to **poly LG** after longer time periods, the current acidity studies suggest that acid release within the tissue will be more gradual and less likely to provoke an inflammatory response.

3.6   CONCLUSIONS

Microscopic analysis, TPM and SEM, of particles prepared from both random and sequenced PLGAs demonstrates that key *in vitro* and *in vivo* properties related to DDS performance (i.e., degradation rate, accumulation and percolation of acidic by-products, microparticle morphology, and foreign body response) can be tuned using precise macromolecular design. These results are consistent with our prior findings that the loss of molecular weight, increase in dispersity, overall swelling, thermal transitions, and erosion during hydrolytic degradation are all a function of LG sequence. In addition, we have confirmed that two-photon microscopy is a viable method for non-invasive monitoring of internal pH that offers advantages relative to CLSM. Future work will focus on improving the loading efficiencies and evaluating the stability and release of acid-sensitive macromolecular payloads for sequence-defined PLGA matrices.

4.0 THE EFFECT OF MONOMER SEQUENCE ON THE RETENTION OF MECHANICAL PROPERTIES DURING HYDROLYTIC DEGRADATION FOR SEQUENCE-DEFINED POLY(LACTIC-*CO*-GLYCOLIC ACID)S

4.1 OVERVIEW

This work presented in this chapter provides new mechanistic insights pertaining to the retention of mechanical properties for sequence-defined and random poly(lactic-*co*-glycolic acid) cylindrical matrices. This chapter is being submitted for publication in a peer-reviewed journal and is summarized in Fig. 28: M.A. Washington, Y. Xue, S. Sant, C. Liu, T.Y. Meyer. "The effect of monomer sequence on the retention of mechanical properties during hydrolytic degradation for sequence-defined poly(lactic-*co*-glycolic acid)s." **2017**.
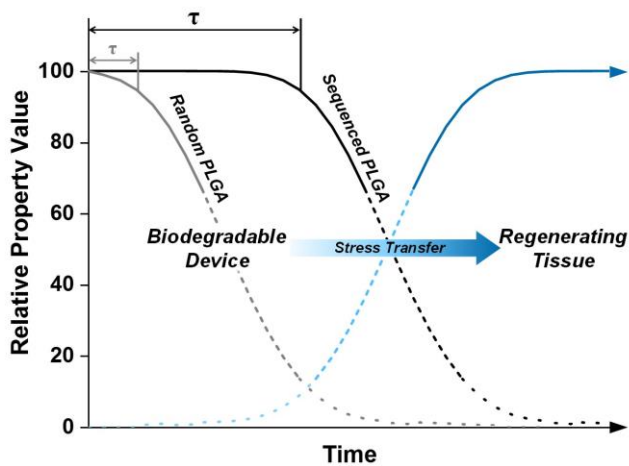
Figure 28. Graphical abstract for Chapter 4 – The effect of monomer sequence on the retention of mechanical properties during hydrolytic degradation for sequence-defined poly(lactic-*co*-glycolic acid)s.

Over the past four decades, biodegradable poly(lactic-*co*-glycolic acid)s (PLGAs) have had minimal success in long-term load bearing orthopedic applications due to their poor retention of mechanical properties. While alternative methods such as self-reinforcement and the addition of synthetic fillers offer initial increases in ultimate strength and modulus, the bulk properties of random PLGAs rapidly decrease due to random and autocatalytic hydrolysis. Controlling monomer sequence in PLGAs has been found, however, to exert a strong influence on a variety of bulk properties including swelling, erosion, and internal acidic microclimate. To investigate the impact of monomer sequence on the relationship between degradation induced microstructural changes and macroscopic bulk properties, cylindrical implants (3 mm x 3 mm) for a set of sequenced and random PLGAs were exposed to physiological conditions over 9 weeks. Microstructural changes were monitored *in vitro* using differential scanning calorimetry (DSC), gel permeation chromatography (GPC), ^{1}H NMR spectroscopy, and powder x-ray diffraction (PXRD) as a function of degradation. The macroscopic mechanical properties, including compressive modulus (CM) and ultimate compressive strength (UCS) were also determined. Overall, the sequence-defined PLGAs exhibited longer hydrolytic induction time periods, τ, and improved retention of mechanical properties compared to random analogues with the same L:G-composition. It is hypothesized that the differences observed are related to the mechanism of hydrolytic cleavage, with sequence copolymers favoring a long-period of chain-end scission prior to the onset of auto-catalytic degradation. Random copolymers, in contrast, exhibited behaviors consistent with a random-chain cleavage mechanism which, in turn, led to a faster onset of auto-catalytic degradation and shorter τ.

4.2   INTRODUCTION

Biodegradable polyesters, specifically poly(lactic acid) (PLA), poly(glycolic acid) (PGA), and poly(lactic-*co*-glycolic acid) (PLGA) have been extensively utilized in various orthopedic and soft tissue regeneration applications due to their osteo-similar mechanical properties, range of degradation profiles, and non-toxicity.[1, 28, 99, 161-162] Unlike metallic implants, biodegradable implants do not require a removal surgery, provide adequate support for regenerating tissues, and degrade at a rate that slowly transfers load to the healing tissues minimizing complications such as stress shielding.[98-99, 163] The initial mechanical strengths of PGA and PLA are similar to that of cortical bone (i.e., compressive strength of 131 – 224 MPa) while PLGA is comparable to cancellous bone (i.e., compressive strength of 5 – 10 MPa).[161] The retention of mechanical strengths are strongly influenced by the composition and microstructure of these polymers (i.e., L:G-ratio, crystallinity, molecular weight).[2, 25, 28, 164] For PLGAs, degradation begins upon *in vivo* implantation and the loss of total strength occurs within the first month. This has limited their use to short-term low-load bearing devices such as sutures, suture anchors, staples, interference screws, and cellular scaffolds.[28, 67, 165-166] While there is considerable evidence that alternative methods such as self-reinforcement,[66, 167-168] addition of nanocomposites,[169-173] polymer blending,[174-176] and introducing chemical crosslinks [177-178] address the mechanical deficiencies of PLGA, methods which produce consistent and predictable time dependent behaviors in the absence of additives remain to be defined.

Our approach to improving the performance of PLGA devices is to use monomer sequence to define the hydrolysis profile, lengthening the time over which mechanical properties are retained without creating a device whose overall degradation is not unacceptably slow. Our rationale for this approach is based on our recent studies on how sequence affects the overall

degradation of various PLGA matrices. We have, for example, demonstrated that sequenced copolymers exhibit more gradual losses of molecular weight, minimal changes in polymer chain dispersity, lower degrees of swelling, and slower erosion than random analogues with the same L:G ratios and molecular weights.[60-62, 179] These trends hold for a variety of matrices including microparticles (2 – 5 and 50 – 150 μm) and compression molded cylindrical implants (3 x 3 and 3 x 1.5 mm). We have also observed sequence-dependent differences in acid distribution within microparticles, the release profile of rhodamine B, and in the *in vivo* inflammatory responses to subcutaneously injected microparticle matrices.[60, 179]

Importantly, our past studies and the ones reported herein contribute also to a growing body of work within the synthetic polymer community that is concerned with characterizing structure/function relationships in sequenced copolymers.[180-182] We and others are motivated not only to address the application-related question posed above but also to develop a deeper understanding of how sequence affects properties and behavior.[33-34, 36, 45] There have been other reports of sequence effects on bulk properties of biodegradable copolymers that are relevant to the focus of the current study. In recent reports by both Sarasua and Albertsson and coworkers, statistical variants of poly(ε-caprolactone-*co*-δ-valerolactone) and triblock copolymers of L-lactide, but-2-ene-1,4-diyl malonate, and ε-caprolactone were found to have superior control over a variety of bulk properties compared to random analogues.[78-79, 124, 183] These studies demonstrate the potential impact of sequence-controlled approaches for tuning the properties of biodegradable matrices.

In the current study we are interested in exploiting high degrees of sequence control in PLGA copolymers to expand our understanding of how degradation induced microstructural changes affect macroscopic bulk properties for sequence-defined PLGAs. Numerous reports

have substantiated that random PLGAs initially undergo ester hydrolysis in sterically accessible glycolic-acid-rich regions.[29, 153, 184-185] This preferential hydrolysis leads to an exponential decrease in molecular weight and concomitant accumulation of lactic acid oligomers. This pattern is particularly important for the retention of mechanical properties as the lower molecular weight species produced by ester scission events rapidly lose mechanical properties. Furthermore, the lower degree of entanglement facilitates increased water absorption leading to elastic modulus-decreasing plasticization. These behaviors are characteristic of biodegradable polyesters which are known to follow a bulk erosion mechanism.[25, 28, 186-187]

Another phenomenon that contributes substantially to the process of degradation is autocatalytic scission of ester bonds due to the local production and slow clearance of acid by-products. Autocatalytic hydrolysis results in the heterogeneous degradation of bulk eroding matrices with diffusion lengths > 10 μm.[187] Tomlins and coworkers determined that the rate of degradation at the center of a specimen is almost an order of magnitude higher than at the surface.[188] This non-uniformity of degradation has been observed in a variety of PLGA matrices and other polyesters and results in polymodal molecular weight distribution, rapid loss of thermal properties, and increased rates of swelling due to osmotic gradient formation.[184, 187, 189-190]

The time scale in which random PLGAs degrade can be tuned to a certain degree through microstructural manipulations (e.g., increasing L:G-ratio, crystallinity, and molecular weight) or decreasing the size/shape of the biodegradable device.[95, 186, 188, 191-192] These strategies aim to slow the rate of degradation of PLGA as well as limit the initial diffusion of water into the matrix. These factors are particularly important as initial water absorption and degradation induced swelling has been reported to play a decisive role both the mass transport mechanisms of

various small molecules (e.g., drugs, water, ions, and degradation products) and retention of various physicochemical properties (i.e., thermal, mechanical, and morphological).[70, 90, 193]

In the current study we utilize compression molded cylindrical implants (3 mm x 3 mm) to evaluate how precise control over monomer sequence effects the relationship between microstructural changes and the retention of macroscopic bulk properties for PLGAs. First, the macroscopic bulk mechanical properties (i.e., compressive modulus and ultimate compressive strength) of wet cylindrical matrices exposed to physiological conditions will be discussed. Then, changes in microstructural composition monitored by differential scanning calorimetry (DSC), gel permeation chromatography (GPC), proton nuclear magnetic resonance spectroscopy (^{1}H-NMR), and powder x-ray diffraction (PXRD) will be compared. Finally, the underlying molecular mechanism of degradation for sequence-defined PLGAs compared to that of random PLGA analogues will be discussed.

4.3   MATERIALS AND METHODS

4.3.1   Materials

Poly(D,L-lactide-*co*-glycolide), acid terminated, with a 50:50 and 65:35 ratio of lactic (L) and glycolic (G) acid derived units were purchased from Durect corporation (Birmingham, AL) as a pelletized solids. Prior to fabrication, the polymers were dissolved in methylene chloride (CH_2Cl_2), precipitated in methanol (MeOH), and dried *in vacuo* yielding off-white amorphous solids. The stereopure random PLGA, poly(L-lactide-*co*-glycolide), acid terminated, with a 50:50 ratio of L:G-derived units was obtained from Changchun SinoBiomaterials Co. Ltd. (Changchun,

China) as a white fibrous solid and was used as provided. Sequenced PLGA copolymers were prepared using previously reported synthetic methods.[55] All sequenced PLGAs were isolated as either white amorphous solids or white fibrous solids. Phosphate buffered saline (PBS; pH = 7.4; 10 mM; certified nuclease free) was purchased from Molecular Biologicals International, Inc. (Irvine, CA).

4.3.2 ^{1}H and ^{13}C NMR spectroscopy

^{1}H and ^{13}C NMR spectra were obtained in CDCl$_3$ using a Bruker Avance III spectrometer (500 MHz) at 293 K. All chemical shifts were reported in ppm (δ) and referenced to the chemical shifts of the residual solvent resonances at δ 7.26 ppm (^{1}H) and δ 77.00 ppm (^{13}C).

4.3.3 Differential scanning calorimetry

DSC analysis was performed using a TA Instruments Q200 calorimeter using a scan range of -10 – 200 °C at a rate of 10 °C/min under a nitrogen atmosphere with a flow rate of 20.0 mL/min. Glass transition temperatures (T$_g$) were calculated as the half Cp extrapolated.

4.3.4 Gel permeation chromatography

Molecular weights and dispersities were acquired using a Waters 717 plus autosampler system (THF, 1 mL/min, 40 °C) equipped with a Waters 2412 refractive index (RI) detector and two styrene-divinylbenzene columns (porosity = 1000 and 100000 Å; Polymer Standard Services).

The RI detector was calibrated using a 9-point calibration based on polystyrene standards (ReadyCal Kit, Polymer Standard Services).

4.3.5 Fabrication of PLGA cylindrical constructs

PLGA cylinders were prepared using heated compression molding in a custom 12 port stainless steel press. Raw polymer (42 – 45 mg) was added to each port of the press which was heated to 20 – 30 °C above the T_g. The samples were compressed for 40 min with a 7,000 lb load using a Carver press (Hydraulic unit model #3912; Wabash, IN) which was heated to 90 – 100 °C. After compression the press was cooled under load to ~34 – 40 °C. The resulting pellets were translucent or opaque depending on the identity of the polymer. The height and width of the specimens were measured using digital calipers with a capability of measuring +/- 0.01 mm. Cylinder masses were recorded using an analytical balance with a 1.0×10^{-4} g uncertainty.

4.3.6 Compression testing methodology

Samples were exposed to physiological conditions (PBS, pH = 7.4, 37 °C, 50 RPM) using a shaker incubator (Lab-Line Orbit Incubator-shaker) over a 9 week time period. After each time point degraded samples (n = 3) were removed from the buffer solution and immediately subjected to uniaxial compression testing. Wet PLGA cylinders were tested at ambient temperature (23 ± 2 °C) and relative humidity (45 ± 5 %) using an MTESTQuattro universal tester (ADMET, Norwood, MA) equipped with a 1 kN load cell operated at a crosshead speed of 0.1 mm/min with a sampling rate of 1 sample/second. The load was applied to the specimen until the yield point was reached or to 45 – 50 % its original thickness if no yield point was observed.

The compressive modulus (CM) and ultimate compressive strength (UCS) were determined as the initial slope (5 – 15 % strain) and the maximum stress at the yield point, respectively. In the absence of a yield point the maximum stress was calculated using the stress at 10 % deformation. All values are reported as the average ± standard error of mean.

4.3.7   *In vitro* thermal properties and molecular weight changes

The changes in thermal properties and molecular weight distribution during degradation were monitored using differential scanning calorimetry (DSC) and gel permeation chromatograph (GPC). PLGA cylinders were removed from the buffer every week for 9 weeks, rinsed 3x with deionized water, flash frozen with liquid nitrogen and lyophilized for 3 d (VirTis Benchtop K freeze dryer, Gardiner, NY; operating at 100 mTorr) prior to testing.

4.3.8   Powder x-ray diffraction

Samples which formed powders during degradation were loaded into quartz capillary tubes (φ = 1.0 mm) prior to goniometer head mounting. The crystallinity of the PLGA powders were evaluated at room temperature with a Bruker X8 Prospector Ultra diffractometer equipped with an APEX II CCD detector and an IμS microfocus Cu Kα source; 45 kV and 0.65 mA (λ = 1.54178 Å). The diffractograms were recorded at a detector distance of 15 cm. PXRD patterns were acquired using the APEX II software package using the PILOT plug-in and were processed using Match! phase identification software to obtain intensity versus d-spacing (Å) plots.

4.4   RESULTS

4.4.1   Naming conventions and characterization of PLGA copolymers

The sequence-defined PLGA copolymers utilized in this study were prepared using segmer assembly polymerization (SAP, Fig. 29 & C1). Using this method, discrete monodisperse sequenced oligomers termed "segmers" are polymerized using condensation conditions which preclude detrimental sequence-scrambling transesterification side-reactions.[55] It is important to note that the synthetic method has been optimized to produce copolymers with a very high degree of sequence fidelity.[147] PLGA copolymers synthesized using SAP are named based on their input segmer, C-side to O-side, where the L-lactic unit, racemic lactic unit, and glycolic unit are abbreviated as **L**, **L**$_{rac}$, and **G**, respectively. As such, a segmer consisting of a racemic lactic and glycolic acid-derived unit, would be termed **L**$_{rac}$**G** and the periodic copolymer would be named **poly L**$_{rac}$**G**. These copolymers are termed "periodic" or "sequence-defined" as they consist of a nearly perfect repetition of the input segmer. The sequence and stereopurity of all sequence-defined copolymers was confirmed via ^{1}H and ^{13}C NMR (Fig C2 – C15). The purchased random copolymers, **PDLGA-50**, **PLLGA-50** and **PDLGA-65** were prepared via ring-opening polymerization (ROP, Fig 29) whose names are derived from their input L:G-ratio and respective lactide stereochemistry. Using this convention, the **PDLGA-50** and **PLLGA-50** copolymers are the racemic and stereopure versions of a random PLGA with a 50:50 L:G-ratio and **PDLGA-65** is the racemic random PLGA derivative with a 65:35 L:G-ratio. The molecular weights of sequence-defined PLGAs and purchased random PLGA controls were comparable, 17 – 30 kDa (Table 3). All PLGAs were amorphous with T$_g$s ranging from 46 – 57 °C after heated compression molding (Table 3).

85
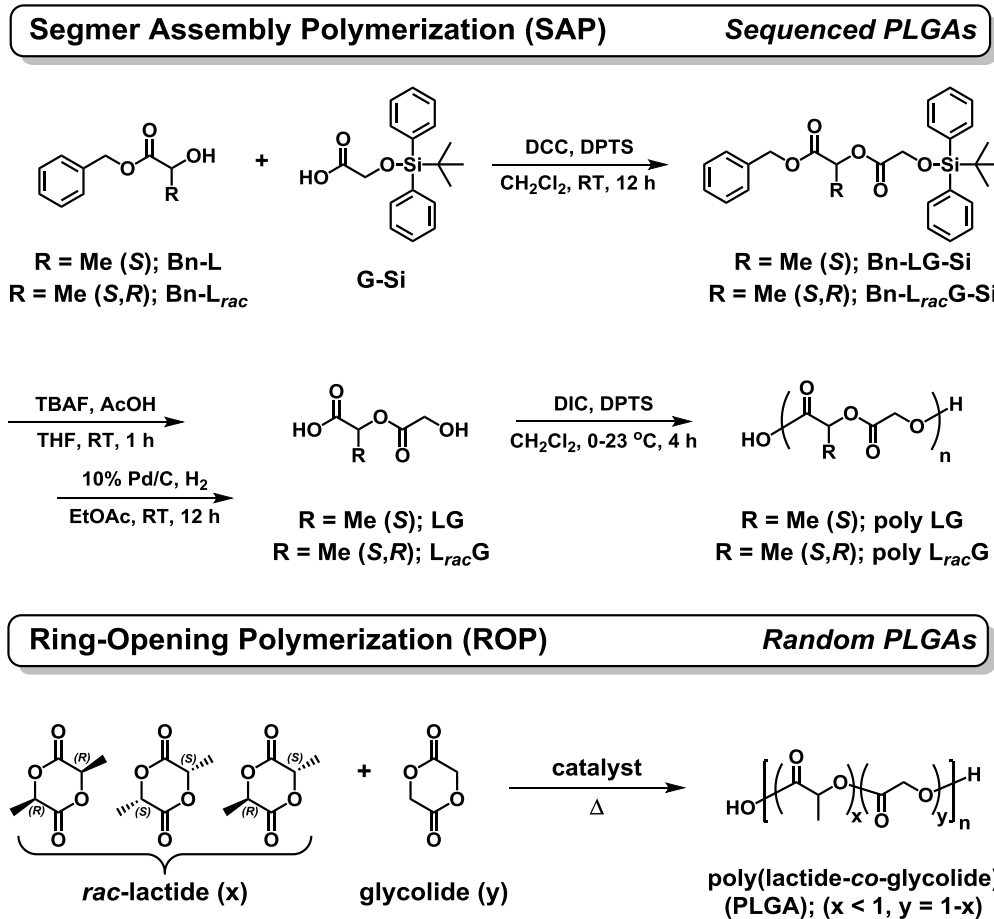
Figure 29. Segmer assembly polymerization (SAP) methodology for synthesizing sequenced-defined PLGAs, poly LG and poly L*rac*G, in addition to the ring-opening polymerization (ROP) of random PLGAs.

Table 3. PLGA characterization data for sequence-defined and random PLGA analogues.

Polymer	M_n^a (kDa)	M_w^a (kDa)	$Đ^a$	T_g (°C)[b]	ratio L:G[c]
Poly LG	22.7	32.1	1.4	48	50:50
Poly L$_{rac}$G	30.2	44.8	1.5	50	50:50
Poly GLLG	16.8	24.6	1.4	48	50:50
Poly LLG	28.9	41.0	1.4	57	66:34
PDLGA-50	21.6	29.5	1.4	46	51:49
PLLGA-50	19.3	29.3	1.5	48	54:46
PDLGA-65	28.2	42.6	1.5	47	65:35

[a] Determined by size exclusion chromatography in THF relative to polystyrene standards.
[b] Obtained in the first heating cycle at 10 °C/min after heated compression molding.
[c] Results based on ^{1}H NMR spectroscopy and presented as the ratio of the lactic (L) and glycolic (G) units.

4.4.2 Mechanical properties of sequenced and random PLGA cylindrical constructs

Degradation induced changes in mechanical properties for a set of four sequenced PLGAs and three random analogue PLGAs were measured using a uniaxial compression testing method over a 9-week time period *in vitro*. The height and width of the cylindrical test samples prepared via heated compression molding were 3.31 ± 0.02 mm and 3.34 ± 0.01 mm, respectively, with an average mass of 34.3 ± 0.2 mg (n = 380). Mechanical properties, compressive modulus (CM) and ultimate compressive strength (UCS), were measured on the wet cylinders (3 samples per time point). The CM and UCS as a function of time are reported in Fig. 30 as the average $\pm$ standard error of mean. Representative stress-strain curves for all PLGAs are included in Fig. C16.
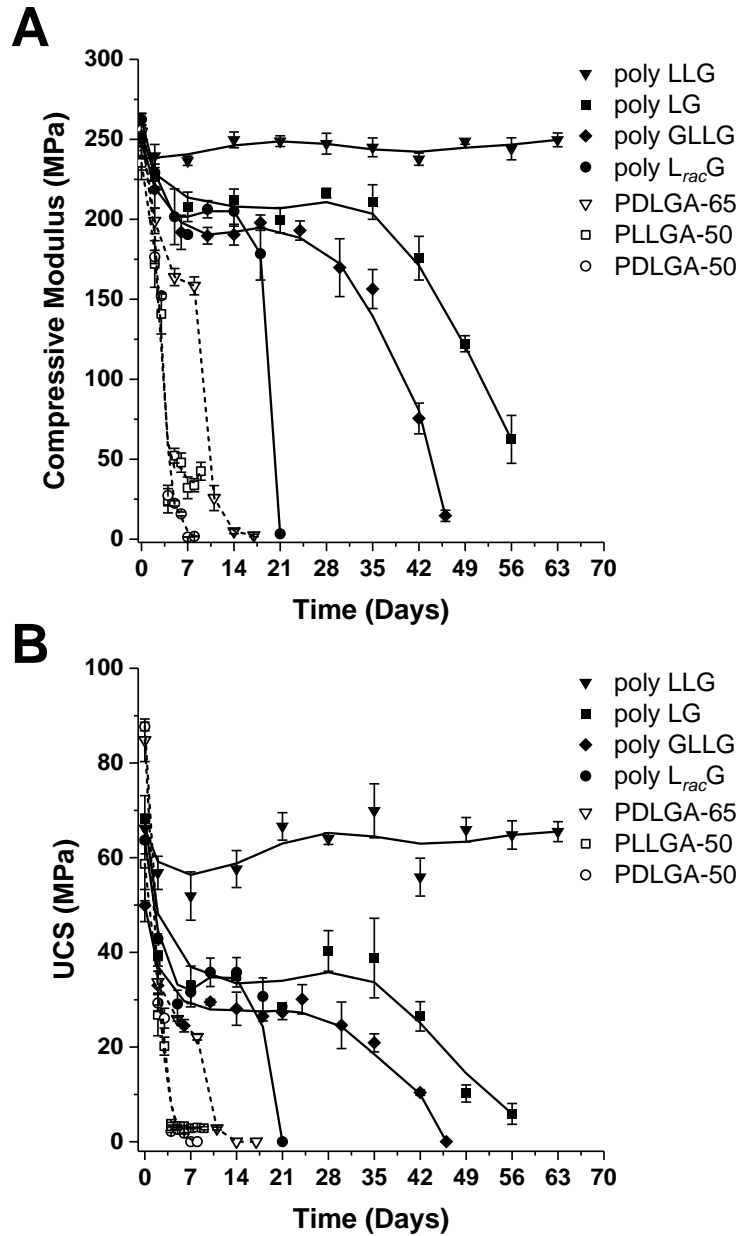
Figure 30. Compressive modulus (CM) (A) and ultimate compressive strength (UCS) (B) versus degradation time for sequenced and random PLGA copolymers. Solid (sequenced PLGAs) and dotted (random PLGAs) lines were fitted using a 1st order binomial smoothing algorithm and error bars represent ± standard error of mean (n = 3).

The initial CM and UCS for all PLGAs were similar, 250 ± 10 MPa and 68 ± 14 MPa, respectively. However, during the course of the experiment, sequenced PLGAs retained their mechanical properties over longer time periods compared to their random analogs. The retention

of mechanical properties for sequence-defined PLGAs ranged from $3 - 9$ weeks compared to $1 -$ 2 weeks for all random PLGAs. Initial decreases in CM and UCS were observed after 2 d of incubation for all PLGAs, with the exception of **poly LLG**. At this time, the CM and UCS of the random PLGAs decreased by 66 ± 12 MPa and 47 ± 14 MPa, respectively. Comparatively, the CM and UCS for sequenced PLGAs decreased by 30 ± 4 MPa and 19 ± 8 MPa, respectively. Throughout the first week of degradation both CM and UCS for the 50:50 L:G-ratio random PLGAs, **PDLGA-50** and **PLLGA-50**, consistently decreased to 90 % and 95 % of their initial values by 4 d, respectively. The mechanical properties for **PDLGA-65** gradually decreased from $199 - 158$ MPa (CM) and $34 - 22$ MPa (UCS) prior to failure at 11 d in contrast to the 50:50 L:G-ratio random PLGAs. All sequence-defined PLGAs showed insignificant changes in mechanical properties during this time period (i.e., $2 - 14$ d) with an average CM and UCS of 214 ± 13 MPa and 39 ± 6 MPa.

Sequenced based changes in mechanical properties were observed after 21 d *in vitro*. At 21 d, a rapid decrease in mechanical properties for **poly L$_{rac}$G** was observed and correlated to CM and UCS losses of 175 MPa and 31 MPa, respectively. In contrast, the mechanical properties for **poly LG** and **poly GLLG** were retained for 5 weeks prior to gradually decreasing over the subsequent 3 weeks. More significant changes in CM and UCS were observed for **poly GLLG** than **poly LG** during this time. It is important to note that the failure mechanism of **poly LG** shifted from a ductile mechanism to a brittle failure mechanism after 35 d *in vitro* (Fig. C17). This behavior was not observed for any additional PLGAs; however, **PLLGA-50** and **poly L$_{rac}$G** did form powders after 35 d which were similar to that of **poly LG** after 63 d. At 42 d, the CM and UCS for **poly GLLG** decreased to 70 % and 79 % of their initial values whereas **poly LG**

only decreased by 31 % and 61 %. No significant changes in CM or UCS were observed for **poly LLG** over the 9 week experimental time period, 245 ± 2 MPa and 62 ± 2 MPa, respectively.

4.4.3   Thermal properties for sequence-defined and random PLGAs as a function of degradation

To understand the relationship between the thermal properties of PLGAs and their degradation, additional differential scanning calorimetry (DSC) analysis was performed on sequence-defined and random PLGA analogues over a 9 week time period after being exposed to physiological conditions. DSC thermograms for lyophilized samples over the course of 9 weeks of degradation are reported in Fig. 31, where the first heating cycles are displayed to reflect the *in situ* thermal properties of the cylinders after hydrolysis.
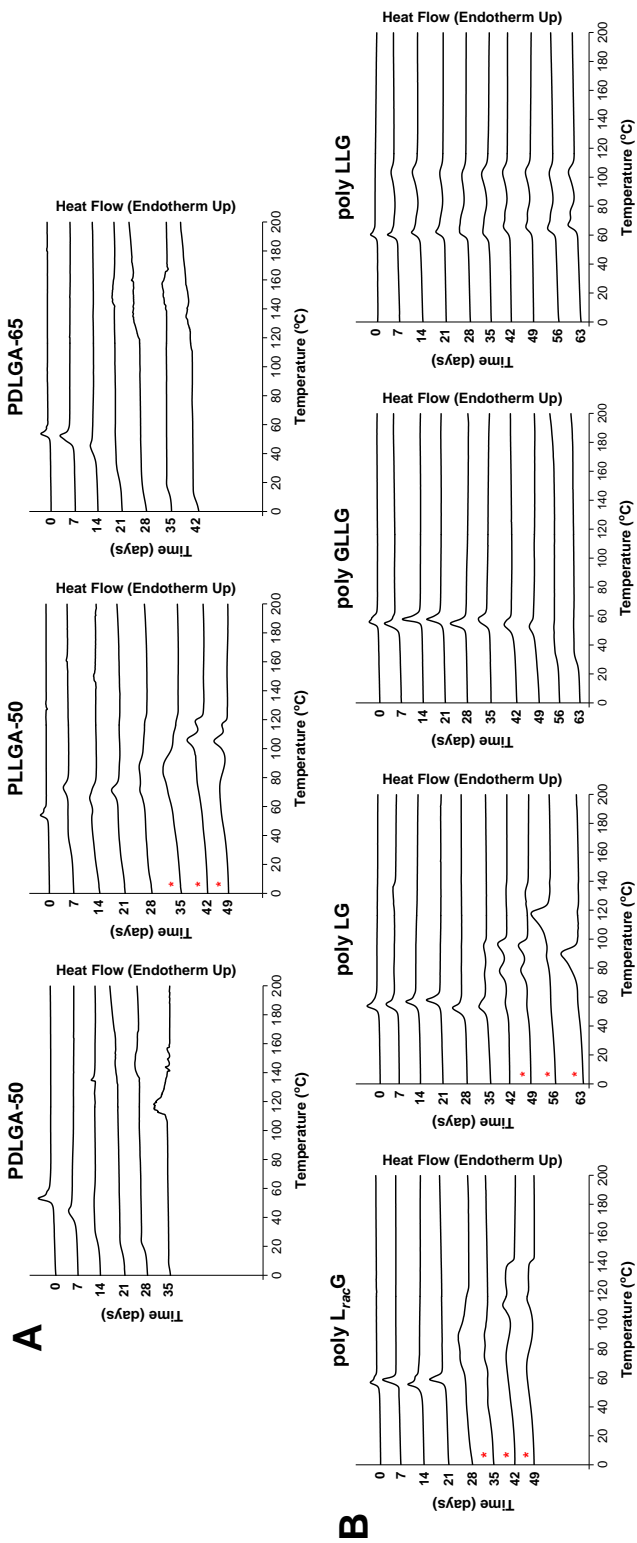
Figure 31. Differential scanning calorimetry thermograms of random (A) and sequenced (B) PLGAs as a function of degradation time. *Crystallinity was analyzed using x-ray diffraction.

The initial thermograms for all PLGAs displayed a single phase transition, T_g ranging from 46 – 58 °C. Dramatic differences in thermal property retention can be seen in the comparison of the DSC traces for random PLGAs, Fig. 31A, and sequenced PLGAs, Fig. 31B. Within the first week of incubation 50:50 L:G-ratio random PLGAs no longer retained their virgin thermal properties. At this point the T_gs approached 37 °C and additional melting transitions appeared at ~ 70 °C for **PLLGA-50**. Sequenced PLGAs retained their original amorphous thermal properties with the exception of **poly LLG** which exhibited semi-crystalline behavior with a T_m of ~ 110 °C. In the subsequent weeks, degradation induced changes in thermal properties were most prominent for random PLGAs. The T_gs of these samples rapidly decreased below physiological temperature by 21 d and high temperature melting transitions (130 – 170 °C) evolved in the racemic random PLGAs. During this time period, no changes in thermal properties were observed for all sequence-defined PLGAs. However, the T_g for **poly L$_{rac}$G** drastically decreased and broad melting transitions were observed from 70 – 130 °C at 21 d. It is important to note that the T_g for **poly L$_{rac}$G** was difficult to identify at this time due to the presence of broad melting transitions which may have overlapped with a T_g. Similar broad melting transitions were also present for **poly LG** after 35 d, however, a clean but slightly shifted T_g remained. After 35 d, all random racemic PLGAs exhibited semi-crystalline behaviors with T_gs < 10 °C and T_ms spanning 115 – 175 °C in contrast to the random stereopure PLGA, **PLLGA-50**, which was crystalline with broad T_ms ranging from 50 – 125 °C. Sequenced stereopure PLGAs retained their original thermal properties over this time period (i.e., 0 – 35 d). At 7 weeks, the glass transition temperatures for **poly LG** and **poly GLLG** began to decrease and differences in thermal behaviors between these samples were observed. **Poly LG** appeared semi-crystalline with a T_g of 48 °C and T_ms of 77 and 97 °C whereas **poly GLLG** was

amorphous with a T_g of 48 °C. In the subsequent weeks the degree of enthalpic relaxation decreased for these copolymers, exemplified by a T_g which no longer appeared as a peak. During week 7, the T_g for **poly GLLG** slowly shifted to 28 °C whereas the T_g for **poly LG** was ~ 40 °C. A clear T_g was no longer present for **poly LG** during weeks 8 – 9; however, large T_ms were observed. Over the course of 9 weeks, **poly LLG** remained semi-crystalline with a T_g of 60 °C and T_m of 102 °C.

4.4.4 Molecular weight distributions for sequence-defined and random PLGAs as a function of degradation

Trends in degradation were further characterized using gel permeation chromatography (GPC). Molecular weight profiles for sequence-defined and random PLGAs over the course of 9 weeks of degradation are shown in Fig. 32.
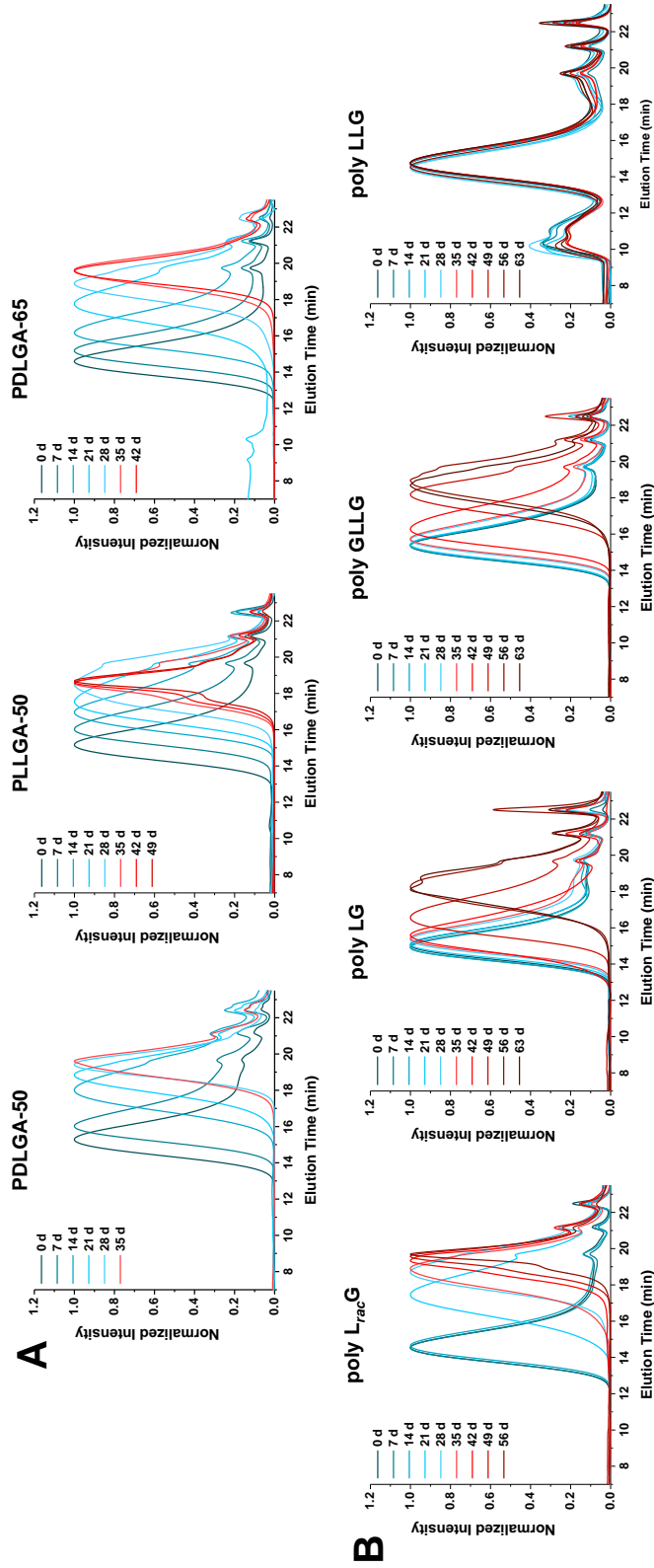
Figure 32. Gel permeation chromatography chromatograms of random (A) and sequenced (B) PLGAs as a function of degradation time.

Initial molecular weights for all PLGAs were similar. Significant reductions in molecular weight and dispersity were observed over shorter time periods for all random PLGAs. The molecular weights for random PLGAs consistently decreased in an exponential fashion while dispersity concomitantly increased throughout 0 – 28 d. The molecular weight profiles for random PLGAs during this time period shifted from a monomodal to a slightly polymodal distribution. The periodic sequenced PLGAs, with the exception of **poly L$_{rac}$G**, preserved their initial molecular weight profiles during this time period. A drastic decrease in molecular weight and increase in dispersity was observed at 21 d for **poly L$_{rac}$G**, while maintaining a monomodal distribution. After 35 d, the molecular weights of random PLGAs plateaued in low molecular regions and dispersity subsequently decreased. Interestingly, higher molecular weight oligomers, $\approx$ 10 % of the original molecular weight remained for **PLLGA-50**, whereas the random racemic PLGAs were $\approx$ 4 % of $M_{n(0)}$. Similar behaviors were observed for **poly L$_{rac}$G** at later time points. The molecular weight profiles for stereopure sequenced defined PLGAs slightly decreased over 35 d of incubation while retaining their original dispersities. Significant shifts in molecular weight for **poly GLLG** and **poly LG** occurred during week 6 and week 7, respectively. Minimal changes in dispersity were observed during these time points. At 63 d the molecular weight profiles for **poly GLLG** and **poly LG** shifted to a polymodal distribution. No significant changes in molecular weight or dispersity were recorded for **poly LLG**; however, unique peaks corresponding to high molecular weight aggregates were present in the GPC traces for this sample throughout the hydrolytic time period.

4.4.5 Characterization of hydrolyzed PLGAs using ^{1}H-NMR

The composition of sequence-defined and random PLGA copolymers as a function of degradation were characterized using proton nuclear magnetic resonance spectroscopy over a 9 week time period. ^{1}H-NMR spectra displaying the chemical shift regions of δ 5.6 − 3.4 ppm and δ 1.8 − 1.3 ppm for all PLGAs as a function of time are included in Figs. C18 − C31. These chemical shift regions contain resonances associated with the methine, methylene, and methyl groups of PLGA. Additional end-group associated resonances appear over the course of degradation in the region of δ 4.5 − 4.2 ppm. An example data set containing only the methine and methylene resonances for **PDLGA-50** and **poly LG** is included in Fig. 33.
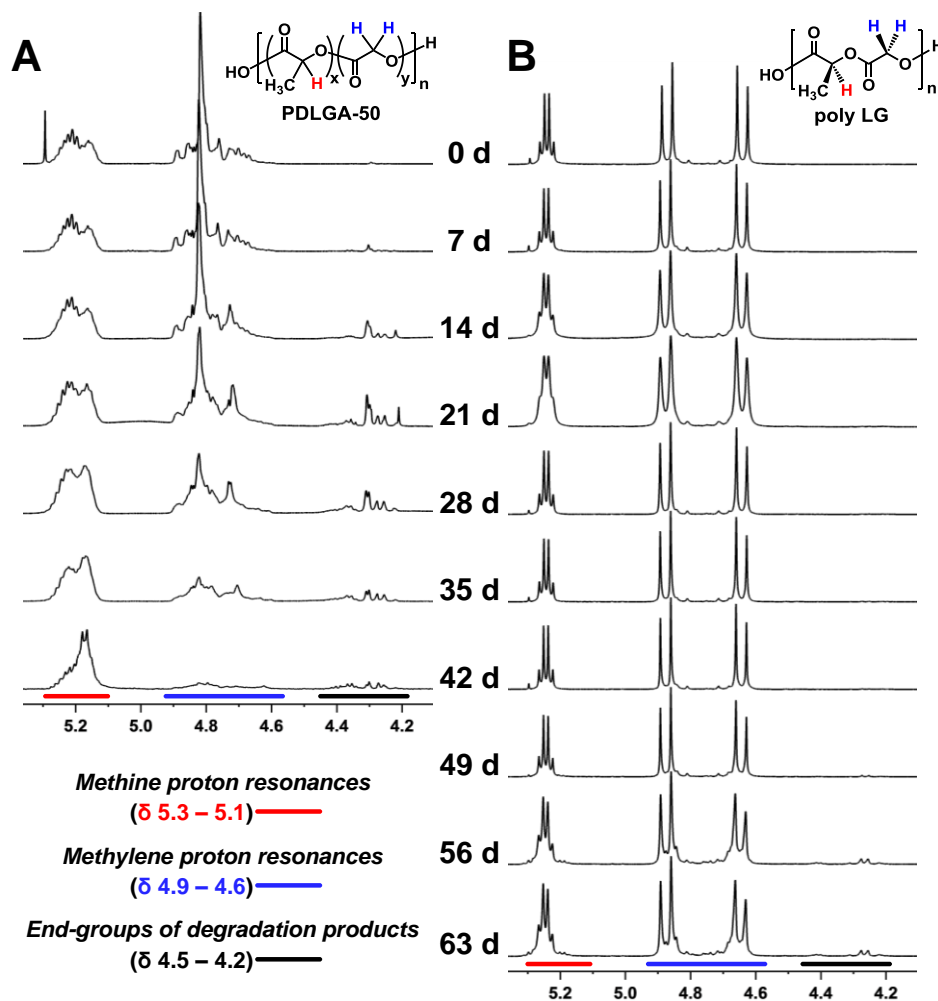
Figure 33. ^{1}H NMR comparison in the region of δ 5.4 – 4.1 ppm for PDLGA-50 (A) and poly LG (B) over the course of 63 d in vitro hydrolysis.

In examining the ^{1}H NMR spectra, it can be seen that the microstructural composition of random PLGAs rapidly changes over the course of degradation compared that of sequence-defined samples. Significant changes in L:G-ratio and the production of hydrolytically generated end-groups occurred more readily for random PLGAs. The L:G-ratios for random PLGAs gradually increased over 42 d exemplified by the prevalence of L-methine resonances (δ 5.3 – 5.1 ppm) and concomitant decreases in G-methylene resonances (δ 4.9 – 4.5 ppm). The rate at which this transition occurred followed the trend of: **PDLGA-50** > **PLLGA-50** > **PDLGA-65**.

After 42 d, the composition of **PLLGA-50** was predominately L-units, which remained unchanged over the subsequent 2 weeks. Sufficient sample quantities for ^{1}H NMR spectrum acquisition was no longer present for the random racemic PLGAs during this time period. In contrast to the random PLGAs, the L:G-ratio for sequence-defined PLGAs remained unchanged over the course of degradation.

The ^{1}H NMR spectra for random PLGAs were also observed to contain larger quantities of hydrolytically generated end-groups resonances compared to those of sequence-defined PLGAs. These resonances appeared during the first week of hydrolysis for all random PLGAs at δ 4.5 − 4.2 ppm. Throughout the first 4 weeks of degradation, end-group associated resonances gradually increased prior to decreasing in the subsequent weeks. The frequency of end-group associated resonances was greatest for random racemic PLGAs, **PDLGA-50** and **PDLGA-65**, compared to the random stereopure PLGA, **PLLGA-50**. End-group associated resonances were not observed in the ^{1}H NMR spectra for sequence-defined PLGAs until week 5. At this time, end-group resonances slowly evolved for **poly L$_{rac}$G** and **poly GLLG** in contrast to **poly LG** and **poly LLG**, which remained unchanged. At 56 and 63 d, changes in the ^{1}H NMR spectra for **poly L$_{rac}$G**, **poly GLLG**, and **poly LG** were observed. No changes were observed for **poly LLG** throughout the course of the experiment.

4.4.6 Degradation induced crystallinity characterized using powder x-ray diffraction

PXRD diffractograms showing the calculated d-spacing (Å) for **PLLGA-50**, **poly L$_{rac}$G**, and **poly LG** are shown in Fig. 34. It is therefore confirmed that **PLLGA-50** and **poly L$_{rac}$G** maintain their respective semi-crystalline structures over the period of 35 − 49 d. In comparison, **poly LG** underwent phase changes from week 7 to week 9, indicated by emergence and

98

disappearance of peaks on the diffractograms. This observation implies that progressive degradation of **poly LG** can lead to re-organization of molecular packing patterns. It is noteworthy to mention that additional peaks corresponding to crystallized salt from the phosphate buffer are occasionally observed in the diffractograms.
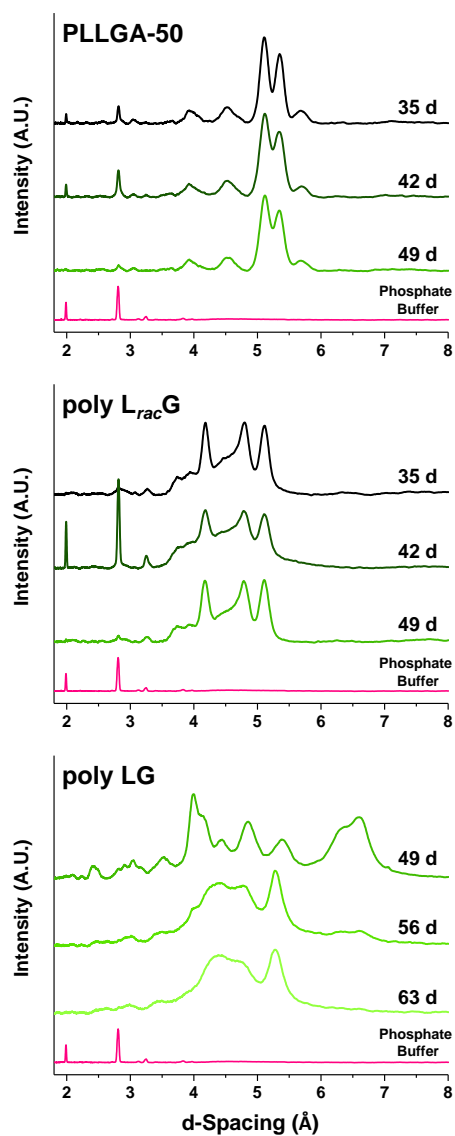

Figure 34. Powder x-ray diffraction diffractograms of PLLGA-50, poly LracG, and poly LG at various time points during the latter stages of degradation.

4.5   DISCUSSION

The dependence of the degradation properties of PLGAs on sequence is unmistakable and the data in this study correlate well with our prior studies. In particular, we found that PLGAs with identical L:G-ratios but different monomer arrangements exhibited dramatically different hydrolytic degradation profiles. The sequenced copolymers lost molecular weight more gradually and retained morphology and bulk mechanical properties for a longer period of time relative to their random analogues. In addition, we observed differences in behavior between sequenced copolymers with differing monomer arrangements and stereochemistry. Sequenced-defined PLGAs which possessed no fast-hydrolyzing G-G linkages (i.e., **poly LLG** and **poly LG**) were found to degrade more gradually than those in which G-G connections were present, (e.g., **poly GLLG**). In addition, stereopure sequenced-defined PLGAs retained their properties over longer time periods compared to racemic analogues (i.e., **poly LG** vs. **poly L$_{rac}$G**). These results are consistent with our previously published results of similarly sized cylindrical implants and smaller microparticle matrices.[60-62, 179]

It is important to note that while the thermal and mechanical properties of these polymers differ significantly as a function of degradation, the initial values of these properties were relatively independent of microstructural composition. The fundamental interchain interactions that control free volume do not appear to depend significantly on the order of the monomers within the chain. Immediately after fabrication, the samples are amorphous and the T_gs of samples with the same L:G ratio and molecular weight are similar. Although most samples develop some crystallinity later in the degradation, the molecular weight profiles at these time points suggest that the crystals comprise primarily oligomers with $M_{n(t)} \leq 0.10 \times M_{n(0)}$. The

stability and composition of these crystalline oligomers were observed to depend on sequence and stereochemistry as illustrated by the DSC thermograms and ^{1}H-NMR spectra. Sequence-defined PLGA oligomers retained their original repeat unit sequence with minimal sequence scrambling throughout the degradation period whereas the oligomers produced from random PLGAs shifted composition such that at later time points the samples comprised primarily L-units. In addition, sequenced and random stereopure PLGAs were observed to persist over longer time periods as higher molecular weight oligomers compared to their racemic analogues. Moreover, in the latter points of degradation, the failure mode of racemic PLGAs was primarily ductile whereas stereopure PLGAs has minimal plastic deformation which was accompanied by brittle fracture.

In order to understand the origin of the sequence-based differences in behavior it is useful to consider the relationship of the various properties as a function of degradation time. Based on the data reported herein, our previously reported findings,[60-62, 179] and poly(α-hydroxy acid) degradation studies reported by others,[28, 84, 94-95, 99, 184-185, 188, 191-192, 194] the properties of solid matrices can be seen to follow the general multi-phase trend pictured in Fig. 35. Here, Phase I of degradation involves the diffusion of water into the construct while molecular weight and T_g are maintained; this induction period, designated τ defines, in many aspects, the time periods involved for later changes. In the second phase, molecular weight decreases due to hydrolysis in a linear fashion prior to transitioning into an exponential decrease due to the aggregation/crystallization of lower molecular weight components. During Phase III, sufficient polymer chain ends and oligomers have been produced to auto-catalytically enhance degradation, molecular entanglement reaches a critical minimum, and water diffusion increases due to the formation of osmotic gradients. Data from the current study and prior studies demonstrate these

changes.[34, 62, 179] In particular, we and others have noted previously that swelling occurs only *after* a significant loss of molecular weight. In the current study, moreover, we observed a correlation between the onset of swelling and the loss of mechanical properties. The initiation of Phase IV occurs only after mechanical properties have reached a minimum, swelling has reached a maximum, and chains have become small enough to become solubilized in water. This multi-phase degradation profile has been observed for biodegradable polyesters.[186, 194-195]
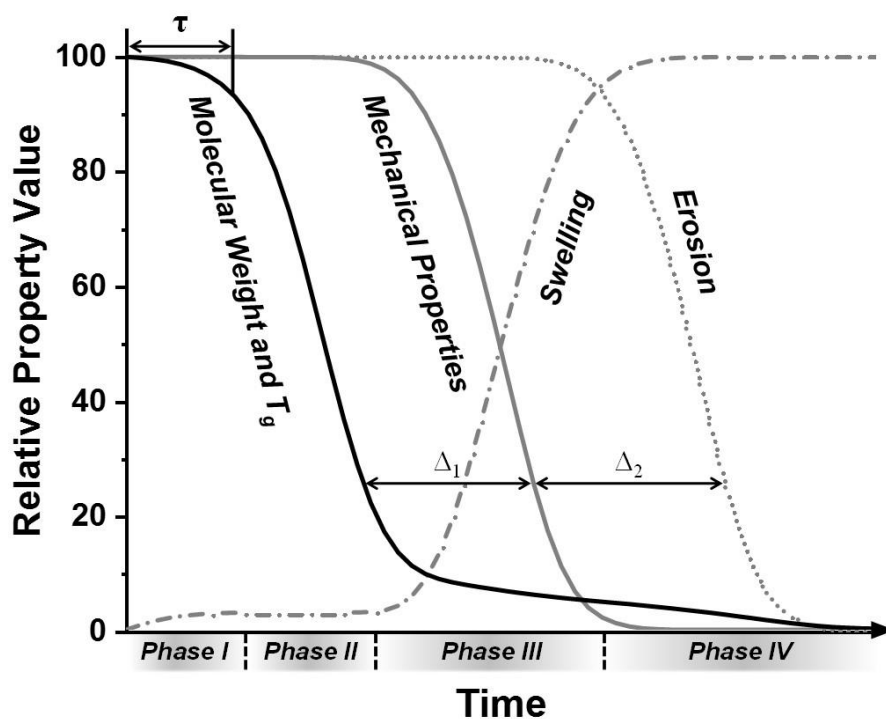
Figure 35. Multi-phase degradation behavior of PLGAs, where Δ_1 and Δ_2 represent differences in property retention times, depend on the microstructural composition of the copolymer, and are not equivalent.

Importantly, the difference in behavior between sequence-defined PLGAs appears to be in the length of the hydrolytic induction time period, τ. During this period, small reductions in all properties are observed. Once molecular weight begins to decrease (and the rate of the drop does also depend on sequence although not as strongly), other molecular-weight dependent properties change rapidly (i.e., thermal, mechanical, morphological). We therefore propose that sequenced-

based differences in τ are largely responsible for the variations in mechanical property retention for these PLGAs.

We hypothesize that the difference in the observed τ's correlates with the molecular mechanism of chain scission and further that the dominant mechanism varies with sequence. In the current study we observe that **poly LG**, **poly GLLG**, and **poly LLG** exhibit similar degradation patterns. These samples retain their mechanical properties over longer time periods, gradually lose molecular weight while maintaining their initial dispersity, have slight changes in T_g over time prior to plasticizing or crystallizing, and have minimal changes in their ^{1}H-NMR spectra. These behaviors are consistent with a chain-end scission mechanism, which due to the relatively slow accumulation of acid, does not become auto-catalytic for a period of time depending on composition (Fig. 36). It has been established that PLA degrades according to this profile as reported by Bikiaris and coworkers.[196] In addition, Gleadeall and Antheunis have shown by modeling that chain-end scission would be expected to give the molecular weight loss patterns similar to those observed for our sequence-defined PLGAs and more generally for many homopolyesters.[194, 197-199] In contrast, the more heterogeneous random copolymers **PLLGA-50**, **PDLGA-50**, and **PDLGA-65** exhibit a degradation pattern that is more consistent with random chain scission mechanisms. Specifically, all show a rapid production of end-group associated resonances, a decrease in G-related ^{1}H-NMR signals, rapid loss of molecular weight, and increases in dispersity.
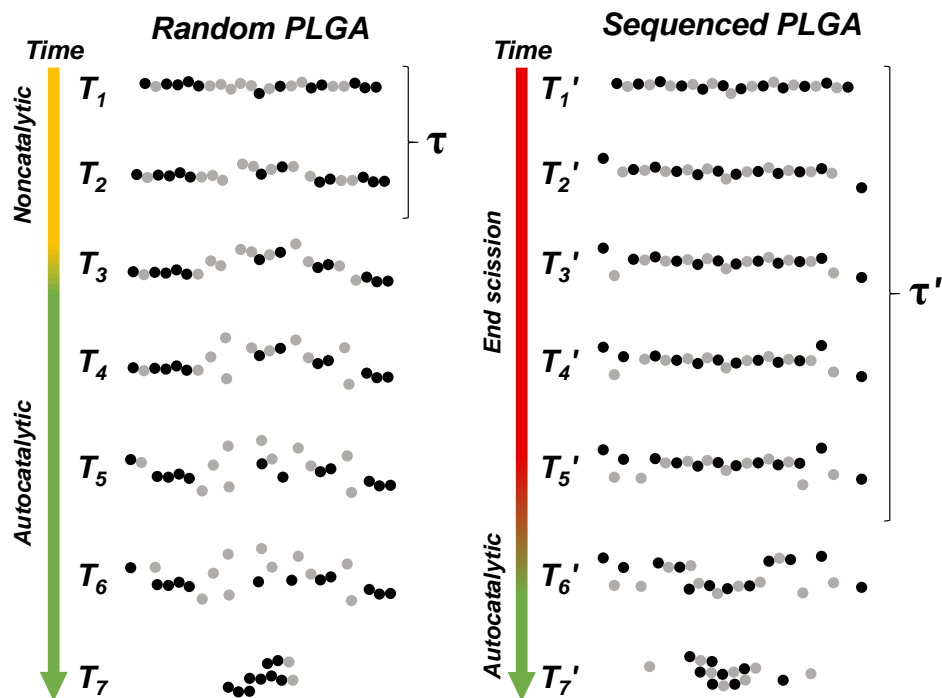
Figure 36. Degradation scheme for random and sequenced PLGA copolymers as a function of hydrolysis time where time $T \neq T'$ and $\tau \neq \tau'$, as these parameters depend on the microstructural composition of the copolymer. Colors correspond to specific hydrolysis mechanisms (i.e., noncatalytic (yellow), autocatalytic (green), and end-scission (red)). Oligomeric crystallization is represented in T_7 and T_7'.

The molecular mechanism contribution to the degradation profile may also be synergistically enhanced by differences in intermolecular packing between the more and less regular polymers and variations in chain-end occupancy volumes.[84] This enhancement could explain, in part, why **poly L$_{rac}$G** degrades more rapidly than the stereopure analogue. Although not clearly reflected in the T_gs (48 °C, **poly LG** vs. 50 °C, **poly L$_{rac}$G** as prepared without significant annealing) it seems likely that the stereopure analog would pack more uniformly and inhibit to some degree random chain scission. Based on this reasoning, all sequenced copolymers may, in general, be expected to favor chain-end scission. With our current data, we cannot, however, determine to what degree differences in chain packing contribute to the observed degradation pattern.

4.6   CONCLUSIONS

This study provides valuable insight into the influence of microstructural chain scission events and macroscopic bulk properties for sequenced PLGAs. The experimental results presented in this study correlate well with our previously reported findings regarding the swelling, erosion, and degradation behaviors of sequence-defined and random PLGA matrices. It was shown that sequence-defined PLGAs retain their mechanical properties over significantly longer induction time periods compared to random PLGAs with that same L:G-ratio. We have identified that the molecular mechanism of degradation for sequence-defined PLGAs primarily proceeds through end-scission events which strongly influences the retention of macroscopic bulk properties. This mechanism differs from conventionally used random PLGAs which degrade through non- and auto-catalytic hydrolysis. These experimental observations support previously published computation models and *in vitro* PLGA degradation studies. Future work will focus on developing a deeper understanding of the *in vivo* performance of sequence-defined PLGAs as craniomaxillofacial fixation devices.

5.0   PROSPECTUS

Using sequence-defined PLGAs, Li and Washington both observed low and inconsistent loading efficiencies of various target molecules using W/O/W and O/W emulsion methods. These encapsulation methodologies have been optimized for random PLGAs. There is considerable evidence to support the conclusion that sequence-defined PLGAs favor more uniform packing and have smaller chain occupancy volumes compared to random PLGAs. Therefore, future work will focus on developing optimized conditions for drug encapsulation. We are particularly interested in investigating the effects of molecular weight, polymer concentration, preparation temperature, and solvent evaporation time which all have been previously reported to influence the internal morphology, glass transition temperatures, drug distribution, and release profiles for PLGA microparticles.[200] Additional methods for improved drug loading have also been reported by Smith, Schwendeman, Elaissari and coworkers.[201-204]

Increasing the loading efficiencies for sequence-defined PLGA microparticle matrices is of particular interest as Li *et al.* observed slower and more gradual rhodamine B release rates from sequence-defined PLGA microparticles. Optimization would allow us to investigate the *in vivo* release of a target molecule that would benefit from a controlled gradual release profile. We hypothesize that sequence-defined PLGAs would efficiently deliver daunorubicin, an antibiotic drug for treatment of proliferative vitreoretinopathy, a complication resulting from retinal detachment. In this application, repeat ocular proliferation is not desired, therefore the release of

daunorubicin must be gradual and controlled within the therapeutic treatment window. In addition, the release and accumulation of acidic by-products from sequence-defined PLGA microparticles occurs at a significantly slower rate compared to random PLGAs. This is particularly advantageous as changes in the pH of the vitreous are known to be detrimental to intraocular tissues.[205-206]

We are also interested in exploring the interactions between sequence-defined PLGAs and large macromolecules such as peptides and proteins. We hypothesize that polymer-protein sequence affinities may enhance the loading efficiencies and offer a more controlled delivery of valuable macromolecular payloads. Applications which would benefit from the high-loading and controlled delivery of peptides and proteins include the treatment of cancer, endometriosis, and diabetes. To test this hypothesis we will utilize an anti-angiogenic protein which is utilized for the treatment of lung cancer, endostar.[207] Currently, a therapeutic effect of this protein is only achieved after multiple high dose injections.[208] Using computational modeling, we will screen various PLGA sequences to identify viable candidates, which have high copolymer-endostar affinities. In a pilot *in vitro* study we will determine the loading efficiencies, monitor the release of endostar from various sequence-defined PLGA microparticle matrices, and evaluate the conformational stability of endostar upon release. As endostar is a recombinant human endostatin with a nine-amino acid tag (i.e., MGGSHHHHH), we are also interested in exploring the effects of end-capping sequence-defined PLGAs with a MGGSHHHHH depsipeptide derivative to enhance polymer-endostar interactions, prolong microparticle degradation rates, and promote a more gradual release profile.

Supporting Information for Chapter 2
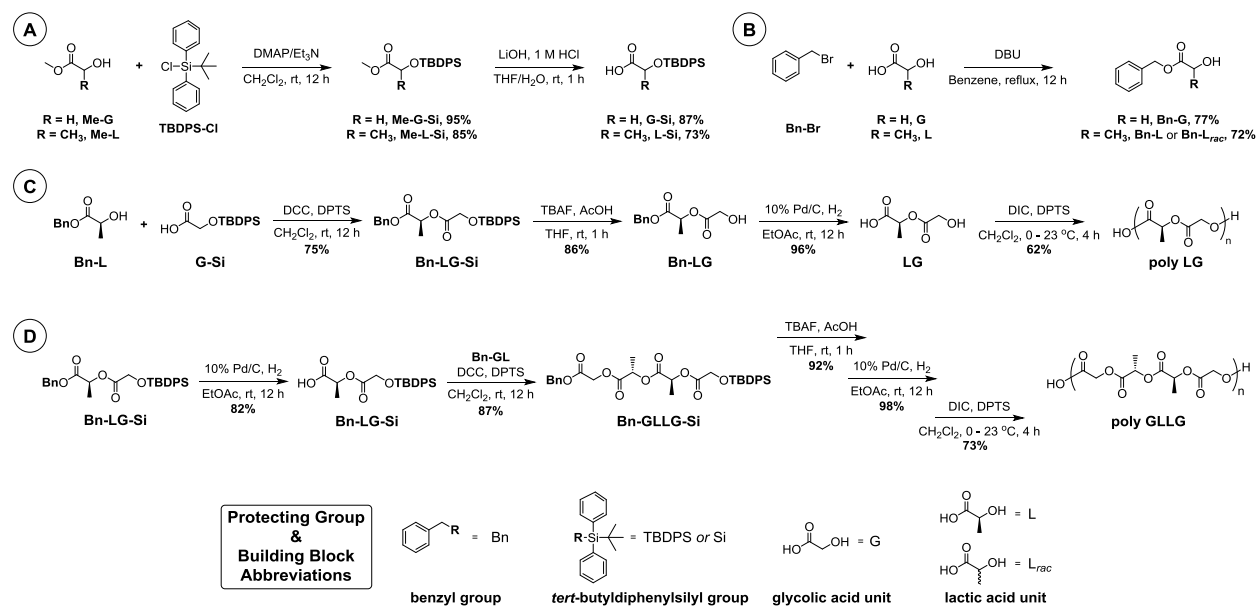
Figure A1. Synthesis of orthogonally protected lactic and glycolic acid building blocks, *tert*-butyldiphenylsilyl

protected alcohols (A) and benzyl protected carboxylic acids (B), and segmer assembly methodology of simple (C)

and complex (D) sequenced poly(lactic-*co*-glycolic acid)s.
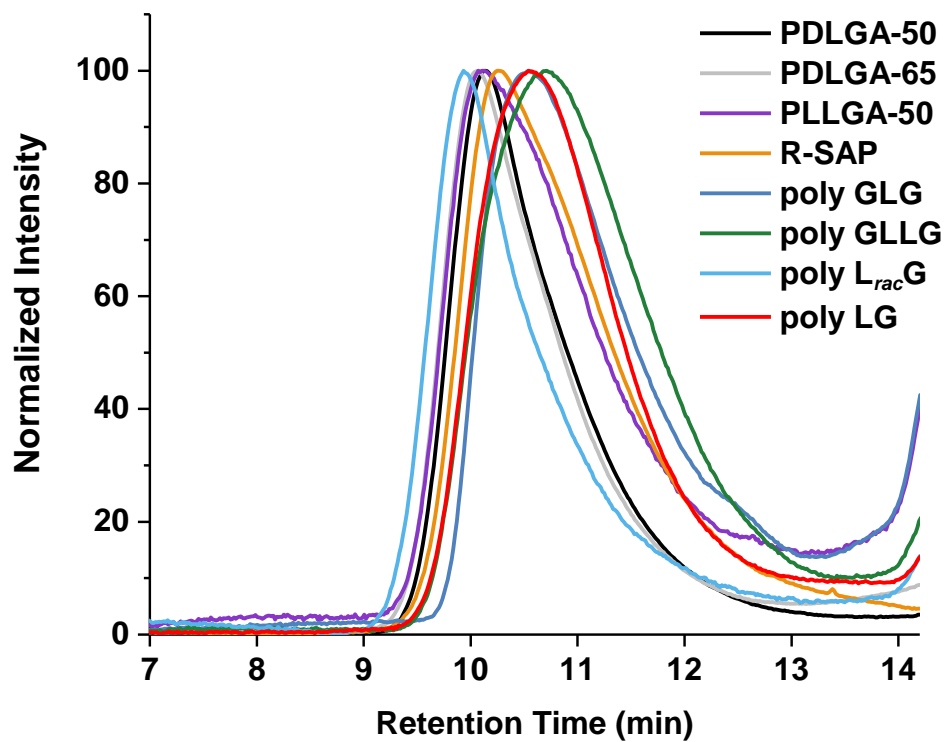
Figure A2. Gel permeation chromatography (GPC) chromatograms of sequenced and random PLGAs acquired using a THF mobile phase, calibrated relative to polystyrene standards.
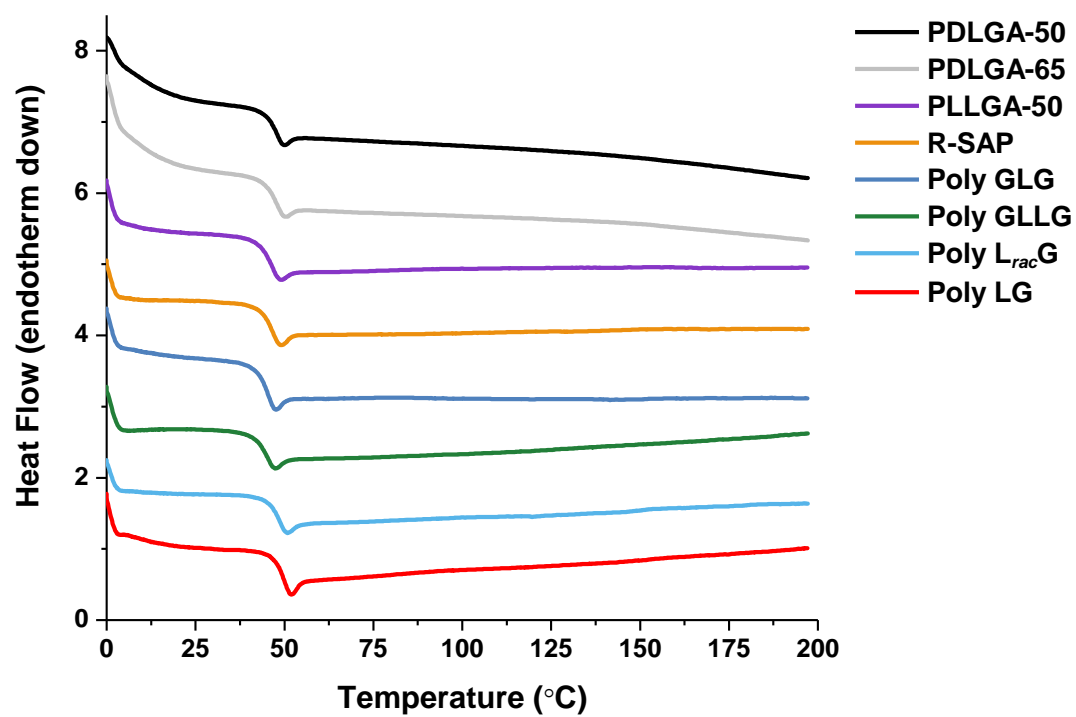
Figure A3. Differential scanning calorimetry (DSC) thermograms of sequenced and random PLGAs acquired from the second heating cycle at a rate of 10 °C/min.
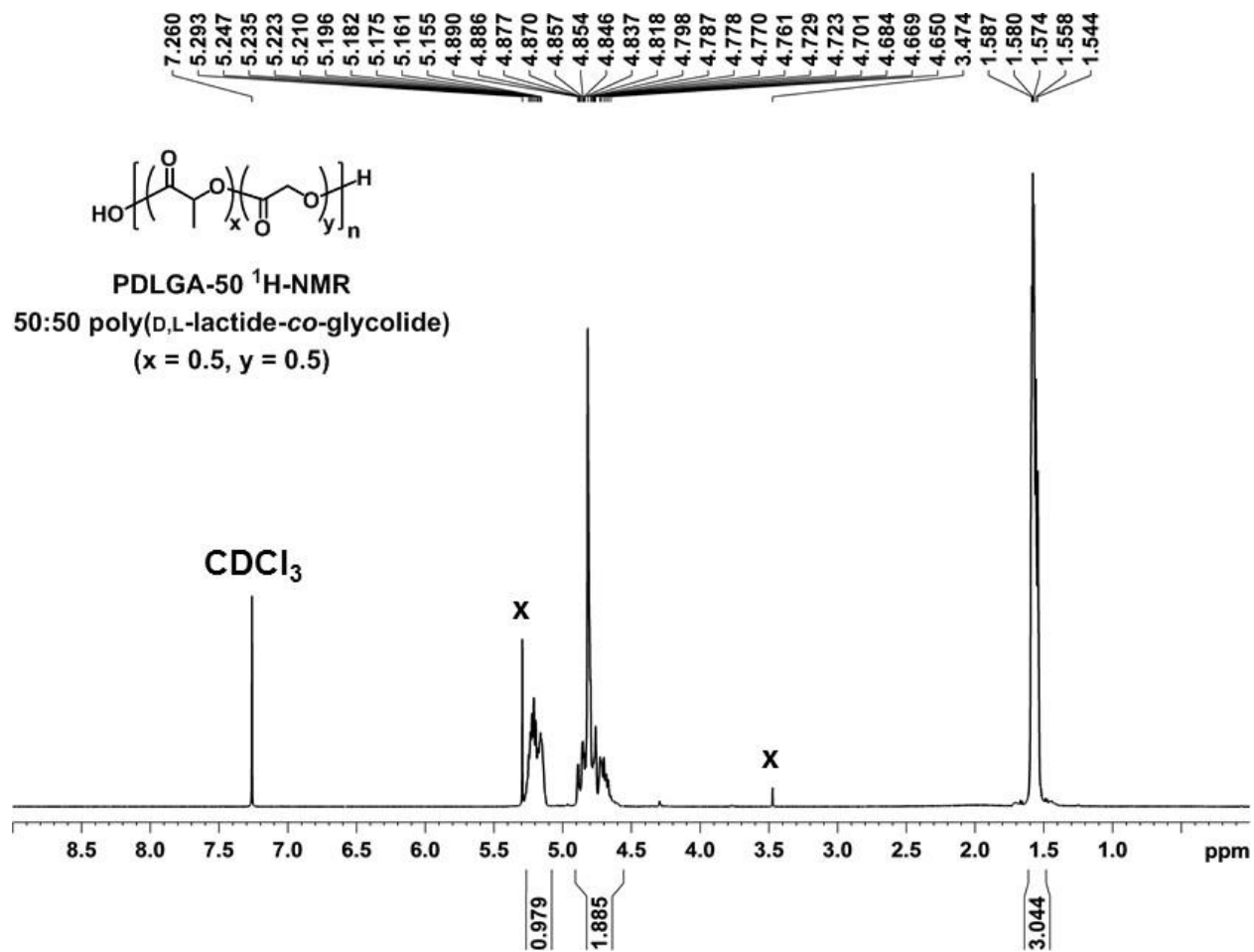
Figure A4. ^{1}H NMR (500 MHz, δ 9.0 – 0.0 ppm) of 50:50 poly(D,L-lactide-*co*-glycolide) (PDLGA-50)
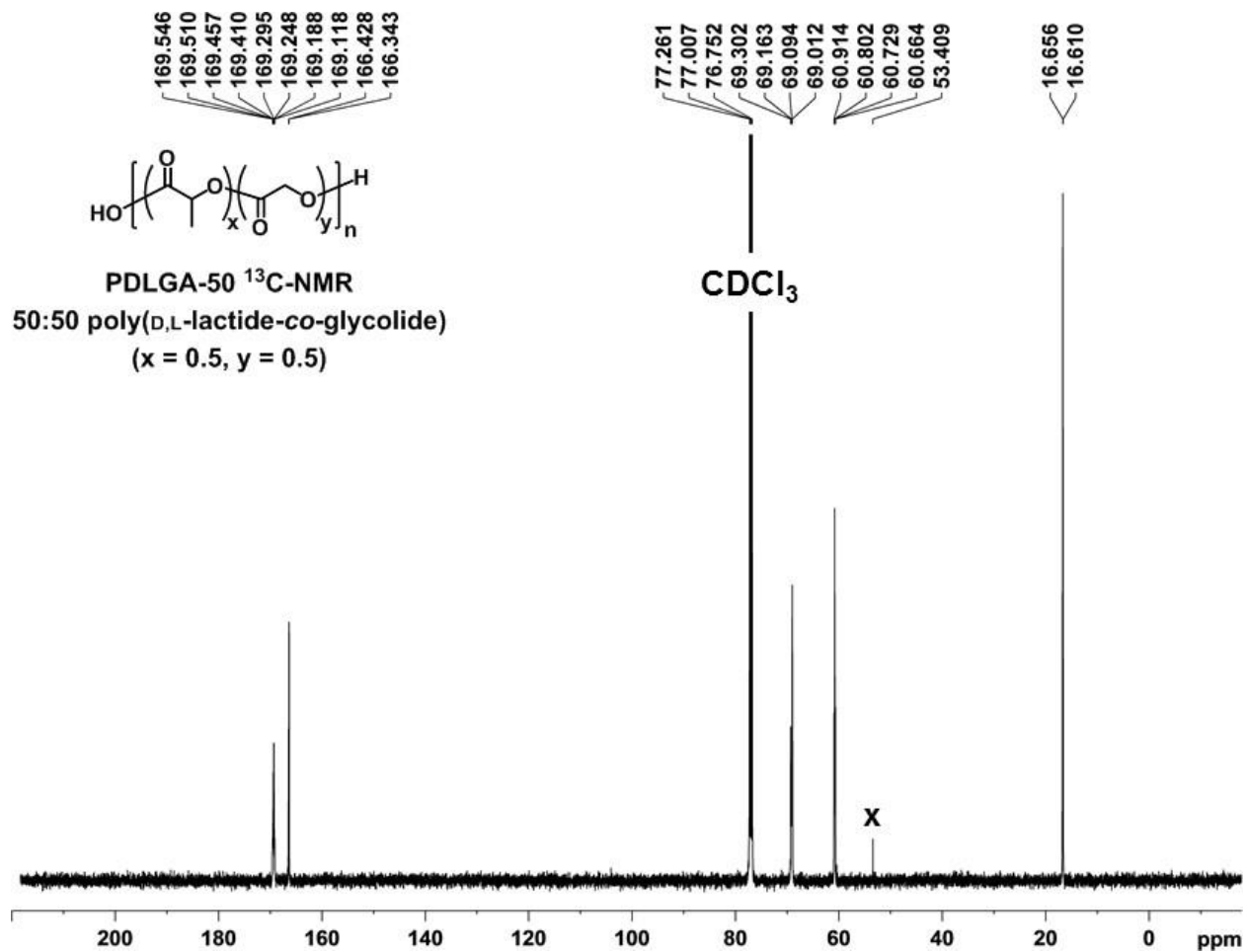
Figure A5. ^{13}C NMR (500 MHz, δ 220 – -10.0 ppm) of 50:50 poly(D,L-lactide-*co*-glycolide) (PDLGA-50).
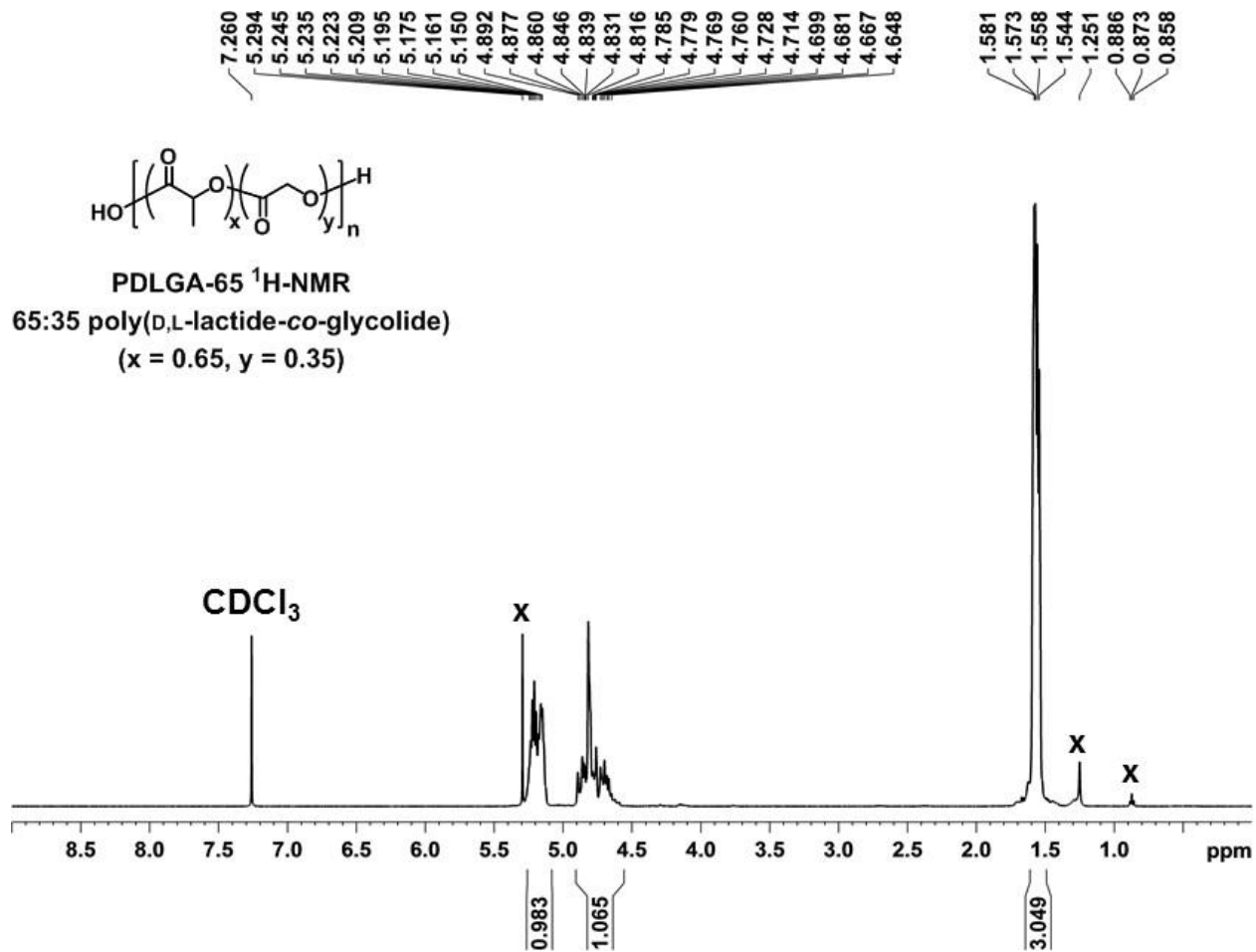
Figure A6. ^{1}H NMR (500 MHz, δ 9.0 – 0.0 ppm) of 65:35 poly(D,L-lactide-*co*-glycolide) (PDLGA-65).
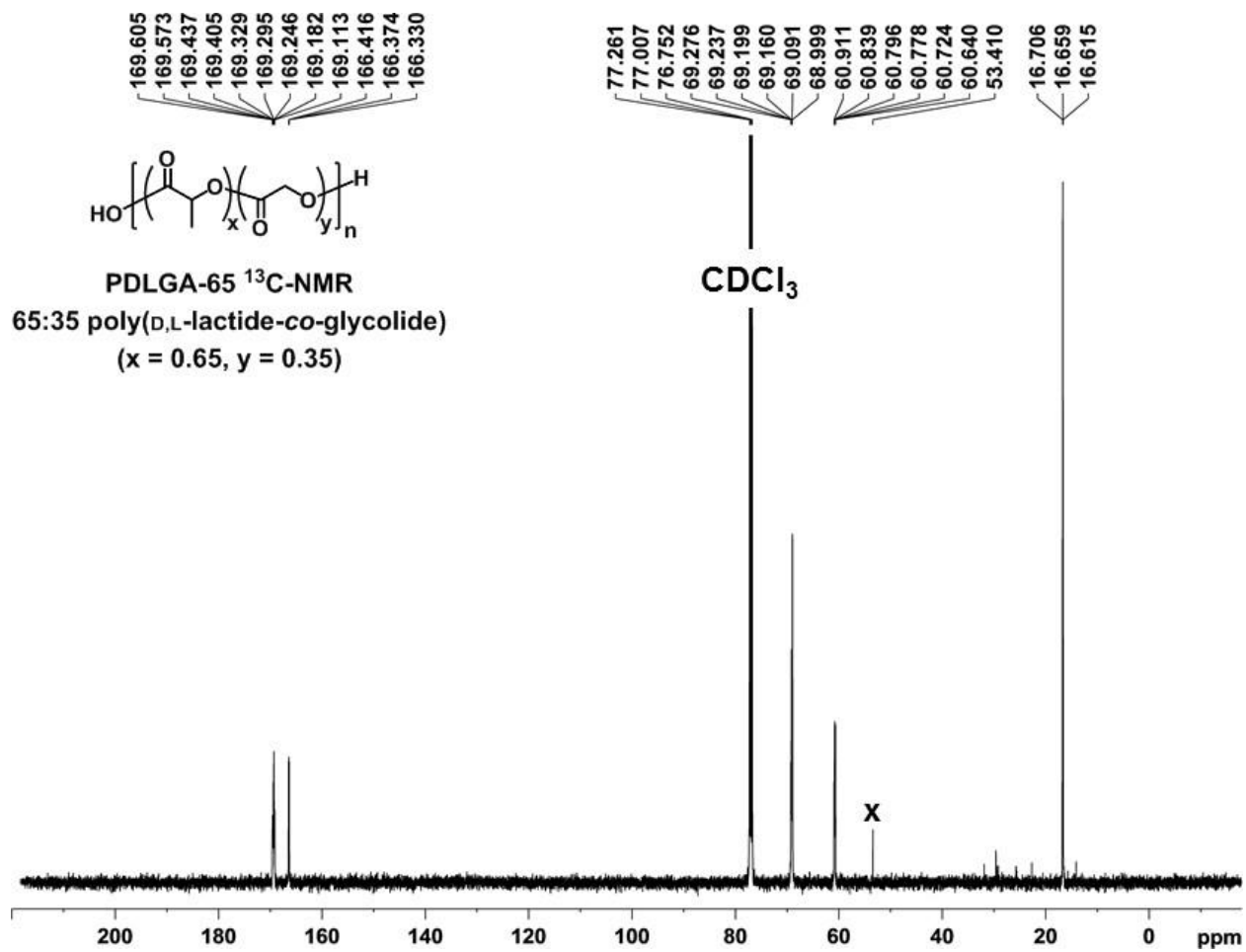
**Figure A7.** ^{13}C NMR (500 MHz, δ 220 – -10.0 ppm) of 65:35 poly(D,L-lactide-*co*-glycolide) (PDLGA-65).
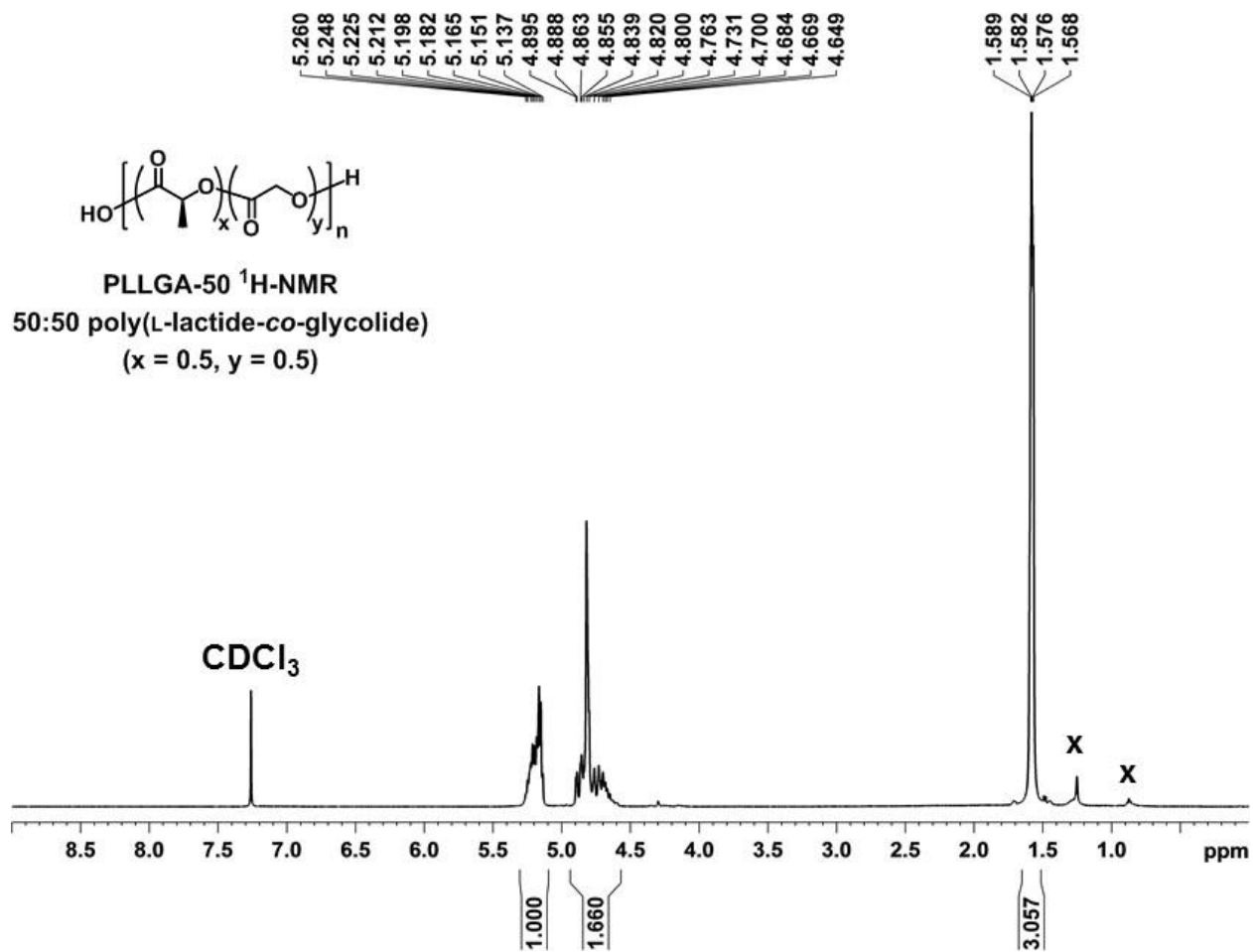
Figure A8. ^{1}H NMR (500 MHz, δ 9.0 – 0.0 ppm) of 50:50 poly(L-lactide-*co*-glycolide) (PLLGA-50).

169.582
169.514
169.446
169.413
169.309
166.492
166.423
166.386
166.341

77.261
77.007
76.753
69.309
69.195
69.101
68.993
68.942
60.924
60.858
60.808
60.735
60.669

16.667
16.620

PLLGA-50 ^{13}C-NMR
50:50 poly(L-lactide-*co*-glycolide)
(x = 0.5, y = 0.5)

CDCl$_3$
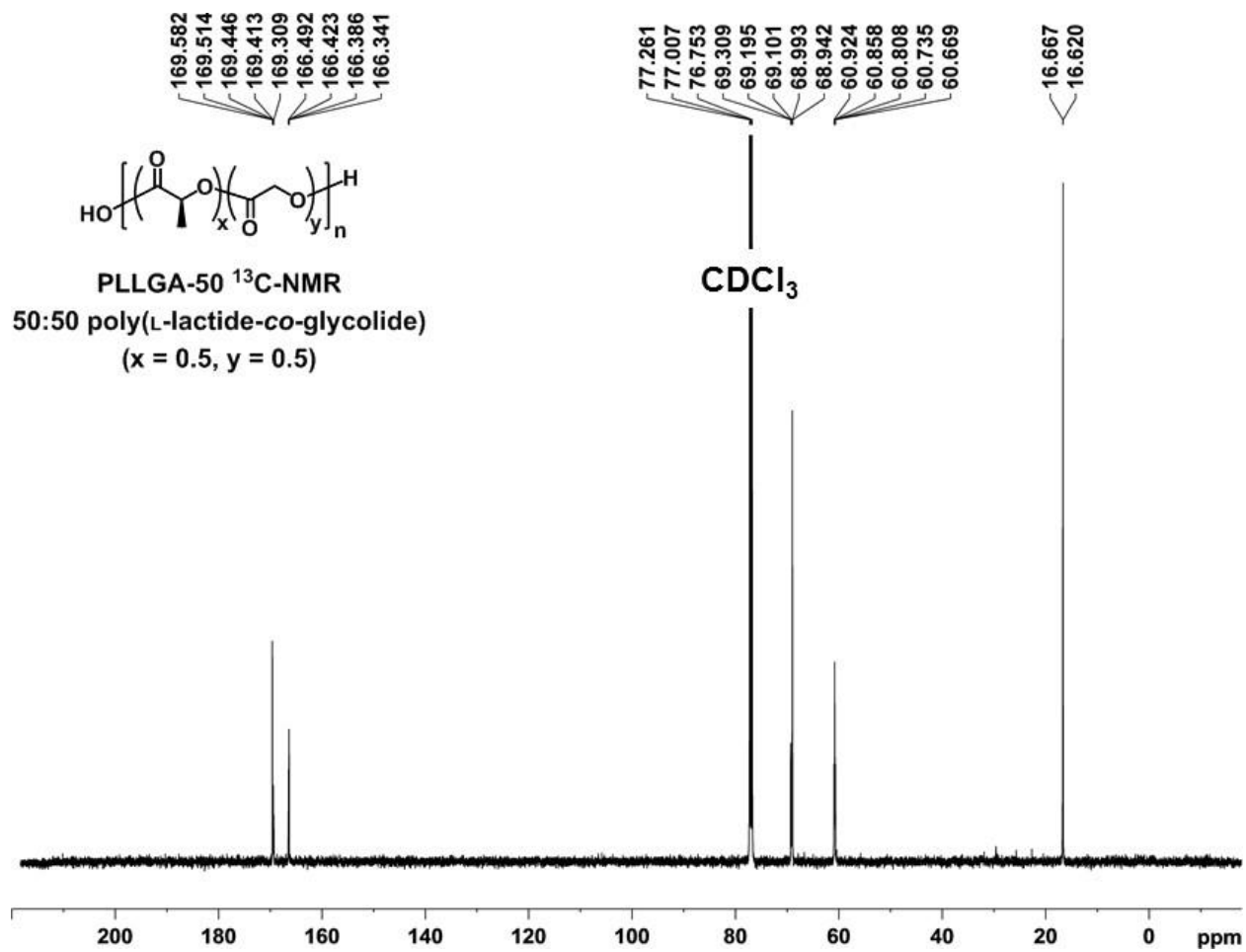
Figure A9. ^{13}C NMR (500 MHz, δ 220 – -10.0 ppm) of 50:50 poly(L-lactide-*co*-glycolide) (PLLGA-50).

116
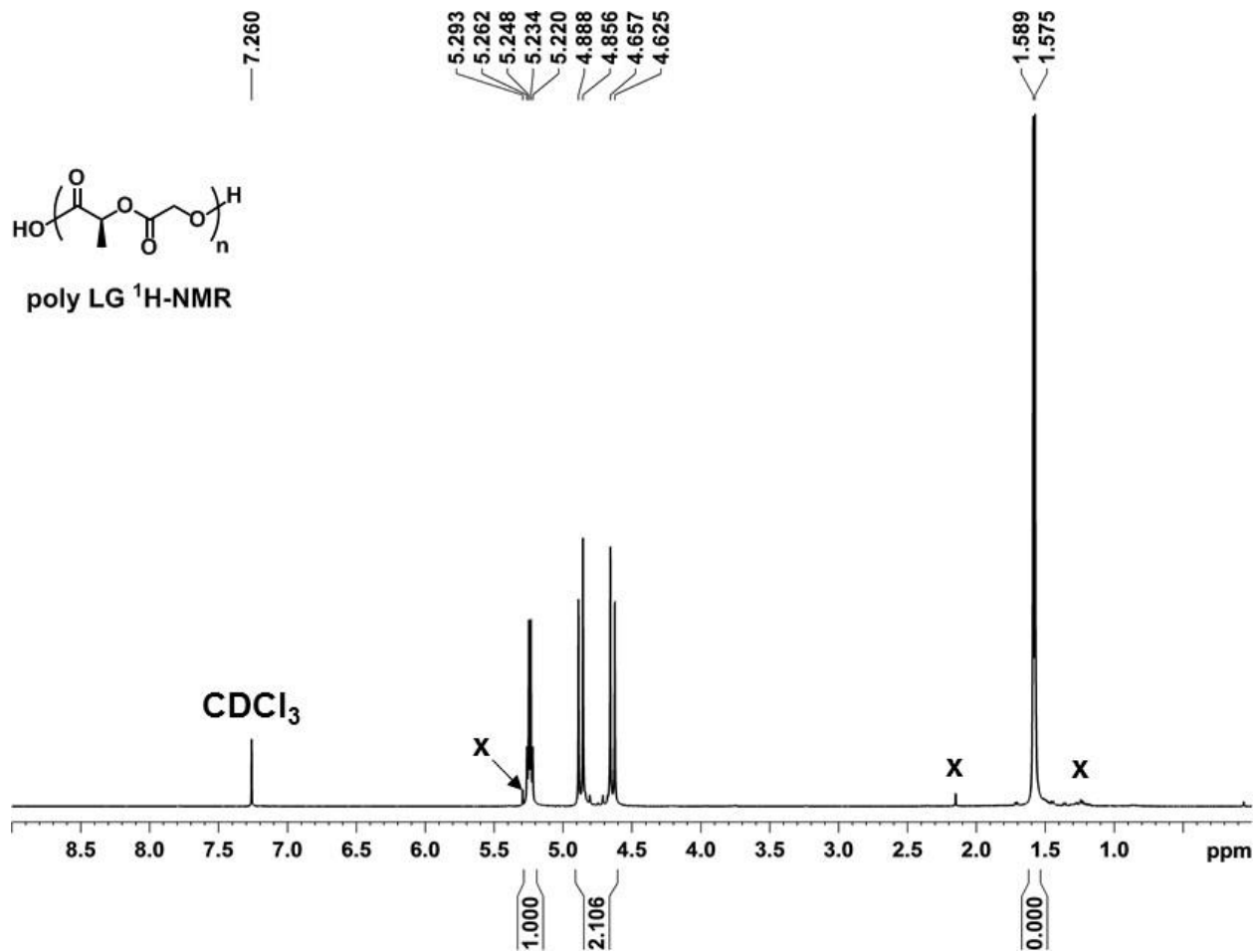
Figure A10. ^{1}H NMR (500 MHz, δ 9.0 – 0.0 ppm) of poly LG.
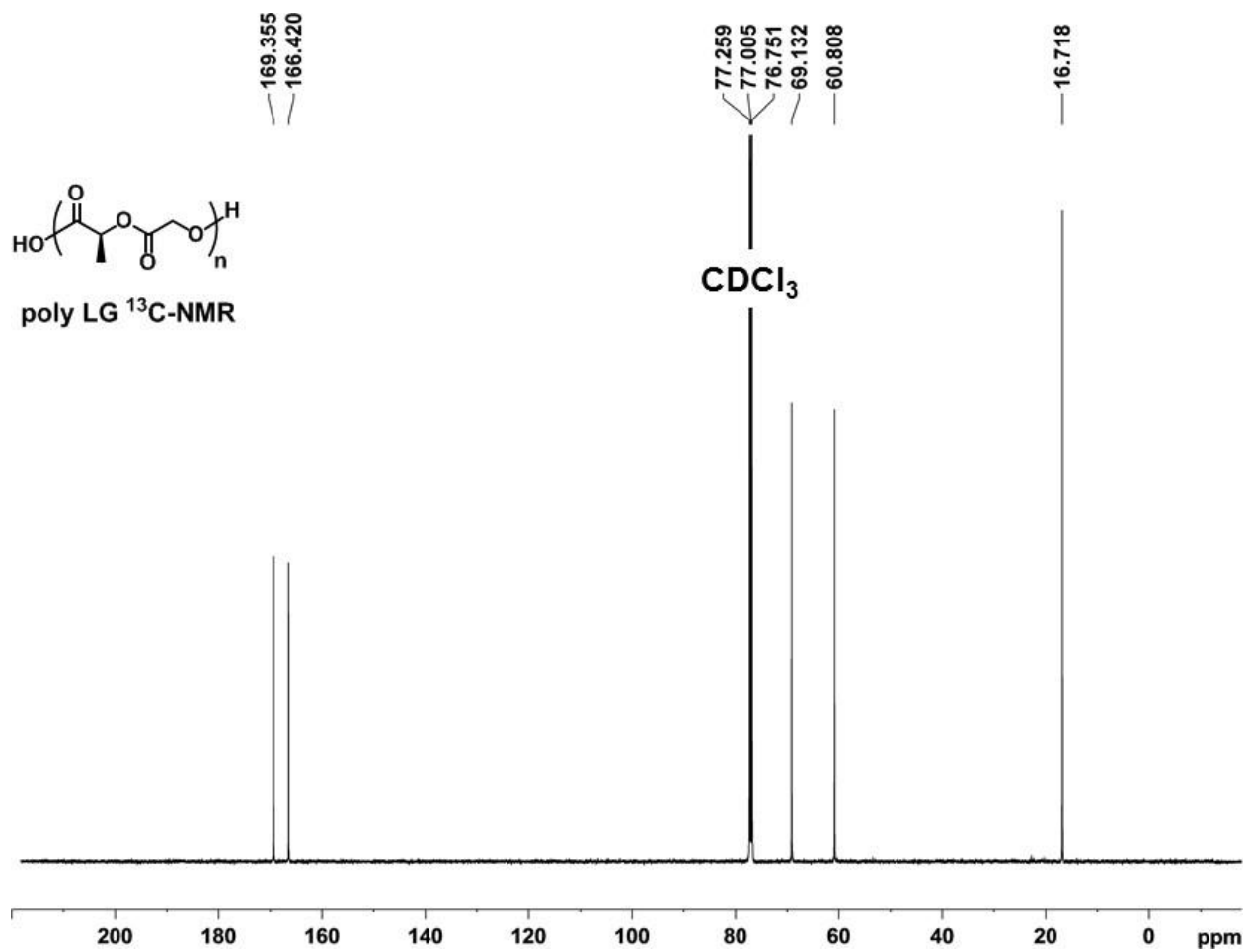
Figure A11. ^{13}C NMR (500 MHz, δ 220 – -10.0 ppm) of poly LG.
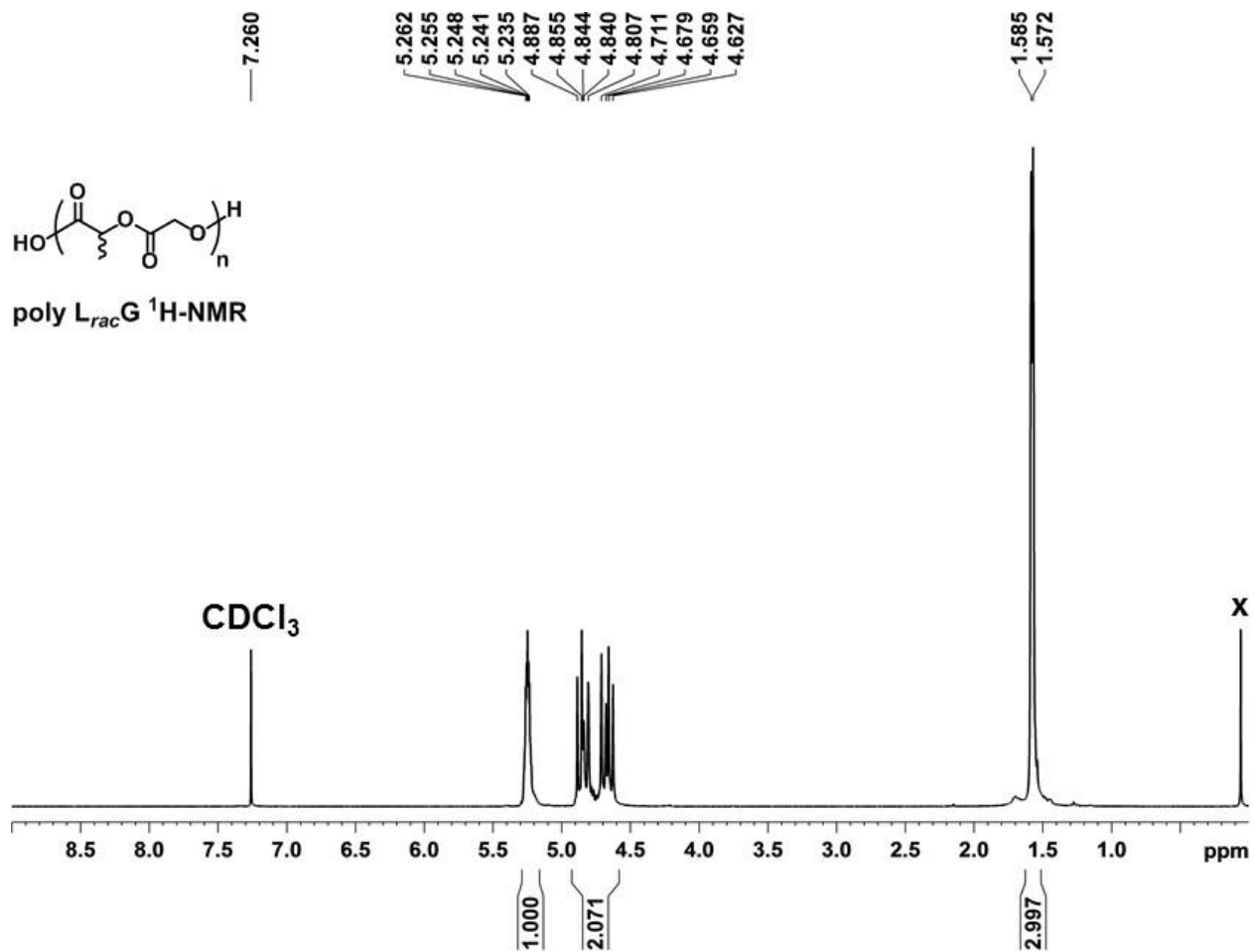
Figure A12. ^{1}H NMR (500 MHz, δ 9.0 – 0.0 ppm) of poly L$_{rac}$G.

119
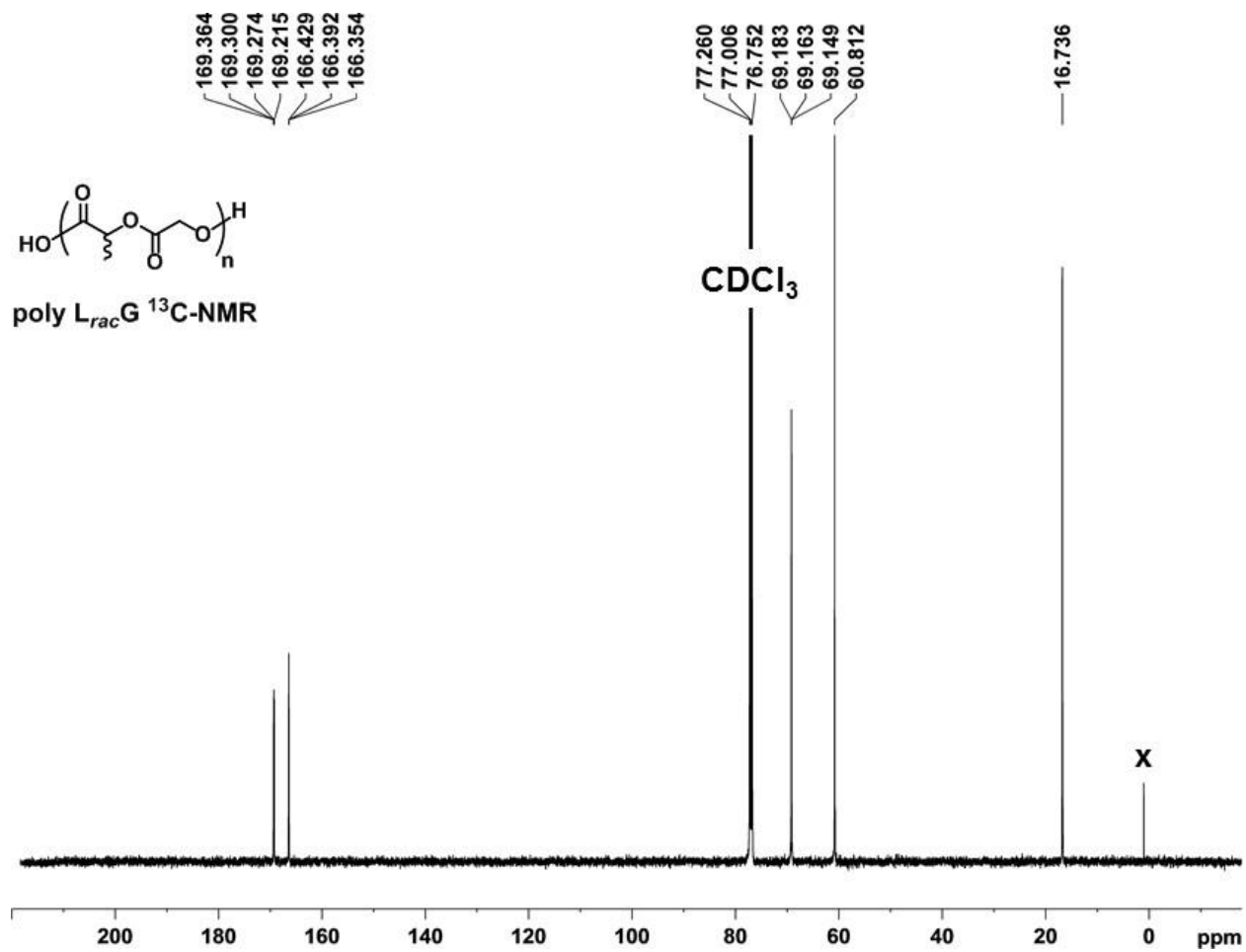
Figure A13. ^{13}C NMR (500 MHz, δ 220 – -10.0 ppm) of poly L$_{rac}$G.
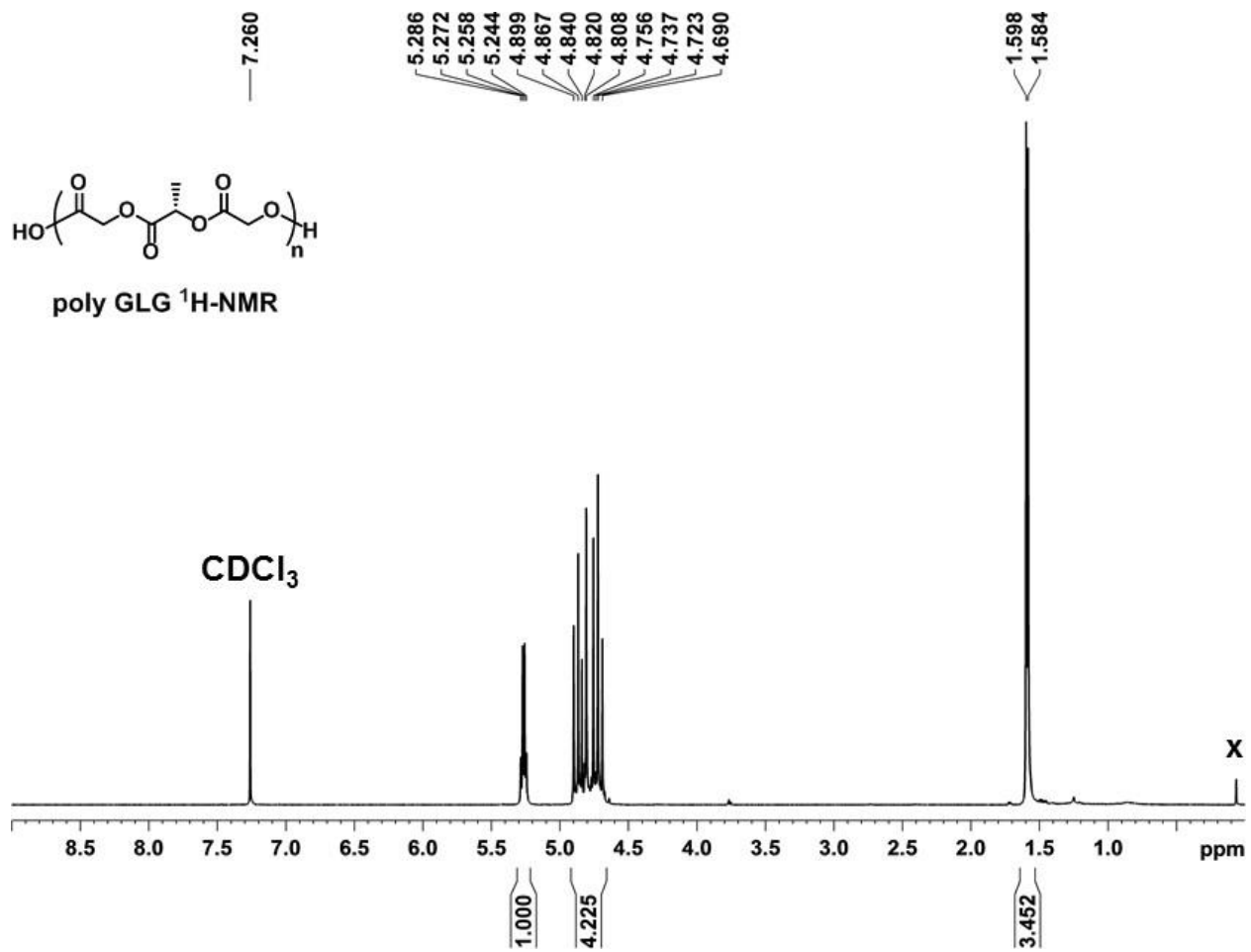
Figure A14. ^{1}H NMR (500 MHz, δ 9.0 – 0.0 ppm) of poly GLG.

Figure A15. ^{13}C NMR (500 MHz, δ 220 – -10.0 ppm) of poly GLG.
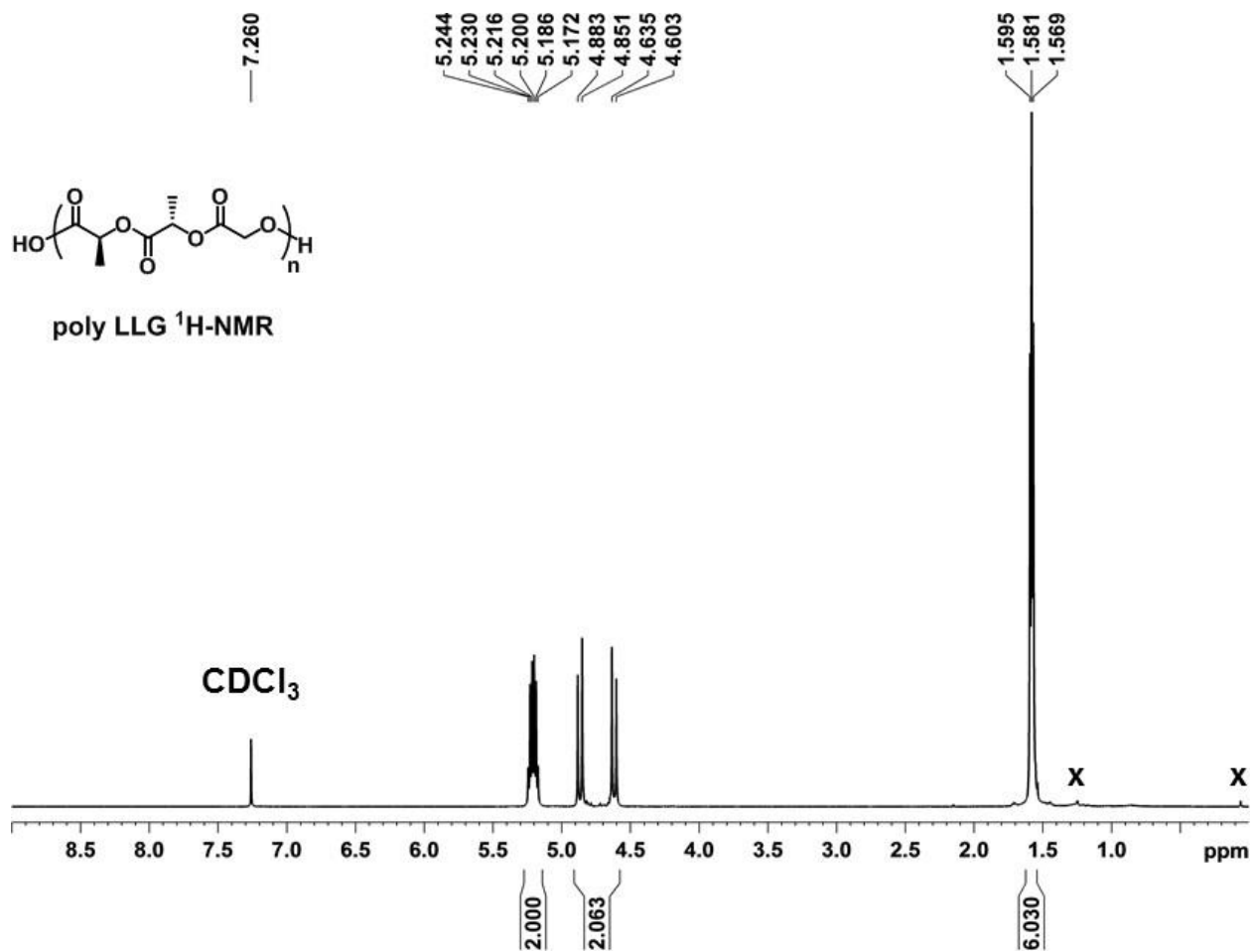
Figure A16. ^{1}H NMR (500 MHz, δ 9.0 – 0.0 ppm) of poly LLG.
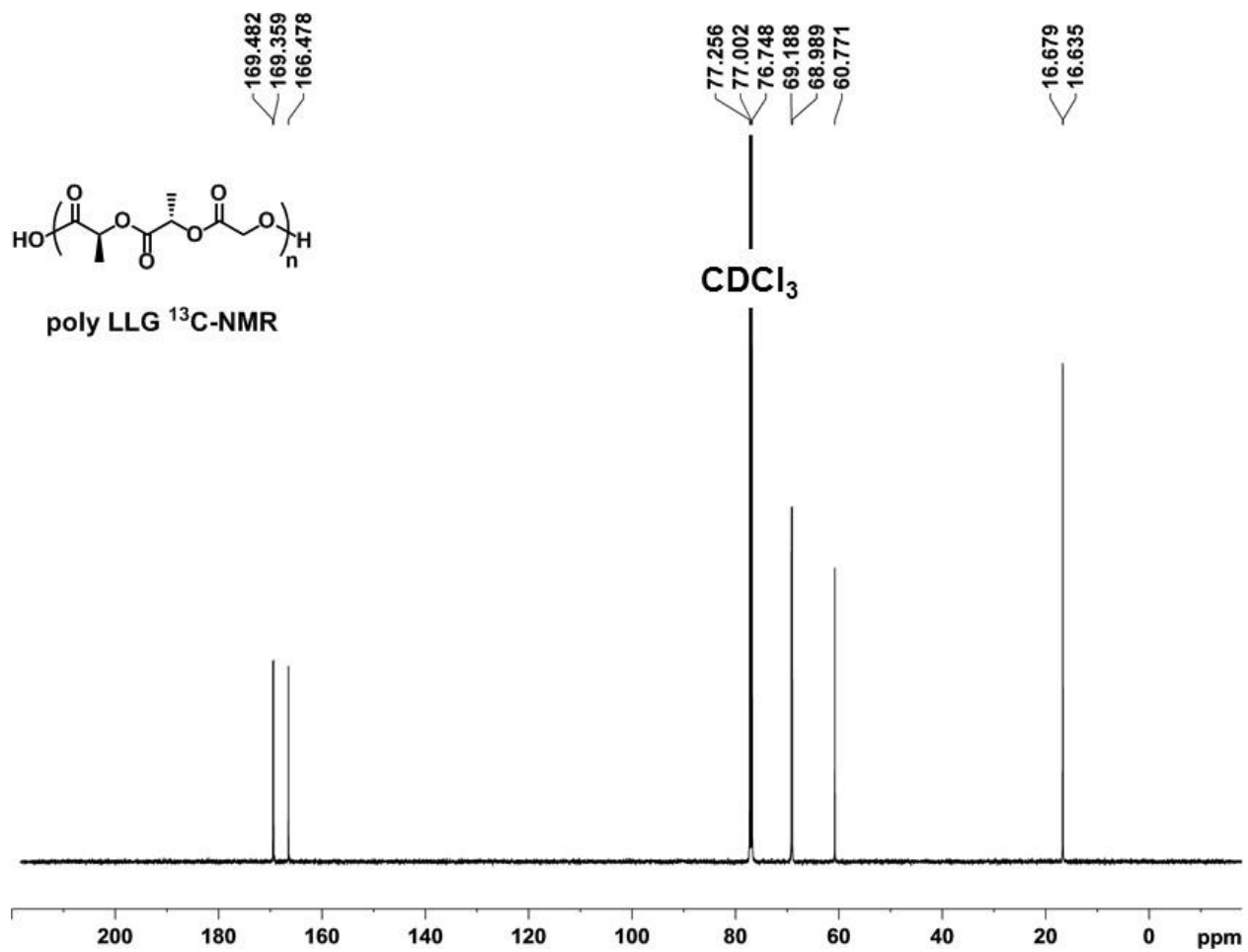
Figure A17. ^{13}C NMR (500 MHz, δ 220 – -10.0 ppm) of poly LLG.
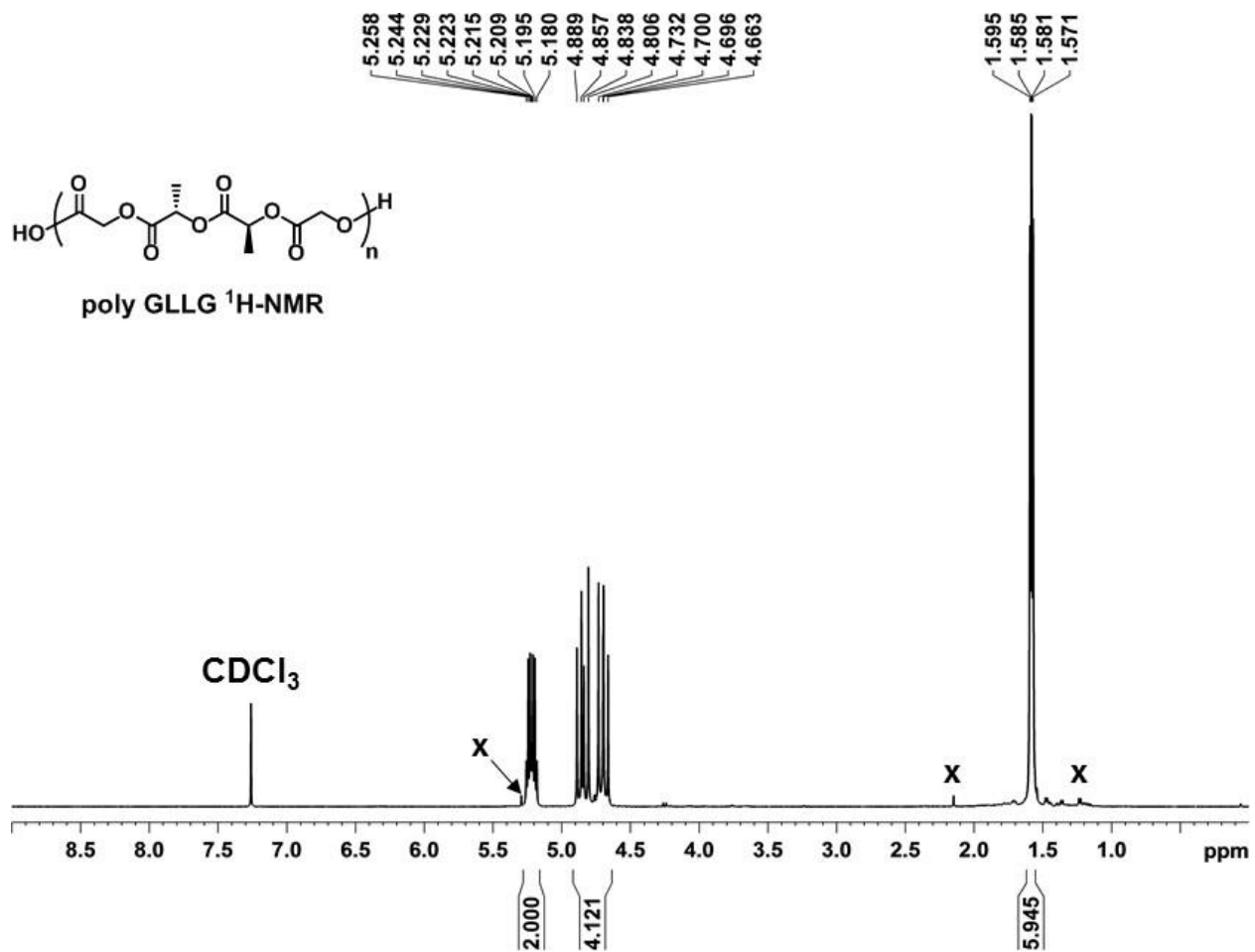
Figure A18. ^{1}H NMR (500 MHz, δ 9.0 – 0.0 ppm) of poly GLLG.
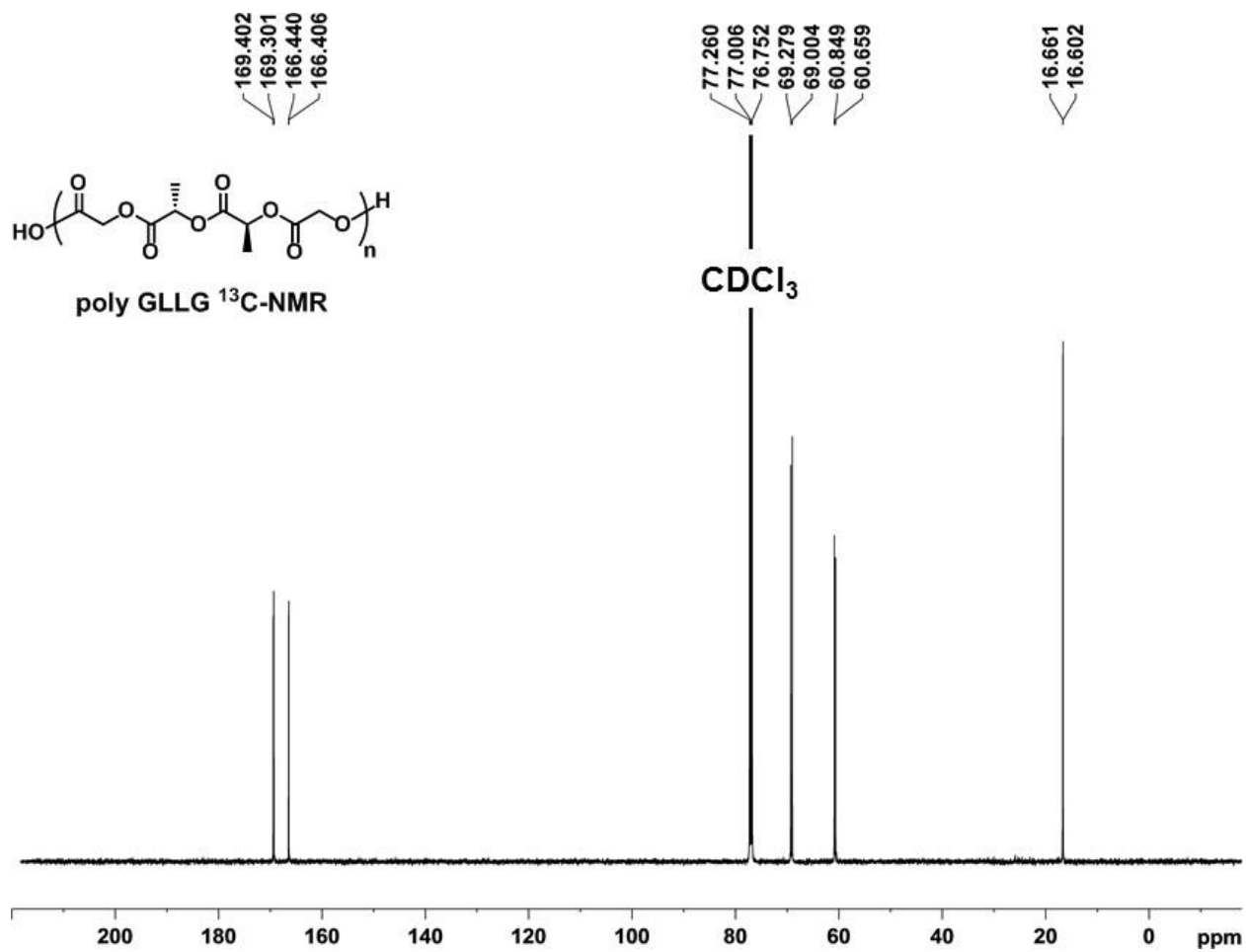
Figure A19. ^{13}C NMR (500 MHz, δ 220 – -10.0 ppm) of poly GLLG.
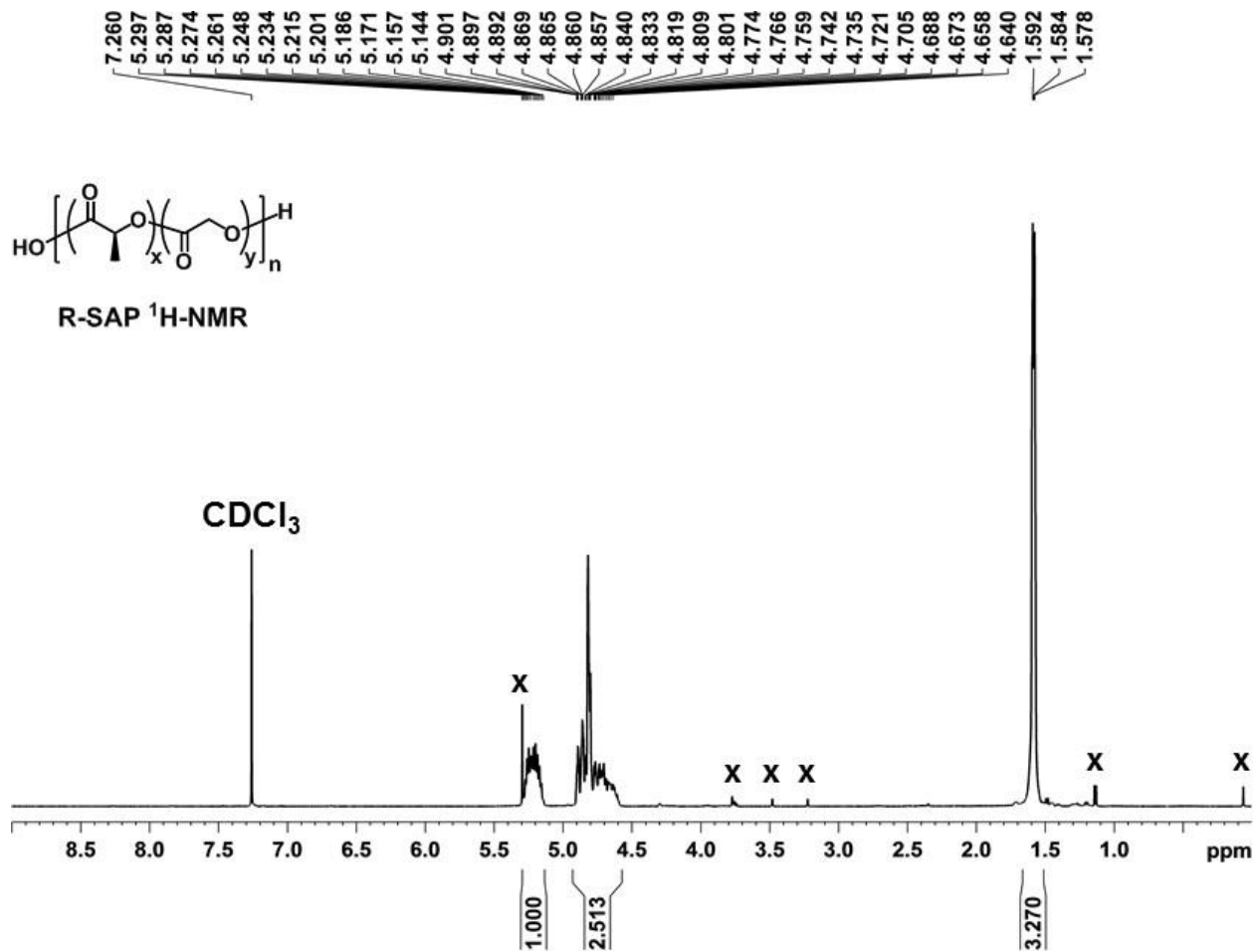
Figure A20. ^{1}H NMR (500 MHz, δ 9.0 – 0.0 ppm) of R-SAP.
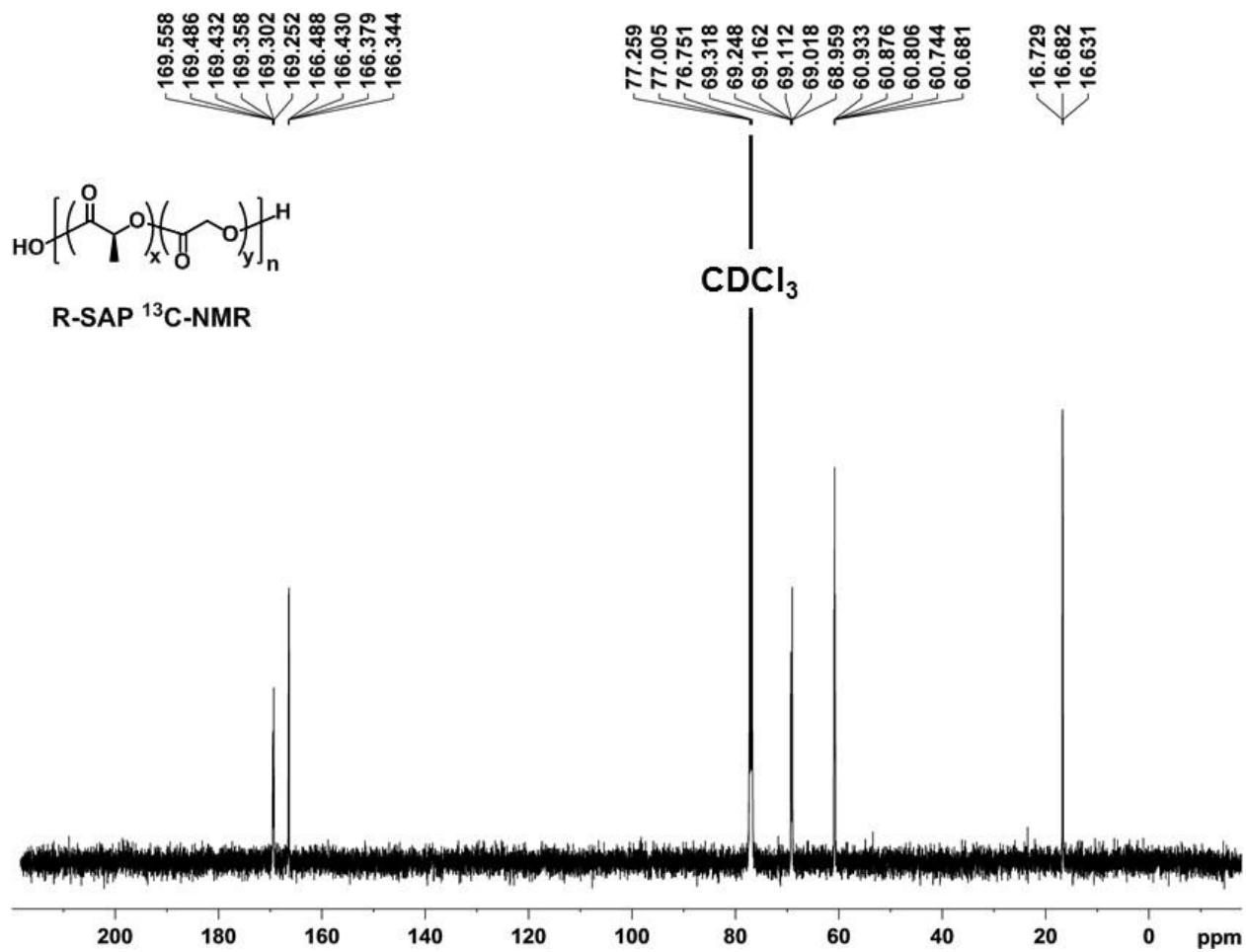
Figure A21. ^{13}C NMR (500 MHz, δ 220 – -10.0 ppm) of R-SAP.
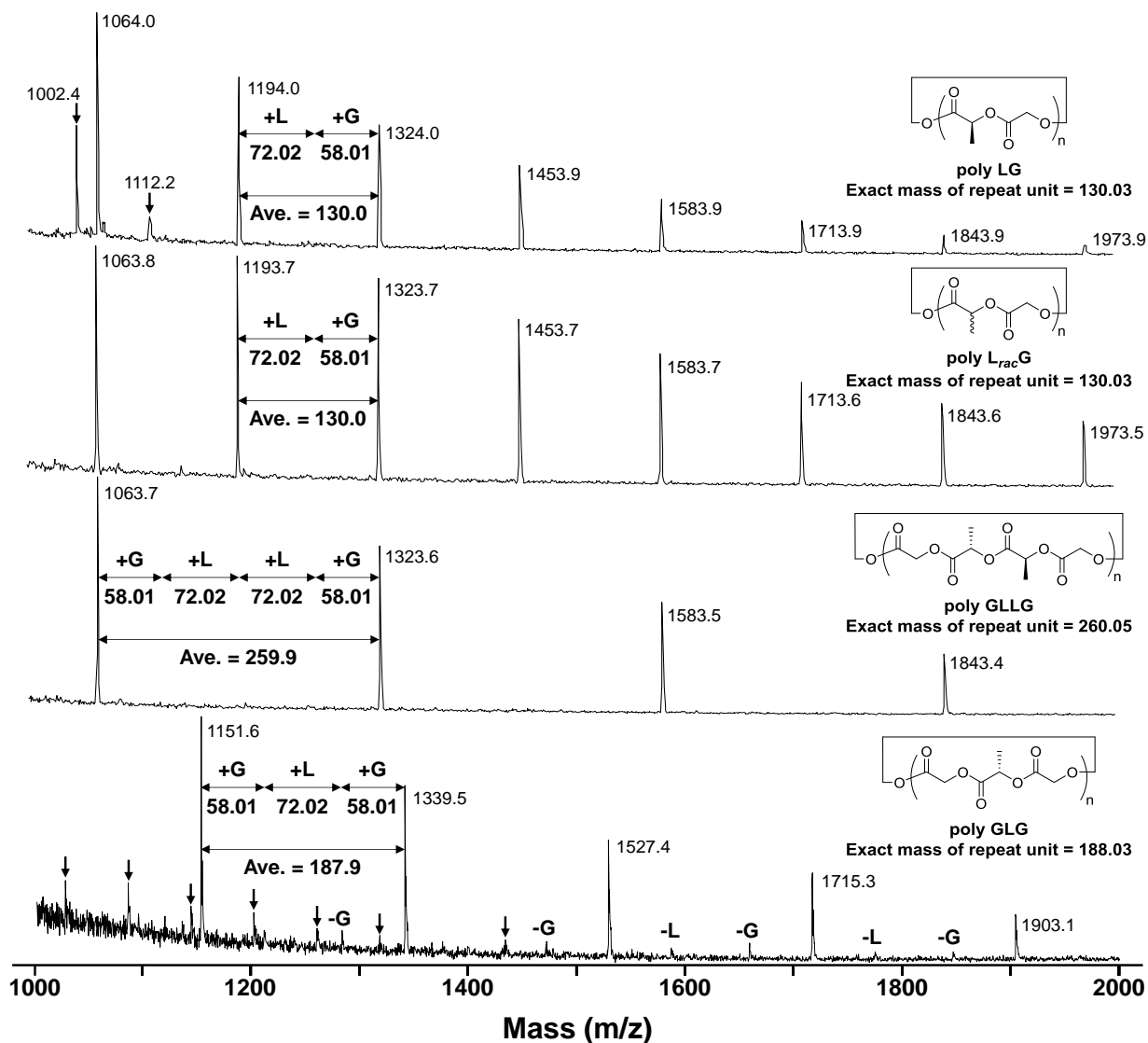
Figure A22. MALDI-ToF-MS spectra acquired in reflector mode of polymers prepared via segmer assembly polymerization in the mass range of 1000-2000 Da. Arrows indicate the presence of impurities while sequence errors are labeled as "–G" or "–L". Note: MALDI-ToF spectra of these polyesters typically consist of only cyclic species. It is not clear if this pattern is due to preferential ionization/volatilization of the cyclics or to the selective formation of cyclics in this molecular weight range.
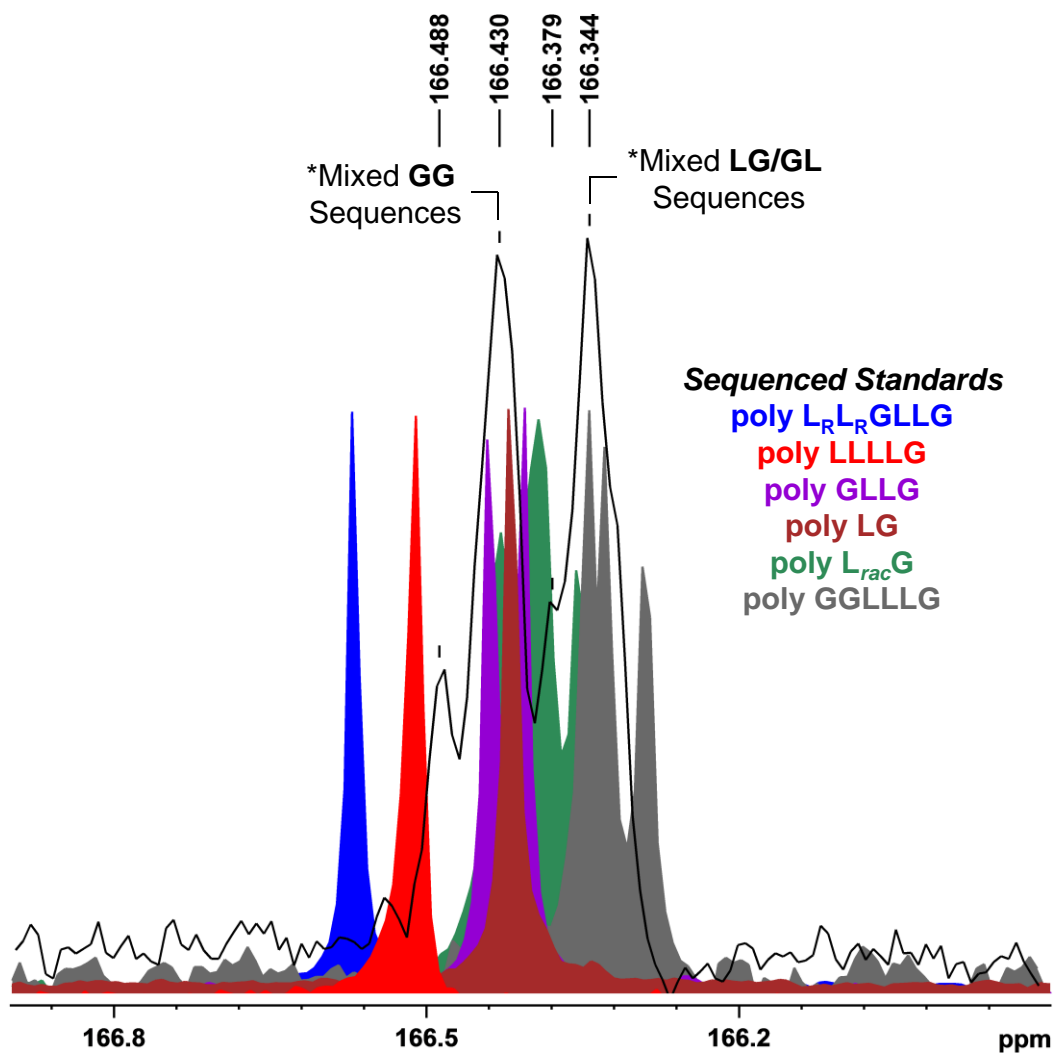
Figure A23. ^{13}C NMR spectral (500 MHz) comparison of R-SAP with several sequenced copolymer standards demonstrating the complexity of glycolyl carbonyl peak assignments. *Chemical shifts of conventional dimeric sequence assignments from PLGAs synthesized via ring-opening polymerization of lactide and glycolide.
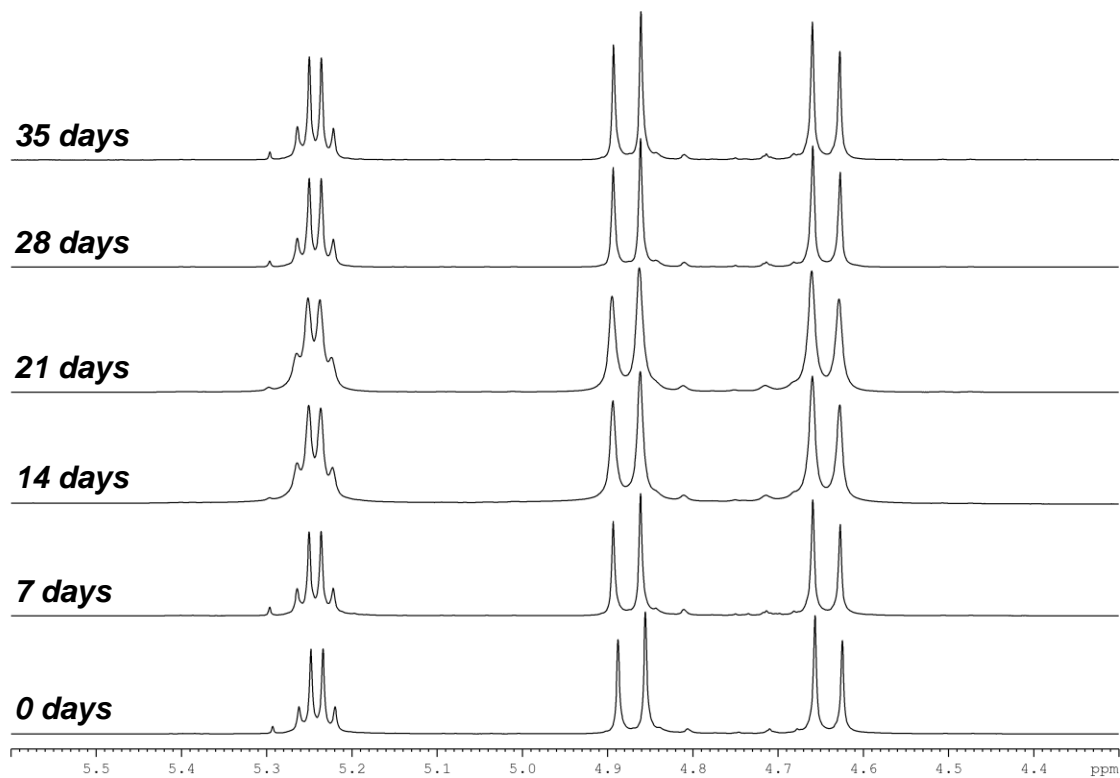
Figure A24. ^{1}H NMR spectra overlay (δ 4.3-5.6 ppm) of poly LG. The small amount of epimerization present in the 0 day sample (δ ~4.7, 4.8 ppm) does not increase with degradation time and no addition resonances appear. Transesterification would be expected to introduce new peaks.
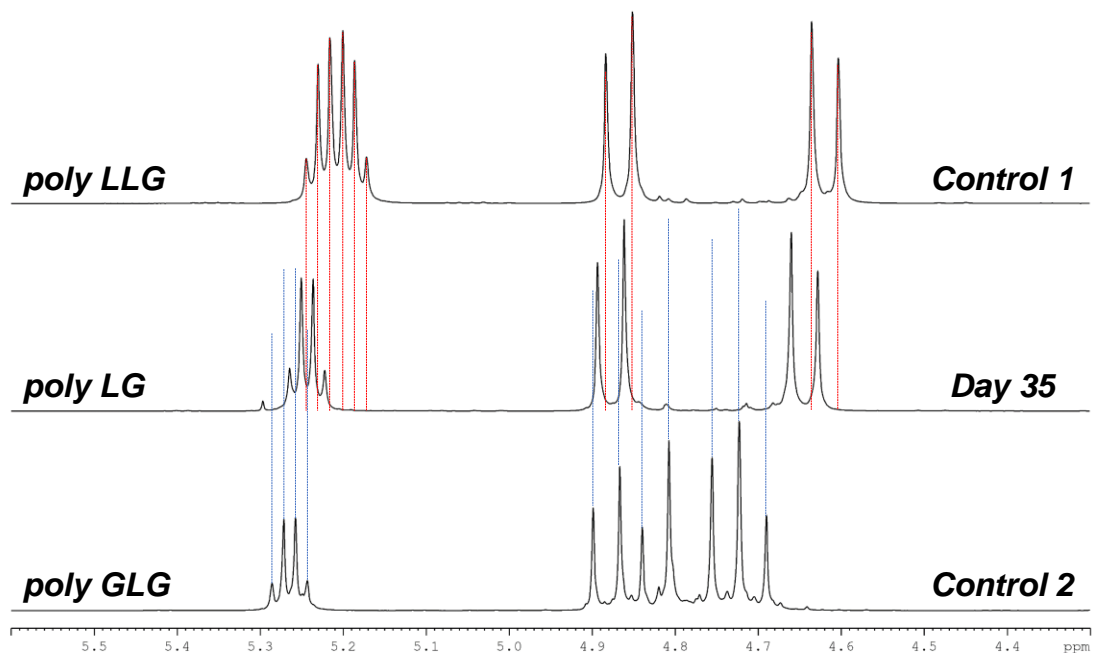
Figure A25. ^{1}H NMR spectra overlay (δ 4.3-5.6 ppm) of poly LG at day 35. The day 35 poly LG sample is compared with spectra of poly GLG and poly LLG to illustrate the chemical shifts that would be expected if the sample was contaminated by transesterification-generated GG and LL units.
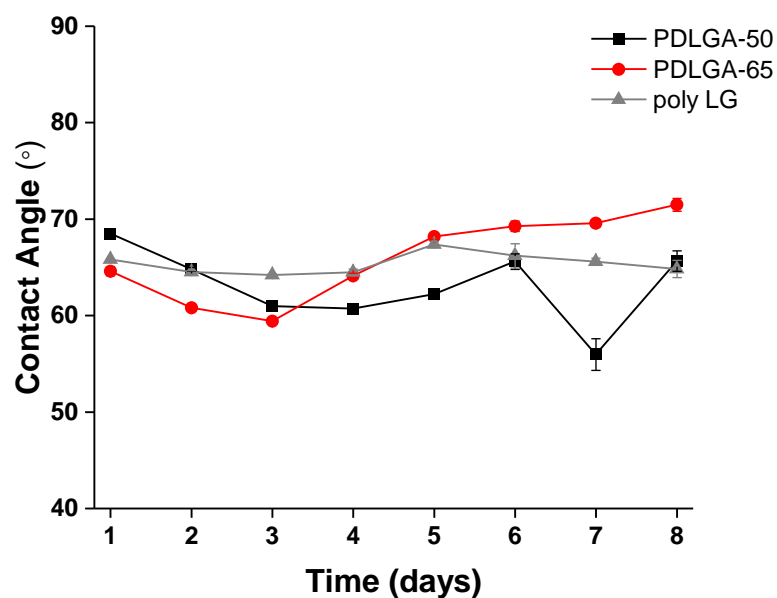
Figure A26. Surface water contact angles of films exposed to physiological conditions over 8 days measured in their hydrated (post-wet) state. The error bars represent ± standard error of the mean (*n*=5). Note: this study was only performed on PDLGA-50 and poly LG because these polymers exhibited the largest differences in swelling and erosion behavior. As their surface contact angles under these conditions were nearly the same, other sequences were not explored. Further evidence for the lack of sensitivity of this measurement to sequence can be found in the comparison of PDLGA-50 with PDLGA-65. Despite the presence of significantly more hydrophobic L units, the contact angle behavior cannot be differentiated from PDLGA-50.
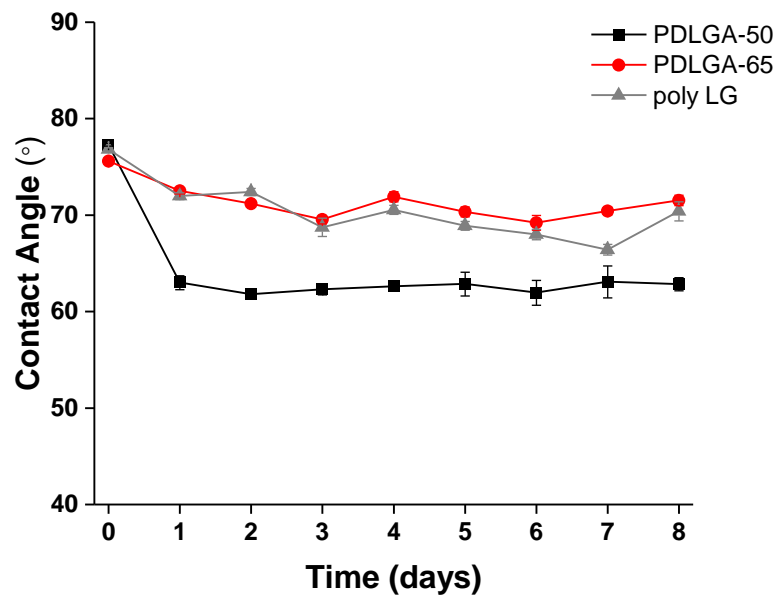
Figure A27. Surface water contact angles of films exposed to physiological conditions over 8 days measured in their lyophilized (post-dry) state. The error bars represent ± standard error of the mean (*n*=5). Note: this study was only performed on PDLGA-50 and poly LG because these polymers exhibited the largest differences in swelling and erosion behavior. As their surface contact angles under these conditions were nearly the same, other sequences were not explored. Further evidence for the lack of sensitivity of this measurement to sequence can be found in the comparison of PDLGA-50 with PDLGA-65. Despite the presence of significantly more hydrophobic L units, the contact angle behavior cannot be differentiated from PDLGA-50.

Supporting Information for Chapter 3
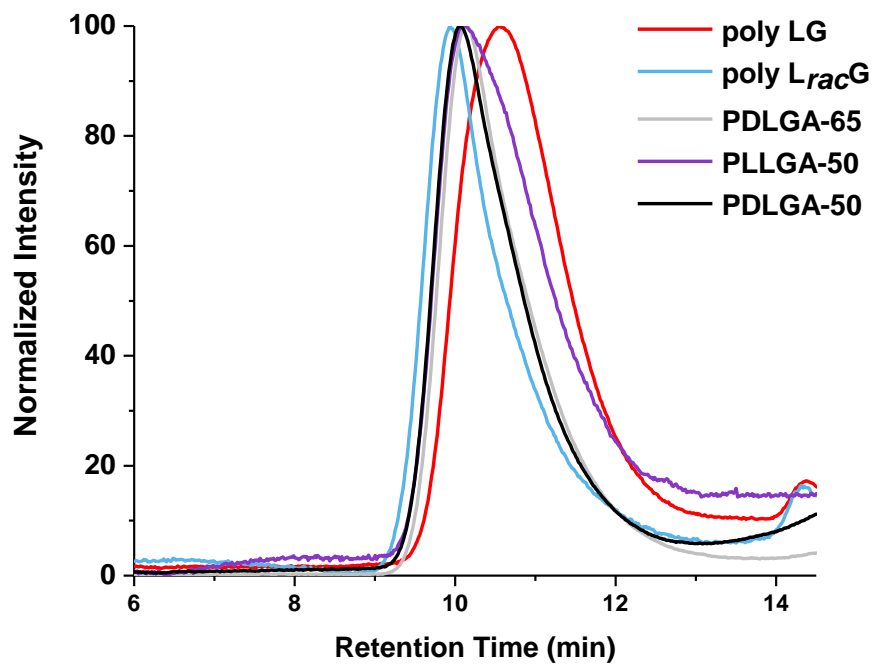
Figure B1. Gel permeation chromatography (GPC) chromatograms of sequenced and random PLGA copolymers.
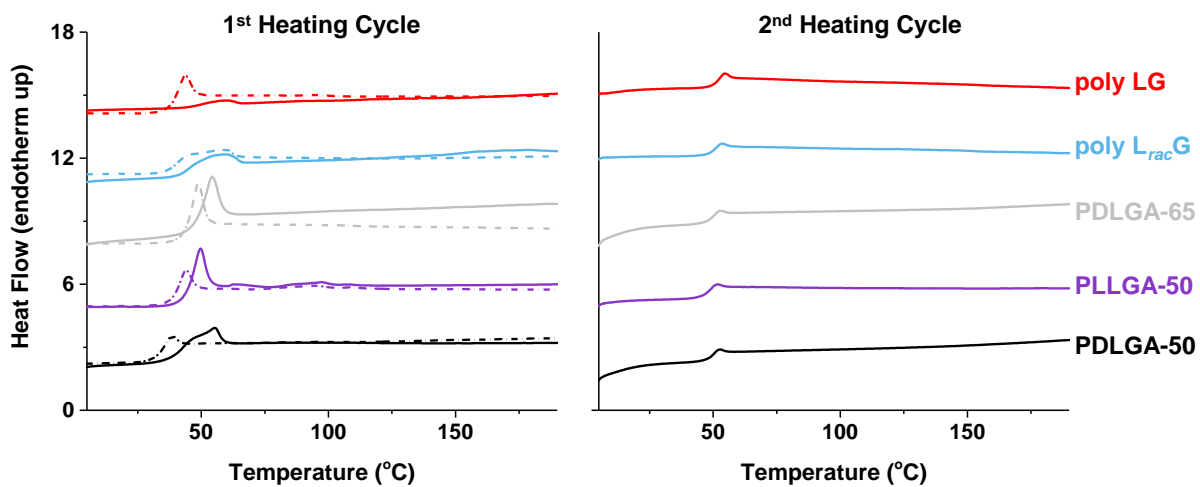
Figure B2. Differential scanning calorimetry (DSC) thermograms of PLGAs. The standard glass transition temperatures of all polymers were measured in the second heating cycle (right). Thermal data for non-loaded (left, solid lines) and LysoSensorTM loaded (left, dotted lines) PLGA microparticles prepared by a single-emulsion (O/W) methodology were determined during the first heating cycle.
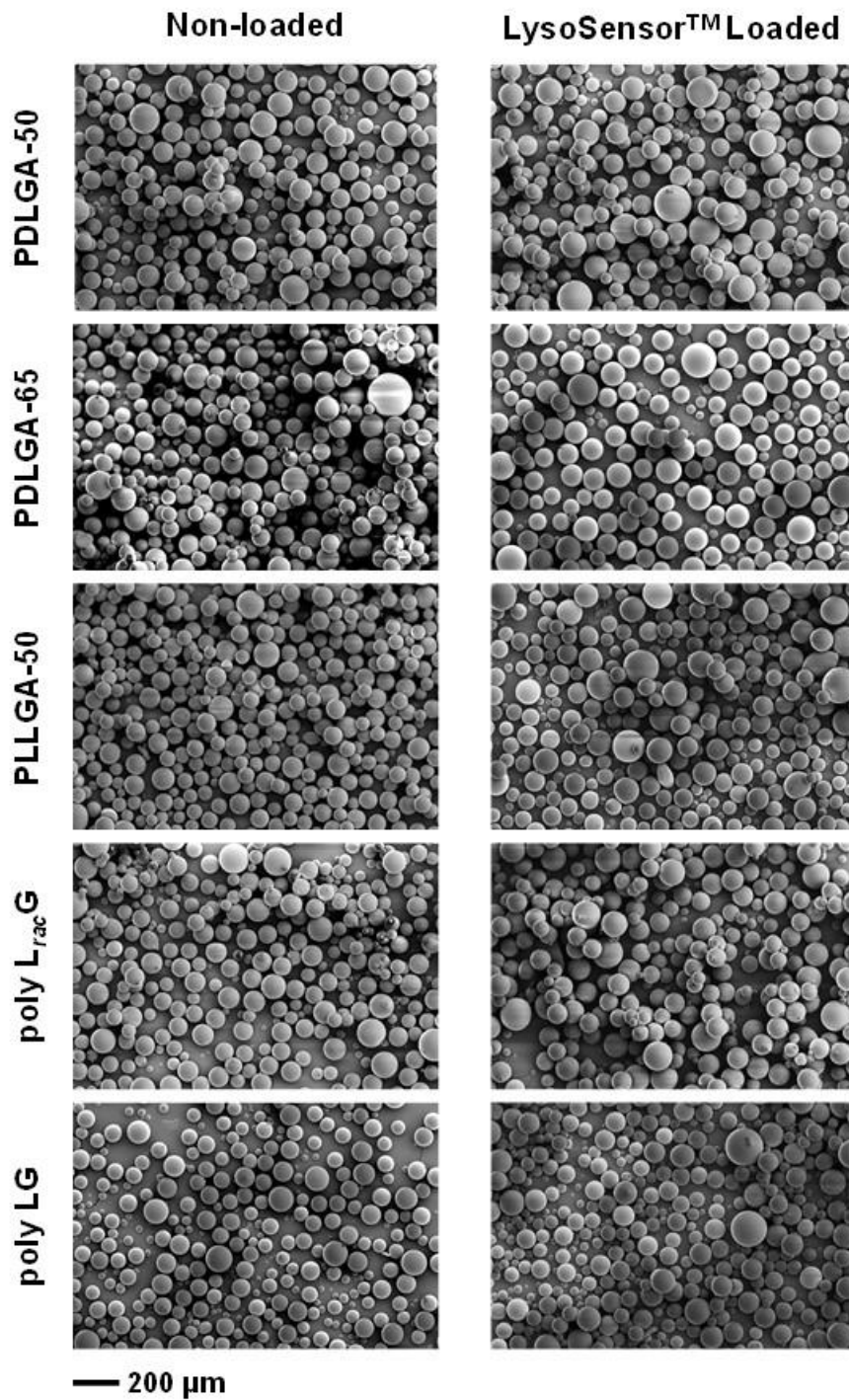
Figure B3. Scanning electron microscopy images (x80) of control (non-loaded) and LysoSensorTM loaded PLGA microparticle prepared via a single-emulsion (O/W) fabrication method.
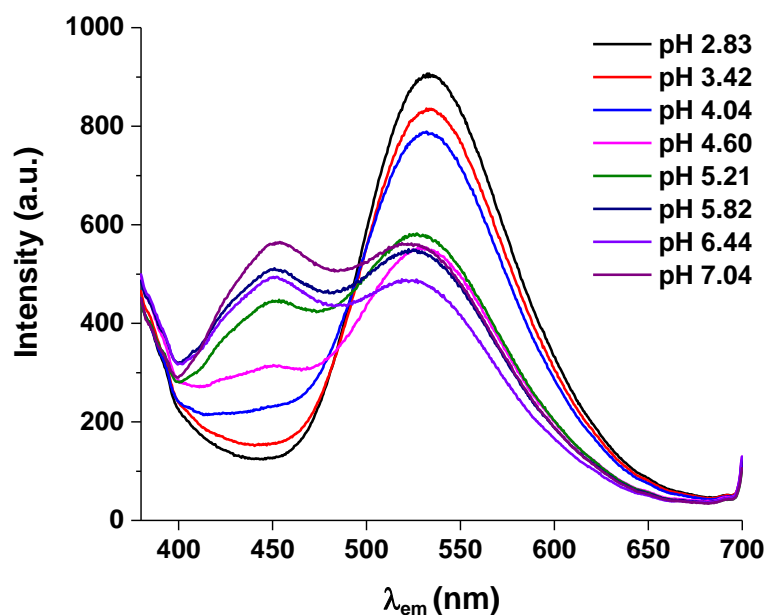
Figure B4. Fluorescence spectra overlay of LysoSensorTM pH probe in various 0.1 M citric acid and 0.2 M Na2HPO4 buffer solutions (pH = 2.83 – 7.04).
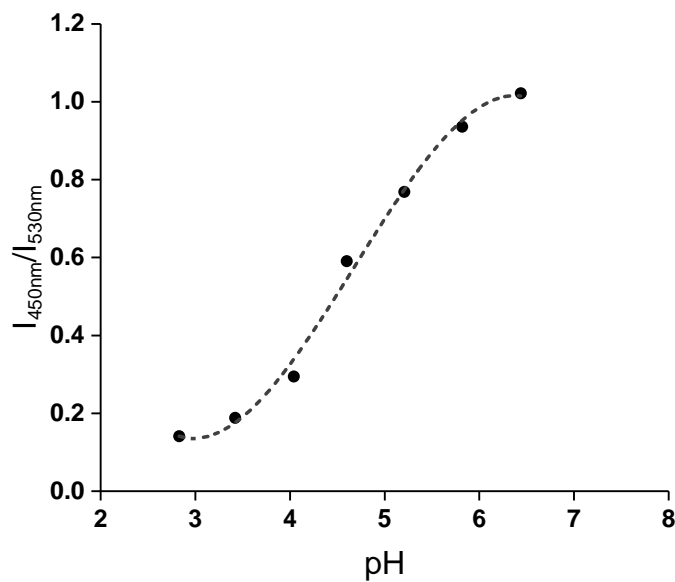
Figure B5. The pH sensitivity of LysoSensorTM Yellow/Blue DND-160 (PDMPO) at concentration 2 µM. The third-order polynomial curve fitting data was y = -0.0449 x3 + 0.6305 x2 - 2.56295 x + 3.36182, where y = I450 nm/I530 nm and x = pH, r2 = 0.994.
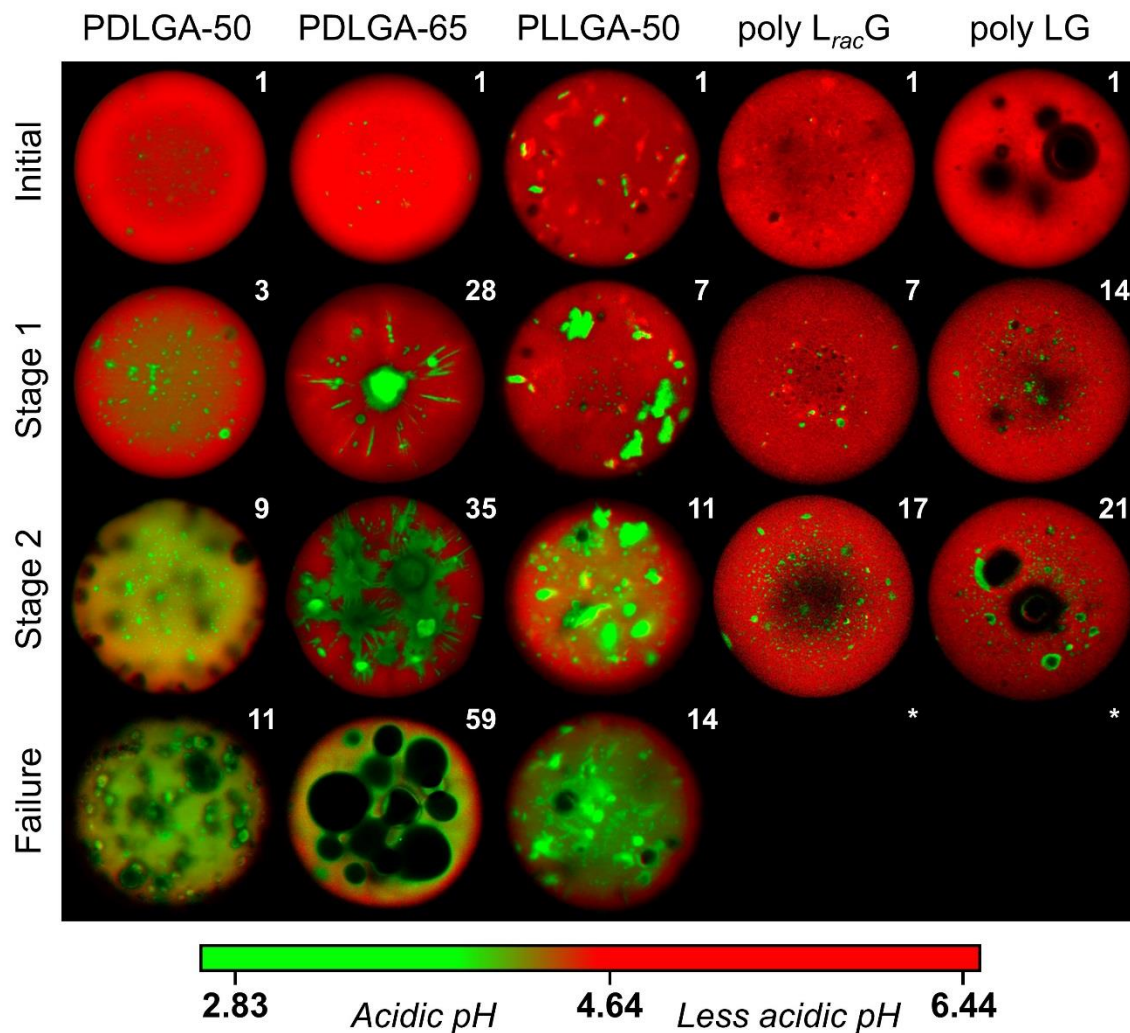
Figure B6. Evolution of characteristic acidic microclimate features monitored using two-photon microscopy. Displayed images are representative of the population at specific time intervals (top right; days). *Data was unable to be acquired due to dye-loss.
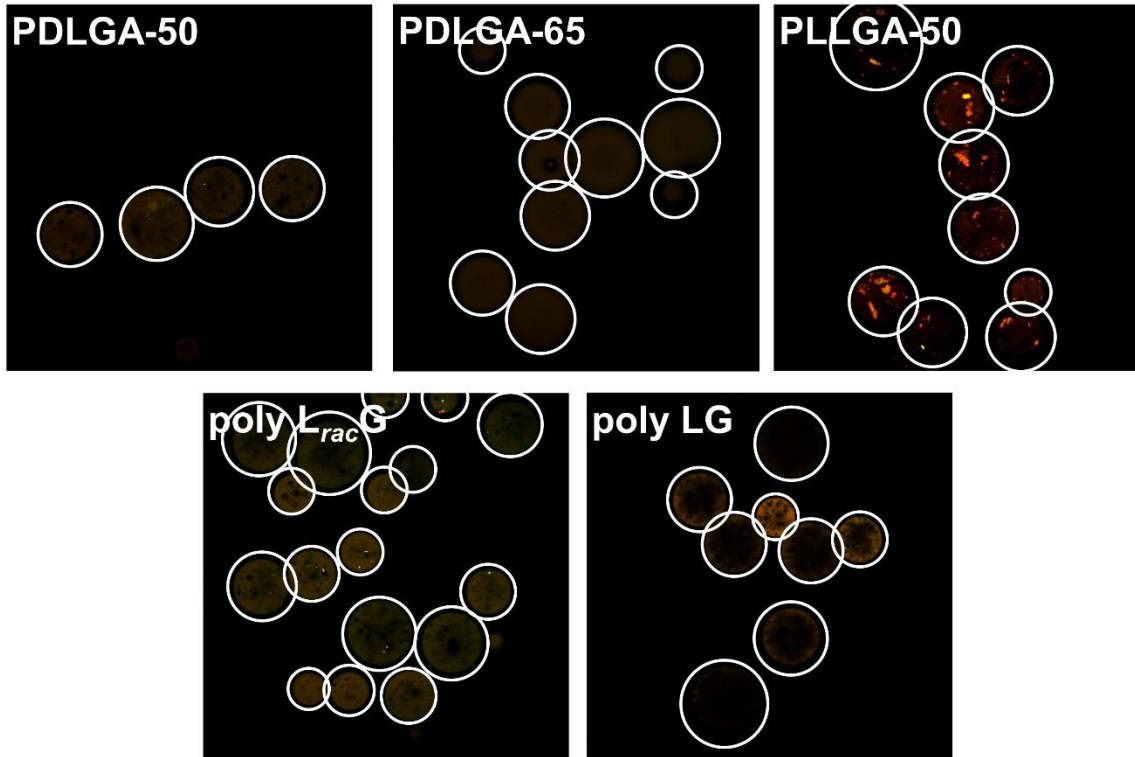
Figure B7. Two-photon microscopy images of hydrated microparticles without encapsulated dye. Images were acquired using λex = 740 nm, 5.40 % intensity. Minimal to no fluorescent interference was detected using the previously described image acquisition settings. Various threshold settings were applied for each polymer: PDLGA-50 (Red (15-255), Green (10-255)), PDLGA-65 (Red (35-255), Green (20-255)), PLLGA-50 (Red (25-255), Green (15-255)), poly LG (Red (80-255), Green (50-255)), poly LracG (Red (75-255), Green (55-255)).
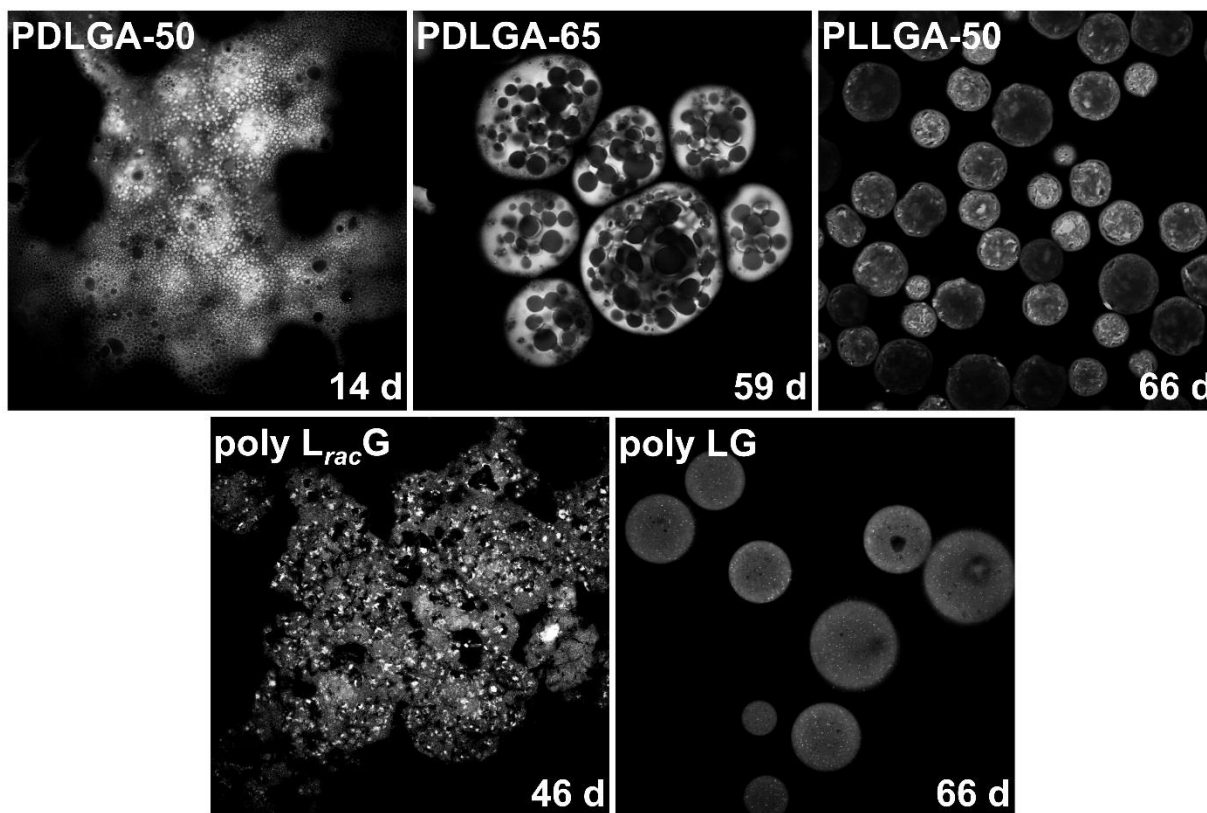
Figure B8. Non-ratiometric two-photon microscopy images illustrating the failure morphologies of sequenced and random PLGAs at specific time points.
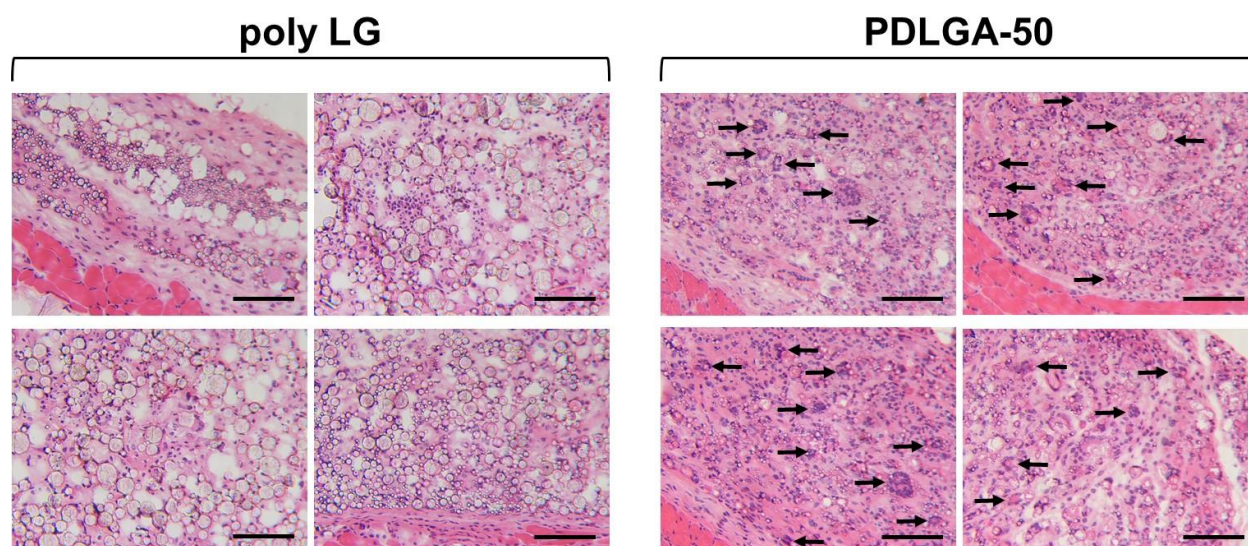
Figure 9. Additional week 4 H&E staining images of subcutaneous tissue microparticle depot injections from two different C57BL/6J wild-type mice (x25). Arrows indicate presence of foreign body giant-cells. Scale bar = 100 μm.

141
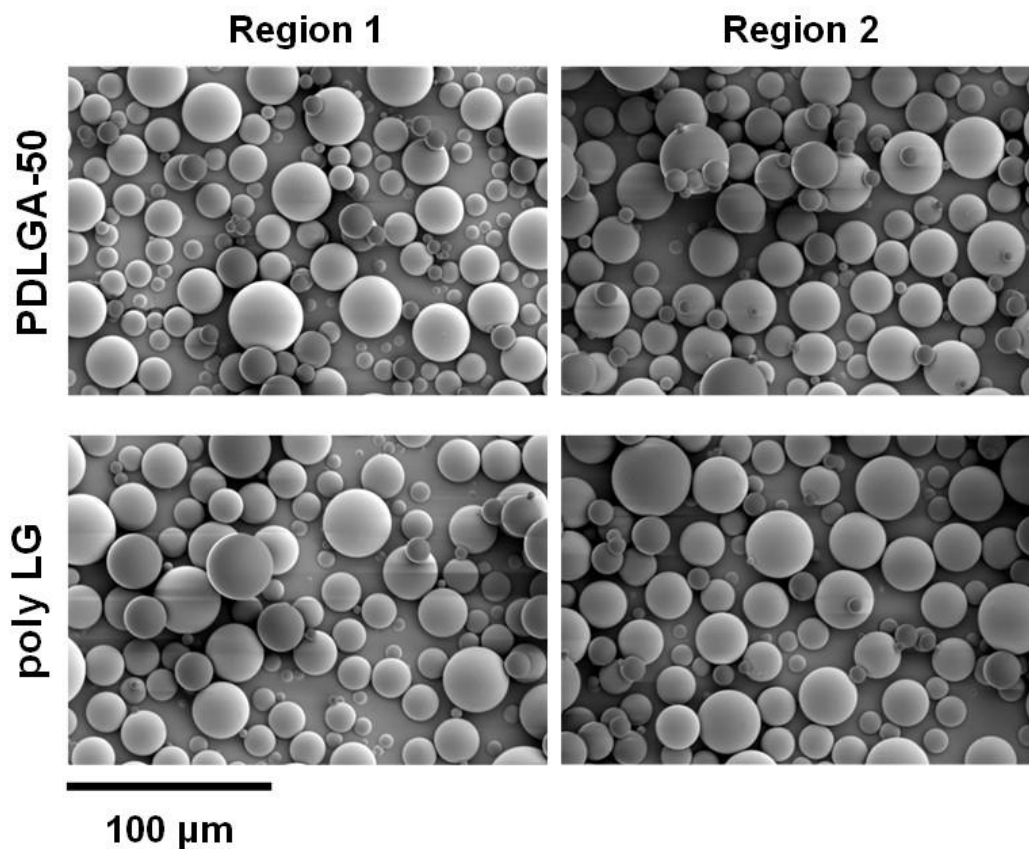
Figure B10. Scanning electron microscopy images (x550) of single-emulsion PDLGA-50 and poly LG microparticles. These samples were injected subcutaneously to evaluate in vivo inflammatory response.

Supporting Information for Chapter 4
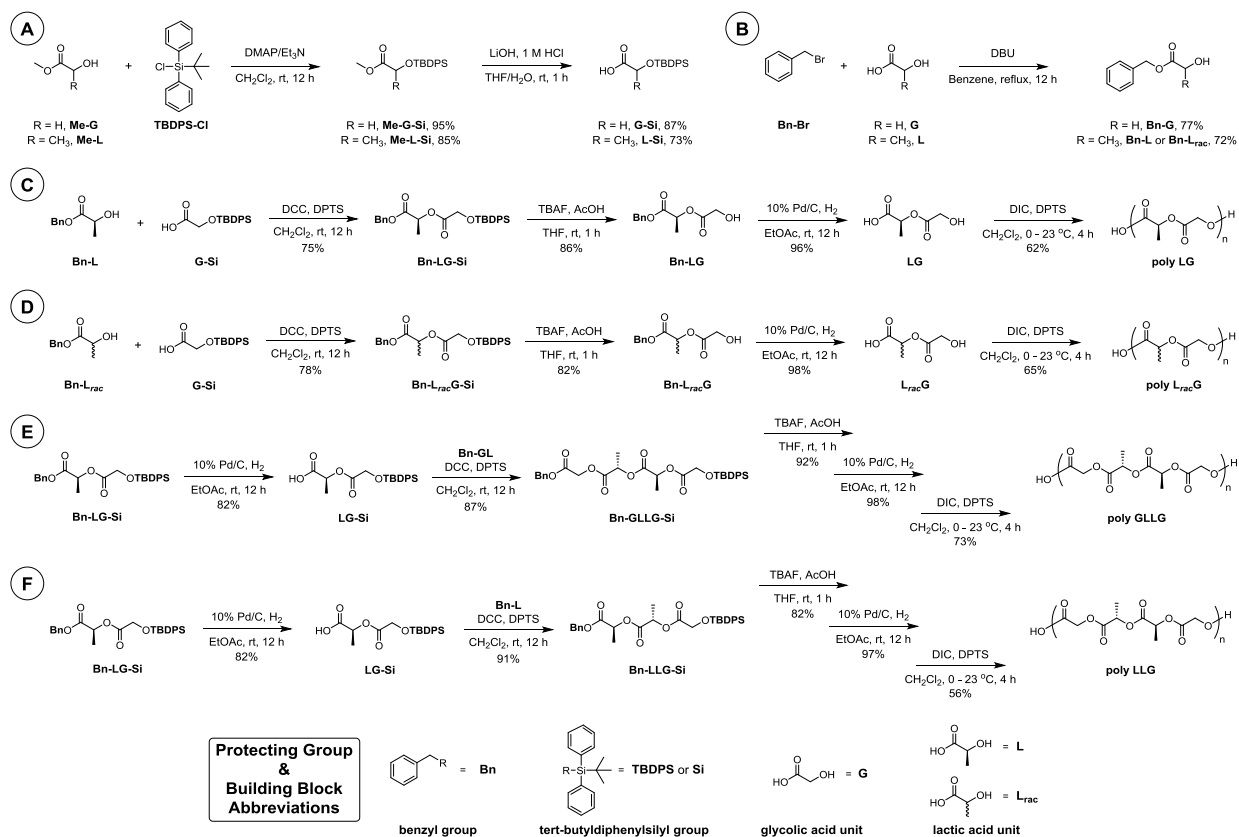
Figure C1. Synthesis of orthogonally protected lactic and glycolic acid building blocks, *tert*-butyldiphenylsilyl protected alcohols (A) and benzyl protected carboxylic acids (B), and segmer assembly polymerization methodology for sequenced poly(lactic-*co*-glycolic acid)s; poly LG (C), poly L*rac*G (D), poly GLLG (E), poly LLG (F).
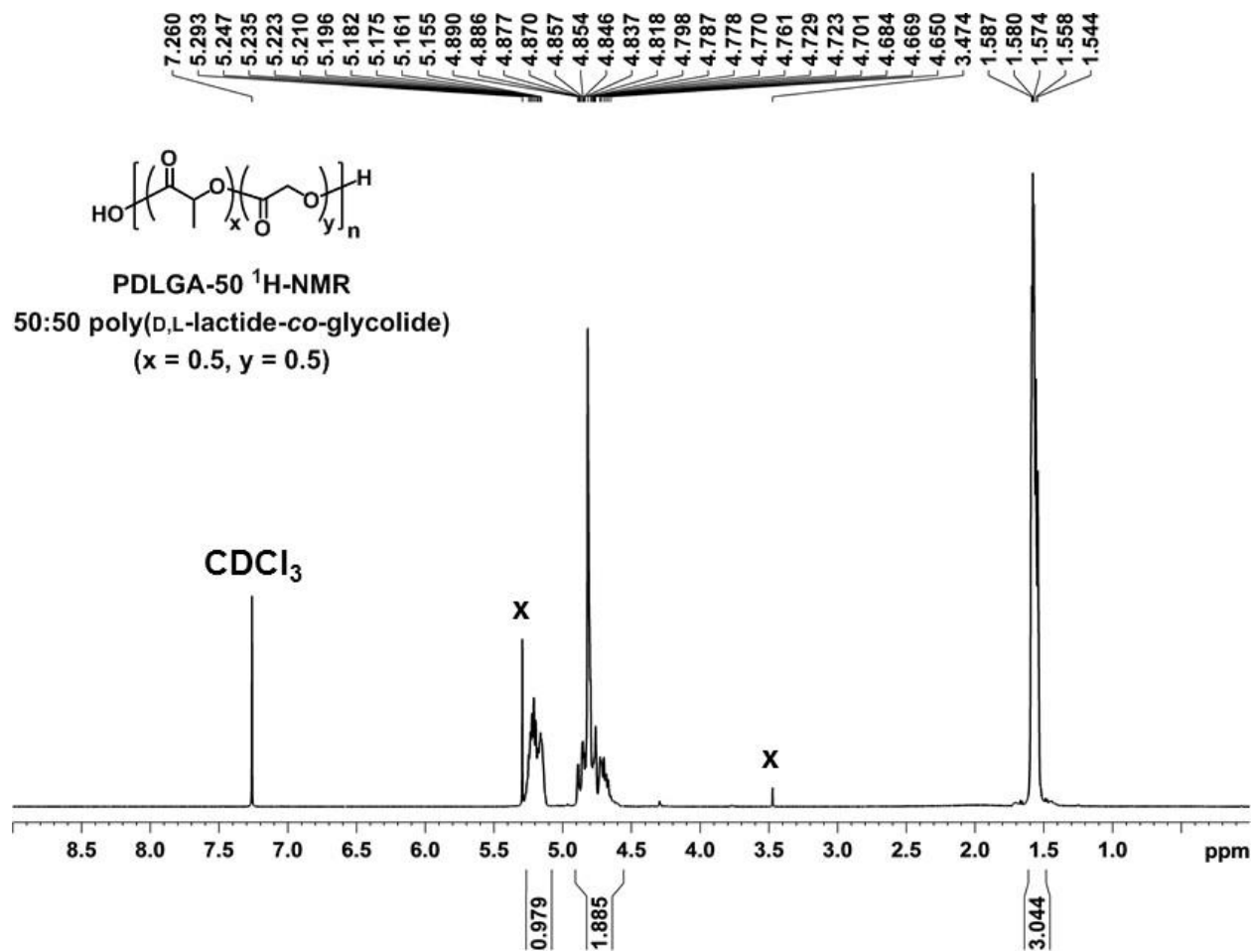
Figure C2. ¹H NMR (500 MHz, δ 9.0 – 0.0 ppm) of 50:50 poly(D,L-lactide-*co*-glycolide) (PDLGA-50)
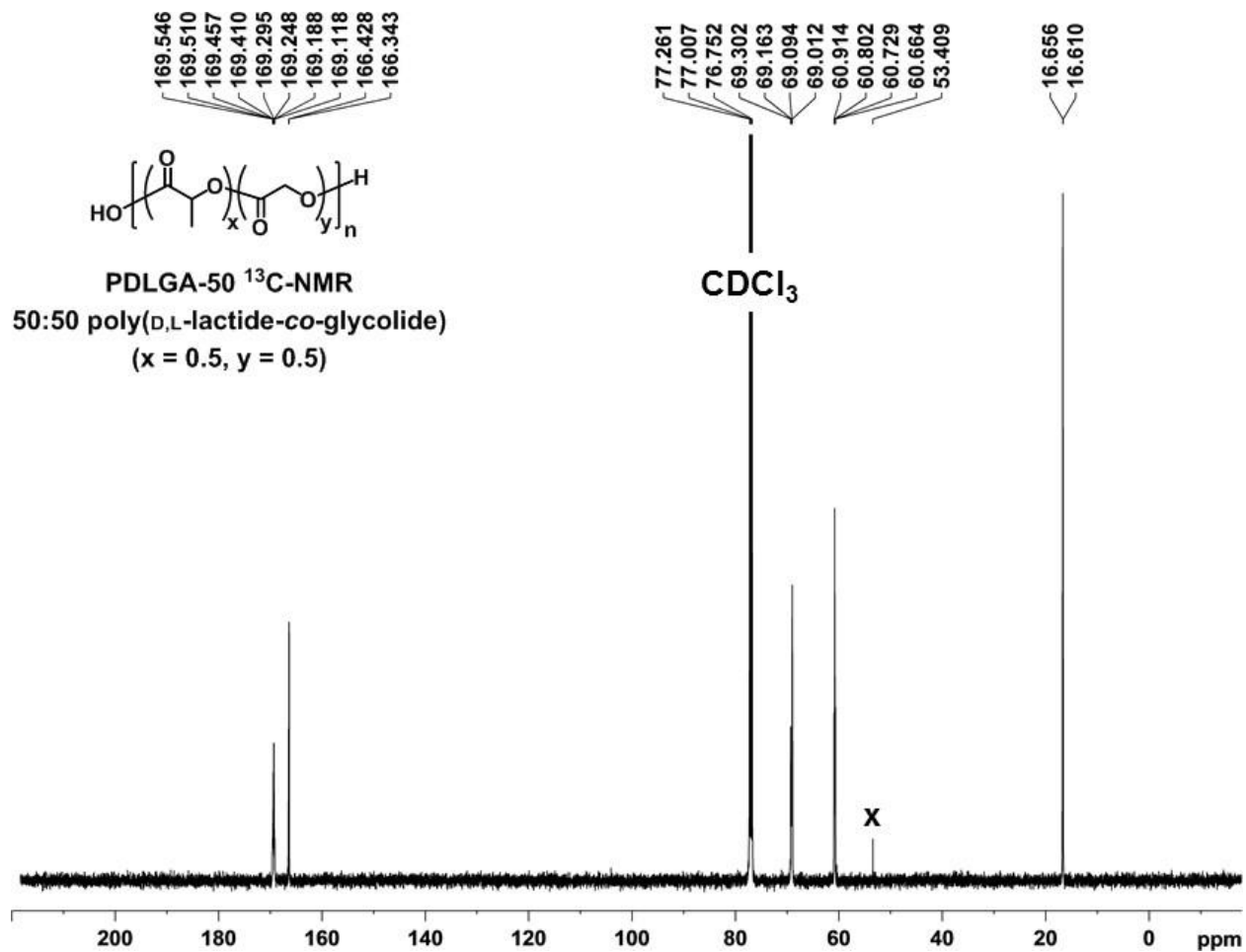
Figure C3. ^{13}C NMR (500 MHz, δ 220 – -10.0 ppm) of 50:50 poly(D,L-lactide-*co*-glycolide) (PDLGA-50).
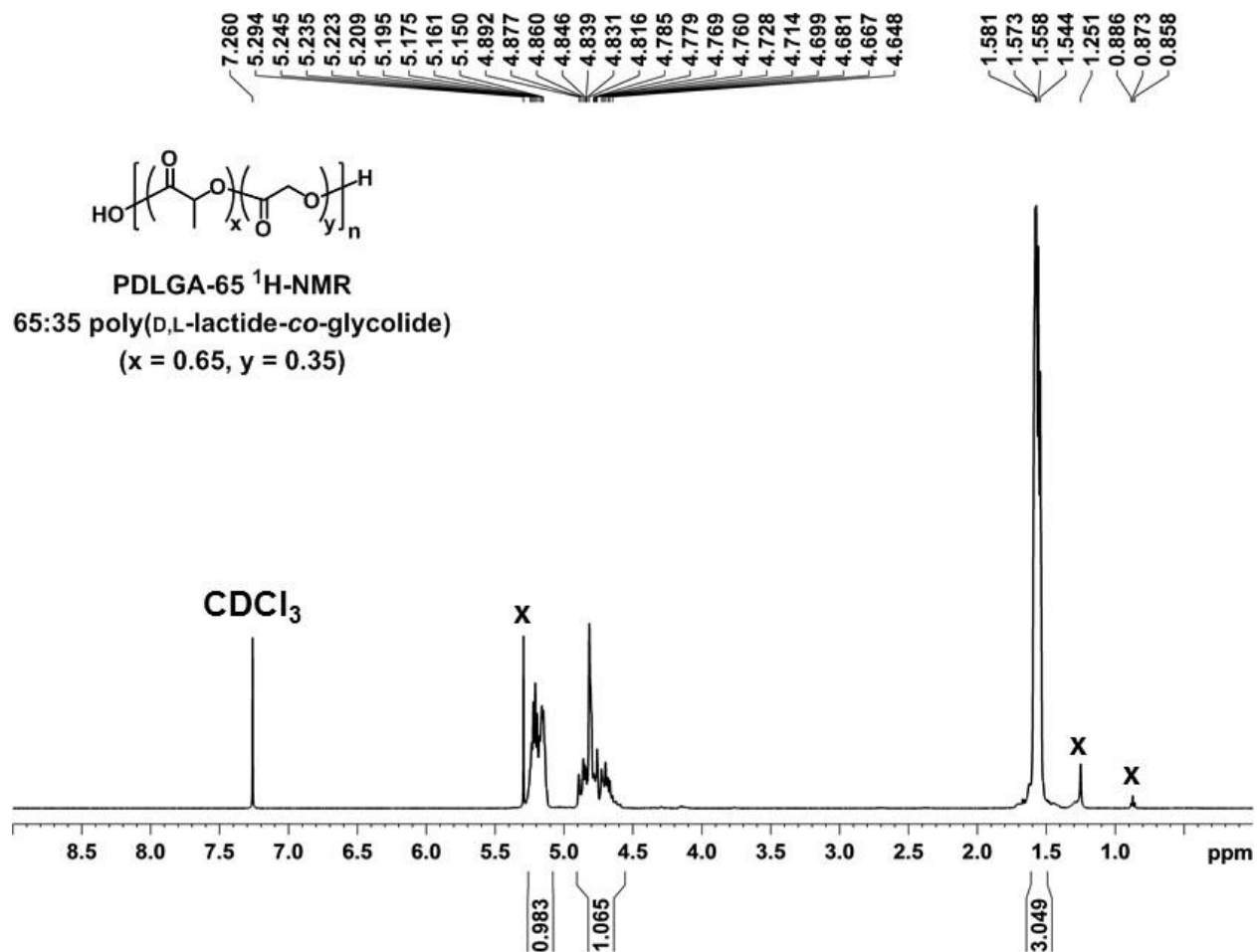
Figure C4. ^{1}H NMR (500 MHz, δ 9.0 – 0.0 ppm) of 65:35 poly(D,L-lactide-*co*-glycolide) (PDLGA-65).

146
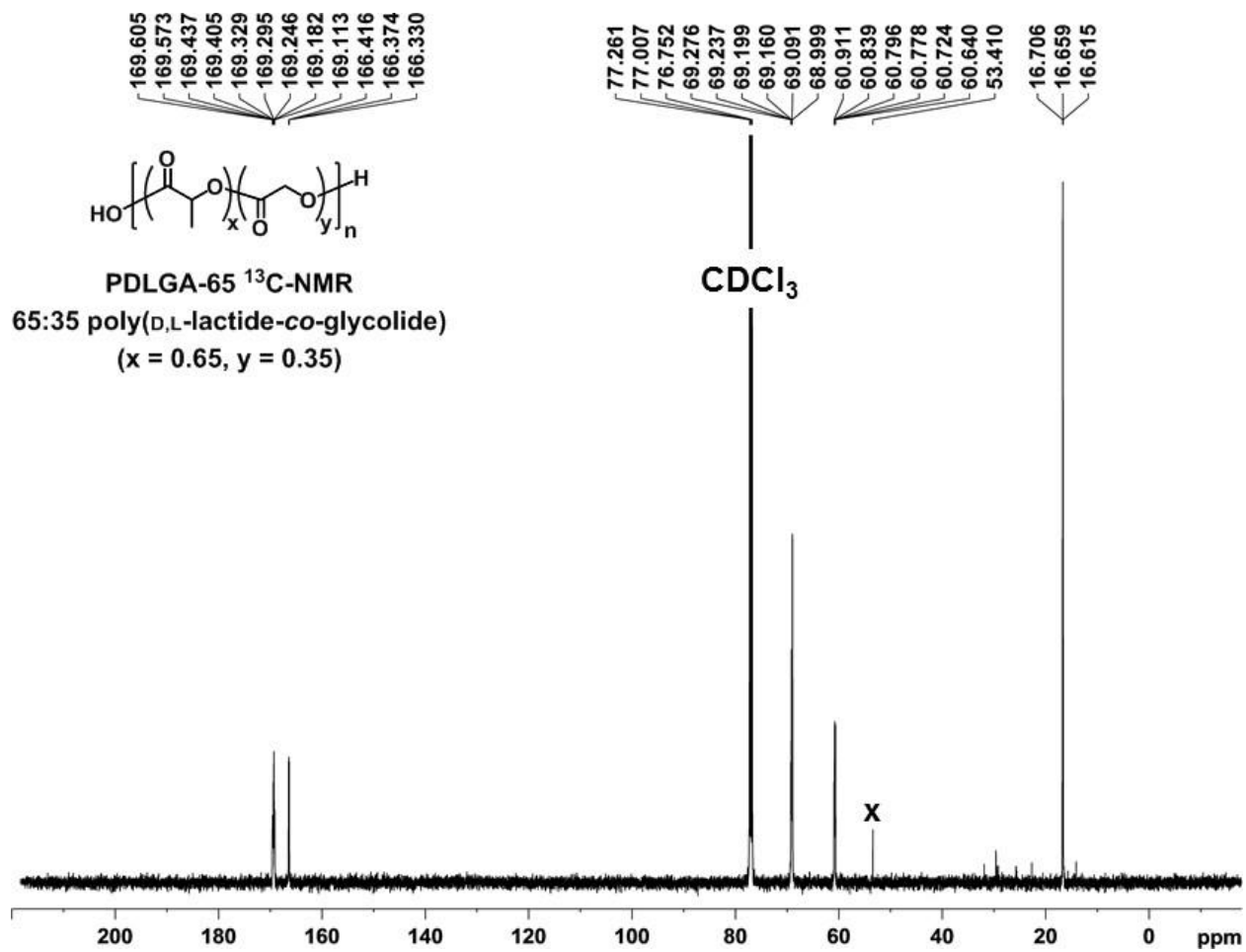
Figure C5. ^{13}C NMR (500 MHz, δ 220 – -10.0 ppm) of 65:35 poly(D,L-lactide-*co*-glycolide) (PDLGA-65).
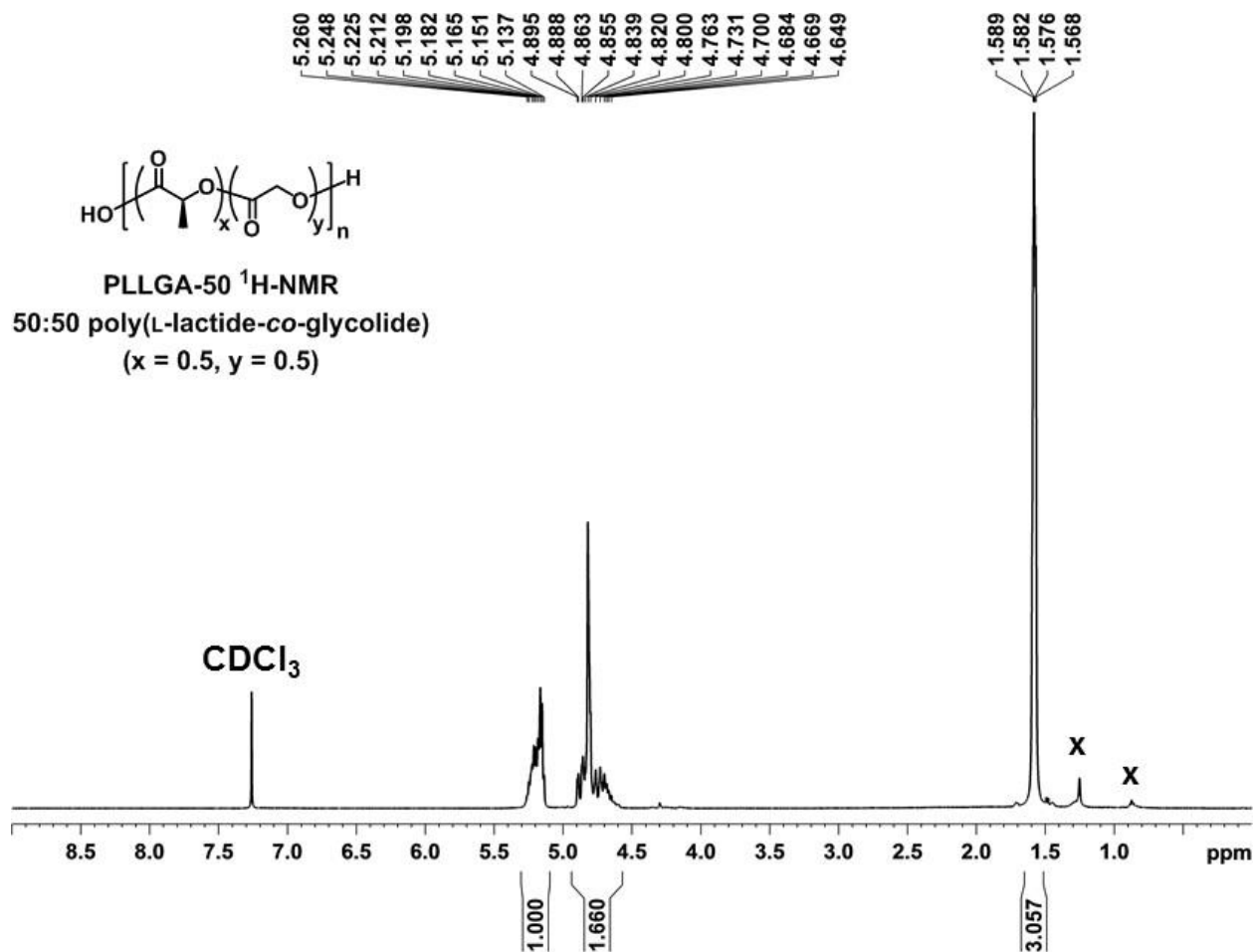
Figure C6. ^{1}H NMR (500 MHz, δ 9.0 – 0.0 ppm) of 50:50 poly(L-lactide-*co*-glycolide) (PLLGA-50).
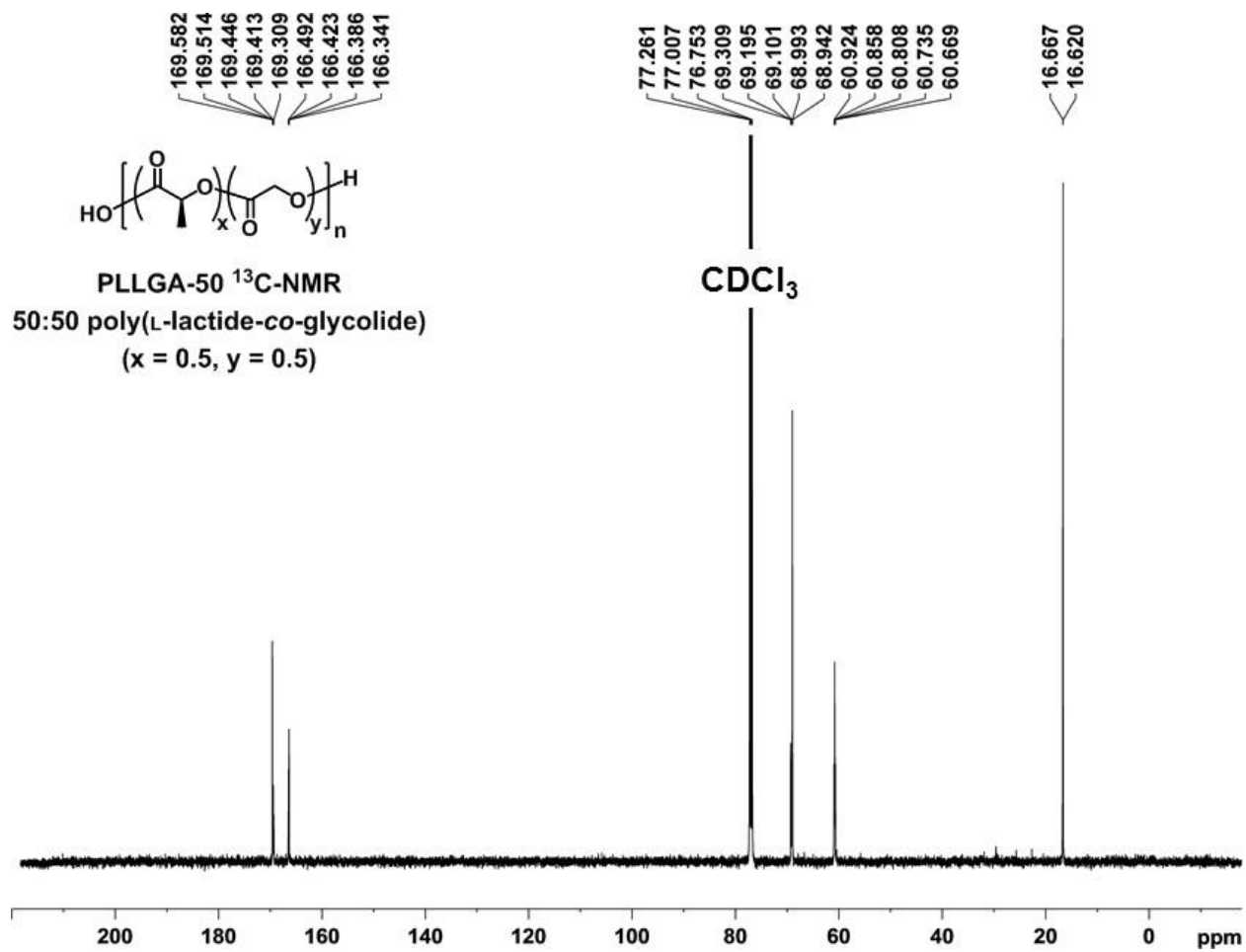
Figure C7. ^{13}C NMR (500 MHz, δ 220 – -10.0 ppm) of 50:50 poly(L-lactide-*co*-glycolide) (PLLGA-50).
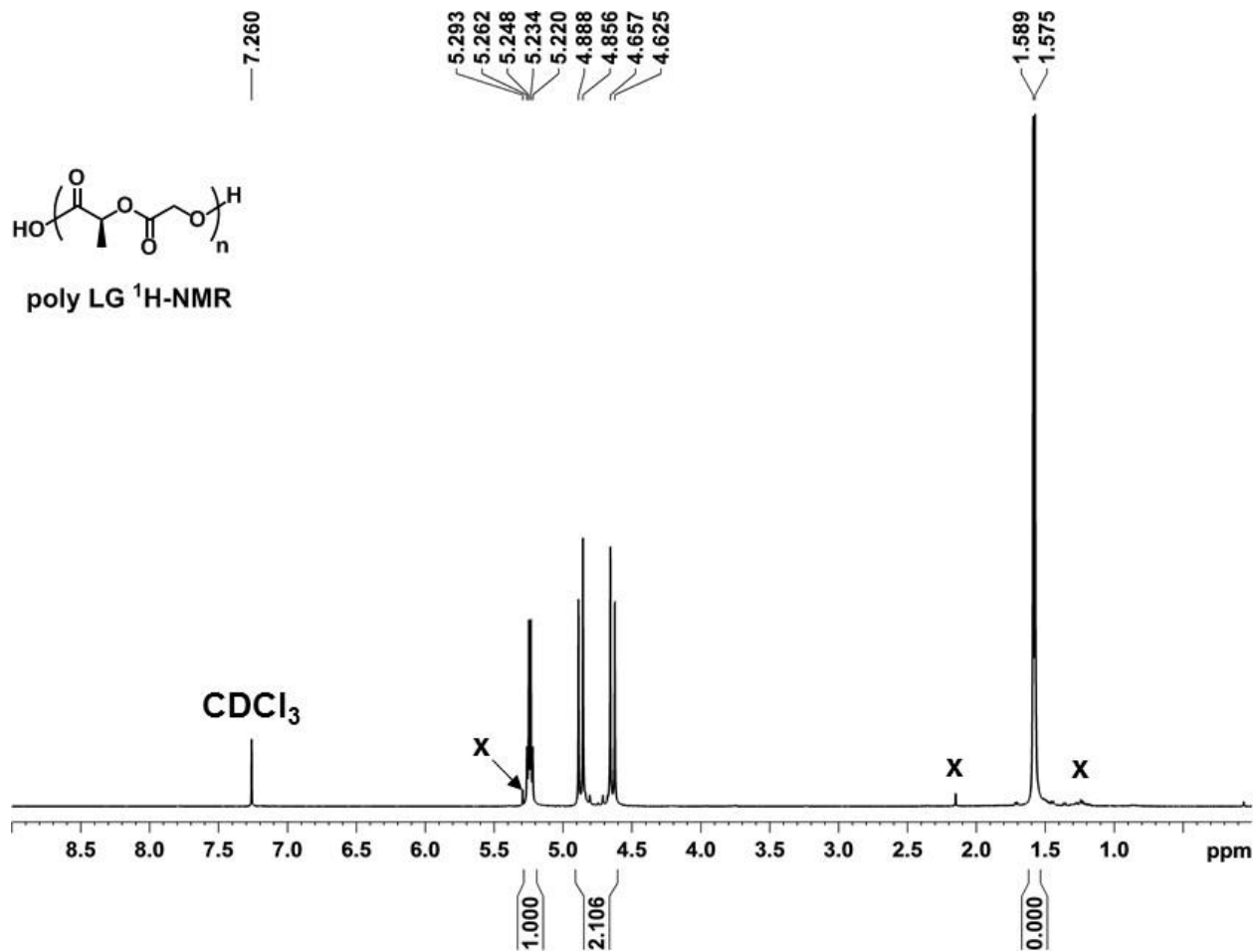
Figure C8. ^{1}H NMR (500 MHz, δ 9.0 – 0.0 ppm) of poly LG.
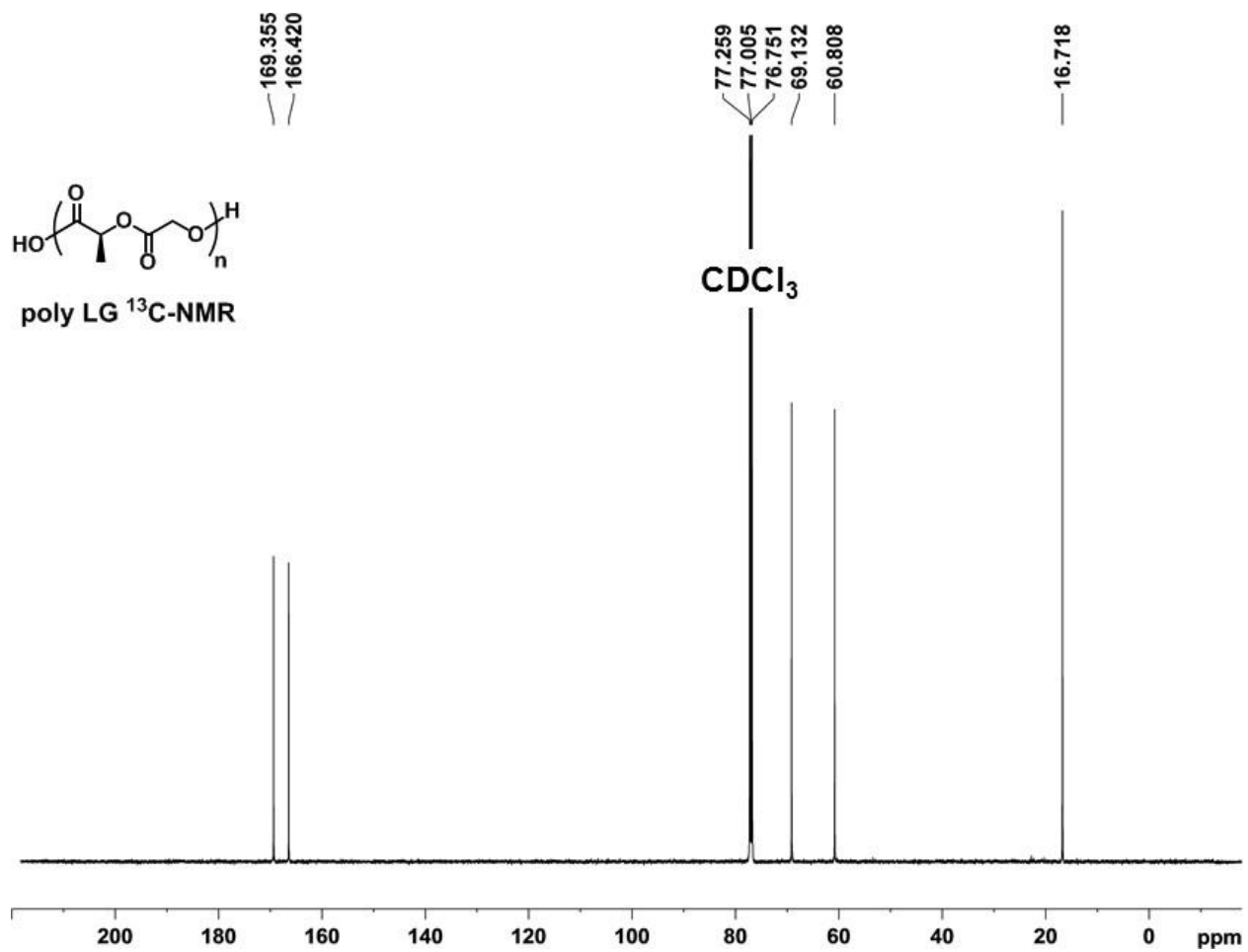
Figure C9. ^{13}C NMR (500 MHz, δ 220 – -10.0 ppm) of poly LG.
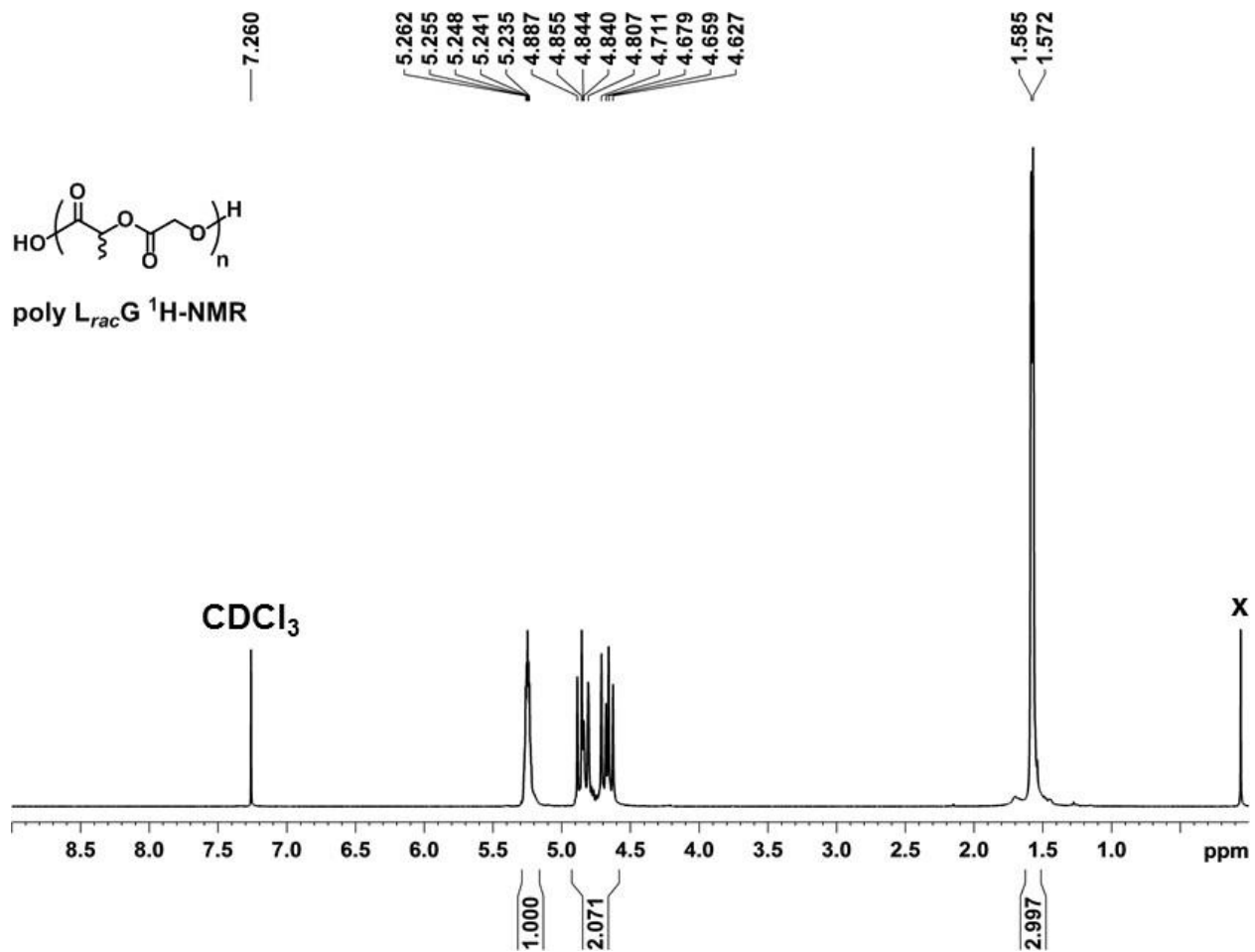
Figure C10. ^{1}H NMR (500 MHz, δ 9.0 – 0.0 ppm) of poly L$_{rac}$G.

152
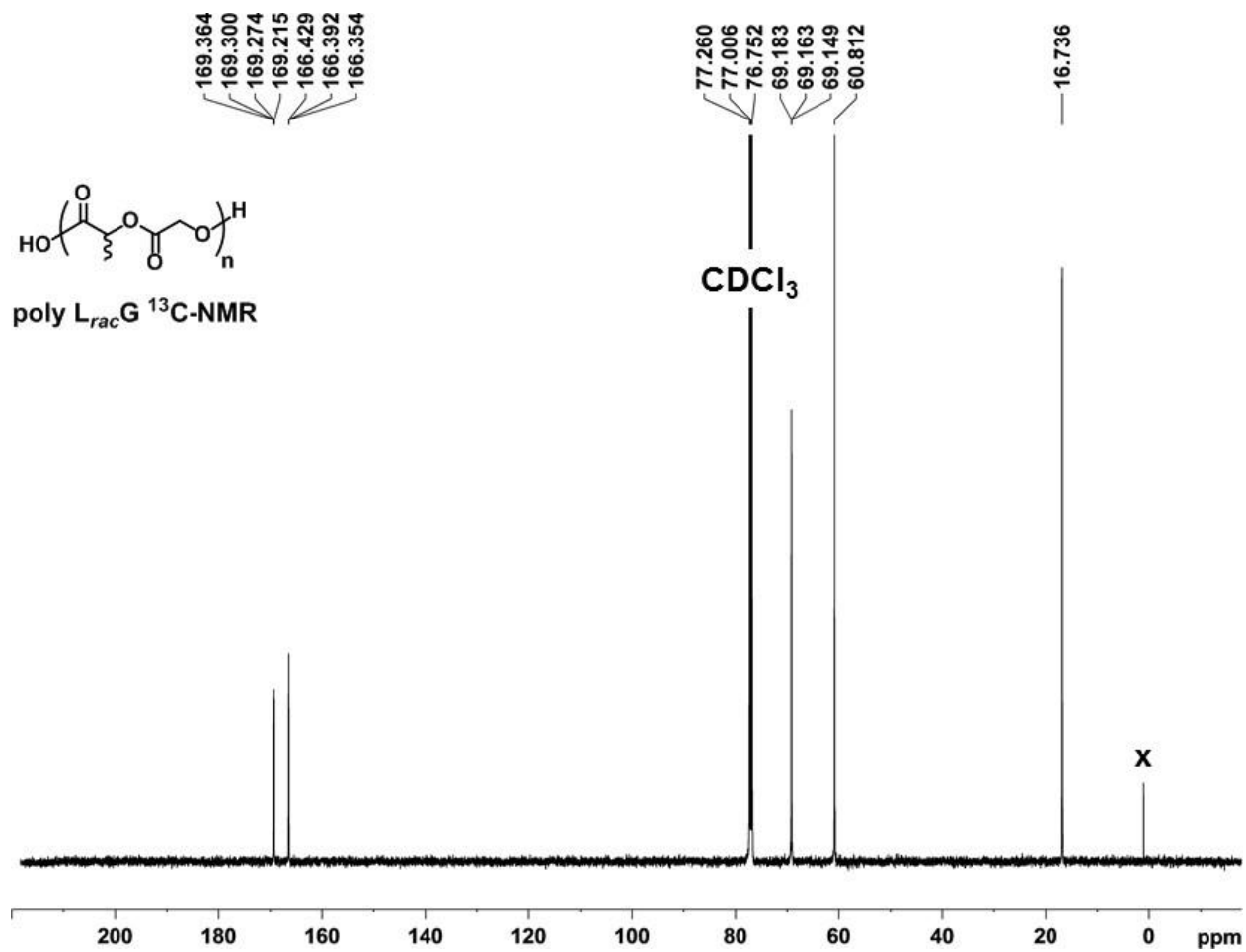
Figure C11. ^{13}C NMR (500 MHz, δ 220 – -10.0 ppm) of poly L$_{rac}$G.

Figure C12. ^{1}H NMR (500 MHz, δ 9.0 – 0.0 ppm) of poly LLG.
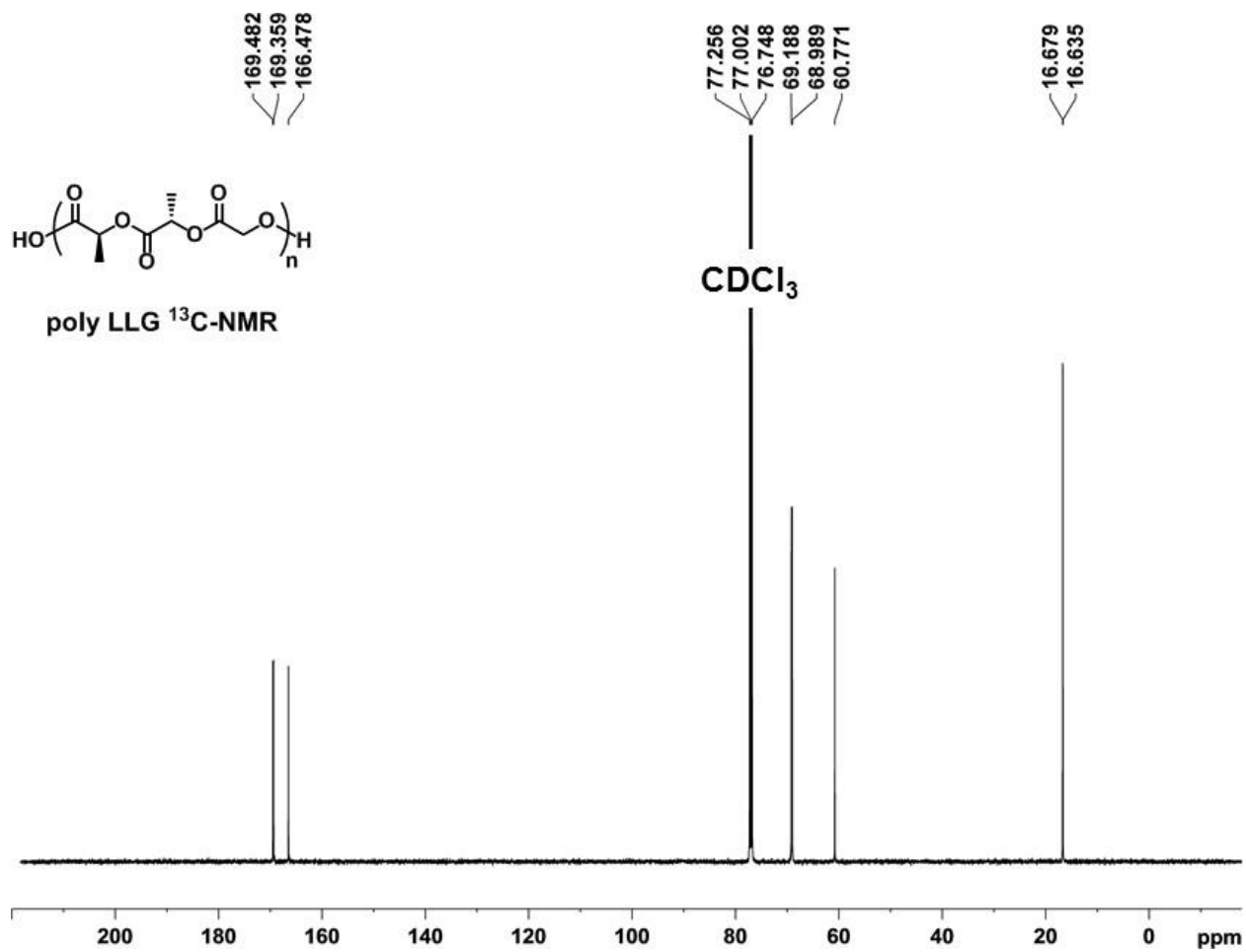
Figure C13. ^{13}C NMR (500 MHz, δ 220 – -10.0 ppm) of poly LLG.
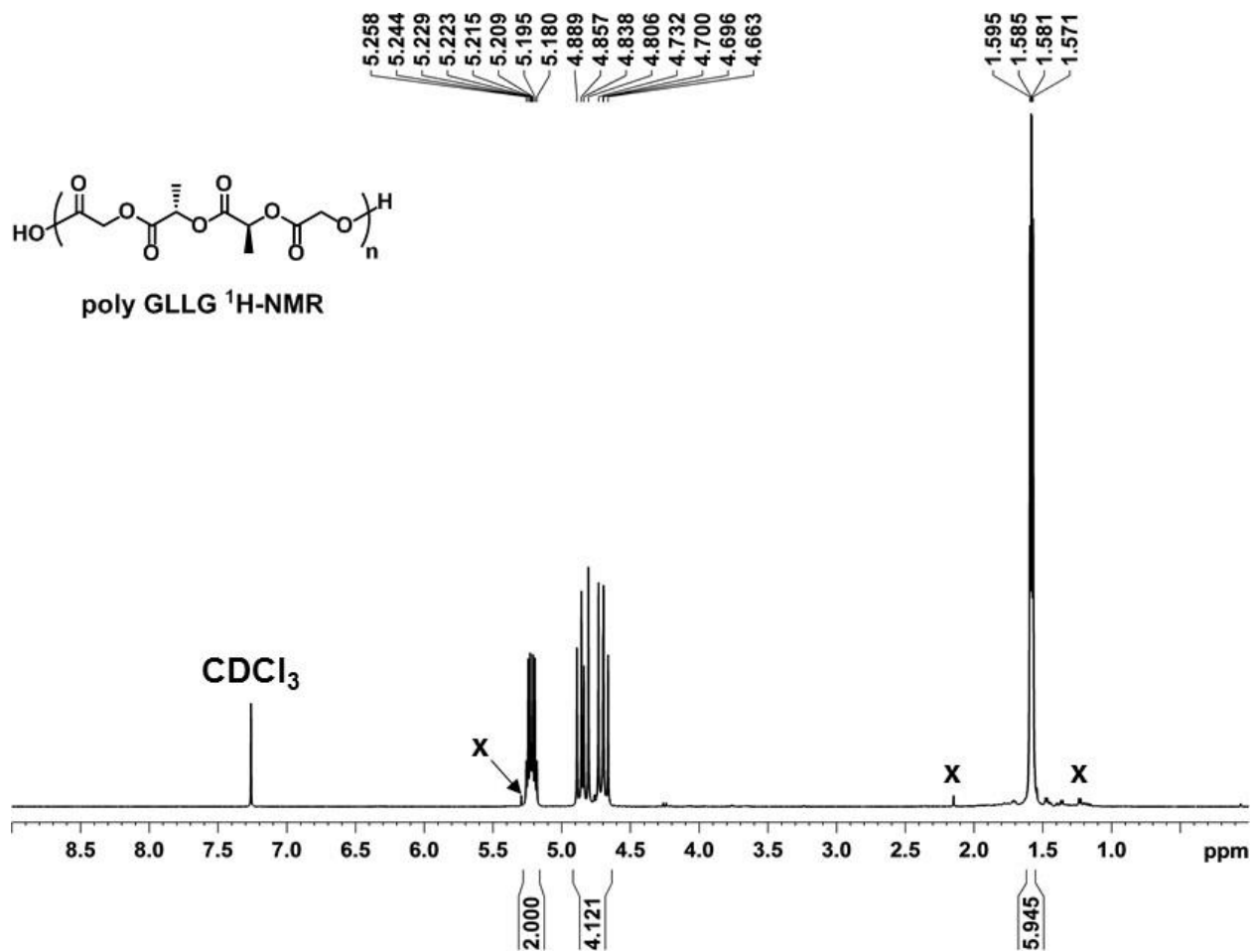
Figure C14. ^{1}H NMR (500 MHz, δ 9.0 – 0.0 ppm) of poly GLLG.
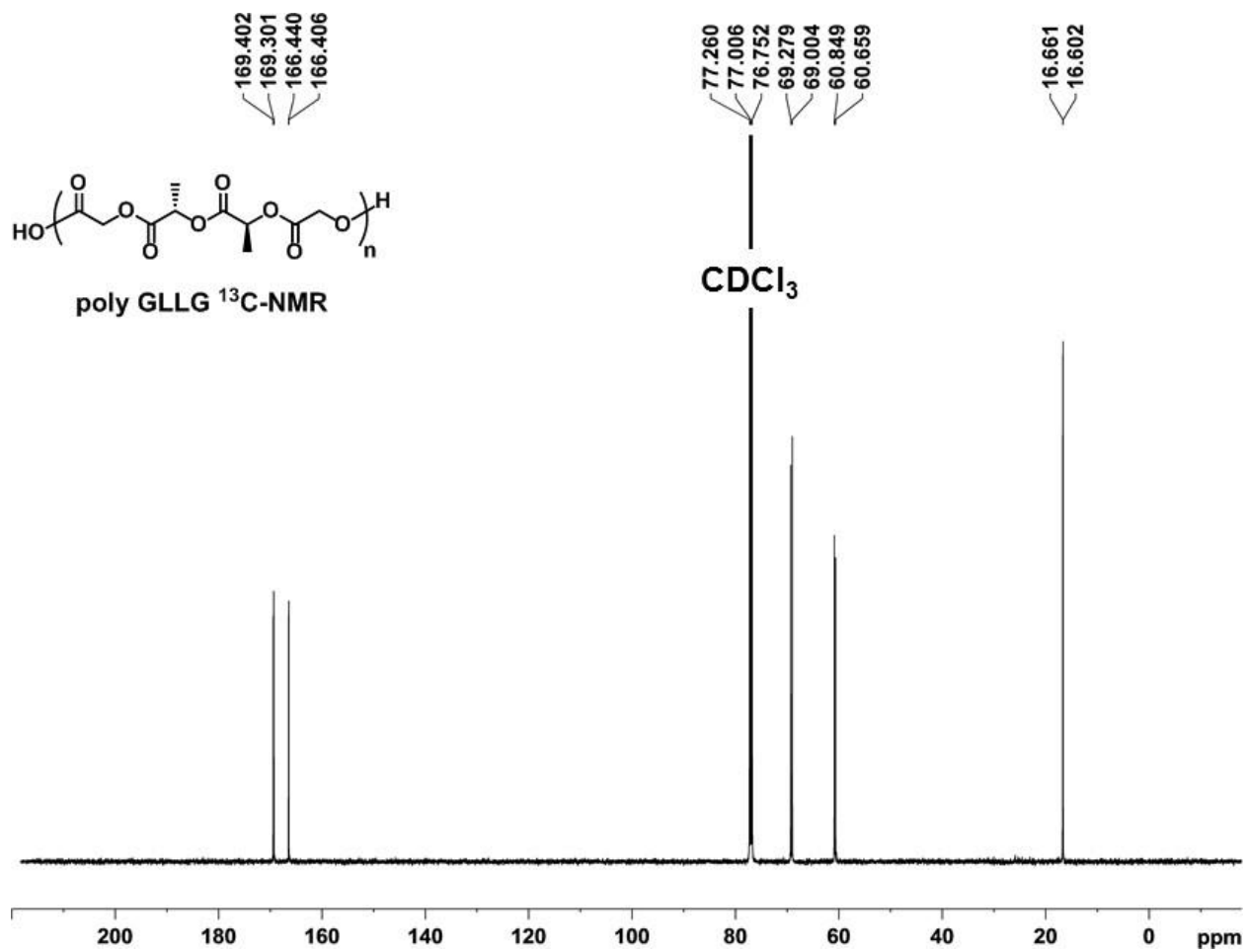
Figure C15. ^{13}C NMR (500 MHz, δ 220 − -10.0 ppm) of poly GLLG.
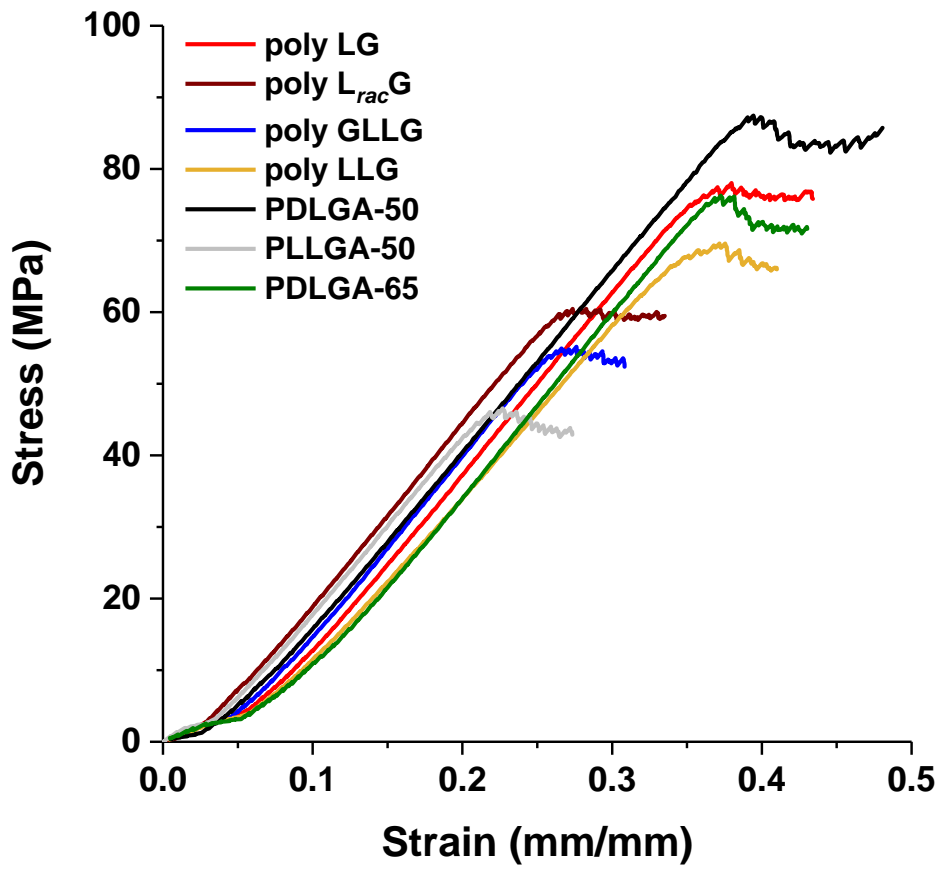
Figure C16. Representative stress-strain curves for sequenced and random PLGAs acquired during compression at a rate of 0.1 mm/min.
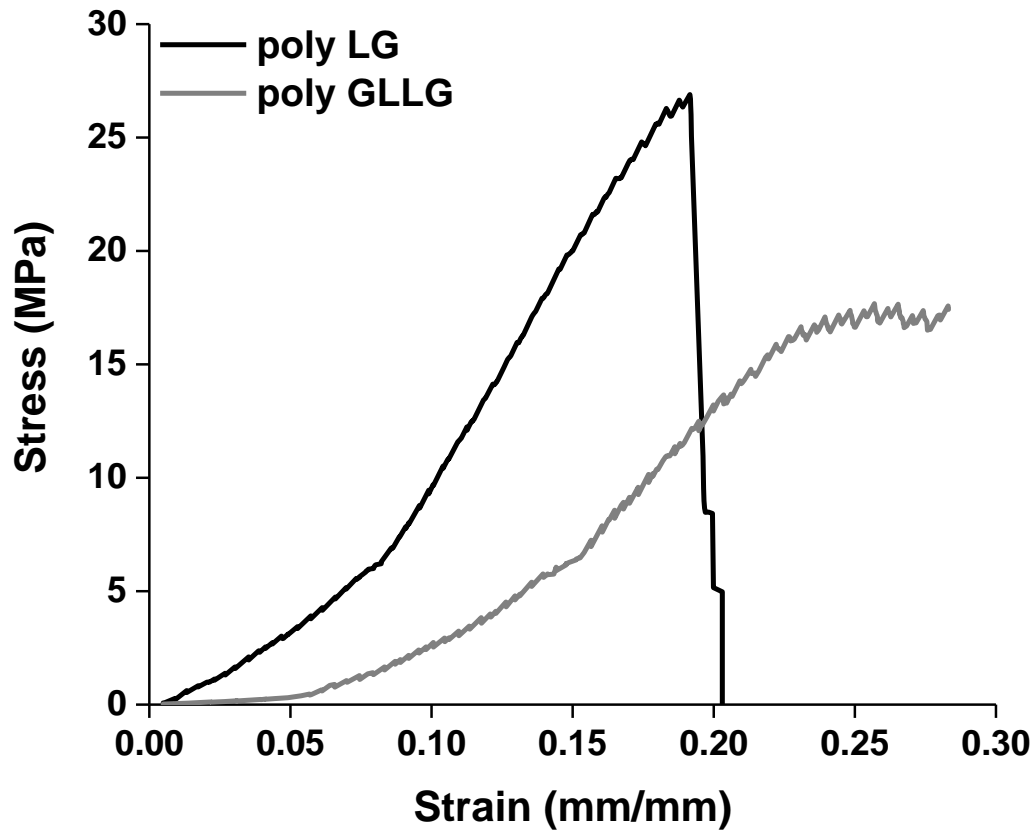
Figure C17. Representative failure mechanism stress-strain curves for poly LG (brittle failure) and poly GLLG (ductile failure) after 35 d *in vitro* acquired during compression at a rate of 0.1 mm/min.
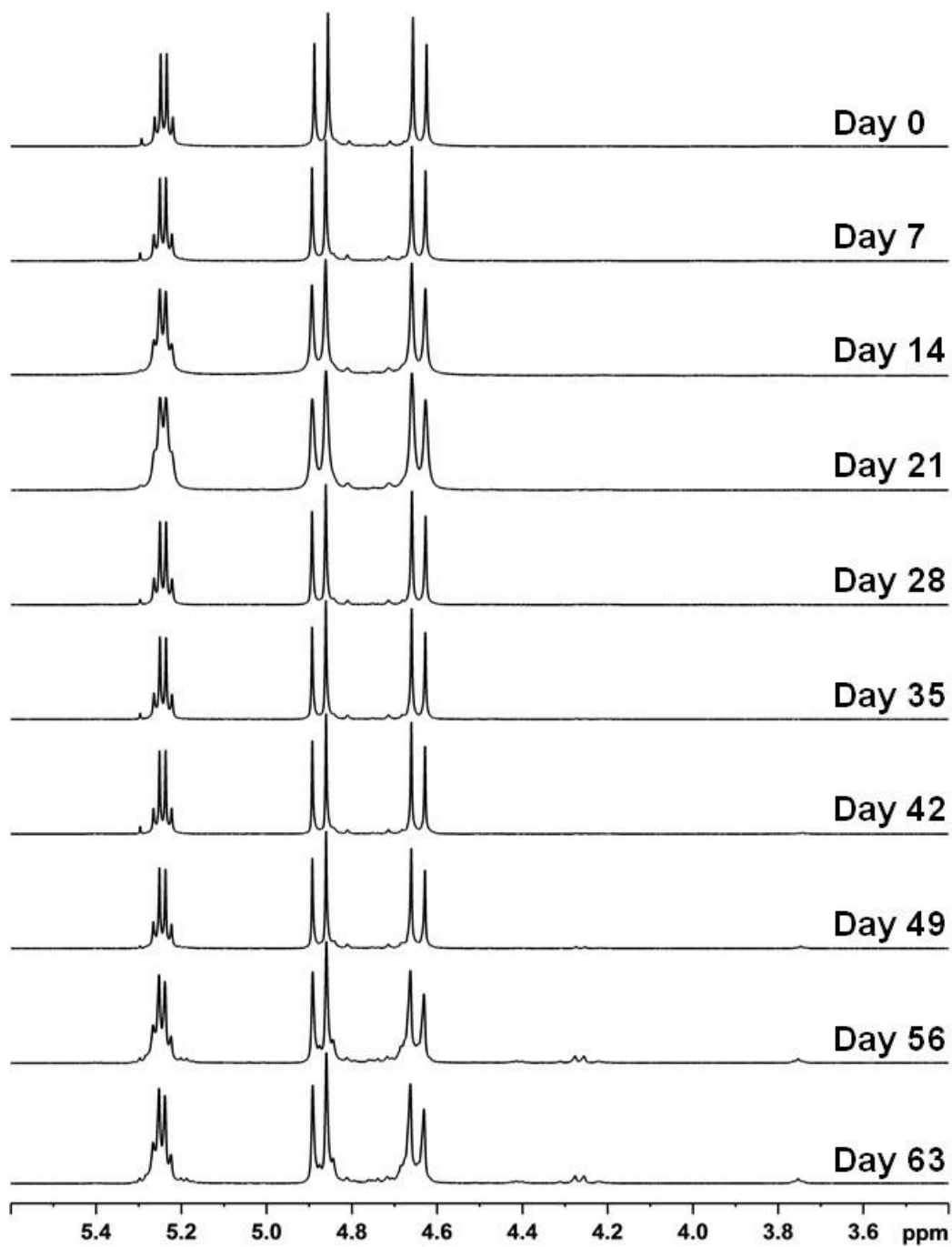
Figure C18. ^{1}H-NMR (500 MHz, CDCl$_3$, δ 5.6 – 3.4 ppm) overlay of poly LG over the course of 63 days *in vitro*.

The regions displayed correlate to the methine (δ 5.3 – 5.2 ppm) and methylene (δ 4.9 – 4.6 ppm) proton resonances.
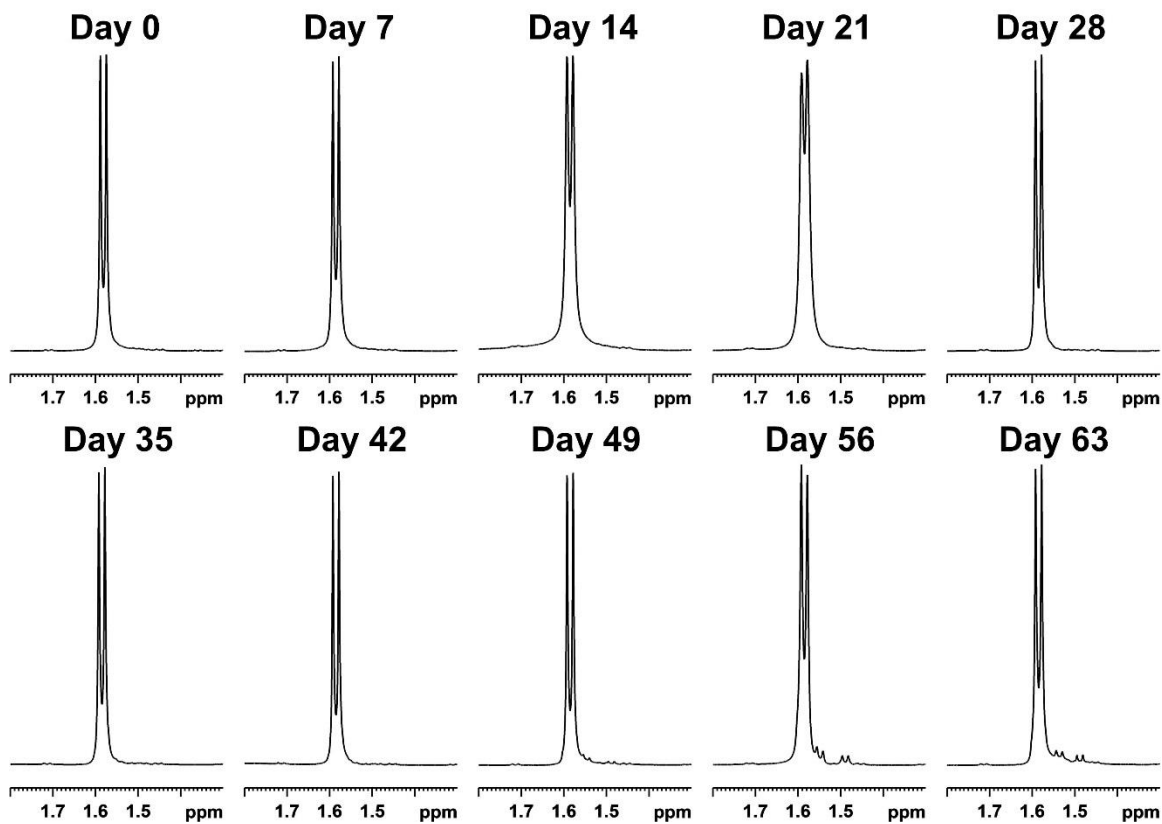
Figure C19. ^{1}H-NMR (500 MHz, CDCl3, δ 1.8 – 1.3 ppm) overlay of poly LG over the course of 63 days in vitro.

The region displayed correlates to the methyl proton resonance.
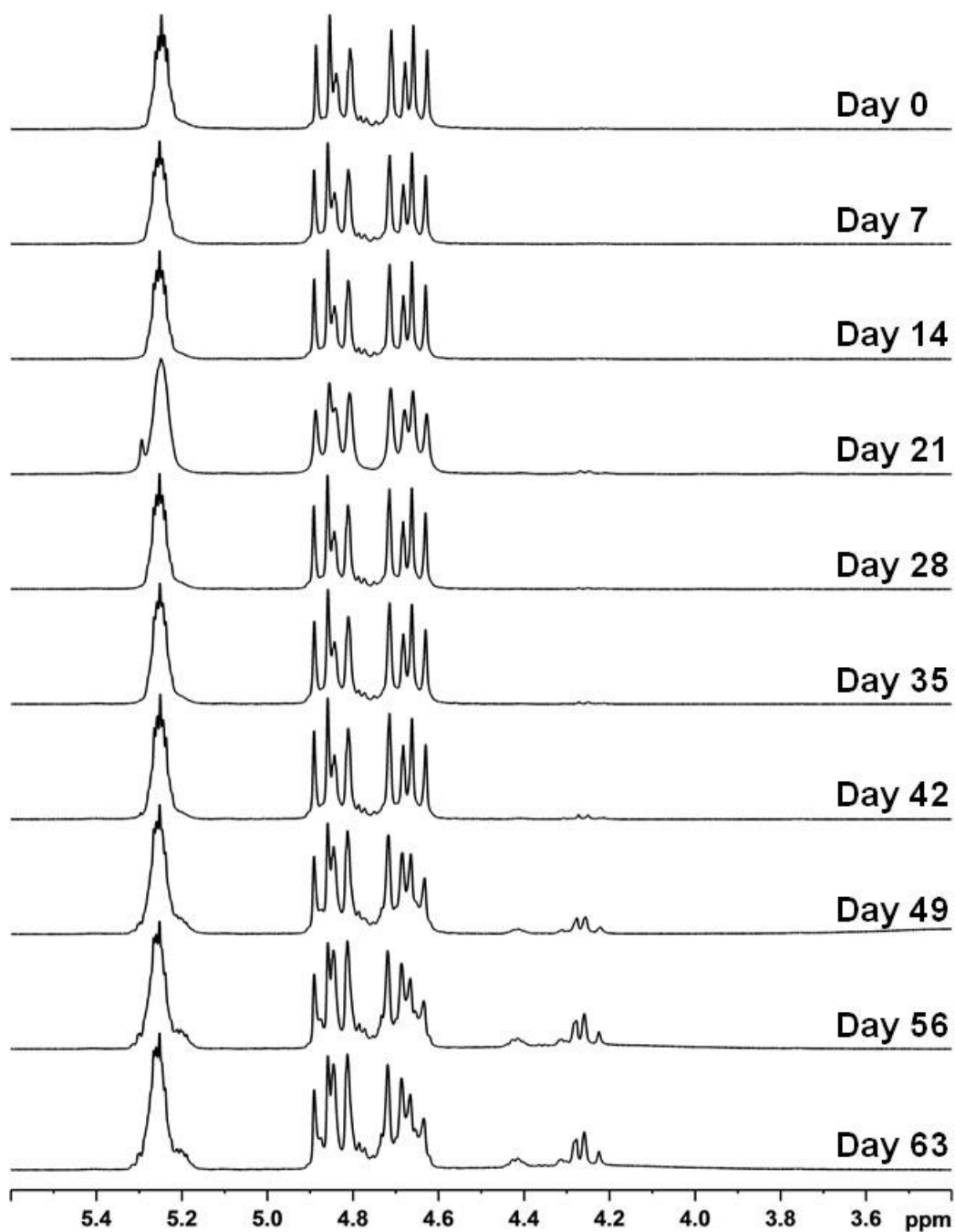
Figure C20. ^{1}H-NMR (500 MHz, CDCl$_3$, δ 5.6 – 3.4 ppm) overlay of poly L$_{rac}$G over the course of 63 days *in vitro*.

The regions displayed correlate to the methine (δ 5.3 – 5.1 ppm) and methylene (δ 4.9 – 4.6 ppm) proton resonances.
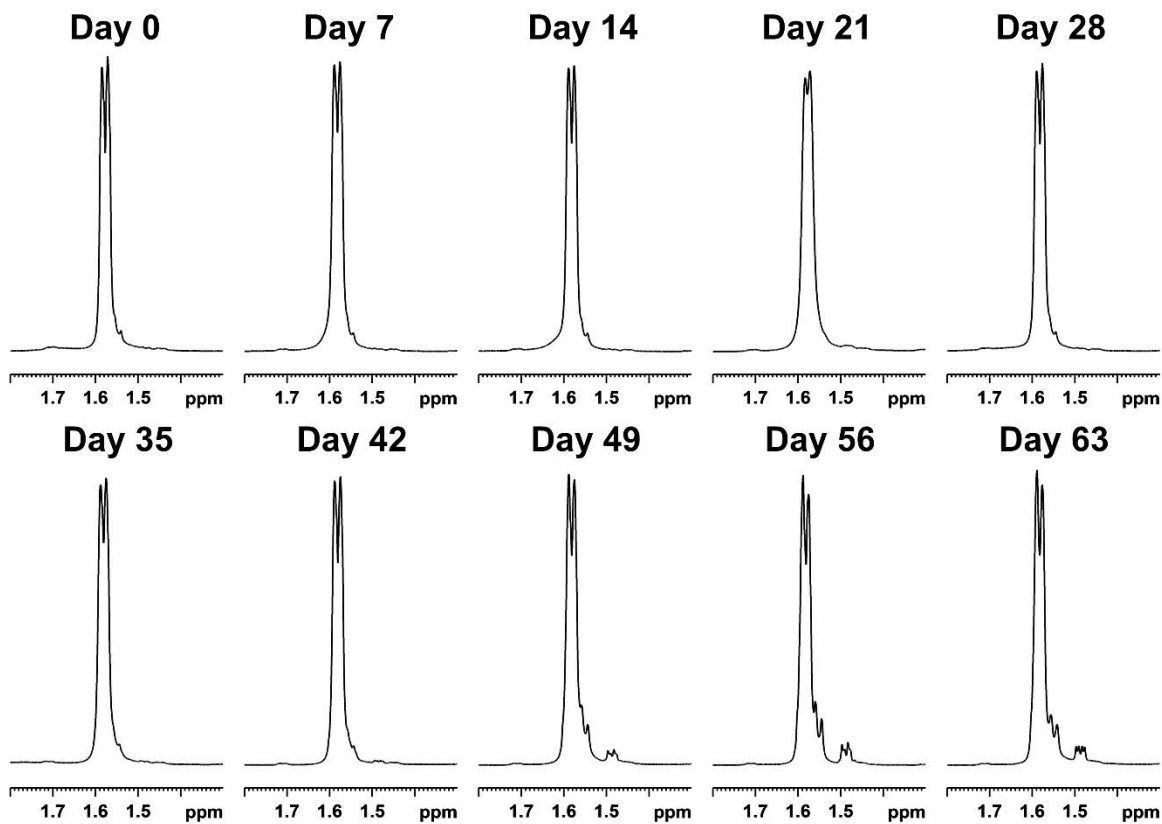
Figure C21. ^{1}H-NMR (500 MHz, CDCl$_3$, δ 1.8 – 1.3 ppm) overlay of poly L$_{rac}$G over the course of 63 days *in vitro*.

The region displayed correlates to the methyl proton resonance.
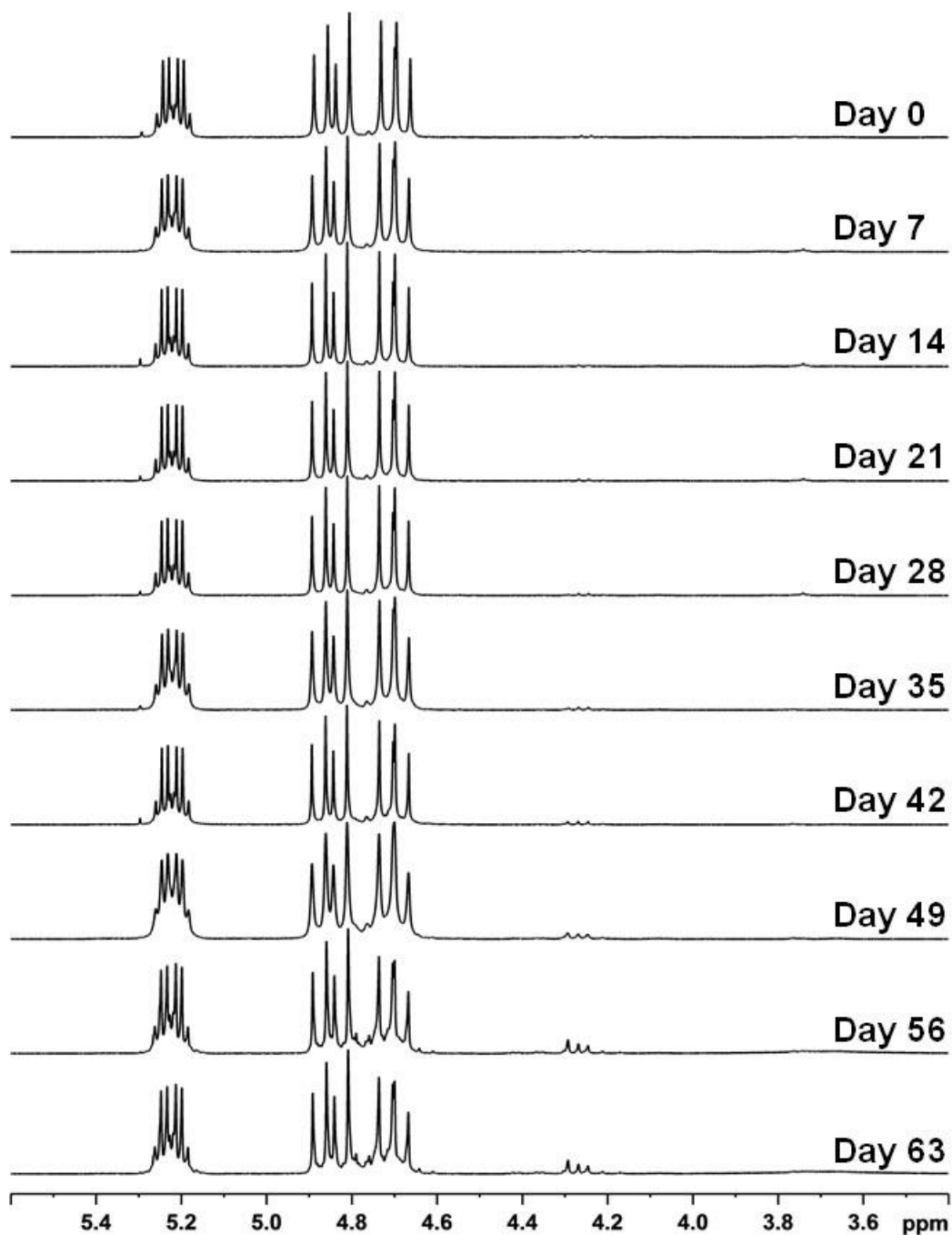
Figure C22. ^{1}H-NMR (500 MHz, CDCl$_3$, δ 5.6 – 3.4 ppm) overlay of poly GLLG over the course of 63 days *in vitro*. The regions displayed correlate to the methine (δ 5.3 – 5.1 ppm) and methylene (δ 4.9 – 4.6 ppm) proton resonances.
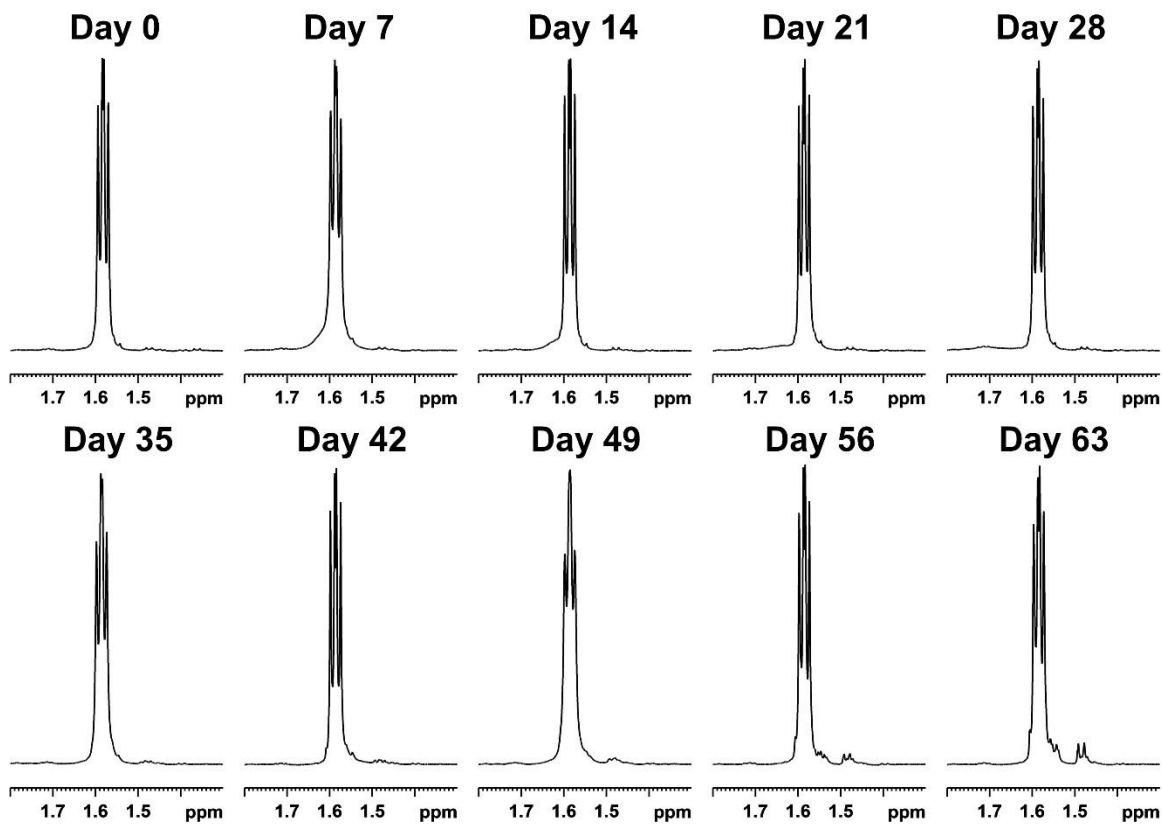
Figure C23. ^{1}H-NMR (500 MHz, CDCl$_3$, δ 1.8 – 1.3 ppm) overlay of poly GLLG over the course of 63 days *in vitro*. The region displayed correlates to the methyl proton resonance.
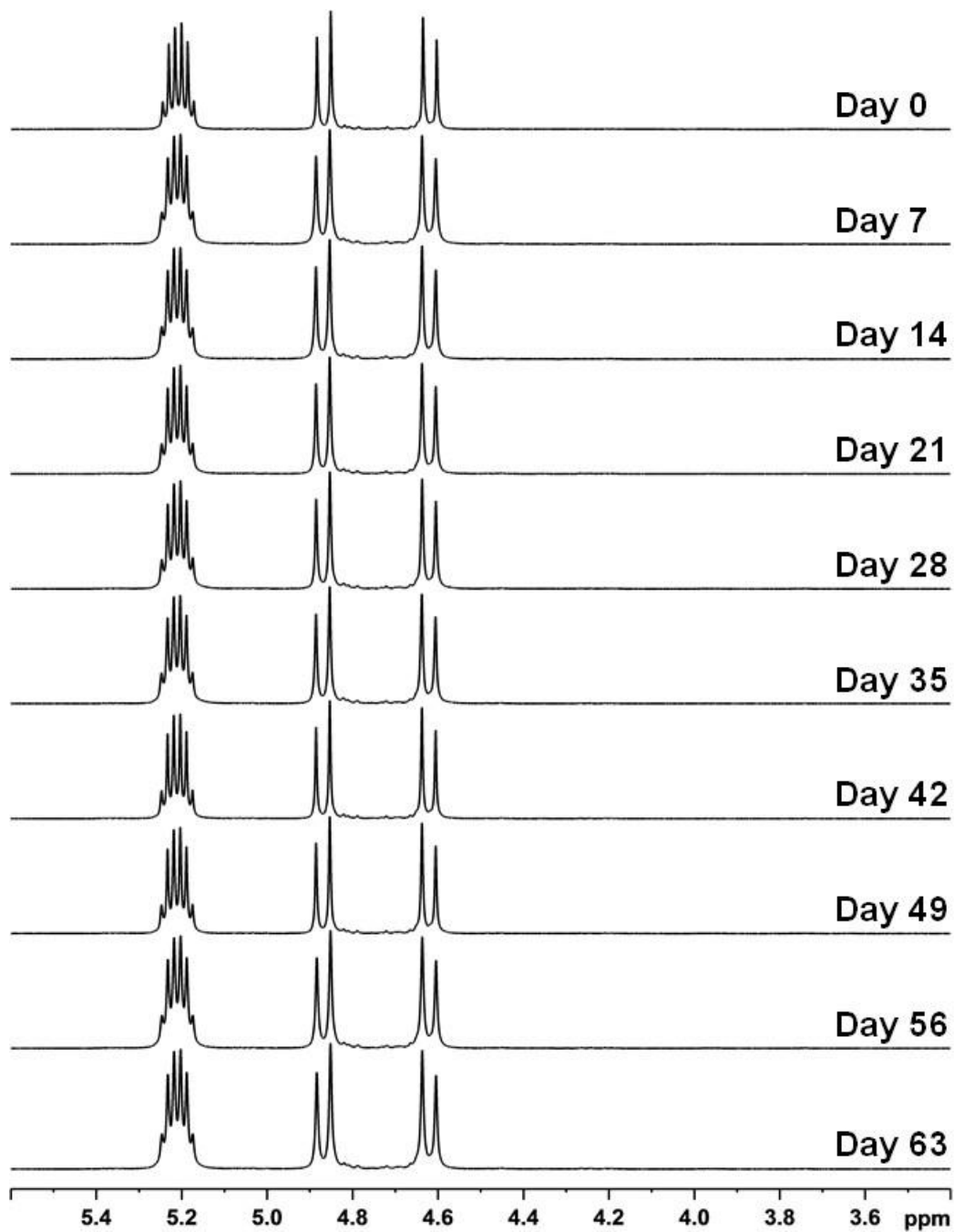
Figure C24. [^1]H-NMR (500 MHz, CDCl₃, δ 5.6 – 3.4 ppm) overlay of poly LLG over the course of 63 days *in vitro*.

The regions displayed correlate to the methine (δ 5.3 – 5.1 ppm) and methylene (δ 4.9 – 4.6 ppm) proton resonances.
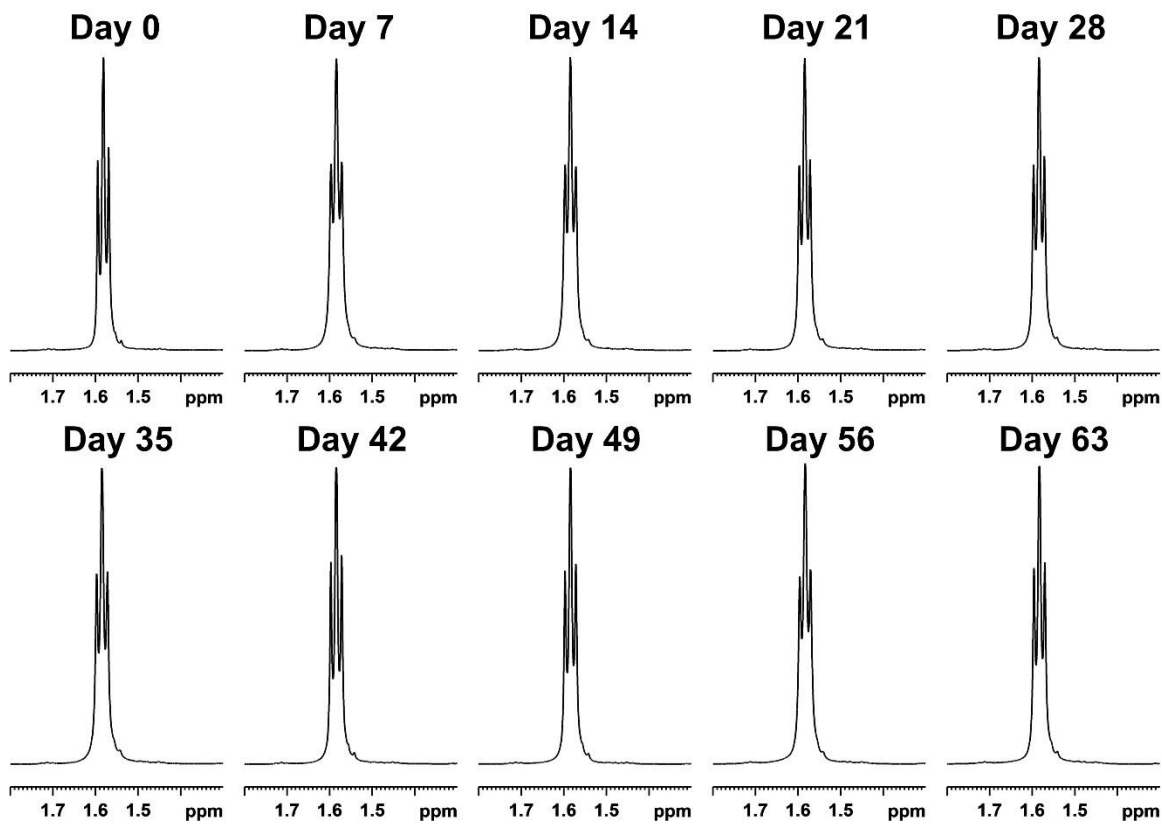
Figure C25. ^{1}H-NMR (500 MHz, CDCl$_3$, δ 1.8 – 1.3 ppm) overlay of poly LLG over the course of 63 days *in vitro*.

The region displayed correlates to the methyl proton resonance.
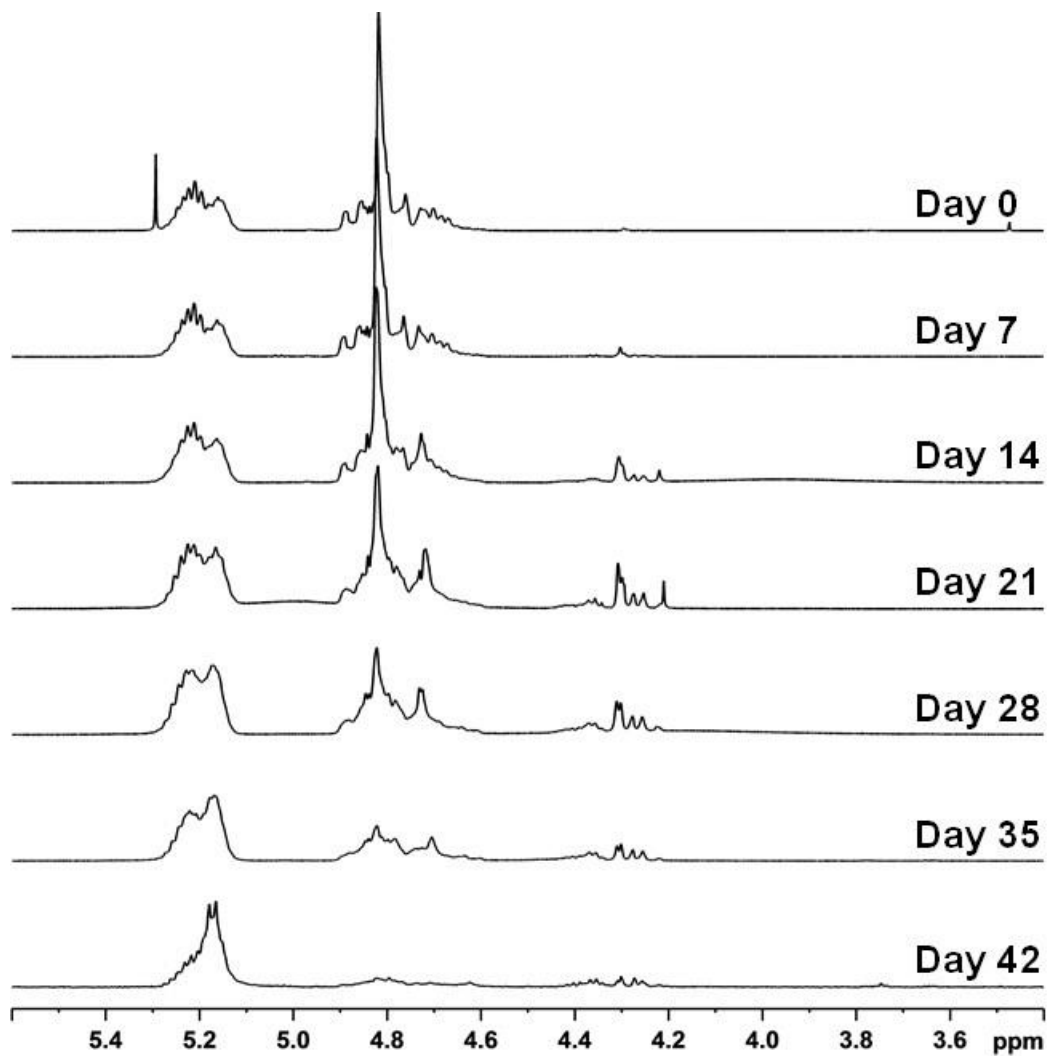
Figure C26. ^{1}H-NMR (500 MHz, CDCl$_3$, δ 5.6 – 3.4 ppm) overlay of 50:50 poly(D,L-lactide-*co*-glycolide)

(PDLGA-50) over the course of 42 days *in vitro*. The regions displayed correlate to the methine (δ 5.3 – 5.1 ppm)

and methylene (δ 4.9 – 4.5 ppm) proton resonances.

168
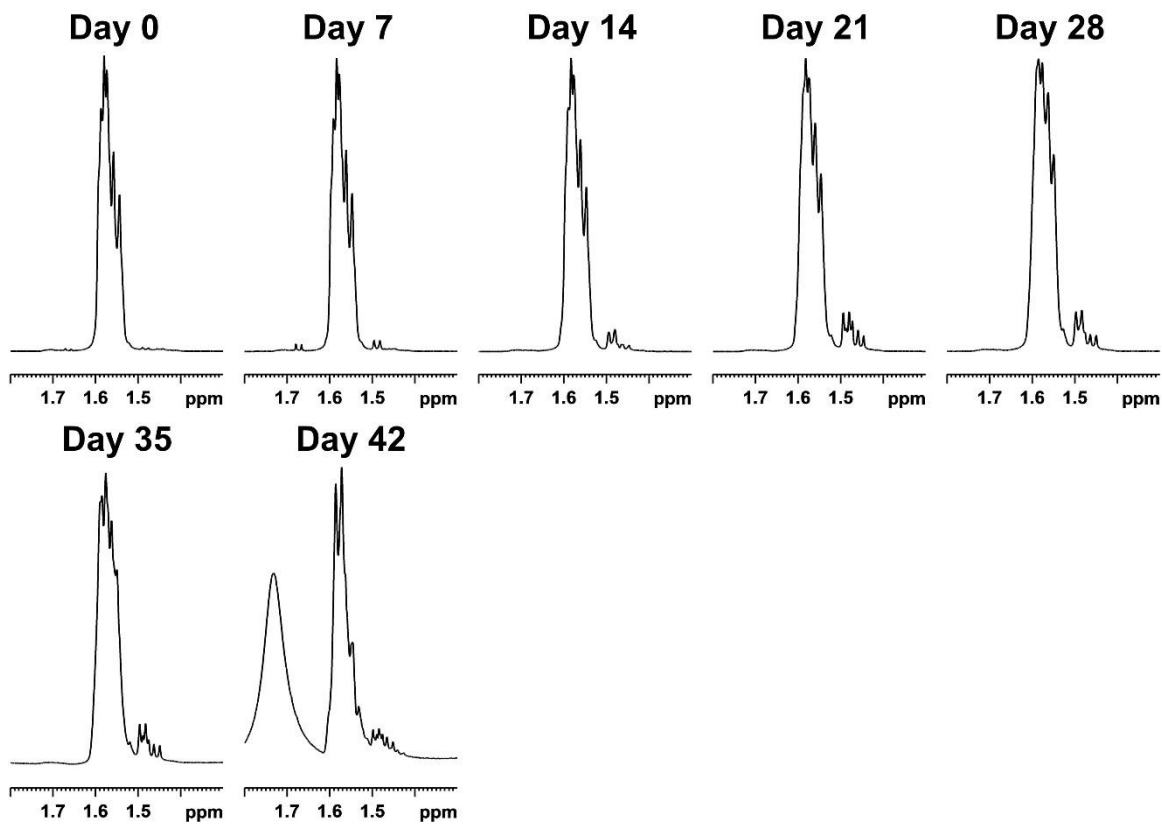
Figure C27. ^{1}H-NMR (500 MHz, CDCl$_3$, δ 1.8 – 1.3 ppm) overlay of 50:50 poly(D,L-lactide-*co*-glycolide)

(PDLGA-50) over the course of 42 days *in vitro*. The region displayed correlates to the methyl proton resonance.
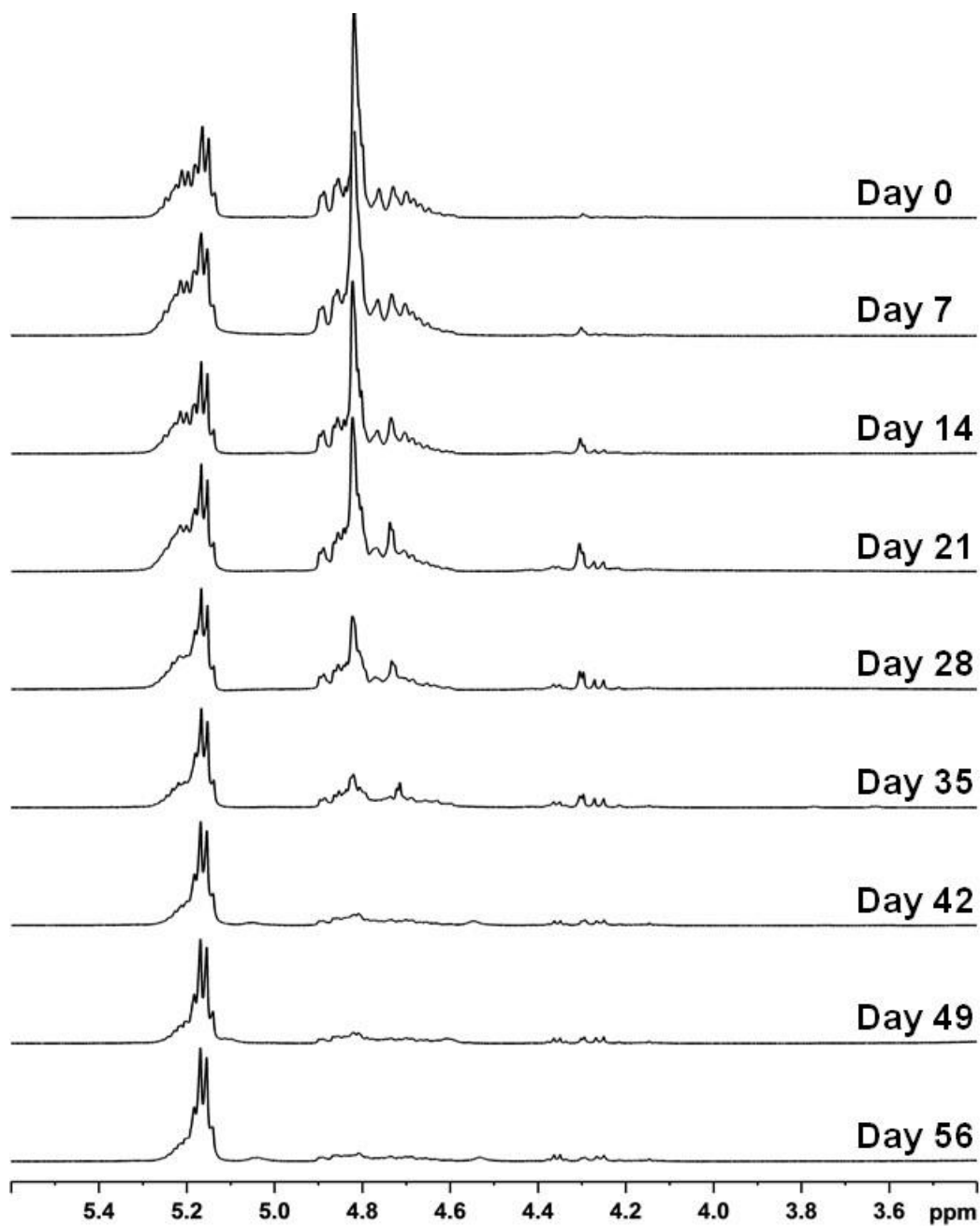
Figure C28. ^{1}H-NMR (500 MHz, CDCl$_3$, δ 5.6 – 3.4 ppm) overlay of 50:50 poly(L-lactide-*co*-glycolide) (PLLGA-50) over the course of 56 days *in vitro*. The regions displayed correlate to the methine (δ 5.3 – 5.1 ppm) and methylene (δ 4.9 – 4.5 ppm) proton resonances.
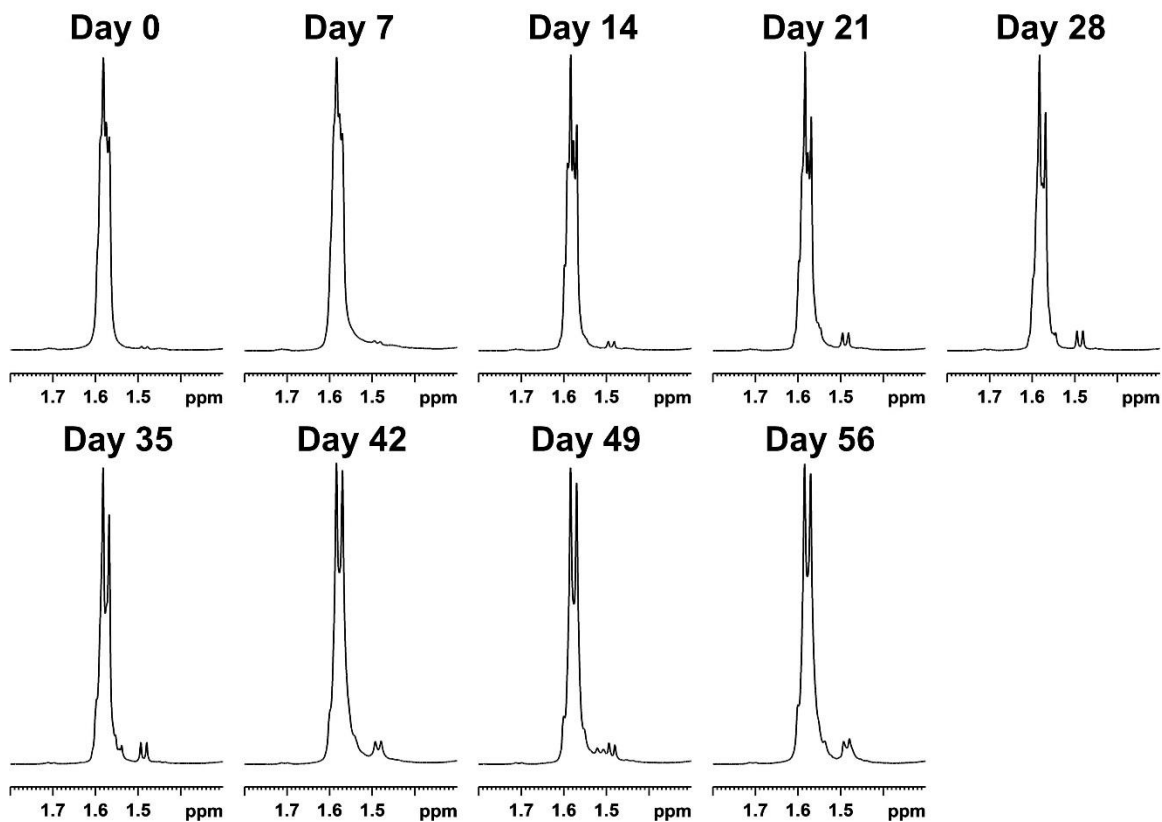
Figure C29. ^{1}H-NMR (500 MHz, CDCl$_3$, δ 1.8 – 1.3 ppm) overlay of 50:50 poly(L-lactide-*co*-glycolide) (PLLGA-50) over the course of 56 days *in vitro*. The region displayed correlates to the methyl proton resonance.
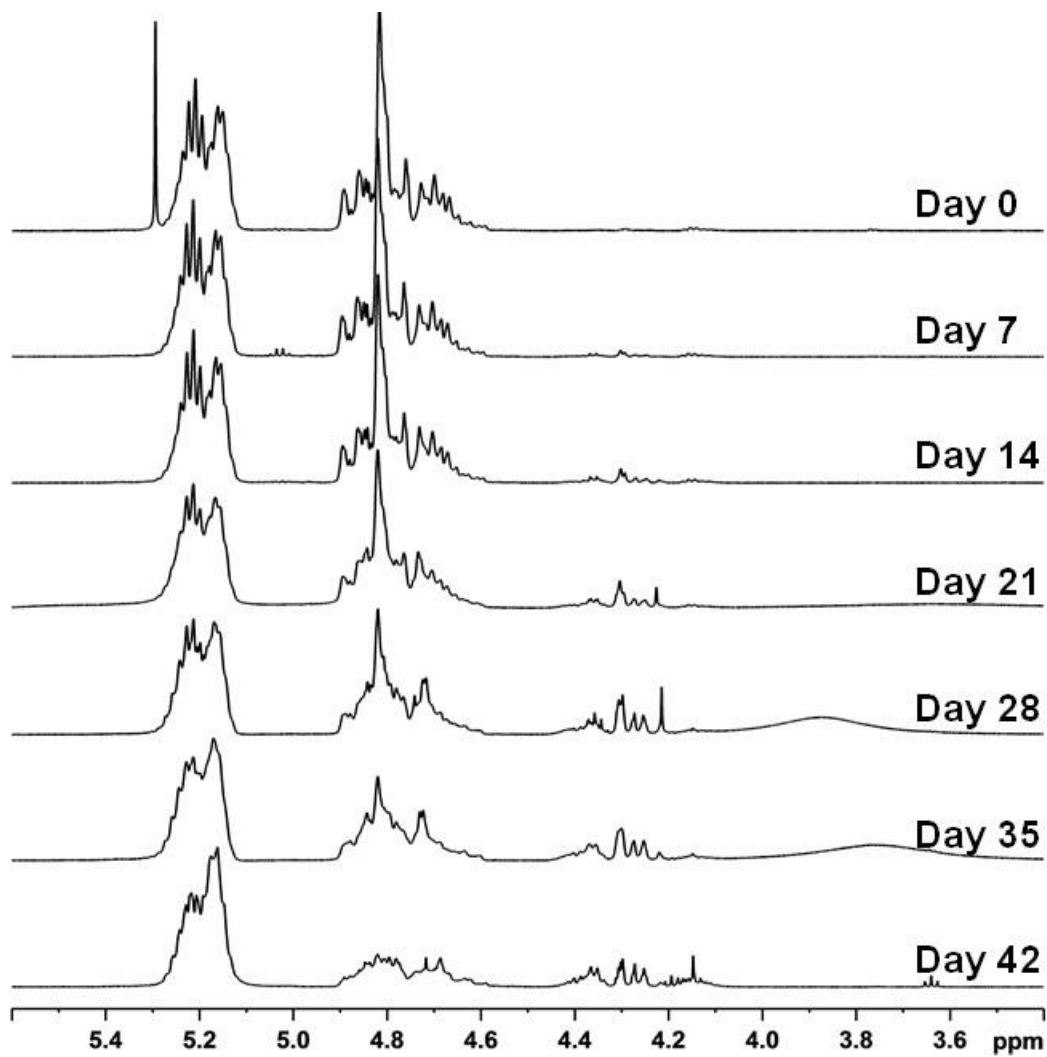
Figure C30. ^{1}H-NMR (500 MHz, CDCl3, δ 5.6 – 3.4 ppm) overlay of 65:35 poly(D,L-lactide-co-glycolide) (PDLGA-65) over the course of 42 days in vitro. The regions displayed correlate to the methine (δ 5.3 – 5.1 ppm) and methylene (δ 4.9 – 4.5 ppm) proton resonances.
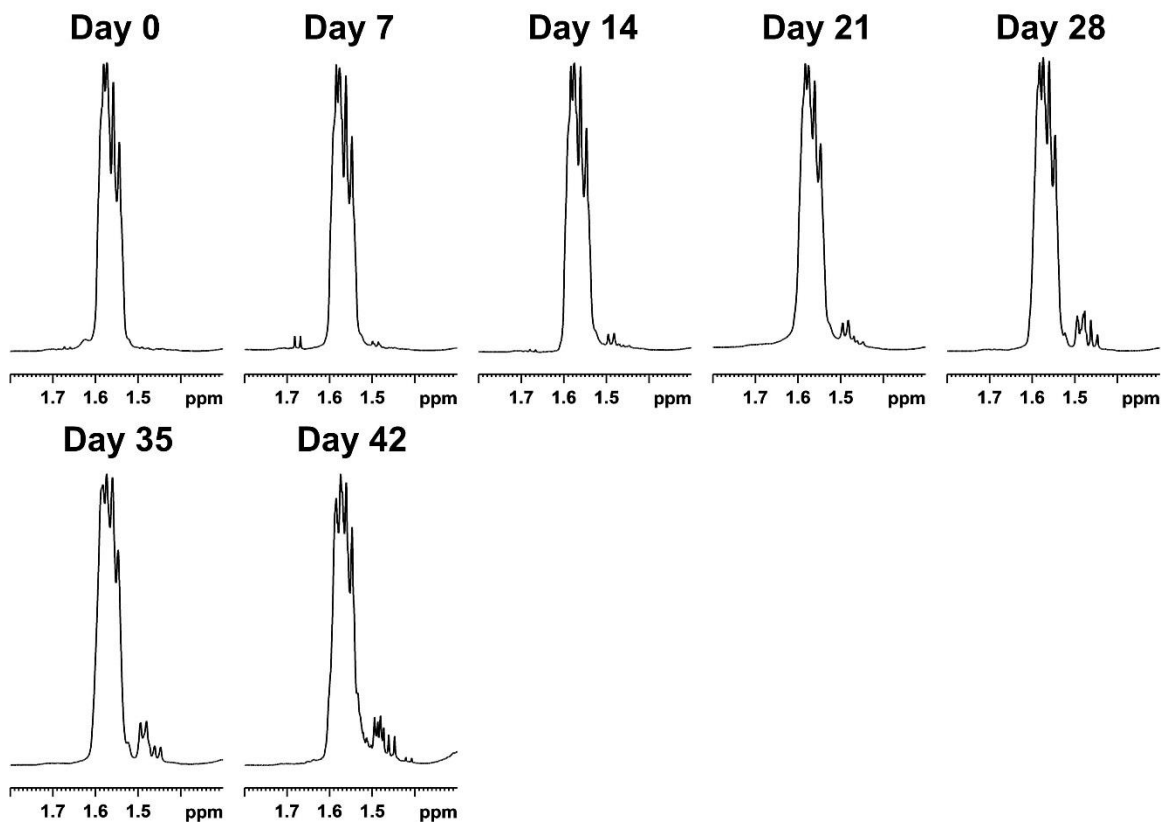
Figure C31. ^{1}H-NMR (500 MHz, CDCl$_3$, δ 1.8 – 1.3 ppm) overlay of 65:35 poly(D,L-lactide-*co*-glycolide)

(PDLGA-65) over the course of 42 days *in vitro*. The region displayed correlates to the methyl proton resonance.

BIBLIOGRAPHY

(1) Ulery, B. D.; Nair, L. S.; Laurencin, C. T., Biomedical Applications of Biodegradable Polymers. *Journal of polymer science. Part B, Polymer physics* **2011,** *49* (12), 832-864.

(2) Gentile, P.; Chiono, V.; Carmagnola, I.; Hatton, P. V., An Overview of Poly(lactic-co-glycolic) Acid (PLGA)-Based Biomaterials for Bone Tissue Engineering. *International Journal of Molecular Sciences* **2014,** *15* (3), 3640-3659.

(3) Singh, G.; Kaur, T.; Kaur, R.; Kaur, A., Recent biomedical applications and patents on biodegradable polymer-PLGA. *International Journal of Pharmacology and Pharmaceutical Sciences* **2014,** *1* (2), 30-42.

(4) Dechy-Cabaret, O.; Martin-Vaca, B.; Bourissou, D., Controlled Ring-Opening Polymerization of Lactide and Glycolide. *Chemical Reviews* **2004,** *104* (12), 6147-6176.

(5) Pounder, R. J.; Dove, A. P., Towards poly(ester) nanoparticles: recent advances in the synthesis of functional poly(ester)s by ring-opening polymerization. *Polymer Chemistry* **2010,** *1* (3), 260-271.

(6) Ajioka, M.; Suizu, H.; Higuchi, C.; Kashima, T., Aliphatic polyesters and their copolymers synthesized through direct condensation polymerization. *Polymer Degradation and Stability* **1998,** *59* (1–3), 137-143.

(7) Gao, Q.; Lan, P.; Shao, H.; Hu, X., Direct Synthesis with Melt Polycondensation and Microstructure Analysis of Poly(L-lactic acid-co-glycolic acid). *Polymer Journal* **2002,** *34* (11), 786-793.

(8) Kasperczyk, J., Copolymerization of glycolide and ε-caprolactone, 1. Analysis of the copolymer microstructure by means of 1H and 13C NMR spectroscopy. *Macromolecular Chemistry and Physics* **1999,** *200* (4), 903-910.

(9) Kasperczyk, J., Microstructural analysis of poly[(L,L-lactide)-co-(glycolide)] by 1H and 13C NMR spectroscopy. *Polymer* **1996,** *37* (2), 201-203.

(10) Stanford, M. J.; Dove, A. P., Stereocontrolled ring-opening polymerisation of lactide. *Chemical Society Reviews* **2010,** *39* (2), 486-494.

(11) Van Wouwe, P.; Dusselier, M.; Vanleeuw, E.; Sels, B., Lactide Synthesis and Chirality Control for Polylactic acid Production. *ChemSusChem* **2016,** *9* (9), 907-921.

(12) Stridsberg, K. M.; Ryner, M.; Albertsson, A. C., Controlled ring-opening polymerization: Polymers with designed macromolecular architecture. In *Degradable Aliphatic Polyesters*, Albertsson, A. C., Ed. Springer-Verlag Berlin: Berlin, 2002; Vol. 157, pp 41-65.

(13) Guillaume, S. M.; Kirillov, E.; Sarazin, Y.; Carpentier, J. F., Beyond Stereoselectivity, Switchable Catalysis: Some of the Last Frontier Challenges in Ring-Opening Polymerization of Cyclic Esters. *Chemistry-a European Journal* **2015,** *21* (22), 7988-8003.

(14) Ovitt, T. M.; Coates, G. W., Stereochemistry of Lactide Polymerization with Chiral Catalysts: New Opportunities for Stereocontrol Using Polymer Exchange Mechanisms. *Journal of the American Chemical Society* **2002,** *124* (7), 1316-1326.

(15) Sun, Y. Y.; Xiong, J.; Dai, Z. R.; Pan, X. B.; Tang, N.; Wu, J. C., Stereoselective Alkali-Metal Catalysts for Highly Isotactic Poly(rac-lactide) Synthesis. *Inorganic Chemistry* **2016,** *55* (1), 136-143.

(16) Ovitt, T. M.; Coates, G. W., Stereoselective ring-opening polymerization of rac-lactide with a single-site, racemic aluminum alkoxide catalyst: Synthesis of stereoblock poly(lactic acid). *Journal of Polymer Science Part a-Polymer Chemistry* **2000,** *38*, 4686-4692.

(17) Ovitt, T. M.; Coates, G. W., Stereoselective ring-opening polymerization of meso-lactide: Synthesis of syndiotactic poly(lactic acid). *Journal of the American Chemical Society* **1999,** *121* (16), 4072-4073.

(18) Cheng, M.; Attygalle, A. B.; Lobkovsky, E. B.; Coates, G. W., Single-site catalysts for ring-opening polymerization: Synthesis of heterotactic poly(lactic acid) from rac-lactide. *Journal of the American Chemical Society* **1999,** *121* (49), 11583-11584.

(19) Spassky, N.; Wisniewski, M.; Pluta, C.; LeBorgne, A., Highly stereoelective polymerization of rac-(D,L)-lactide with a chiral Schiff's base/aluminium alkoxide initiator. *Macromolecular Chemistry and Physics* **1996,** *197* (9), 2627-2637.

(20) von Schenck, H.; Ryner, M.; Albertsson, A. C.; Svensson, M., Ring-Opening Polymerization of Lactones and Lactides with Sn(IV) and Al(III) Initiators. *Macromolecules* **2002,** *35* (5), 1556-1562.

(21) Dong, C.-M.; Qiu, K.-Y.; Gu, Z.-W.; Feng, X.-D., Synthesis of poly(D,L-lactic acid-alt-glycolic acid) from D,L-3-methylglycolide. *Journal of Polymer Science Part A: Polymer Chemistry* **2000,** *38* (23), 4179-4184.

(22) Auras, R., *Poly(lactic acid) : synthesis, structures, properties, processing, and applications*. Wiley: Hoboken, N.J., 2010; p xxiii, 499 p.

(23) Gilding, D. K.; Reed, A. M., Biodegradable polymers for use in surgery—polyglycolic/poly(lactic acid) homo- and copolymers: 1. *Polymer* **1979,** *20* (12), 1459-1464.

(24) Leenslag, J. W.; Pennings, A. J.; Bos, R. R. M.; Rozema, F. R.; Boering, G., Resorbable materials of poly(l-lactide). VI. Plates and screws for internal fracture fixation. *Biomaterials* **1987,** *8* (1), 70-73.

(25) Gunatillake, P. A.; Adhikari, R., Biodegradable synthetic polymers for tissue engineering. *European Cells and Materials* **2003,** *5*, 1-16; discussion 16.

(26) Razak, S.; Sharif, N.; Rahman, W., Biodegradable polymers and their bone applications: a review. *Internation Journal of Basic & Applied Sciences* **2012,** *12*, 31-49.

(27) Gentile, P.; Chiono, V.; Carmagnola, I.; Hatton, P. V., An overview of poly(lactic-co-glycolic) acid (PLGA)-based biomaterials for bone tissue engineering. *International Journal of Molecular Sciences* **2014,** *15* (3), 3640-59.

(28) Middleton, J. C.; Tipton, A. J., Synthetic biodegradable polymers as orthopedic devices. *Biomaterials* **2000,** *21* (23), 2335-2346.

(29) Park, T. G., Degradation of poly(lactic-co-glycolic acid) microspheres - Effect of copolymer composition *Biomaterials* **1995,** *16* (15), 1123-1130.

(30) Alexis, F., Factors affecting the degradation and drug-release mechanism of poly(lactic acid) and poly[(lactic acid)-co-(glycolic acid)]. *Polymer International* **2005,** *54* (1), 36-46.

(31) Vert, M., Degradation of polymeric systems aimed at temporary therapeutic applications: Structure-related complications. In *e-Polymers*, 2005; Vol. 5, p 70.

(32)   Watson, J. D.; Crick, F. H., Molecular structure of nucleic acids; a structure for deoxyribose nucleic acid. *Nature* **1953,** *171* (4356), 737-8.

(33)   Lutz, J. F.; Lehn, J. M.; Meijer, E. W.; Matyjaszewski, K., From precision polymers to complex materials and systems. *Nature Reviews Materials* **2016,** *1* (5), 1-14.

(34)   Lutz, J. F.; Ouchi, M.; Sawamoto, M.; Meyer, T. Y., *Sequence-Controlled Polymers: Synthesis, Self-Assembly, and Properties*. American Chemical Society: 2014; Vol. 1170, p 408.

(35)   Lutz, J. F.; Ouchi, M.; Liu, D. R.; Sawamoto, M., Sequence-Controlled Polymers. *Science* **2013,** *341* (6146).

(36)   Cole, J. P.; Hanlon, A. M.; Rodriguez, K. J.; Berda, E. B., Protein-Like Structure and Activity in Synthetic Polymers. *Journal of Polymer Science Part A - Polymer Chemistry* **2017,** *55* (2), 191-206.

(37)   Matyjaszewski, K.; Xia, J., Atom Transfer Radical Polymerization. *Chemical Reviews* **2001,** *101* (9), 2921-2990.

(38)   Moad, G.; Rizzardo, E.; Thang, S. H., Radical addition–fragmentation chemistry in polymer synthesis. *Polymer* **2008,** *49* (5), 1079-1131.

(39)   Hawker, C. J.; Bosman, A. W.; Harth, E., New Polymer Synthesis by Nitroxide Mediated Living Radical Polymerizations. *Chemical Reviews* **2001,** *101* (12), 3661-3688.

(40)   Bielawski, C. W.; Grubbs, R. H., Living ring-opening metathesis polymerization. *Progress in Polymer Science* **2007,** *32* (1), 1-29.

(41)   Hibi, Y.; Ouchi, M.; Sawamoto, M., A strategy for sequence control in vinyl polymers via iterative controlled radical cyclization. *Nature Communications* **2016,** *7*, 11064.

(42)   Matyjaszewski, K., Architecturally Complex Polymers with Controlled Heterogeneity. *Science* **2011,** *333* (6046), 1104-1105.

(43)   Matyjaszewski, K., Atom Transfer Radical Polymerization (ATRP): Current Status and Future Perspectives. *Macromolecules* **2012,** *45* (10), 4015-4039.

(44)   Gody, G.; Zetterlund, P. B.; Perrier, S.; Harrisson, S., The limits of precision monomer placement in chain growth polymerization. *Nature Communications* **2016,** *7*, 10514.

(45)   Badi, N.; Chan-Seng, D.; Lutz, J. F., Microstructure Control: An Underestimated Parameter in Recent Polymer Design. *Macromolecular Chemistry and Physics* **2013,** *214* (2), 135-142.

(46)   Badi, N.; Lutz, J.-F., Sequence control in polymer synthesis. *Chemical Society Reviews* **2009,** *38* (12), 3383-3390.

(47)   Tsarevsky, N. V.; Sumerlin, B. S.; Matyjaszewski, K., Step-Growth "Click" Coupling of Telechelic Polymers Prepared by Atom Transfer Radical Polymerization. *Macromolecules* **2005,** *38* (9), 3558-3561.

(48)   Porel, M.; Alabi, C. A., Sequence-Defined Polymers via Orthogonal Allyl Acrylamide Building Blocks. *Journal of the American Chemical Society* **2014,** *136* (38), 13162-13165.

(49)   Deng, X.-X.; Li, L.; Li, Z.-L.; Lv, A.; Du, F.-S.; Li, Z.-C., Sequence Regulated Poly(ester-amide)s Based on Passerini Reaction. *Acs Macro Letters* **2012,** *1* (11), 1300-1303.

(50)   Stayshich, R. M.; Meyer, T. Y., Preparation and microstructural analysis of poly(lactic-alt-glycolic acid). *Journal of Polymer Science Part a-Polymer Chemistry* **2008,** *46* (14), 4704-4711.

(51)   Al Ouahabi, A.; Charles, L.; Lutz, J. F., Synthesis of Non-Natural Sequence-Encoded Polymers Using Phosphoramidite Chemistry. *Journal of the American Chemical Society* **2015,** *137* (16), 5629-5635.

(52)   Roy, R. K.; Meszynska, A.; Laure, C.; Charles, L.; Verchin, C.; Lutz, J. F., Design and synthesis of digitally encoded polymers that can be decoded and erased. *Nature Communications* **2015,** *6*, 8.

(53) Laure, C.; Karamessini, D.; Milenkovic, O.; Charles, L.; Lutz, J. F., Coding in 2D: Using Intentional Dispersity to Enhance the Information Capacity of Sequence-Coded Polymer Barcodes. *Angewandte Chemie-International Edition* **2016,** *55* (36), 10722-10725.

(54) Hartmann, L.; Börner, H. G., Precision Polymers: Monodisperse, Monomer-Sequence-Defined Segments to Target Future Demands of Polymers in Medicine. *Advanced Materials* **2009,** *21* (32-33), 3425-3431.

(55) Stayshich, R. M.; Meyer, T. Y., New Insights into Poly(lactic-co-glycolic acid) Microstructure: Using Repeating Sequence Copolymers To Decipher Complex NMR and Thermal Behavior. *Journal of the American Chemical Society* **2010,** *132* (31), 10920-10934.

(56) Swanson, J. P.; Martinez, M. R.; Cruz, M. A.; Mankoci, S. G.; Costanzo, P. J.; Joy, A., A coacervate-forming biodegradable polyester with elevated LCST based on bis-(2-methoxyethyl) amine. *Polymer Chemistry* **2016,** *7* (28), 4693-4702.

(57) Gokhale, S.; Xu, Y.; Joy, A., A Library of Multifunctional Polyesters with "Peptide-Like" Pendant Functional Groups. *Biomacromolecules* **2013,** *14* (8), 2489-2493.

(58) Weiss, R. M.; Jones, E. M.; Shafer, D. E.; Stayshich, R. M.; Meyer, T. Y., Synthesis of Repeating Sequence Copolymers of Lactic, Glycolic, and Caprolactic Acids. *Journal of Polymer Science Part a-Polymer Chemistry* **2011,** *49* (8), 1847-1855.

(59) Stayshich, R. M.; Weiss, R. M.; Li, J.; Meyer, T. Y., Periodic Incorporation of Pendant Hydroxyl Groups in Repeating Sequence PLGA Copolymers. *Macromolecular Rapid Communications* **2011,** *32* (2), 220-225.

(60) Li, J.; Rothstein, S. N.; Little, S. R.; Edenborn, H. M.; Meyer, T. Y., The Effect of Monomer Order on the Hydrolysis of Biodegradable Poly(lactic-co-glycolic acid) Repeating Sequence Copolymers. *Journal of the American Chemical Society* **2012,** *134* (39), 16352-16359.

(61) Li, J.; Stayshich, R. M.; Meyer, T. Y., Exploiting Sequence To Control the Hydrolysis Behavior of Biodegradable PLGA Copolymers. *Journal of the American Chemical Society* **2011,** *133* (18), 6910-6913.

(62) Washington, M. A.; Swiner, D. J.; Bell, K. R.; Fedorchak, M. V.; Little, S. R.; Meyer, T. Y., The impact of monomer sequence and stereochemistry on the swelling and erosion of biodegradable poly(lactic-co-glycolic acid) matrices. *Biomaterials* **2017,** *117*, 66-76.

(63) Mu, L.; Feng, S. S., A Novel Controlled Release Formulation for the Anticancer Drug Paclitaxel (Taxol®): PLGA Nanoparticles Containing Vitamin E TPGS. *Journal of Controlled Release* **2003,** *86* (1), 33-48.

(64) Fonseca, C.; Simões, S.; Gaspar, R., Paclitaxel-loaded PLGA Nanoparticles: Preparation, Physicochemical Characterization and in vitro Anti-tumoral Activity. *Journal of Controlled Release* **2002,** *83* (2), 273-286.

(65) Derakhshandeh, K.; Erfan, M.; Dadashzadeh, S., Encapsulation of 9-nitrocamptothecin, A Novel Anticancer Drug, in Biodegradable Nanoparticles: Factorial Design, Characterization and Release Kinetics. *European Journal of Pharmaceutics and Biopharmaceutics* **2007,** *66* (1), 34-41.

(66) Tiainen, J.; Soini, Y.; Törmälä, P.; Waris, T.; Ashammakhi, N., Self-Reinforced Polylactide/Polyglycolide 80/20 Screws Take More than 1½ Years to Resorb in Rabbit Cranial Bone. *Journal of Biomedical Materials Research Part B: Applied Biomaterials* **2004,** *70B* (1), 49-55.

(67) Pan, Z.; Ding, J. D., Poly(lactide-co-glycolide) Porous Scaffolds for Tissue Engineering and Regenerative Medicine. *Interface Focus* **2012,** *2* (3), 366-377.

(68) Wang, Y.; Wen, Q.; Choi, S. H., FDA's Regulatory Science Program for Generic PLA/PLGA-Based Drug Products. *American Pharmaceutical Review* **2016**.

(69) Makadia, H. K.; Siegel, S. J., Poly(lactic-co-glycolic acid) (PLGA) as Biodegradable Controlled Drug Delivery Carrier. *Polymers* **2011,** *3* (3), 1377-1397.

(70) Rothstein, S. N.; Little, S. R., A "Tool Box" for Rational Design of Degradable Controlled Release Formulations. *Journal of Materials Chemistry* **2011,** *21* (1), 29-39.

(71) Norris, B. N.; Zhang, S.; Campbell, C. M.; Auletta, J. T.; Calvo-Marzal, P.; Hutchison, G. R.; Meyer, T. Y., Sequence Matters: Modulating Electronic and Optical Properties of Conjugated Oligomers via Tailored Sequence. *Macromolecules* **2013,** *46* (4), 1384-1392.

(72) Weiss, R. M.; Short, A. L.; Meyer, T. Y., Sequence-Controlled Copolymers Prepared via Entropy-Driven Ring-Opening Metathesis Polymerization. *Acs Macro Letters* **2015,** *4* (9), 1039-1043.

(73) Zhang, S.; Hutchison, G. R.; Meyer, T. Y., Sequence Effects in Conjugated Donor–Acceptor Trimers and Polymers. *Macromolecular Rapid Communications* **2016**, 882-887.

(74) Fernández, J.; Etxeberria, A.; Sarasua, J. R., Synthesis, structure and properties of poly(L-lactide-co-epsilon-caprolactone) statistical copolymers. *Journal of the Mechanical Behavior of Biomedical Materials* **2012,** *9*, 100-112.

(75) Fernández, J.; Etxeberria, A.; Sarasua, J. R., In vitro degradation studies and mechanical behavior of poly(epsilon-caprolactone-co-delta-valerolactone) and poly(epsilon-caprolactone-co-L-lactide) with random and semi-alternating chain microstructures. *European Polymer Journal* **2015,** *71*, 585-595.

(76) Fernández, J.; Etxeberria, A.; Sarasua, J. R., Effects of repeat unit sequence distribution and residual catalyst on thermal degradation of poly(L-lactide/epsilon-caprolactone) statistical copolymers. *Polymer Degradation and Stability* **2013,** *98* (7), 1293-1299.

(77) Fernández, J.; Etxeberria, A.; Ugartemendia, J. M.; Petisco, S.; Sarasua, J. R., Effects of chain microstructures on mechanical behavior and aging of a poly(L-lactide-co-epsilon-caprolactone) biomedical thermoplastic-elastomer. *Journal of the Mechanical Behavior of Biomedical Materials* **2012,** *12*, 29-38.

(78) Fernández, J.; Larrañaga, A.; Etxeberria, A.; Sarasua, J. R., Tensile behavior and dynamic mechanical analysis of novel poly(lactide/delta-valerolactone) statistical copolymers. *Journal of the Mechanical Behavior of Biomedical Materials* **2014,** *35*, 39-50.

(79) Fernández, J.; Larrañaga, A.; Etxeberría, A.; Sarasua, J. R., Effects of chain microstructures and derived crystallization capability on hydrolytic degradation of poly(l-lactide/epsilon-caprolactone) copolymers. *Polymer Degradation and Stability* **2013,** *98* (2), 481-489.

(80) Sun, S.; Li, J.; Li, X.; Lan, B.; Zhou, S.; Meng, Y.; Cheng, L., Episcleral drug film for better-targeted ocular drug delivery and controlled release using multilayered poly-ε-caprolactone (PCL). *Acta Biomaterialia* **2016,** *37*, 143-154.

(81) Costa, E. F.; Barros, N. M.; Coppini, L. P.; Neves, R. L.; Carmona, A. K.; Penha, F. M.; Rodrigues, E. B.; Dib, E.; Magalhaes, O., Jr.; Moraes-Filho, M. N.; Lima Filho, A. A.; Maia, M.; Farah, M. E., Effects of light exposure, pH, osmolarity, and solvent on the retinal pigment epithelial toxicity of vital dyes. *Am J Ophthalmol* **2013,** *155* (4), 705-12, 712.e1.

(82) Rahman, C. V.; Ben-David, D.; Dhillon, A.; Kuhn, G.; Gould, T. W.; Muller, R.; Rose, F. R.; Shakesheff, K. M.; Livne, E., Controlled release of BMP-2 from a sintered polymer scaffold enhances bone repair in a mouse calvarial defect model. *J Tissue Eng Regen Med* **2014,** *8* (1), 59-66.

(83) Anderson, J. M.; Shive, M. S., Biodegradation and biocompatibility of PLA and PLGA microspheres. *Advanced Drug Delivery Reviews* **1997,** *28* (1), 5-24.

(84) von Burkersroda, F.; Schedl, L.; Gopferich, A., Why degradable polymers undergo surface erosion or bulk erosion. *Biomaterials* **2002,** *23* (21), 4221-4231.

(85) Gopferich, A., Mechanisms of polymer degradation and erosion. *Biomaterials* **1996,** *17* (2), 103-114.

(86) Gopferich, A., Polymer bulk erosion. *Macromolecules* **1997,** *30* (9), 2598-2604.

(87) Gopferich, A., Erosion of composite polymer matrices. *Biomaterials* **1997,** *18* (5), 397-403.

(88) Gopferich, A., Polymer degradation and erosion: Mechanisms and applications. *European Journal of Pharmaceutics and Biopharmaceutics* **1996,** *42* (1), 1-11.

(89) Gopferich, A.; Tessmar, J., Polyanhydride degradation and erosion. *Advanced Drug Delivery Reviews* **2002,** *54* (7), 911-931.

(90) Gasmi, H.; Danede, F.; Siepmann, J.; Siepmann, F., Does PLGA microparticle swelling control drug release? New insight based on single particle swelling studies. *Journal of Controlled Release* **2015,** *213*, 120-127.

(91) Takizawa, K.; Nulwala, H.; Hu, J.; Yoshinaga, K.; Hawker, C. J., Molecularly defined (L)-lactic acid oligomers and polymers: Synthesis and characterization. *Journal of Polymer Science Part A: Polymer Chemistry* **2008,** *46* (18), 5977-5990.

(92) Qian, H.; Wohl, A. R.; Crow, J. T.; Macosko, C. W.; Hoye, T. R., A Strategy for Control of "Random" Copolymerization of Lactide and Glycolide: Application to Synthesis of PEG-b-PLGA Block Polymers Having Narrow Dispersity. *Macromolecules* **2011,** *44* (18), 7132-7140.

(93) Kreiser-Saunders, I.; Kricheldorf, H. R., Polylactones, 39. Zn lactate-catalyzed copolymerization of L-lactide with glycolide or ε-caprolactone. *Macromolecular Chemistry and Physics* **1998,** *199* (6), 1081-1087.

(94) Vey, E.; Rodger, C.; Booth, J.; Claybourn, M.; Miller, A. F.; Saiani, A., Degradation kinetics of poly(lactic-co-glycolic) acid block copolymer cast films in phosphate buffer solution as revealed by infrared and Raman spectroscopies. *Polymer Degradation and Stability* **2011,** *96* (10), 1882-1889.

(95) Vey, E.; Rodger, C.; Meehan, L.; Booth, J.; Claybourn, M.; Miller, A. F.; Saiani, A., The impact of chemical composition on the degradation kinetics of poly(lactic-co-glycolic) acid copolymers cast films in phosphate buffer solution. *Polymer Degradation and Stability* **2012,** *97* (3), 358-365.

(96) Keles, H.; Naylor, A.; Clegg, F.; Sammon, C., Investigation of factors influencing the hydrolytic degradation of single PLGA microparticles. *Polymer Degradation and Stability* **2015,** *119*, 228-241.

(97) Eglin, D.; Alini, M., Degradable polymeric materials for osteosynthesis: Tutorial. *European Cells & Materials* **2008,** *16*, 80-91.

(98) Ciccone II, W. J.; Motz, C.; Bentley, C.; Tasto, J. P., Bioabsorbable implants in orthopaedics: new developments and clinical applications. *The Journal of the American Academy of Orthopaedic Surgeons* **2001,** *9* (5), 280-8.

(99) Athanasiou, K. A.; Agrawal, C. M.; Barber, F. A.; Burkhart, S. S., Orthopaedic applications for PLA-PGA biodegradable polymers. *Arthroscopy* **1998,** *14* (7), 726-737.

(100) Siepmann, J.; Elkharraz, K.; Siepmann, F.; Klose, D., How Autocatalysis Accelerates Drug Release from PLGA-Based Microparticles: A Quantitative Treatment. *Biomacromolecules* **2005,** *6* (4), 2312-2319.

(101) Liu, Y.; Yin, Y.; Wang, L.; Zhang, W.; Chen, X.; Yang, X.; Xu, J.; Ma, G., Surface hydrophobicity of microparticles modulates adjuvanticity. *Journal of Materials Chemistry B* **2013,** *1* (32), 3888-3896.

(102) Mei, F. F.; Peng, Y.; Lu, S. T.; Sun, F.; Zhang, Y.; Ge, C.; Zhang, Y.; Gu, H. L.; Wang, Y. D.; Zhao, X. W.; Wang, G. Y., Synthesis and Characterization of Biodegradable Poly(lactic-co-glycolic acid). *Journal of Macromolecular Science Part B-Physics* **2015,** *54* (5), 562-570.

(103) Fredenberg, S.; Wahlgren, M.; Reslow, M.; Axelsson, A., The mechanisms of drug release in poly(lactic-co-glycolic acid)-based drug delivery systems-A review. *International Journal of Pharmaceutics* **2011,** *415* (1-2), 34-52.

(104) Kamaly, N.; Yameen, B.; Wu, J.; Farokhzad, O. C., Degradable Controlled-Release Polymers and Polymeric Nanoparticles: Mechanisms of Controlling Drug Release. *Chemical Reviews* **2016,** *116* (4), 2602-2663.

(105) Seyednejad, H.; Ghassemi, A. H.; van Nostrum, C. F.; Vermonden, T.; Hennink, W. E., Functional aliphatic polyesters for biomedical and pharmaceutical applications. *Journal of Controlled Release* **2011,** *152* (1), 168-176.

(106) Xu, X. J.; Sy, J. C.; Shastri, V. P., Towards developing surface eroding poly(alpha-hydroxy acids). *Biomaterials* **2006,** *27* (15), 3021-3030.

(107) Li, S. M.; Garreau, H.; Vert, M., Structure-property relationships in the case of the degradation of massive poly(α-hydroxy acids) in aqueous media. *Journal of Materials Science: Materials in Medicine* **1990,** *1* (3), 131-139.

(108) Saha, S. K.; Tsuji, H., Hydrolytic Degradation of Amorphous Films of L-Lactide Copolymers with Glycolide and D-Lactide. *Macromolecular Materials and Engineering* **2006,** *291* (4), 357-368.

(109) López-Santos, C.; Terriza, A.; Portolés, J.; Yubero, F.; González-Elipe, A. R., Physiological Degradation Mechanisms of PLGA Membrane Films under Oxygen Plasma Treatment. *The Journal of Physical Chemistry C* **2015,** *119* (35), 20446-20452.

(110) Miller, R. A.; Brady, J. M.; Cutright, D. E., Degradation rates of oral resorbable implants (polylactates and polyglycolates): Rate modification with changes in PLA/PGA copolymer ratios. *Journal of Biomedical Materials Research* **1977,** *11* (5), 711-719.

(111) Schadlich, A.; Kempe, S.; Mader, K., Non-invasive in vivo characterization of microclimate pH inside in situ forming PLGA implants using multispectral fluorescence imaging. *Journal of Controlled Release* **2014,** *179*, 52-62.

(112) Zolnik, B. S.; Burgess, D. J., Effect of acidic pH on PLGA microsphere degradation and release. *Journal of Controlled Release* **2007,** *122* (3), 338-344.

(113) Fu, K.; Pack, D. W.; Klibanov, A. M.; Langer, R., Visual evidence of acidic environment within degrading poly(lactic-co-glycolic acid) (PLGA) microspheres. *Pharmaceutical Research* **2000,** *17* (1), 100-106.

(114) Rothstein, S. N.; Federspiel, W. J.; Little, S. R., A simple model framework for the prediction of controlled release from bulk eroding polymer matrices. *Journal of Materials Chemistry* **2008,** *18* (16), 1873-1880.

(115) Rothstein, S. N.; Federspiel, W. J.; Little, S. R., A unified mathematical model for the prediction of controlled release from surface and bulk eroding polymer matrices. *Biomaterials* **2009,** *30* (8), 1657-1664.

(116) Brunner, A.; Mader, K.; Gopferich, A., pH and osmotic pressure inside biodegradable microspheres during erosion. *Pharmaceutical Research* **1999,** *16* (6), 847-853.

(117) Danhier, F.; Ansorena, E.; Silva, J. M.; Coco, R.; Le Breton, A.; Preat, V., PLGA-based nanoparticles: an overview of biomedical applications. *Journal of Controlled Release* **2012,** *161* (2), 505-522.

(118) Dragan, U.; Magdalena, S., Poly(lactide-co-glycolide)-based Micro and Nanoparticles for the Controlled Drug Delivery of Vitamins. *Current Nanoscience* **2009,** *5* (1), 1-14.

(119) Knight, A. S.; Zhou, E. Y.; Francis, M. B.; Zuckermann, R. N., Sequence Programmable Peptoid Polymers for Diverse Materials Applications. *Advanced Materials* **2015,** *27* (38), 5665-5691.

(120) Qu, C. K.; He, J. P., Recent developments in the synthesis of sequence controlled polymers. *Science China-Chemistry* **2015,** *58* (11), 1651-1662.

(121) Schulz, M. D.; Wagener, K. B., Precision Polymers through ADMET Polymerization. *Macromolecular Chemistry and Physics* **2014,** *215* (20), 1936-1945.

(122) Tabata, Y.; Abe, H., Synthesis and Properties of Alternating Copolymers of 3-Hydroxybutyrate and Lactate Units with Different Stereocompositions. *Macromolecules* **2014,** *47* (21), 7354-7361.

(123) Tabata, Y.; Abe, H., Effects of composition and sequential structure on thermal properties for copolymer of 3-hydroxybutyrate and lactate units. *Polymer Degradation and Stability* **2013,** *98* (9), 1796-1803.

(124) Fernández, J.; Larrañaga, A.; Etxeberria, A.; Wang, W.; Sarasua, J. R., A new generation of poly(lactide/epsilon-caprolactone) polymeric biomaterials for application in the medical field. *Journal of Biomedical Materials Research Part A* **2014,** *102* (10), 3573-3584.

(125) Fernandez, J.; Meaurio, E.; Chaos, A.; Etxeberria, A.; Alonso-Varona, A.; Sarasua, J. R., Synthesis and characterization of poly (L-lactide/epsilon-caprolactone) statistical copolymers with well resolved chain microstructures. *Polymer* **2013,** *54* (11), 2621-2631.

(126) Hakkarainen, M.; Höglund, A.; Odelius, K.; Albertsson, A. C., Tuning the Release Rate of Acidic Degradation Products through Macromolecular Design of Caprolactone-Based Copolymers. *Journal of the American Chemical Society* **2007,** *129* (19), 6308-6312.

(127) van de Weert, M.; Hennink, W. E.; Jiskoot, W., Protein Instability in Poly(lactic-co-glycolic acid) Microparticles. *Pharmaceutical Research* **2000,** *17* (10), 1159-1167.

(128) Xie, S.; Zhu, Q.; Wang, B.; Gu, H.; Liu, W.; Cui, L.; Cen, L.; Cao, Y., Incorporation of tripolyphosphate nanoparticles into fibrous poly(lactide-co-glycolide) scaffolds for tissue engineering. *Biomaterials* **2010,** *31* (19), 5100-5109.

(129) Gu, B.; Wang, Y.; Burgess, D. J., In vitro and in vivo performance of dexamethasone loaded PLGA microspheres prepared using polymer blends. *International Journal of Pharmaceutics* **2015,** *496* (2), 534-540.

(130) Eisenächer, F.; Schädlich, A.; Mäder, K., Monitoring of internal pH gradients within multi-layer tablets by optical methods and EPR imaging. *International Journal of Pharmaceutics* **2011,** *417* (1–2), 204-215.

(131) Mäder, K.; Gallez, B.; Liu, K. J.; Swartz, H. M., Non-invasive in vivo characterization of release processes in biodegradable polymers by low-frequency electron paramagnetic resonance spectroscopy. *Biomaterials* **1996,** *17* (4), 457-461.

(132) Liu, Y.; Schwendeman, S. P., Mapping Microclimate pH Distribution inside Protein-Encapsulated PLGA Microspheres Using Confocal Laser Scanning Microscopy. *Molecular Pharmaceutics* **2012,** *9* (5), 1342-1350.

(133)   Ding, A. G.; Schwendeman, S. P., Acidic Microclimate pH Distribution in PLGA Microspheres Monitored by Confocal Laser Scanning Microscopy. *Pharmaceutical Research* **2008,** *25* (9), 2041-2052.

(134)   Li, L.; Schwendeman, S. P., Mapping neutral microclimate pH in PLGA microspheres. *Journal of Controlled Release* **2005,** *101* (1-3), 163-173.

(135)   Kang, J. C.; Schwendeman, S. P., Determination of diffusion coefficient of a small hydrophobic probe in poly(lactide-co-glycolide) microparticles by laser scanning confocal microscopy. *Macromolecules* **2003,** *36* (4), 1324-1330.

(136)   Shenderova, A.; Burke, T. G.; Schwendeman, S. P., Evidence for an acidic microclimate in PLGA microspheres. *Proceedings of the Controlled Release Society* **1998,** (25), 265-266.

(137)   Liu, Y.; Ghassemi, A. H.; Hennink, W. E.; Schwendeman, S. P., The microclimate pH in poly(d,l-lactide-co-hydroxymethyl glycolide) microspheres during biodegradation. *Biomaterials* **2012,** *33* (30), 7584-7593.

(138)   Rothstein, S. N.; Huber, K. D.; Sluis-Cremer, N.; Little, S. R., In Vitro Characterization of a Sustained-Release Formulation for Enfuvirtide. *Antimicrobial Agents and Chemotherapy* **2014,** *58* (3), 1797-1799.

(139)   Heidemann, W.; Jeschkeit-Schubbert, S.; Ruffieux, K.; Fischer, J. H.; Jung, H.; Krueger, G.; Wintermantel, E.; Gerlach, K. L., pH-stabilization of predegraded PDLLA by an admixture of water-soluble sodiumhydrogenphosphate—results of an in vitro- and in vivo-study. *Biomaterials* **2002,** *23* (17), 3567-3574.

(140)   Shenderova, A.; Ding, A. G.; Schwendeman, S. P., Potentiometric method for determination of microclimate pH in poly(lactic-co-glycolic acid) films. *Macromolecules* **2004,** *37* (26), 10052-10058.

(141)   Ding, A. G.; Shenderova, A.; Schwendeman, S. P., Prediction of microclimate pH in poly(lactic-co-glycolic acid) films. *Journal of the American Chemical Society* **2006,** *128* (16), 5384-5390.

(142)   Bennewitz, M. F.; Watkins, S. C.; Sundd, P., Quantitative intravital two-photon excitation microscopy reveals absence of pulmonary vaso-occlusion in unchallenged Sickle Cell Disease mice. *Intravital* **2014,** *3* (2), e29748.

(143)   Watkins, S. C., St. Croix, Claudette *Current Protocols Select: Methods and Applications in Microscopy and Imaging.* 1 ed.; John Wiley & Sons, Inc.: Hoboken, New Jersey, 2013.

(144)   Denk, W.; Strickler, J. H.; Webb, W. W., Two-photon laser scanning fluorescence microscopy. *Science* **1990,** *248*, 73+.

(145)   Park, H. J.; Lim, C. S.; Kim, E. S.; Han, J. H.; Lee, T. H.; Chun, H. J.; Cho, B. R., Measurement of pH Values in Human Tissues by Two-Photon Microscopy. *Angewandte Chemie-International Edition* **2012,** *51* (11), 2673-2676.

(146)   Jhunjhunwala, S.; Raimondi, G.; Thomson, A. W.; Little, S. R., Delivery of rapamycin to dendritic cells using degradable microparticles. *Journal of Controlled Release* **2009,** *133* (3), 191-197.

(147)   Weiss, R. M.; Li, J.; Liu, H. H.; Washington, M. A.; Giesen, J. A.; Grayson, S. M.; Meyer, T. Y., Determining Sequence Fidelity in Repeating Sequence Poly(lactic-co-glycolic acid)s. *Macromolecules* **2017,** 550-560.

(148)   Lee, J. H.; Lee, S.; Gho, Y. S.; Song, I. S.; Tchah, H.; Kim, M. J.; Kim, K. H., Comparison of confocal microscopy and two-photon microscopy in mouse cornea in vivo. *Experimental Eye Research* **2015,** *132*, 101-108.

(149) Wanapun, D.; Kestur, U. S.; Kissick, D. J.; Simpson, G. J.; Taylor, L. S., Selective Detection and Quantitation of Organic Molecule Crystallization by Second Harmonic Generation Microscopy. *Analytical Chemistry* **2010,** *82* (13), 5425-5432.

(150) Wampler, R. D.; Kissick, D. J.; Dehen, C. J.; Gualtieri, E. J.; Grey, J. L.; Wang, H.; Thompson, D. H.; Cheng, J.; Simpson, G. J., Selective Detection of Protein Crystals by Second Harmonic Microscopy. *Journal of the American Chemical Society* **2008,** *130* (43), 14076-14077.

(151) Lyu, S.; Untereker, D., Degradability of Polymers for Implantable Biomedical Devices. *International Journal of Molecular Sciences* **2009,** *10* (9), 4033-4065.

(152) Vert, M.; Li, S.; Garreau, H.; Mauduit, J.; Boustta, M.; Schwach, G.; Engel, R.; Coudane, J., Complexity of the hydrolytic degradation of aliphatic polyesters. *Die Angewandte Makromolekulare Chemie* **1997,** *247* (1), 239-253.

(153) Engineer, C.; Parikh, J.; Raval, A., Effect of copolymer ratio on hydrolytic degradation of poly(lactide-co-glycolide) from drug eluting coronary stents. *Chemical Engineering Research & Design* **2011,** *89* (3A), 328-334.

(154) Shenderova, A.; Burke, T. G.; Schwendeman, S. P., The acidic microclimate in poly(lactide-*co*-glycolide) microspheres stabilizes camptothecins. *Pharmaceutical Research* **1999,** *16* (2), 241-248.

(155) Anderson, J. M.; Rodriguez, A.; Chang, D. T., Foreign body reaction to biomaterials. *Seminars in immunology* **2008,** *20* (2), 86-100.

(156) Anderson, J. M.; Shive, M. S., Biodegradation and biocompatibility of PLA and PLGA microspheres. *Advanced Drug Delivery Reviews* **2012,** *64*, 72-82.

(157) Athanasiou, K. A.; Niederauer, G. G.; Agrawal, C. M., Sterilization, toxicity, biocompatibility and clinical applications of polylactic acid/ polyglycolic acid copolymers. *Biomaterials* **1996,** *17* (2), 93-102.

(158) Zandstra, J.; Hiemstra, C.; Petersen, A. H.; Zuidema, J.; van Beuge, M. M.; Rodriguez, S.; Lathuile, A. A.; Veldhuis, G. J.; Steendam, R.; Bank, R. A.; Popa, E. R., Microsphere size influences the foreign body reaction. *European Cells & Materials* **2014,** *28*, 335-347.

(159) Hickey, T.; Kreutzer, D.; Burgess, D. J.; Moussy, F., In vivo evaluation of a dexamethasone/PLGA microsphere system designed to suppress the inflammatory tissue response to implantable medical devices. *Journal of Biomedical Materials Research* **2002,** *61* (2), 180-187.

(160) Anderson, J. M.; Lanza, R.; Thomson, J. A.; Nerem, R. M., Biocompatibility and Bioresponse to Biomaterials. In *Principles of Regenerative Medicine*, Academic Press: San Diego, 2008; pp 704-723.

(161) Sheikh, Z.; Najeeb, S.; Khurshid, Z.; Verma, V.; Rashid, H.; Glogauer, M., Biodegradable Materials for Bone Repair and Tissue Engineering Applications. *Materials* **2015,** *8* (9), 5273.

(162) Athanasiou, K. A.; Zhu, C.; Lanctot, D. R.; Agrawal, C. M.; Wang, X., Fundamentals of biomechanics in tissue engineering of bone. *Tissue Engineering* **2000,** *6* (4), 361-81.

(163) Waris, E.; Ashammakhi, N.; Kaarela, O.; Raatikainen, T.; Vasenius, J., Use of Bioabsorbable Osteofixation Devices in the Hand. *Journal of Hand Surgery (British and European Volume)* **2004,** *29* (6), 590-598.

(164) Södergård, A.; Stolt, M., Properties of lactic acid based polymers and their correlation with composition. *Progress in Polymer Science* **2002,** *27* (6), 1123-1163.

(165) Agrawal, C. M.; Ray, R. B., Biodegradable polymeric scaffolds for musculoskeletal tissue engineering. *Journal of Biomedical Materials Research* **2001,** *55* (2), 141-150.

(166) Stähelin, A. C.; Weiler, A.; Rüfenacht, H.; Hoffmann, R.; Geissmann, A.; Feinstein, R., Clinical degradation and biocompatibility of different bioabsorbable interference screws: A report of six cases. *Arthroscopy: The Journal of Arthroscopic & Related Surgery* **1997,** *13* (2), 238-244.

(167) Tiainen, J.; Veiranto, M.; Suokas, E.; Törmälä, P.; Waris, T.; Ninkovic, M.; Ashammakhi, N., Bioabsorbable Ciprofloxacin-Containing and Plain Self-Reinforced Polylactide-Polyglycolide 80/20 Screws: Pullout Strength Properties in Human Cadaver Parietal Bones. *Journal of Craniofacial Surgery* **2002,** *13* (3), 427-433.

(168) Törmälä, P., Biodegradable self-reinforced composite materials; Manufacturing structure and mechanical properties. *Clinical Materials* **1992,** *10* (1-2), 29-34.

(169) Liu, H.; Webster, T. J., Mechanical properties of dispersed ceramic nanoparticles in polymer composites for orthopedic applications. *International Journal of Nanomedicine* **2010,** *5*, 299-313.

(170) Park, J. J.; Yu, E. J.; Lee, W.; Ha, C., Mechanical properties and degradation studies of poly(D,L-lactide-co-glycolide) 50:50/graphene oxide nanocomposite films. *Polymers for Advanced Technologies* **2014,** *25* (1), 48-54.

(171) Armentano, I.; Dottori, M.; Fortunati, E.; Mattioli, S.; Kenny, J. M., Biodegradable polymer matrix nanocomposites for tissue engineering: A review. *Polymer Degradation and Stability* **2010,** *95* (11), 2126-2146.

(172) Virlan, M. J. R.; Miricescu, D.; Totan, A.; Greabu, M.; Tanase, C.; Sabliov, C. M.; Caruntu, C.; Calenic, B., Current Uses of Poly(lactic-co-glycolic acid) in the Dental Field: A Comprehensive Review. *Journal of Chemistry* **2015,** *2015*, 12.

(173) Scholz, M. S.; Blanchfield, J. P.; Bloom, L. D.; Coburn, B. H.; Elkington, M.; Fuller, J. D.; Gilbert, M. E.; Muflahi, S. A.; Pernice, M. F.; Rae, S. I.; Trevarthen, J. A.; White, S. C.; Weaver, P. M.; Bond, I. P., The use of composite materials in modern orthopaedic medicine and prosthetic devices: A review. *Composites Science and Technology* **2011,** *71* (16), 1791-1803.

(174) Zhu, G. Q.; Wang, F. G.; Gao, Q. C.; Liu, Y. Y., Physicochemical Properties of Poly(lactic acid-co-glycolic acid) Film Modified via Blending with Poly(butyl acrylate-co-methyl methacrylate). *Polimeros-Ciencia E Tecnologia* **2013,** *23* (5), 619-623.

(175) Zhu, G. Q.; Wang, F. G.; Tan, H. S.; Gao, Q. C.; Liu, Y. Y., Properties of poly(lactic acid-co-glycolic acid) film modified by blending with polyurethane. *Chemical Papers* **2014,** *68* (2), 246-252.

(176) McDonald, P. F.; Geever, L. M.; Lyons, J. G.; Higginbotham, C. L., Physical and Mechanical Properties of Blends Based on Poly (dl-lactide), Poly (l-lactide-glycolide) and Poly (epsilon-caprolactone). *Polymer-Plastics Technology and Engineering* **2010,** *49* (7), 678-687.

(177) Hasirci, V.; Litman, A. E.; Trantolo, D. J.; Gresser, J. D.; Wise, D. L.; Margolis, H. C., PLGA bone plates reinforced with crosslinked PPF. *Journal of Materials Science: Materials in Medicine* **2002,** *13* (2), 159-167.

(178) Phong, L.; Han, E. S. C.; Xiong, S.; Pan, J.; Loo, S. C. J., Properties and hydrolysis of PLGA and PLLA cross-linked with electron beam radiation. *Polymer Degradation and Stability* **2010,** *95* (5), 771-777.

(179) Washington, M. A.; Balmert, S. C.; Fedorchak, M. V.; Little, S. R.; Watkins, S. C.; Meyer, T. Y., Monomer sequence in PLGA microparticles: Effects on acidic microclimates and *in vivo* inflammatory response. *Submitted for publication* **2017**.

(180) Middleton, L. R.; Trigg, E. B.; Schwartz, E.; Opper, K. L.; Baughman, T. W.; Wagener, K. B.; Winey, K. I., Role of Periodicity and Acid Chemistry on the Morphological Evolution and Strength in Precise Polyethylenes. *Macromolecules* **2016,** *49* (21), 8209-8218.

(181) Rana, D.; Mounach, H.; Halary, J. L.; Monnerie, L., Differences in mechanical behavior between alternating and random styrene-methyl methacrylate copolymers. *Journal of Materials Science* **2005,** *40* (4), 943-953.

(182) Versteegen, R. M.; Kleppinger, R.; Sijbesma, R. P.; Meijer, E. W., Properties and morphology of segmented copoly(ether urea)s with uniform hard segments. *Macromolecules* **2006,** *39* (2), 772-783.

(183) Målberg, S.; Höglund, A.; Albertsson, A. C., Macromolecular Design of Aliphatic Polyesters with Maintained Mechanical Properties and a Rapid, Customized Degradation Profile. *Biomacromolecules* **2011,** *12* (6), 2382-2388.

(184) Li, S. M.; Garreau, H.; Vert, M., Structure property relationships in the case of the degradation of massive aliphatic poly-(alpha-hydroxy acids) in aqueous-media. .2. Degradation of lactide-glycolide copolymers - PLA37.5GA25 and PLA75GA25. *Journal of Materials Science-Materials in Medicine* **1990,** *1* (3), 131-139.

(185) Vey, E.; Roger, C.; Meehan, L.; Booth, J.; Claybourn, M.; Miller, A. F.; Saiani, A., Degradation mechanism of poly(lactic-co-glycolic) acid block copolymer cast films in phosphate buffer solution. *Polymer Degradation and Stability* **2008,** *93* (10), 1869-1876.

(186) Pietrzak, W. S.; Sarver, D. R.; Verstynen, M. L., Bioabsorbable polymer science for the practicing surgeon. *J Craniofac Surg* **1997,** *8* (2), 87-91.

(187) Lu, L.; Garcia, C. A.; Mikos, A. G., In vitro degradation of thin poly(DL-lactic-co-glycolic acid) films. *Journal of Biomedical Materials Research* **1999,** *46* (2), 236-244.

(188) Maxwell, A. S.; Tomlins, P. E., New approaches to mapping through-thickness variations in the degradation in poly (lactide-co-glycolide). *Polymer Degradation and Stability* **2011,** *96* (5), 1015-1021.

(189) Li, S. M.; Garreau, H.; Vert, M., Structure property relationships in the case of the degradation of massive aliphatic poly-(alpha-hydroxy acids) in aqueous-media. 1.poly(D,L-lactic acid). *Journal of Materials Science-Materials in Medicine* **1990,** *1* (3), 123-130.

(190) Li, S. M.; Garreau, H.; Vert, M., Structure property relationships in the case of the degradation of massive aliphatic poly-(alpha-hydroxy acids) in aqueous-media. 3. Indluence of the morphology of poly(L-lactic acid). *Journal of Materials Science-Materials in Medicine* **1990,** *1* (4), 198-206.

(191) Shirazi, R. N.; Aldabbagh, F.; Erxleben, A.; Rochev, Y.; McHugh, P., Nanomechanical properties of poly(lactic-co-glycolic) acid film during degradation. *Acta Biomaterialia* **2014,** *10* (11), 4695-4703.

(192) Shirazi, R. N.; Aldabbagh, F.; Ronan, W.; Erxleben, A.; Rochev, Y.; McHugh, P., Effects of material thickness and processing method on poly(lactic-co-glycolic acid) degradation and mechanical performance. *Journal of Materials Science-Materials in Medicine* **2016,** *27* (10), 12.

(193) Félix Lanao, R. P.; Jonker, A. M.; Wolke, J. G. C.; Jansen, J. A.; van Hest, J. C. M.; Leeuwenburgh, S. C. G., Physicochemical Properties and Applications of Poly(lactic-co-glycolic acid) for Use in Bone Regeneration. *Tissue Engineering. Part B, Reviews* **2013,** *19* (4), 380-390.

(194) Lyu; Schley, J.; Loy, B.; Lind, D.; Hobot, C.; Sparer, R.; Untereker, D., Kinetics and Time−Temperature Equivalence of Polymer Degradation. *Biomacromolecules* **2007,** *8* (7), 2301-2310.

185

(195) Hakkarainen, M.; Albertsson, A.-C.; Karlsson, S., Weight losses and molecular weight changes correlated with the evolution of hydroxyacids in simulated in vivo degradation of homo- and copolymers of PLA and PGA. *Polymer Degradation and Stability* **1996,** *52* (3), 283-291.

(196) Beslikas, T.; Gigis, I.; Goulios, V.; Christoforides, J.; Papageorgiou, G. Z.; Bikiaris, D. N., Crystallization study and comparative in vitro-in vivo hydrolysis of PLA reinforcement ligament. *Int J Mol Sci* **2011,** *12* (10), 6597-618.

(197) Pitt, C. G.; Zhong-wei, G., Modification of the rates of chain cleavage of poly(ϵ-caprolactone) and related polyesters in the solid state. *Journal of Controlled Release* **1987,** *4* (4), 283-292.

(198) Pitt, C. G.; Chasalow, F. I.; Hibionada, Y. M.; Klimas, D. M.; Schindler, A., Aliphatic polyesters. I. The degradation of poly(ϵ-caprolactone) in vivo. *Journal of Applied Polymer Science* **1981,** *26* (11), 3779-3787.

(199) Gleadall, A.; Pan, J. Z.; Kruft, M. A.; Kellomaki, M., Degradation mechanisms of bioresorbable polyesters. Part 1. Effects of random scission, end scission and autocatalysis. *Acta Biomaterialia* **2014,** *10* (5), 2223-2232.

(200) Vay, K.; Friess, W.; Scheler, S., A detailed view of microparticle formation by in-process monitoring of the glass transition temperature. *European Journal of Pharmaceutics and Biopharmaceutics* **2012,** *81* (2), 399-408.

(201) Han, F. Y.; Thurecht, K. J.; Whittaker, A. K.; Smith, M. T., Bioerodable PLGA-Based Microparticles for Producing Sustained-Release Drug Formulations and Strategies for Improving Drug Loading. *Frontiers in Pharmacology* **2016,** *7*, 185.

(202) Wang, J.; Schwendeman, S. P., Mechanisms of solvent evaporation encapsulation processes: Prediction of solvent evaporation rate. *Journal of Pharmaceutical Sciences* **1999,** *88* (10), 1090-1099.

(203) Wischke, C.; Schwendeman, S. P., Principles of encapsulating hydrophobic drugs in PLA/PLGA microparticles. *International Journal of Pharmaceutics* **2008,** *364* (2), 298-327.

(204) Iqbal, M.; Zafar, N.; Fessi, H.; Elaissari, A., Double emulsion solvent evaporation techniques used for drug encapsulation. *International Journal of Pharmaceutics* **2015,** *496* (2), 173-190.

(205) Herrero-Vanrell, R.; Bravo-Osuna, I.; Andrés-Guerrero, V.; Vicario-de-la-Torre, M.; Molina-Martínez, I. T., The potential of using biodegradable microspheres in retinal diseases and other intraocular pathologies. *Progress in Retinal and Eye Research* **2014,** *42*, 27-43.

(206) Nan, K.; Ma, F.; Hou, H.; Freeman, W. R.; Sailor, M. J.; Cheng, L., Porous silicon oxide– PLGA composite microspheres for sustained ocular delivery of daunorubicin. *Acta Biomaterialia* **2014,** *10* (8), 3505-3512.

(207) Ling, Y.; Yang, Y.; Lu, N.; You, Q.-d.; Wang, S.; Gao, Y.; Chen, Y.; Guo, Q.-L., Endostar, a novel recombinant human endostatin, exerts antiangiogenic effect via blocking VEGF-induced tyrosine phosphorylation of KDR/Flk-1 of endothelial cells. *Biochemical and Biophysical Research Communications* **2007,** *361* (1), 79-84.

(208) Chen, W.; Hu, S., Suitable carriers for encapsulation and distribution of endostar: comparison of endostar-loaded particulate carriers. *International Journal of Nanomedicine* **2011,** *6*, 1535-1541.